Université du Québec
Institut National de la Recherche Scientifique
Centre Eau Terre Environnement

LES ÉMISSIONS DE GAZ À EFFET DE SERRE ET LES COMMUNAUTÉS MICROBIENNES DES MARES ASSOCIÉES AU DÉGEL DU PERGÉLISOL DANS L'ARCTIQUE

Par

Karita NEGANDHI
M.Sc. Biologie marine

Thèse présentée pour l'obtention du grade de
Philosophiae doctor (Ph.D.)
en Sciences de l'eau

Jury d'évaluation

Président du jury et examinateur externe	Dr. Philippe Constant Institut Armand-Frappier
Examinateur externe	Dr. Alison Derry Université du Québec à Montréal
Examinateur interne	Dr. Paul Drevnick Institut national de la recherche scientifique
Directrice de recherche	Dr. Isabelle Laurion Institut national de la recherche scientifique
Codirectrice de recherche	Dr. Connie Lovejoy Université Laval

RÉSUMÉ

Plusieurs mares dans l'Arctique sont associées au dégel du pergélisol, incluant les mares thermokarstiques générées par le réchauffement accéléré du climat et l'érosion du pergélisol. L'étendue de leur couverture spatiale et les propriétés limnologiques de ces mares sont préoccupantes parce qu'elles émettent une quantité substantielle mais variable de gaz à effet de serre (GES). À l'Île Bylot, les mares polygonales et les mares *allongées* sont deux formations géomorphologiques courantes du paysage des polygones en coins de glace. Cette thèse explore la possibilité que ces différentes formations influencent les émissions de GES par l'entremise de leurs propriétés limnologiques et leurs assemblages microbiens distincts. Les concentrations de GES dissous dans les mares ont été mesurées sur trois ans et variaient de 1.8 à 609 µM pour le dioxyde de carbone (CO_2), et de 0.1 à 25 µM pour le méthane (CH_4). Les émissions des mares *allongées* étaient systématiquement plus élevées que celles des mares polygonales pour le CO_2 (+17.0 comparé à -1.7 mmol m^{-2} d^{-1}) et pour le CH_4 (+0.7 par rapport à +0.2 mmol m^{-2} d^{-1}). Les analyses multivariées indiquent que les différences de production de GES selon la formation géomorphologique sont expliquées par les communautés bactériennes des sédiments et les sources de carbone. D'autres facteurs, incluant la structure de archées et communautés pélagiques de bactéries, n'étaient pas nettement séparés, à travers la diversité de l'UTO et leurs fonctions inférées, en fonction des formations géomorphologiques. Pour ce qui est des communautés bactériennes, il y avait proportionnellement plus de méthanotrophes (consommateurs de CH_4) ainsi que des signatures isotopiques $\delta^{13}C$-CO_2 et $\delta^{13}C$-CH_4 indiquant une plus grande oxydation du CH_4 dans les mares polygonales, et ultimement des émissions plus faibles de CH_4 par comparaison aux mares *allongées*. La présence de méthanotrophes semble réguler les concentrations en CH_4 et ainsi leurs émissions, avec une relation négative entre les concentrations dissoutes de CH_4 et le nombre de méthanotrophes (1 – 20%) dans les sédiments de surface ($r=-0.895$, $P=0.040$), tandis qu'aucune relation n'existe avec les méthanogènes ($r=-0.331$, $P=0.669$). Les sédiments des mares *allongées*, soumis expérimentalement à des températures plus élevées (+5°C), ont démontré une augmentation de la production en CO_2 et CH_4. Les communautés bactériennes des sédiments sont devenues plus diversifiées à température plus élevée, mais sans augmentation des méthanotrophes, ce qui pourrait expliquer l'augmentation de production nette de CH_4. En général, les mares *allongées* semblent prédisposées à une production de GES plus élevée et provenant d'une source de carbone plus grande et plus ancienne, et ainsi ont le potentiel d'agir plus directement sur le climat global. De

plus, leurs propriétés géomorphologiques instables empêchent l'établissement de tapis microbiens de cyanobactéries qui puisent efficacement le CO_2 et produisent de l'O_2. Ainsi ses mares abritent moins de méthanotrophes pour oxyder le CH_4, et une communauté bactérienne pouvant soutenir une production accrue de CH_4 en réaction au réchauffement planétaire.

Mots-clés : méthane (CH_4), dioxyde de carbone (CO_2), méthanogènes, méthanotrophes, carbone, mares thermokarstiques, mares de dégel, pergélisol, Arctic

ABSTRACT

Under a warming climate, thermokarst and thaw ponds formation is associated with thawing permafrost. The extent and characteristics of these ponds is of concern because they emit substantial, but highly variable greenhouse gases (GHG). On Bylot Island, polygonal and runnel ponds originate from two different geomorphological formations. In this thesis, the possibility that the different geomorphological formations influence GHG emissions through distinct limnological properties and microbial assemblages was explored. The dissolved GHG concentrations in the ponds was measured over 3 years and varied from 1.8-609 µM for carbon dioxide (CO_2), and 0.1-25 µM for methane (CH_4). Runnel ponds had consistently higher emissions than polygonal ponds for CO_2 (17.0 compared to -1.7 mmol m^{-2} d^{-1}) and for CH_4 (0.7 compared to 0.2 mmol m^{-2} d^{-1}). Using multivariate analysis GHG production differences between the geomophologically distinct ponds was explained by differences in the sediment bacterial community and carbon (C)-source. Other factors including sediment archaeal communities and water bacterial communities did not have clear a separation, through OTUs diversity and inferred functions, between pond formations. For the bacterial communities, there were proportionally more methanotrophs (CH_4 consumers) in the polygonal ponds along with $\delta^{13}C$-CO_2 and $\delta^{13}C$-CH_4 signatures indicating CH_4 oxidation, and ultimately less CH_4 released into the water compared to runnel ponds. Occurrence of methanotrophs seems to regulate CH_4 concentrations, with a negative relationship between dissolved CH_4 concentrations and the number of surface sediment methanotrophs (1 - 20%, r=-0.895, P=0.040), compared to no relationship with methanogens (r=-0.331, P=0.669). Runnel pond sediment, experimentally subjected to warmer temperatures (+5°C) showed increased CO_2 and CH_4. The sediment bacterial communities become more diverse under increased temperature, but with no increase in methanotrophs, possibly explaining the increase in CH_4 production. Overall runnel ponds seemed to be predisposed to higher and more climate-relevant GHG production through access to larger and older carbon supplies. In addition, their geomorphological origin allows for an absence of cyanobacterial mats to take up CO_2 and produce O_2, fewer methanotrophs to oxidize CH_4, and a bacterial community supporting increased CH_4 production in response to a warming climate.

Keywords: methane (CH_4), carbon dioxide (CO_2), methanogens, methanotrophs, carbon, thermokarst ponds, thaw ponds, permafrost, Arctic

AVANT-PROPOS

Cette thèse comprend des recherches originales sur les émissions de gaz à effet de serre (GES), les communautés microbiennes et les caractéristiques de carbone dans l'Arctique mares de thermokarts (fonte) de l'île Bylot. Elle est composée de quatre parties, la première partie consistant en une synthèse à présenter le contexte de la recherche, les objectifs, les résultats, et une conclusion résumée. Le second est le cœur de la thèse composé de trois articles, qui sont énumérés ci-dessous. Suivie par les troisième et quatrième parties contenant les référence bibliographiques et une annexe.

Articles de la these

Negandhi K, Laurion I, Whiticar MJ, Galand PE, Xiaomei X, and Lovejoy C (2013) Small thaw ponds: an unaccounted source of methane in the Canadian high Arctic. *PLOS ONE* 8: e78204. doi:10.1371/journal.pone.0078204

Negandhi K, Laurion I, and Lovejoy C (2013/4) Arctic thaw pond morphology influences bacterial communities and associated greenhouse gas emissions (soumis à *Polar biology*).

Negandhi K, Laurion I., and Lovejoy C. (2014) Arctic thaw ponds sensitivity to increased temperature: DNA and RNA bacterial community and GHG production rate (en préparation).

REMERCIEMENTS

I would like to thank firstly my advisor Isabelle Laurion, not only for taking a chance on a student from Florida to work in the Arctic, but also for many more important things. Throughout my PhD, she has always supported me, allowing me to learn and acquire too much to list. A main attribute I have learned from her that will always stay with me is best put as "For every fact there is an infinity of hypotheses" by Robert M. Pirsig.

I would also very much like to thank my co-advisor Connie Lovejoy. The amazing lab she has set up, has allowed me to learn an unimaginable amount working at. This is not to discredit the highly unforgettable time spent with Connie. I would also like to take the time to thank everyone in her lab, as each one has helped me out, and especially André Comeau.

I would also like to thank my co-authors on my first article: Pierre Galand, Michael Whiticar, and Xiaomei Xo. This was very much a result of collaborative work, which I fully enjoyed learning and working on it.

I can undoubtedly say that the best part of my PhD was working with amazing people. This experience has given me confidence, not only in science but also to keep pursuing within the scientific field. I present my thesis under the words of John Muir "When one tugs at a single thing in nature, he finds it attached to the rest of the world", with hopes that it inspires further science.

TABLE DES MATIÈRES

GLOSSAIRE DES ABBRÉVIATIONS (EN FRANÇAIS)

ADN : acide désoxyribonucléique

ARN : acide ribonucléique bactérienne

AT : azote total

BYL# : Île Bylot, avec un nombre représentant des étangs spécifiques

C : carbone

CO : carbone organique

COD : carbone organique dissous

GES : gaz à effet de serre

MA : méthanogénèse acétoclastique

MH : méthanogénèse hydrogénique

MO : matière organique

MOD : matière organique dissoute

MODC : matière organique dissoute chromophorique

MOS : matière organique du sol

PT : phosphore total

PCR : réaction en chaîne polymérase

Q_{10} : coefficient de température pour la vitesse de changement en raison d'un changement de température de 10 C

SRP : phosphate réactif soluble

UTO : unité taxonomique opérationnelle

LISTE DES TABLEAUX

LISTE DES FIGURES

LES ÉMISSIONS DE GAZ À EFFET DE SERRE ET LES COMMUNAUTÉS MICROBIENNES DES MARES ASSOCIÉES AU DÉGEL DU PERGÉLISOL DANS L'ARCTIQUE

SYNTHÈSE

1 SYNTHÈSE

1.1 Introduction

1.1.1 Pergélisol et formation des mares de dégel

Le climat rigoureux des écosystèmes polaires crée de nombreux traits propres aux paysages du cryosphère ainsi qu'une terminologie associée. Une telle caractéristique est le pergélisol ou le sol cryotique. Le pergélisol inclut le sol, les roches, la glace et la matière organique qui persistent à ou en bas de 0°C pour un minimum de deux ans consécutifs (van Everdingen, 1998). Il existe des variations de cette définition, par exemple, en Russie, il s'agit de trois ans avec une température en bas de 0°C et la présence de glace est nécessaire (Kudryavtsev, 1978). En Arctique les régions où 90 - 100 % du sol est pergélisol sont dénommées pergélisol continu. Il s'agit de pergélisol discontinu si le pergélisol constitue 10 - 90 % du sol (Brown *et al.*, 1997). En tout le pergélisol se retrouve sur plus de 24 % des surfaces terrestres de l'hémisphère Nord (Tarnocai *et al.*, 2009) (Figure 1.1).

La majorité du pergélisol présent s'est formé dans la dernière période glaciale et a subsisté des milliers d'années. Le pergélisol a diminué les années ayant des températures plus chaudes. Quand les températures moyennes augmentent chaque année, la couche active, une couche de sol qui dégèle l'été pour ensuite regeler de nouveau, approfondit avec le temps. La variation extrême de températures de la couche active est de +15°C à -35°C selon la température annuelle de l'air (Wagner *et al.*, 2008). En association avec le dégel de cette couche active est la formation de mares thermokarst. À mesure que la couche de pergélisol dégel, la terre non gelée persiste et érode, créant des dépressions qui favorisent la formation de mares de dégel (Figure 1.2 a & b). L'eau qui remplit les dépressions peut provenir de la pluie et de la fonte de glace et de neige, mais la provenance de chaque source n'est pas connue et varie probablement entre les saisons.

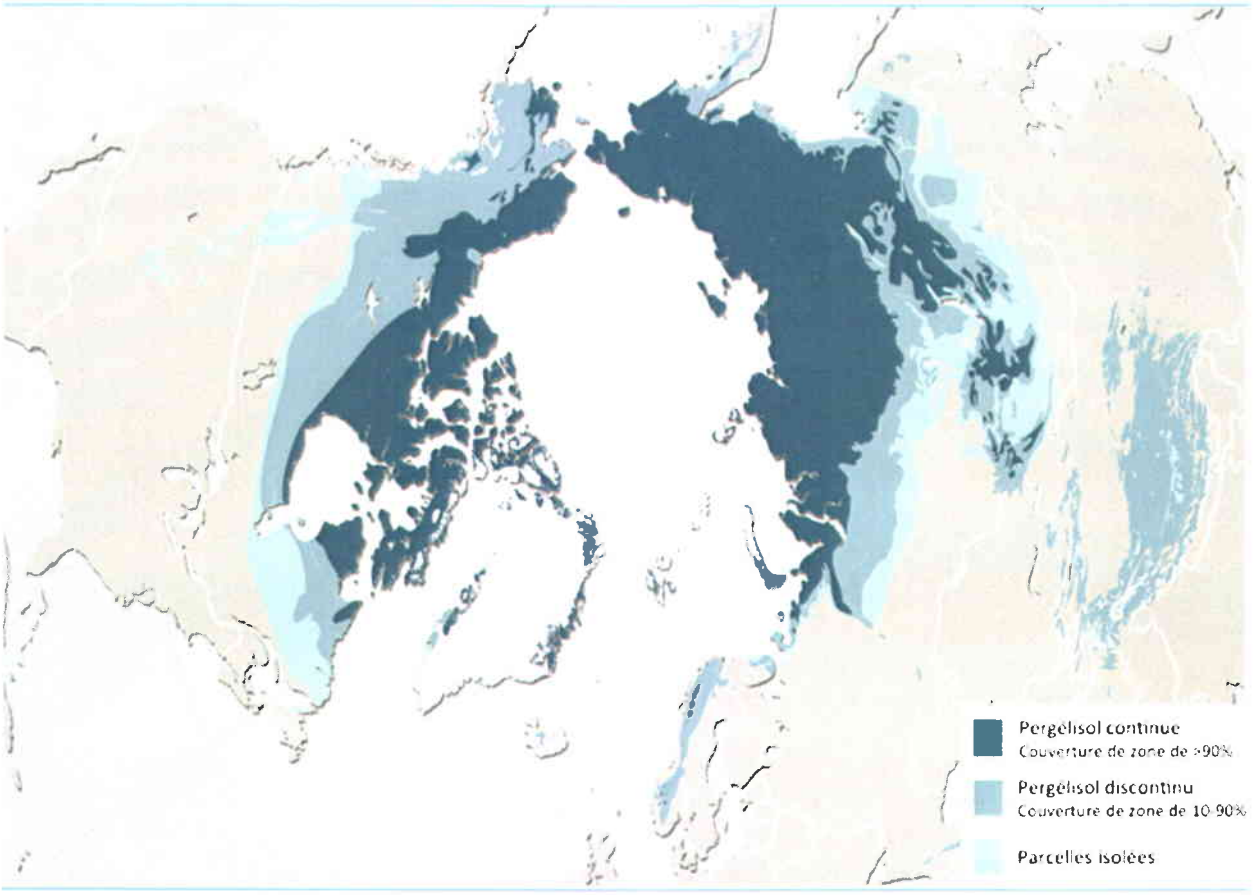

Figure 1.1 La distribution des endroits de pergélisol continu et discontinu dans l'hémisphère Nord. Modifé de Brown, et al. 1997. Association internationale du pergélisol, circum- Arctic carte de pergélisol et de la glace du sol en Arctique, Échelle 1:10,000,000. U.S. Geological Survey.

Figure 1.2 a) Une mare (de fonte) thermokarst en Arctique, classée comme une mare *allongées* à l'île Bylot, avec du pergélisol qui érode la rive en raison d'une couche active intense en dégel à cause du changement climatique. b) Une mare de dégel en Arctique, classée comme une mare polygone à l'île Bylot, un phénomène naturel associé avec le dégel de la couche active n'ayant aucune érosion.

Les mares et les lacs thermokarst en pergélisol peuvent démontrer une caractéristique distincte, le talik (Fig. 1.3 a). L'origine du mot provient du mot Russe pour fonte, *tait*. Un talik est une région du sol située en dessous des lacs ou des mares et ce sol demeure non gelé toute au long de l'année (van Everdingen, 1998). Il peut même se produire dans des régions de pergélisol continu si les lacs sont si profonds qu'ils ne gèlent pas jusqu'au fond. Ce phénomène a lieu, par exemple, en Sibérie et en Alaska au fond des lacs thermokarst profonds (Walter *et al.*, 2008). Une deuxième formation unique associée aux lacs et aux mares thermokarst est les coins de glace (Fig. 1.3 b). Les coins de glace forme après plusieurs cycles de gel et dégel de la couche active. Les contractions thermiques lors de la saison froide de l'hiver créent des craques dans le sol puis, dans le printemps, ces contractions thermiques se remplissent d'eau de fonte qui gèle en hiver. Des fissurations et des gels continus produisent des coins de glace plus larges et plus profonds, créant ainsi un réseau de polygones de tourbe (Washburn, 1980). Les mares de dégel peu profondes se forment sur le paysage de coins de glace, soit sur les polygones à centre concave, soit sur les coins de glace fondants.

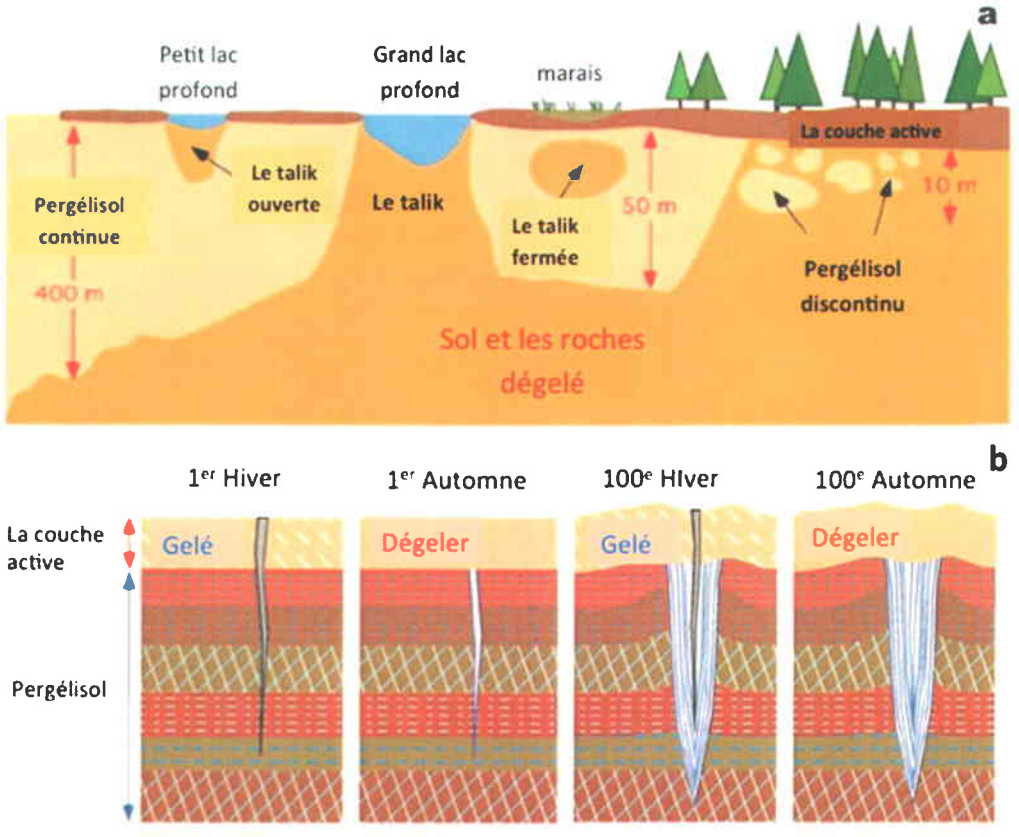

Figure 1.3. Une illustration de la couche active associée à la formation de a) taliks et de b) coins de glace dans la région de pergélisol continu. Modifé de Pidwirny, M. (2006). "Periglacial Processes and Landforms". *Fundamentals of Physical Geography, 2nd Edition*. 19 septembre 2013. http://www.physicalgeography.net/fundamentals/10ag.html

1.1.2 La pertinence des mares de dégel

Malgré que l'aire totale des mares de dégel soit incertaine, des études récentes ont démontré que les petites étendues d'eau constituent la majorité de l'eau potable sur la Terre. Les plus anciennes études ont déclaré que 1.3 - 1.8 % de la surface de la planète est couverte par des lacs et des mares (Wetzel, 1990; Meybeck, 1995), incluant les plans d'eau entre 0.01 - 1 km^2. Cette couverture a augmenté à plus que 3 % (Downing *et al.*, 2006). L'activité microbienne de ces nombreux étendues d'eau est donc importante pour les cycles globaux de nutriments (Figure 1.4 ; Bardgett *et al.*, 2008).

Les cycles globaux accorder une importance particulière au cycle de carbone (C) par rapport aux mares et aux lacs de fonte parce qu'ils peuvent produire une quantité appréciable de gaz à effet de serre (GES) (Zimov *et al.*, 1997; Wagner *et al.*, 2005; Walter *et al.*, 2006; Zona *et al.*, 2008; Laurion *et al.*, 2010). Malgré que la rétroaction biogéochimique globale reliée au réchauffement climatique des systèmes de pergélisol inondés soit relativement faible en comparaison avec les émissions humaines (Gao *et al.*, 2013), la véritable ampleur de leurs émissions de GES est peu connue. La contribution globale des lacs fut estimée entre 8 – 48 Tg CH_4 an^{-1}, ce qui 6 – 16 % des émissions naturelles de CH_4, et 1.6 – 9.6 % des émissions totales (Bastviken *et al.*, 2004). Il a été suggéré que les milieux humides de l'Arctique (>50°N), y compris les mares et les lacs de fonte, sont la plus grande source naturelle de CH_4, responsables de ~25 % (Bousquet *et al.*, 2006). L'importance des mares de dégel les plus petites est facilement oubliée en raison de leur taille, parce qu'elles sont difficiles à percevoir avec l'imagerie satellite (Smith *et al.*, 2007; Walter *et al.*, 2008), mais également à cause de la grande variabilité des émissions observée de ces divers écosystèmes. Par exemple, les petites mares de dégel sont responsables de 35 – 62% des émissions estivales des plans d'eau, mais elles peuvent entreposer du C temporairement pendant d'autres périodes de l'année (Abnizova *et al.*, 2013). La diversité des propriétés géomorphologiques, physicochimiques and biologiques des mares de dégel (Breton *et al.*, 2009, Laurion *et al.*, 2010) aggrave la difficulté de déchiffrer les tendances qui correspondent à leurs émissions de GES variables.

Des études précédentes ont établit plusieurs propriétés des lacs qui influencent le cycle de C et qui mènent à des incertitudes des estimés de GES d'efflux. Par exemple, Christensen et al. (2007) a trouvé que l'efflux de dioxyde de carbone (CO_2) par aire est plus important pour les petits lacs que pour les plus grands. L'explication pour ceci est que les émissions des lacs plus petits ont des sources de C terrestres, couplant ainsi leur cycle de C à des processus terrestres (Kortelainen *et al.*, 2006). Les estimations de flux des lacs sont compliquées par un facteur unique additionnel, le temps de la fonte de glace. Dix pourcent des émissions de CO_2 de 79 356 lacs suédois de 57° à 68°N fut relâché immédiatement à la fonte de la glace (Algesten *et al.*, 2004). De plus, les émissions de glace étaient plus élevées pour les lacs recevant des intrants des tourbières (Striegl *et al.*, 2001), liant l'hydrologie aux émissions de CO_2. Les émissions peuvent aussi varier entre les saisons et à travers la progression trophique des lacs étant donné que plus de C labile est réduit lors des premiers stades (Striegl *et al.*, 2001, Zona *et al.*, 2008). Indépendamment de la large gamme de propriétés physico-chimiques, la majorité des mares de dégel est supersaturée en GES (Breton *et al.*, 2009), probablement en raison des intrants

terrestres de C (Tank *et al.*, 2009). Malgré les difficultés d'étudier les lacs éloignés de l'Arctique, leur abondance et leur potentiel d'agir comme des conduites de gaz requièrent plus d'efforts d'échantillonnage (Vincent *et al.*, 2008; Prowse *et al.*, 2006).

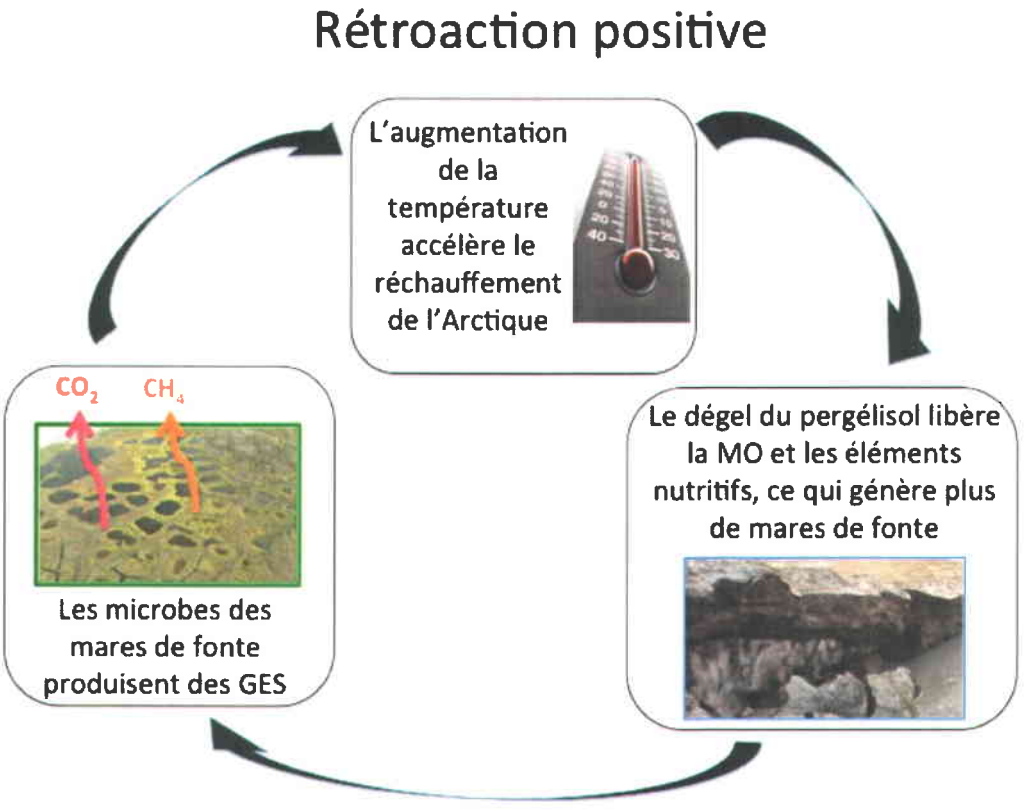

Figure 1.4 Le rôle des mares de dégel en tant qu'acteurs de rétroaction, en raison de l'augmentation de la température, induit un dégel de pergélisol plus important, ce qui génère plus de mares de dégel, qui sont des producteurs importants de GES, augmentant ainsi davantage le réchauffement de l'Arctique.

Les écosystèmes de pergélisol arctiques et boréaux entreposent deux fois plus de carbone organique (CO) que ce qui se retrouve dans l'atmosphère (Zimov *et al.*, 2006; Schuur *et al.*, 2008). Uniquement à l'intérieur du Canada, 147 Gt de CO de sol, ou 56% de tous les sols canadiens, est capté dans le pergélisol (Tarnocai *et al.*, 2009). En conséquence, fur à mesure que le pergélisol dégèle, une fourniture énorme d'CO est libérée et peut être utilisée par des microbes, produisant ainsi des GES (Schuur *et al.*, 2008; Grosse *et al.*, 2011). La pertinence de cette nouvelle source d'CO mobilisée comme un mécanisme de rétroaction du climat est

actuellement inconnue. Une combinaison de 11 modèles a prédit que 100 Pg C d'émissions du pergélisol dégelera d'ici 2100, mais il y a un taux d'incertitude de 56% avec ces modèles (Schaefer *et al.*, 2012; Gao *et al.*, 2013). Cette incertitude peut être attribuée en partie à la lacune de connaissances de la dégradabilité de C et de la formation future de caractéristiques typiques des thermokarst et des traits associés (Camill *et al.*, 2001; Schaefer et al., 2012; Koven *et al.*, 2013).

L'accumulation de C entreposé dans les hautes latitudes est causée par la présence de sols humides et froids qui inhibent la décomposition de tissus végétaux morts et, par conséquence, augmentent leur intégration dans le réservoir de matière organique du sol (MOS) (McGuire *et al.*, 2009). Il est tenu pour acquis que ceci a permis une accumulation de C dans les sols dégelés datant d'avant le dernier maximum glaciaire (~20 kyrs A.P.; Zimov *et al.*, 2006), mais dans les sols de l'Arctique canadien, cette accumulation a débuté après l'Holocène (~12 kyrs A.P.; Fortier & Allard 2004). Globalement le C utilisé pour la production de CO_2 and CH_4 peut provenir de trois grandes catégories comprenant le métabolisme des plantes (photosynthétats récents), la décomposition de plantes mortes récemment, et la décomposition de vieille MOS suite au dégel du pergélisol (Schuur *et al.*, 2009). Donc, les GES émis dans l'Arctique canadien pourraient provenir de ce vieux C accumulé, selon sa labilité comparée aux intrants de C plus récents par des plantes terrestres ou aquatiques (Figure 1.5).

La labilité de carbone influence l'activité microbienne (Berggren *et al.*, 2010; Guillemette & delGiorgio 2011). Par exemple, même si le pergélisol peut constituer une source importante de C, il peut être de faible qualité, causant un métabolisme microbien limité par le substrat (Wagner *et al.* 2005). Par contre, le C du sol peut soutenir une production microbienne plus efficace que prévue (Berggren *et al.*, 2010), étant donné que les sols de pergélisol et de la couche active exposée à des communautés bactériennes lacustrines ont démontré une dégradation rapide de l'CO du pergélisol et des émissions de CH_4 (Mazeas *et al.*, 2009; Roehm *et al.*, 2009).

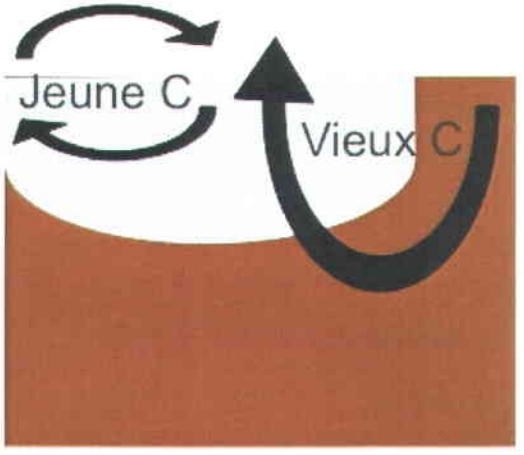

Figure 1.5 Le cycle de vieux versus jeune C pour la production de GES dans les mares de dégel peut influencer l'importance des émissions des mares de dégel comme un mécanisme de rétroaction positive pour le changement climatique.

Afin de déterminer si la source de C plus ancienne est utilisée pour la production des GES, la datation par radio carbone (^{14}C) est utile. Les plantes vivantes échangent ^{14}C avec l'atmosphère, alors ils ont la même valeur ^{14}C value que l'atmosphère au moment spécifique quand il a été fixé. Quand les plantes meurent, il n'y a plus d'échange de ^{14}C avec l'atmosphère, laissant le ^{14}C à diminuer à partir de la désintégration radioactive. Ce processus permet les valeurs de ^{14}C des MOS de servir comme de marqueur pour le taux ou la source de C (O'Brien & Stout 1978; Trumbore *et al.*, 1990).

1.1.3 Dégradation microbienne de C et production de GES

Afin de mieux comprendre et d'investiguer la transformation de CO du pergélisol en GES, les communautés microbiennes des mares de dégel doivent être caractérisées parce que les communautés microbiennes sont les contributeurs principaux, encore plus que les facteurs environnementaux, aux variations spatiales et temporelles de la dynamique du C des écosystèmes (Strickland *et al.*, 2009). Avant que soit CO_2 ou CH_4 puissent être produits, le C présent initialement doit être dégradé dans une forme utilisable. Ces étapes initiales de dégradation de C transforment C par des processus hydrolytiques, fermentatives, et syntrophiques (Whiticar *et al.*, 1986; Padmanabhan *et al.*, 2003).

La labilité du C, qui peut être difficile à déterminer, est le facteur principal qui affecte la dégradation initiale de C. Même si la source principale de C provient des molécules terrestres humiques, qui sont reconnues d'être peu labile, la photolyse des molécules peut augmenter sa labilité. La photolyse inclut une modification structurale à une molécule qui la rend plus petite et, par conséquence, plus labile, ainsi augmentant l'activité microbienne (Bertilsson & Allard 1996; Anesio *et al.*, 2005). La matière organique dissoute (MOD) des mares de dégel est largement influencé par la photolyse et, donc, est un facteur important à tenir en compte lors des calculs des taux de dégradation microbienne de C, surtout lors des étés arctiques quand il y a plus que 24 heures d'ensoleillement (Laurion & Mladenov 2013).

Les méthanogènes sont des acteurs clefs dans les émissions des GES. Des méthanogènes connus appartenant actuellement au domaine d'Archaea. Récemment, une étude liant des espèces archées indicatrices avec leur habitat a démontré que le seul habitat sans espèces indicatrices fut les sédiments d'eaux douces comparé à six autres habitats, comprenant l'eau douce, le sol, l'eau marine, le sédiment marin, l'hypersaline, et les cheminées hydrothermiques (Auguet *et al.*, 2009). Ce résultat a pu être en raison du manque d'études des sédiments d'eaux douces et le besoin pour plus d'investigations portant sur les archées, mais pourrait aussi refléter une faible occurrence des archées dans ces genres de sédiments.

Parmi les archées sont des méthanogènes qui ont le rôle de formation de CH_4 (Garcia *et al.*, 2000). Dans les milieux humides froids et les sols pergélisols, CH_4 est produit par 2 voies. Le premier groupe fonctionnel se sert de H_2 pour réduire CO_2 en CH_4 et est nommé méthanogénèse hydrogénique (MH). Le deuxième inclut la fermentation de l'acétate en CH_4 et CO_2 et s'appelle méthanogénèse acétoclastique (MA) (Deppenmeier *et al.*, 1996; Conrad 2005).

La détermination de la voie métabolique utilisée aidera à prédire les émissions de CH_4 et de CO_2 en fonction des conditions environnementales qui changent rapidement actuellement en Arctique. Par exemple, la distribution spatiale des émissions de CH_4 dans les milieux humides tempérés fut expliquée par les voies méthanogéniques (Hornibrook *et al.*, 1997). La présence d'MA ou MH est causée par les changements de la source des substrats de C labile. Par exemple, la disponibilité de CO frais et labile favorise MA, en comparaison avec du CO de tourbe plus récalcitrant qui favorise le MH (Miyajima *et al.*, 1997, Hornibrook *et al.,* 2000). La voie méthanogènique utilisée (MA ou MH) pour la production de CH_4 peut être déterminée par les signatures $\delta^{13}C$ et $\delta^{2}H$ de CO_2 et de CH_4 (Whiticar, 1999).

En dehors de la disponibilité des substrats, le taux de production de CH_4 peut également être limité par des facteurs tel le potentiel de rédox et le pH. Par exemple, les accepteurs d'électrons électronégatifs (NO_3^-, SO_4^{2-}, Fe^{3+}) supplantent les méthanogènes pour le H_2, et ainsi limitent la production de CH_4 (Valentine *et al.*, 1994). En plus, certaines bactéries, comme les bactéries sulfato-réductrice entrent également en compétition avec les méthanogènes pour le H_2 (Abram & Nedwell *et al.*, 1978). Cela rend les propriétés physicochimiques d'eau, les bactéries, les méthanogènes et la disponibilité de substrat, des facteurs importants à considérer pour la production de CH_4.

Les méthanotrophes sont aussi un élément clef des cycles des GES. Ceux-ci sont des consommateurs de CH_4 qui oxydent le CH_4 en CO_2 et qui jouent un rôle important dans la régulation de la quantité de CH_4 qui se rend à l'atmosphère (Bastviken *et al.*, 2008). Une fois le CH_4 est produit dans les sédiments et relâché dans la colonne d'eau, une fraction peut être oxydée en CO_2 par les méthanotrophes avant qu'il se rend à l'atmosphère. Par exemple, un lac finnois a démontré que, sur une base annuelle, 79 % du CH_4 produit fut consommé par des méthanotrophes, et que seulement le 21% qui restait fut relâché à l'atmosphère (Kankaala *et al.*, 2006). D'ailleurs cette étude a démontré que le flux de CH_4 entre l'interface sédiment-eau ne prévoyait pas le flux de CH_4 entre l'eau et l'atmosphère. Malgré que l'impact de l'oxydation de CH_4 méthanotrophe peut varier parmi les lacs selon la profondeur, la structure verticale et les régimes de mélange contribuent tous à les émissions de GES variables (Michmerhuizen *et al.*, 1996; Striegl *et al.*, 1998).

Contrairement à la production de CH_4, qui se limite aux benthos, la production de CO_2 peut se retrouver autant dans le benthos que dans le pélagos à travers plusieurs processus bactériens. En plus des méthanotrophes, diverses bactéries hétérotrophes font la respiration pélagique et sédimentaire. Le CO_2 peut aussi être produit physiquement par la photo-oxydation, où la MOD est photolysée (Jonsson *et al.*, 2001). L'importance de la photo-oxydation pour la production de CO_2 peut être relativement faible en comparaison avec la respiration (Jonsson *et al.*, 2001). Similaire à la méthanotrophie de CH_4, la photosynthèse agit comme un puits microbien de CO_2, principalement par des tapis cyanobactériennes dans les mares de dégel (Vézina & Vincent 1997; Figure 1.6).

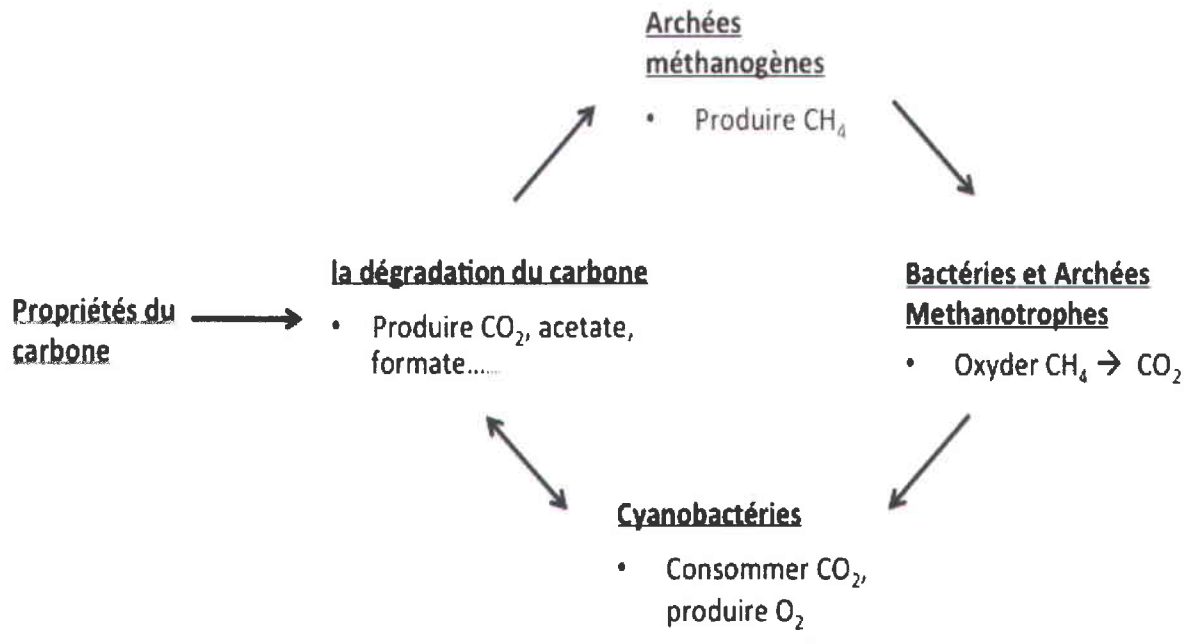

Figure 1.6 Des rôles variés des bactéries et des archées dans la production de GES dans les mares de dégel de l'Arctique

Il a un lien direct entre les bactéries qui dégradent le C qui sont responsables pour la transformation initiale de C en une forme appropriée pour les producteurs et consommateurs de CH_4, et plusieurs types de bactéries qui régulent la production de CO_2. Donc, le Domaine bactérienne autant que le règne d'archée est importante à étudier afin de déceler le cycle de C et la production de GES, démontrant un besoin pour des études plus poussées pour identifier les membres bactériennes et archées impliqués parmi les divers habitats arctiques.

1.1.4 Le transport de méthane à travers la colonne d'eau

En plus de l'oxydation méthanotrophique d'une fraction de CH_4 produite dans les sédiments de lac, il y a une autre complication pour l'estimation des émissions de CH_4, soit son transport à travers la colonne d'eau. Il y a trois processus de transport de CH_4 de sédiment benthique à l'atmosphère: le transport par les plantes, la diffusion et l'ébullition (Figure 1.7; Whalen, 2005). Les trois processus doivent être considérés pour estimer correctement les émissions totales d'un lac ou d'une mare. Par exemple, les racines de plantes ont aérenchyme qui transfèrent CH_4

du sédiment à travers la plante jusqu'à l'atmosphère (Shannon *et al.*, 1996), représentant possiblement 2 - 23% du CH_4 émis (Bastviken *et al.*, 2004 et références qui y figurent), mais ceci n'a pas été rapporté pour les écosystèmes influencés par le pergélisol. Le flux diffusive est le plus souvent mesuré, variant considérablement entre systèmes aquatiques et influencés par les grandes variations de turbulence à la surface de l'eau (MacIntyre *et al.*, 2010). Par exemple dans les lacs boréaux suédois et les lacs thermokarst sibériens, les taux peuvent être aussi faibles que 0.48 mmol m^{-2} j^{-1} (Zimov *et al.*, 2001; Batsviken *et al.*, 2004) comparés aux taux de la Baie d'Hudson qui atteignent 48 mmol m^{-2} j^{-1} (Hamilton *et al.*, 1994). Par contre, plus récemment, ce processus s'est révélé de constituer qu'une petite partie des émissions totales en raison de la faible solubilité de CH_4 dans l'eau (Baker-Blocker *et al.*, 1977; Cicerone et Shetter 1981; Bartlett *et al.*, 1988; Casper *et al.*, 2000). L'ébullition a été moins étudiée parce qu'elle est même plus variable dans l'espace et dans le temps (Walter *et al.*, 2006), mais dans les lieux étudiés à date, les taux d'ébullition sont généralement considérés plus élevés que les taux de diffusion (Walter *et al.*, 2010).

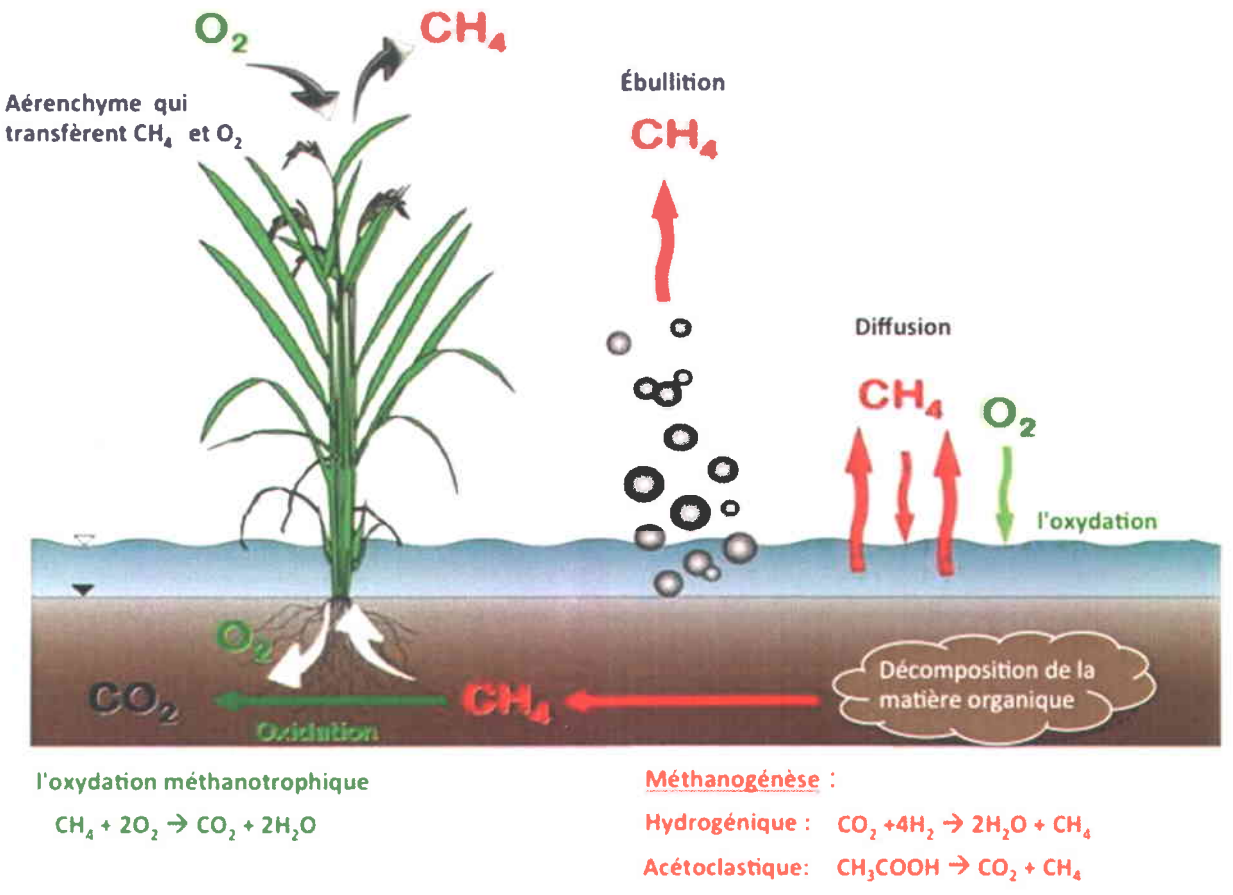

Figure 1.7 Section transversale d'une mare de dégel illustrant les trois modes possibles de transport de CH_4 à l'atmosphère: les plantes, l'ébullition et la diffusion. La photo provient de l'Institute of biogeochemistry and pollutant dynamics; www1.ethz.ch/ibp/research/environmentalmicrobiology/research/Wetlands

L'importance de distinguer le transport de l'ébullition par rapport au transport diffusif relève de leurs impacts sur l'oxydation de CH_4, parce que le CH_4 transporté par l'ébullition est moins susceptible d'être consommé par des méthanotrophes (Figure 1.7). Par exemple, le CH_4 de l'ébullition des « hot spot » et des « point source » est associé avec des bulles plus rapides et plus larges qui transitent dans la colonne d'eau, et ont donc moins de chances d'être oxydées que les micro-bulles et les gaz dissous (Prairie & del Giorgio 2013). Les gaz dissous peuvent quand même s'échapper à l'atmosphère s'ils ne passent pas à travers une zone de méthanotrophie (Chanton & Martens 1988).

Les mécanismes d'ébullition ont été classés récemment pour les lacs thermokarst arctiques comme «background source », « point source », et « hot spots » (Walter *et al.*, 2007). L'ébullition background est considérée comme étant des évènements d'ébullition aléatoires et plus faibles qui ont lieu sporadiquement à plusieurs endroits dans un lac. En comparaison, les point source et hot spots sont des sources d'ébullition plus localisées et continues. Ces diverses formes d'ébullition doivent être considérées comme elles impliquent des techniques d'échantillonnage différentes (des entonnoirs immergés ou une technique l'espace de l'air dans la bouteille, la fréquence d'échantillonnage, la hétérogénéité spatiotemporelle; voir plus bas) et elles semblent être produites à partir de sources de C datées (Walter *et al.*, 2008). L'ébullition « point source » et « hot spot » a les signatures de C les plus anciennes et sont apparemment produites à partir des sédiments les plus profonds des lacs thermokarst sibériens et alaskiens (11 355 – 42 900 ^{14}C ans), en comparaison à l'ébullition background (1 345 – 8 845 ^{14}C ans) et l'ébullition background des sédiments de surface remués (> moderne à 3 965 ans). Le CH_4 dissous est censé, en ce moment, être le plus jeune, mais, à nos connaissances, ceci n'a pas été vérifié. La détermination de l'âge du C des GES émis a des implications pour l'équilibre de C, avec CH_4 daté étant le plus vieux, représentant une rétroaction positive et pertinente du climat en comparaison au C fixé récemment (Elmendorf *et al.*, 2012). Étant donné que l'ébullition point source et hot spot constituent la majorité des émissions CH_4 des lacs thermokarst sibériens (70%), leur production sont provient d'une façon marquée de C ancien et représente donc une rétroaction positive du climat (Walter *et al.*, 2007).

Avant que ces pourcentage d'ébullition de CH_4 dissous soient attribués à des âges de C pour l'équilibre de C, ce modèle doit être confirmé dans d'autres systèmes thermokarst d'ailleurs en Arctique où la géomorphologie et la morphologie des lacs peuvent varier considérablement et influenceraient ces modèles. Par exemple, les taliks, tel étudiés auparavant dans des lacs thermokarst, n'existent pas en dessous des mares de dégel peu profondes de l'île Bylot et, en conséquence, la production des hot spots n'est peut-être pas possible à l'intérieur d'une couche active de ~60 cm de profondeur. De plus, la composition structurale de tourbe, y inclut le contenu de sable, d'argile et de la glace, ainsi que la pression atmosphérique, peuvent jouer un rôle décisif dans l'accumulation et la relâche de bulles de surface de CH_4 (Coulthard *et al.*, 2009; Tokida *et al.*, 2007).

1.1.5 Les effets de la température sur le cycle du C des mares de dégel

Avec la prévision de le Groupe d'experts intergouvernemental sur l'évolution du climat (IPCC) d'une augmentation de la température de 2 à 9 °C, selon le modèle et les scénarios de forçage, à la fin du 21^{ième} siècle pour les régions arctiques (2007), l'occurrence de mares de dégel augmentera probablement dans les régions de pergélisol continu. Le degré de stimulation de la production de GES serait stimulée par les étés plus chaudes et plus longues est inconnu mais très probable en raison de quelques activités de respiration microbienne avec un écart Q_{10} de 1.7 – 3.4 (Anderson, 2010; Bekku *et al.*, 2003). Par contre, d'autres points sensibles des températures Q_{10} très variables ont été reportés, menant à une prévision que les valeurs de respiration Q_{10} au delà de 2.5 reflètent probablement une interaction des sources de substrat en plus de la température (Davidson *et al.*, 2006). En fait, des taux de production de CH_4 accrus des milieux humides du Nord et de l'Arctique constituaient des réponses à la disponibilité augmentée des substrats (Anderson, 2010) en raison la température améliorant les taux de fermentation (Valentine *et al.*, 1994). Le nouveau réservoir de C libéré grâce au réchauffement du climat pourrait ainsi être un facteur principal de la stimulation de la production de GES selon la biodisponibilité (Wagner *et al.*, 2005; Guillemette & delGiorgio 2011). De plus, la réponse de la composition de la communauté microbienne arctique est inconnue. Par exemple, une activité méthanotrophique accrue (oxydation de CH_4 en CO_2) pourrait mitiger la production de CH_4.

Un changement de température peut influencer la quantité de C disponible qui se décompose, à cause d'un changement de la communauté microbienne (MacDonald *et al.*, 1995; Zogg *et al.*, 1997). Particulièrement, Zogg *et al.* (1997) ont trouvé qu'une augmentation de température entraine une quantité plus importante de C respiré ainsi qu'une biomasse microbienne active plus petit et une source de C plus grand. Ceci a souligné que l'augmentation de C respiré n'est pas à cause de plus d'activité microbienne mais plutôt en raison d'un changement dans la communauté microbienne (Figure 1.8). De plus, les températures plus clémentes ont augmenté la quantité de vieux C utilisée par les microbes attribuée à un changement de la composition de la communauté microbienne et à les réactions enzymatiques entre 5, 20 and 35°C, étant donné que la taille de la communauté est inchangée. Une décomposition accrue de vieux C peut aussi arrivée à des températures plus élevés avec l'ajout d'azote et sans changement de communauté microbienne (Waldrop & Firestone 2004). Donc, n'importe quel changement de la communauté microbienne des mares de dégel sous des températures plus élevées peut influencer la source de C utilisée pour la production de GES. L'utilisation préférentielle d'une source C est fortement

déterminée par les bactéries (de fermentation) de dégradation de C parce qu'ils offrent les substrats nécessaires pour la méthanogènese (Valentine *et al.*, 1994). Ultimement, une augmentation des émissions de CH_4 peut arriver s'il y a une source de composées fermentables (Westermann *et al.*, 1989), ou une baisse d'activités méthanotrophiques.

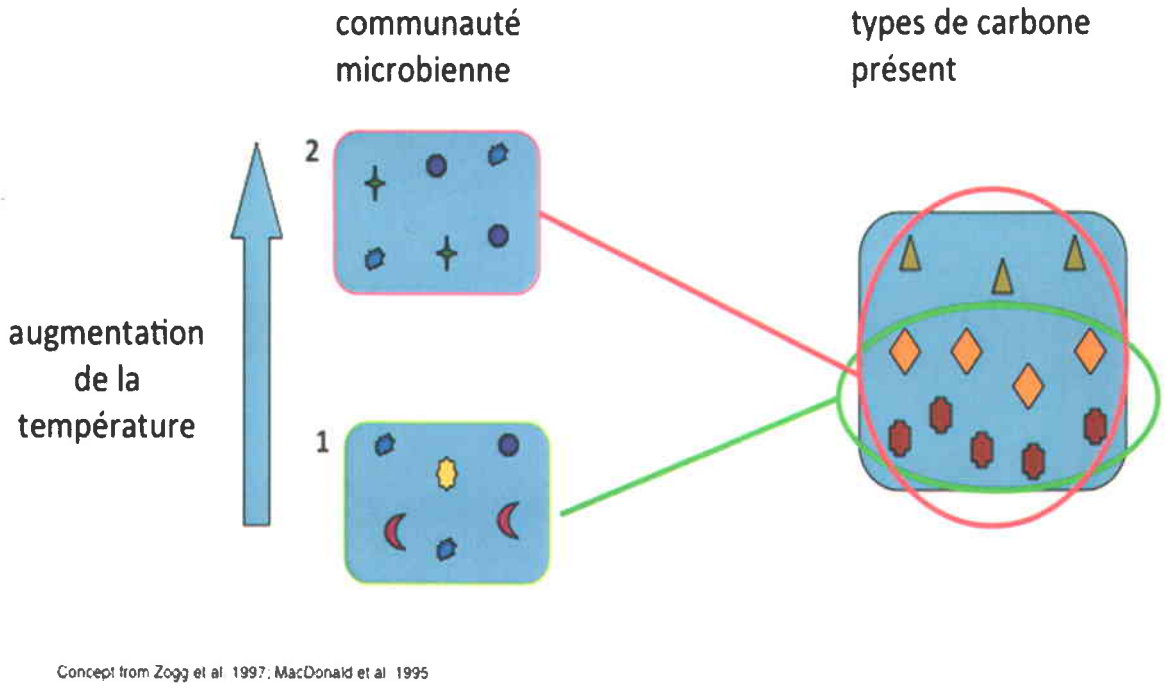

Figure 1.8 L'effet possible d'une augmentation de température sur le type de carbone utilisé par les bactéries et éventuellement utilisé pour produire les GES.

En tout il y a trois facteurs principaux à considérer afin de prévoir la production future de GES et de mieux comprendre les causes de sa variabilité parmi les mares de dégel, et ceci sera traité dans cette thèse : les sources de carbone utilisées pour la production de GES, l'identification de la communauté microbienne présente en termes de production de GES, et comment la communauté bactérienne et la production de GES peuvent répondre à les augmentations de température.

1.2 Site d'étude

L'île Bylot est située dans le pergélisol continu de l'Arctique canadien, nord de l'île de Baffin. L'échantillonnage a eu lieu au parc national Sirmilik dans une vallée pro-glaciaire à 73° 09'N, 79° 59'W (Fig. 1.9). La station de recherche et la station météorologique (station du réseau SILA du Centre d'études nordiques) ont enregistré de 1994 - 2007 une température annuelle moyenne de -14.5°C et une précipitation de 94 mm de juin à aout. Le paysage caractérisé par les polygones de la vallée étudiée s'est caractérisé par une unité de tourbe d'une épaisseur de ~ 2.5 m, avec une couche active de 40 cm en 2002 (Fortier & Allard 2004) et jusqu'à 60 cm en 2012 (D. Fortier, comm. pers.). Entourant les mares de dégel se retrouve une végétation comprenant des carex, des gazons et des mousses brunes. Les mares de dégel de l'île Bylot ont été qualifiées comme étant riches en CO et en nutriments, et des émetteurs significatives de CH_4 et occasionnellement de CO_2 (Breton *et al.*, 2009; Laurion *et al.*, 2010).

Les mares de dégel au site d'étude peuvent être catégorisés en deux groupes de formations géomorphologiques nommés mares polygones et mares *allongées*. Les deux gèlent jusqu'au fond en hiver, avec des thermisteurs de 2008 - 2009 indiquant l'eau libre pour ~111 jours par an. Les mares *allongées* se forment sur des coins de glace en fonte avec des profondeurs souvent moins que 0.5 m (Fig. 1.10). Elles sont devenues plus apparentes dans les dernières années à cause du dégel accéléré du pergélisol, probablement responsable de l'érosion du sol observé dans ces mares. Les mares polygones sont des environnements plus stables associés naturellement avec les cycles de gel-dégel de la couche active, avec des profondeurs de 0.5 à 1.5 m (Fig. 1.11). La structure thermique de la colonne d'eau est différente selon la formation de la mare. Les mares *allongées* sont stratifiées, avec BYL28 ayant une thermocline à 0.2 m en 2009. Les mares polygones ont une structure thermique homogène, ainsi qu'une topographie à l'abri du vent et à fetch légèrement plus forte (Laurion & Mladenov 2013). Ainsi une différence de production de GES entre ces deux formations de mares pourrait expliquer une partie de la variabilité reporté dans ces systèmes de pergélisol, en plus a localisation de domaines d'intérêt pour des efforts futurs.

La vallée pro-glaciaire étudiée a une aire de ~65 km^2, dont les mares de dégel et les lacs couvrent 4.2 % (Bégin, 2012). À ce site d'étude, il y a des endroits où soit les mares polygone, soit les mares *allongées* dominent, et où les deux sont présentes (Figure 1.12). Les mares *allongées* contribuent environ 44% de l'aire de surface d'eau libre, avec une formation commune de réseaux peu profonds mais allongés.

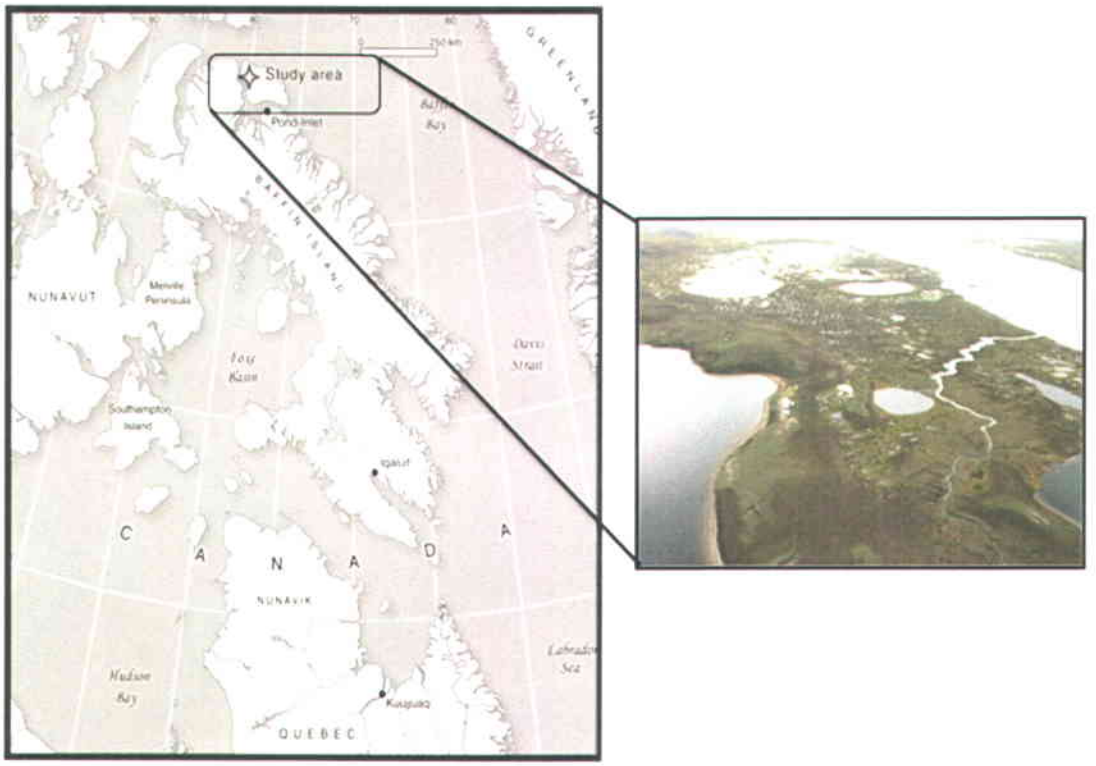

Figure 1.9 Une carte illustrant la localisation du site d'étude à l'île Bylot, Nunavut, Canada, et une vue aérienne du site d'étude de la vallée proglaciaire

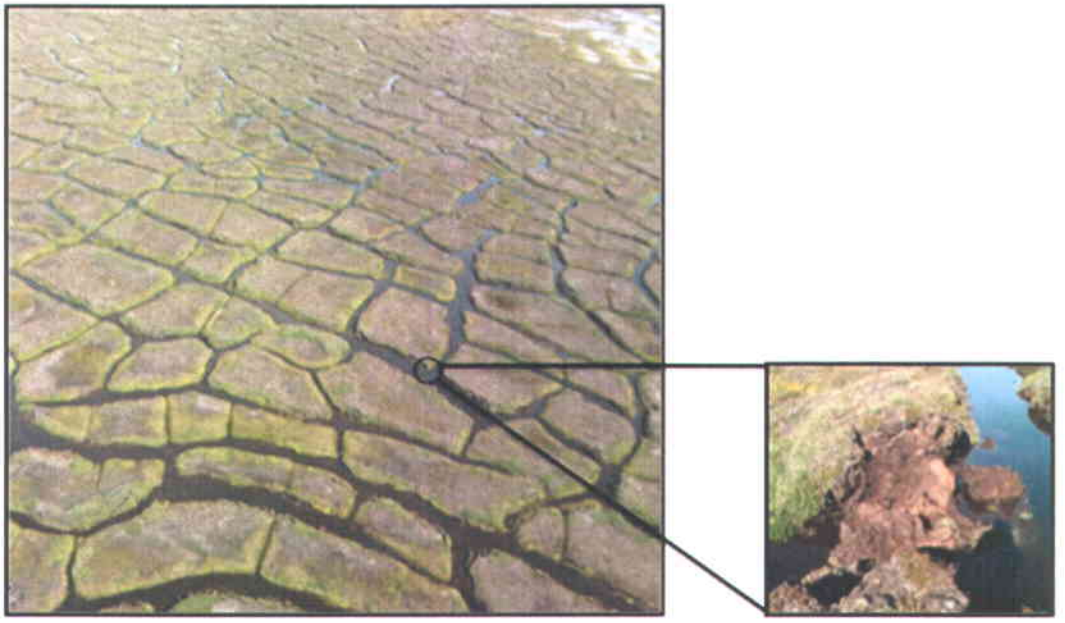

Figure 1.10 Des paysages de pergélisol dominés par des mares de dégel *allongées*, avec de l'érosion.

Figure 1.11 Des paysages de pergélisol dominés par des mares de dégel polygone

Figure 1.12 Paysage (polygone) de pergélisol ayant à la fois les mares polygone ainsi que les mares *allongées*

1.3 Objectifs et Hypothèses

L'objectif global de cette thèse était de déterminer si les petites mares de dégel dans l'Arctique de l'Est canadien ont le potentiel d'agir comme un mécanisme de rétroaction positive sur le réchauffement du climat. Les trois chapitres qui constituent le coeur de la thèse sont résumés et reliés les uns aux autres en se référant à la Figure 1.4. Dans le chapitre 1, l'utilisation de MO libéré de la fonte du pergélisol et utilisé pour la production de GES est adressée. Ici l'accent est mis sur la production et méthanogènes CH_4. Dans le chapitre 2, la communauté bactérienne et leur rôle commun dans la production de GES est décrit. L'effet d'une augmentation de la température a sur la production de GES dégel de l'étang et de la communauté bactérienne associée est présenté au chapitre 3. Ensemble, ces trois chapitres permettent de mieux comprendre le rôle des mares de dégel en tant qu'acteurs de retroaction.

Chapitre 1. Les petites mares de dégel: une source non comptabilisée de méthane dans le haut Arctique canadien

Objectifs

1) Décrire la communauté méthanogène des mares de dégel polygonales et *allongées* à l'île Bylot et comment elle se compare à celle des autres environnements de pergélisol tels que la tourbe gelée et les milieux humides arctiques.

2) Identifier si la méthanogénèse acétoclastique (MA) et/ou la méthanogénèse hydrogénotrophique (MH) produisent le CH_4 relâché par diffusion et par ébullition dans les mares de dégel de l'île Bylot.

3) Déterminer si les méthanogènes utilisent le vieux C provenant de la tourbe déposée au cours de l'Holocène et libéré par le dégel du pergélisol ou plutôt le C récemment fixé par les plantes ou les cyanobactéries.

4) Déterminer si les flux d'ébullition sont plus importants que la diffusion dans les petites mares de dégel de l'île Bylot, tel que reporté dans le cas des lacs thermokarstiques de plus grande taille en Sibérie et en Alaska.

5) Comparer les caractéristiques limnologiques et les communautés méthanogènes des mares polygonales et des mares *allongées*, étant donné que ces dernières augmenteront probablement dans le futur proche en raison du réchauffement climatique accéléré.

Hypothèses

1) Les communautés méthanogènes trouvées dans les mares de dégel de l'île Bylot sont uniques comparativement aux autres milieux de pergélisol.

2) Les communautés méthanogènes des mares polygonales et allongées sont distinctes.

3) Les voies de production du CH_4 (AM ou HM) transporté par diffusion et ébullition sont distinctes dans mares de dégel de Bylot.

4) Les mares allongées, avec l'érosion de la tourbe, utilisent une source plus ancienne de carbone pour la production de GES par rapport aux mares polygonales.

Chapitre 2. Influence des communautés fonctionnelles de bactéries sur les émissions de gaz à effet de serre par les petites mares de dégel du haut Arctique canadien

Objectifs

1) Déterminer si la géomorphologie des mares de dégel, et les propriétés physicochimiques associées, influencent les assemblages bactériens.

2) Déterminer s'il y a une différence entre les communautés bactériennes des sédiments de surface et celles qui colonisent la colonne d'eau des mares de dégel.

3) Déterminer une différence dans la diversité fonctionnelle des communautés bactériennes explique la différence des efflux de GES observée entre les mares *allongées* et polygonales.

Hypothèses

1) La géomorphologie des mares de dégel, et les propriétés physicochimiques associées, influencent les communautés bactériennes de l'eau et des sédiments de surface.

2) Les communautés bactériennes distinctes retrouvées dans les mares de dégel *allongées* et polygonales expliquent leurs différentes émissions de GES.

Chapitre 3. La réponse des mares de dégel du haut Arctique canadien à une hausse de la température: communautés bactériennes selon l'ADN et l'ARN et taux de production des gaz à effet de serre

Objectifs

1) Déterminer si la production de CO_2 et de CH_4 des mares polygonales et *allongées* réagit de façon similaire sous des conditions plus chaudes.

2) Identifier si le temps entre la récolte d'échantillons (*in situ*) et le début des expériences d'incubation (T1) affecte les communautés bactériennes totales (ADN) et le potentiel de synthèse des protéines (ARN).

3) Déterminer si les communautés bactériennes réagissent à une augmentation de température de 5°C par une modification de la communauté (ADN) ou une augmentation de l'activité de synthèse des protéines (ARN).

4) Identifier comment les changements de la communauté bactérienne d'une mare *allongée* fortement productive peuvent être liés à sa production de GES.

Hypothèses

1) Le taux de production de CO_2 et de CH_4 des mares polygonales et allongées augmente de façon similaire sous des conditions plus chaudes.

2) Le court délais entre le prélèvement des échantillons (*in situ*) et le début des expériences d'incubation (T1) affecte la communauté bactérienne active (ARN), mais pas la communauté totale (ADN).

3) Une augmentation de 5°C en température favorise à la fois une augmentation de la diversité des communautés bactériennes totales et actives, de sorte que la production de GES est accélérée.

1.4 Matériel et méthode

Voici un bref survol de la méthode d'échantillonnage effectué. Chaque chapitre présentera les détails techniques, mais ici se retrouve l'approche scientifique utilisée pour répondre aux objectifs de la thèse. Les méthodes ne sont pas divisées en chapitres, parce que plusieurs des méthodes ont été appliquées à tous les chapitres. L'échantillonnage pour cette thèse a été limité aux mois d'été (Juin - Aout), comme le dur climat de l'Arctique limite l'accès à la station de recherche à quelques mois d'été (Table 1.1).

Tableau 1.1 Sommaire des échantillons de mare de dégel présentées dans cette thèse. POL = mares polygone; RUN = mares *allongées*; COD=carbone organique dissous; GES incluent CO_2 and CH_4; l'ébullition inclut CH_4 relâché en bulles; la voie de production inclut CH_4 produit par méthanogénèse acétoclastique (MA) ou méthanogénèse hydrogenotrophique (MH); CO=carbone organique ; MODC=matière organique dissoute colorée.

		Year	Total ponds (POL: RUN)	Method
Dissolved GES	GES flux	2009 - 2011	92 (33: 58)	Concentrations dissoues
	Production pathway	2009	19 (9: 10)	Isotopes stables
	Diurnal variations	2011	2 (2 POL)	Mesures de flux à l'heure
Ébullition	Ébullition flux	2011	2 (2 POL)	Entonnoirs
	Production pathway	2011	4 (2: 2)	Isotopes stables
	C-source (age)	2011	4 (2: 2)	Datation ^{14}C
Microbial Diversity	Archaea de sédiment de surface	2009	4 (2: 2)	Pyro-séquençage
	Bactérie de sédiment de surface	2009	5 (2: 3)	Pyro-séquençage
	Bactérie de l'eau	2009	5 (2: 3); 2 (1: 1)	Pyro-séquençage & Libraires de clonage
Environnement	Limnologie	2009 - 2011	17 (9: 8)	Nutriments, pH, temp, O_2
	Source de C de l'eau	2009 - 2011	17 (9: 8)	Quantité & composition de MODC
	Source de C du sédiment	2011	17 (9: 8)	% CO
Incubations	Taux de production GES	2009 - 2010	4 (2: 2)	Over 16 days at 4°C and 9°C
	Communauté total de bactérie sédimentaire	2010	1 (1 RUN)	Pyro-séquençage *in situ*, t_0, t_{16}-4°C and t_{16}-9°C
	Synthèse des protéines potentiel des sédiments communauté bactérienne	2010	1 (1 RUN)	Pyro-séquençage *in situ*, t_0, t_{16}-4°C and t_{16}-9°C

1.4.1 Les propriétés physicochimiques et l'échantillonnage de GES

Les propriétés limnologiques des mares de dégel ont été échantillonnées afin d'examiner les relations entre les communautés microbiennes des mares polygone et *allongées*. La température, l'O_2 dissous, la conductivité et le pH ont été mesurés par Yellow Spring Instrument (YSI, 600R sonde multiparamétrique). Le phosphore total (PT), l'azote total (AT), le phosphate réactif soluble (SRP), les cations, et les anions ont aussi été mesurés chaque année.

Les concentrations de GES dissous ont été récoltées sur trois ans (2009 - 2011) pour cette thèse. À partir des concentrations dissoutes, un flux correspondant a été estimé selon la loi de Fick utilisant le modèle basé sur le vent de Cole et Caraco (1998) afin de calculer le coefficient de l'échange de gaz, avec un facteur de correction développé à partir d'une série de mares où le flux direct des mesures a pris avec une chambre flottante. Le facteur de correction tient compte que la turbulence est contrôlée par une échange de chaleur plutôt que par le vent dans les petites mares de dégel et donc la turbulence est plus faible comparée aux estimées obtenues par des modèles basées sur uniquement sur le vent (MacIntyre *et al.*, 2010). En plus des mesures de flux dissous, le flux d'ébullition a aussi été obtenu de deux mares polygone en 2011, avec des entonnoirs immergées (Figure 1.13). Les taux d'ébullition ont été mesurés par une accumulation passive des gaz dans les entonnoirs inversé immergées sur une période de 21 à 121 heures, tandis qu'un flux dissous est toujours estimé à partir d'un échantillon discret de gaz et calculé à partir d'un modèle de transfert de gaz qui utilise la vitesse du vent des deux heures précédentes. La grande variabilité de turbulence au cours d'une journée pour les estimées de flux diffus combinée avec la large variabilité spatiotemporelle des évènements d'ébullition (Walter *et al.*, 2010) excluent des extrapolations simples.

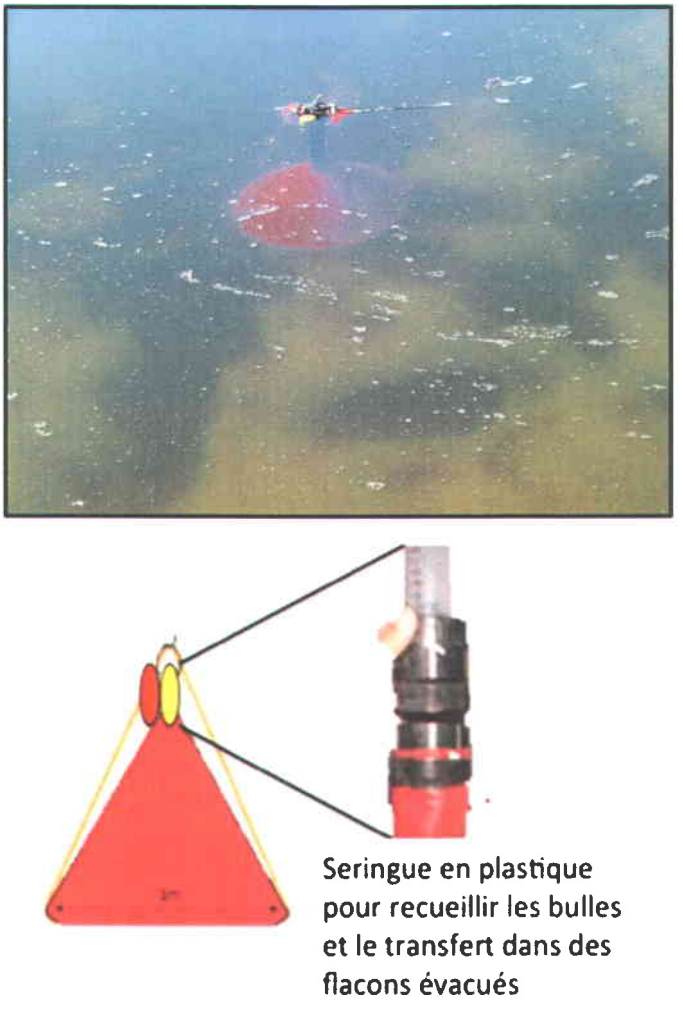

Figure 1.13 Entonnoir immergé utilisé pour prélever les échantillons d'ébullition flottant au delà de la glace toujours présente au fond des mares de dégel tôt en juillet 2011

Afin d'investiguer les cycles du C et du CH_4 dans les mares de dégel, les signatures isotopiques $\delta^{13}C$ et $\delta^{2}H$ ont été mesurées sur les échantillons de GES dissous et d'ébullition. Ces signatures ont permis de déterminer quelles voies métaboliques ont servi à la production de CH_4, la méthanogénèse acétoclastique ou la méthanogénèse hydrogénotrophique (MA ou MH). De plus, ces valeurs permettent de déterminer le niveau d'oxydation du CH_4 ainsi que la provenance possible des sources de C. Par exemple, un faible enrichissement en $\delta^{13}C$ indique une faible oxydation et une source de CH_4 provenant du benthos (bulles), tandis qu'un enrichissement plus élevé en $\delta^{13}C$ révèle une source pelagique (dissous) (Kendall & McDonnel 1998). Ces signatures isotopiques sont utiles pour identifier des voies métaboliques (AM ou HM) mais ne fournissent pas de renseignements sur les limites de la disponibilité du substrat ou des pourcentages exacts pour chaque voie de production (Alstad and Whiticar 2011). La datation

par radiocarbone a aussi été appliquée aux GES d'ébullition pour déterminer si le C plus ancien relâché par le pergélisol en dégel est utilisé par les microbes pour la production de GES, et si ce processus diffère entre les mares polygonales et *allongées*.

En plus de l'utilisation des isotopes stables, les propriétés d'absorption et de fluorescence de la matière organique dissoute chromophorique (MODC) ont été utilisées pour caractériser une fraction du CO utilisé par des microbes des mares de dégel. Les échantillons d'eau filtrés à travers 0.2 μm ont été scannés par un spectrophotomètre et un spectrofluoromètre (détails plus bas). La courbe du spectre d'absorption de MODC qui en résultait peut être utilisée pour estimer le ratio d'acides fulviques à humiques et corréler le poids moléculaire de la MOD (Helms *et al.*, 2008, Holmes *et al.*, 2008), tandis que le coefficient d'absorption de la MOD (e.g. à 320 nm, a_{320}) est utilisé pour quantifier la MODC, ou l'efficacité d'absorption de la MOD lorsque donné par unité de carbone organique dissous (COD) (Breton *et al.*, 2009).

1.4.2 Les communautés microbiennes

Les communautés d'archées et des bactéries ont été examinées en ciblant les gènes 16S ARNr utilisant de l'acide désoxyribonucléique (ADN) comme un template. Ces communautés d'ADN ont été examiné de l'eau de surface et du sédiment des mares polygone et *allongées* ponds avec du pyro-séquencage haut débit. Le ciblage et le séquençage les gènes 16S ARNr utilisant de l'acide ribonucléique (ARN) bactérien ont été également utilisés pour explorer le potentiel de synthèse des protéines de la communauté des sédiments bactériennes. En termes plus simples, une communauté ARN est souvent désignée comme la communauté «active» par rapport à la communauté ADN qui représente toutes les bactéries présentes. Toutefois, les données d'ARN ne représentent pas seulement les ribosomes actifs pour la synthèse des protéines, mais aussi des ribosomes inactifs (Blazewicz *et al.*, 2013).

Tandis qu'un sous-ensemble plus large de 20 mares de dégel ont été investigués pour leurs propriétés physicochimiques et leurs flux de GES, quatre mares ont été choisies pour étudier en détails les communautés microbiennes. Initialement ces quatre mares ont inclut deux mares polygone (BYL 1 & 22) et deux mares *allongées* ponds (BYL24 & 38). Les communautés archées ont été étudiées en particulier dans le sédiment, où les méthanogènes anoxiques sont souvent limités. Les communautés bactériennes impliquées dans la respiration hétérotrophique pélagique, la respiration sédimentaires, et l'oxydation de CH_4 oxydation ont été investiguées

dans l'eau de surface ainsi que dans le sédiment par clonage par Séquençage Sanger et par le pyro-séquençage haut débit.

La technologie relativement nouvelle du pyro-séquençage haut débit, comparée à les clonages par Séquençage Sanger, est devenue plus présente au début de ce projet. Le pyro-séquençage est bénéfique en raison de sa capacité de générer un grand nombre de séquences (reads; fragments de séquences courtes) utilisé pour les identités microbiennes de taille intermédiaire (Margulies *et al.*, 2005). Par exemple, dans cette étude ~2,000 reads ont été produits par échantillons, comparés à une librairie de clonage par Séquençage Sanger qui en produit ~90 séquencés, selon les efforts de clonage. Ceci permet une vision beaucoup plus détaillée de la communauté microbienne, ainsi que l'identification des micro-organismes abondants (≥ 1% de la communauté entière) et rares (< 1% de la communauté entière). Le pyro-séquençage permit donc une augmentation du pouvoir statistique pour une description de la communauté microbienne et une approfondissement des connaissances de l'importance écologique d'une communauté écologique.

Brièvement, le pyro-séquençage avec la technologie Roche 454 est effectué avec des fragments ciblés d'ADN bactériennes ou archéales amplifiés avec une réaction en chaîne polymérase (PCR) (Fig. 1.14 a) et chaque fragment étant capturé sur une perle unique (perle d'émulsion). Chaque perle est recouverte d'huile d'émulsion où la PCR contenue a lieu. Le résultat est que chaque perle a des millions de matrices uniques d'ADN (Fig. 1.14 b). L'huile d'émulsion est brisée et chaque perle tombe dans un puits (Fig. 1.14 c). Une fois dans le puits, une série de bases (A, T, G, C) est lavée sur la plaque de puits, et quand une base complémentaire est présente la synthèse a lieu par une réaction chimique qui cause produit une émission de lumière (Margulies *et al.*, 2005). Le terme "pyro" séquençage provient du fait que les intensités lumineuses, produite à partir de l'enzyme de pyrophosphate (PPi), servent pour la détermination de la séquence d'ADN. La différence méthodologique apparente entre le pyro-séquençage et le clonage par Séquençage Sanger est qu'aucun sous-clonage à l'intérieur des bactéries ou manipulation fastidieuse des clones individuels n'est employé avec le pyro-séquençage.

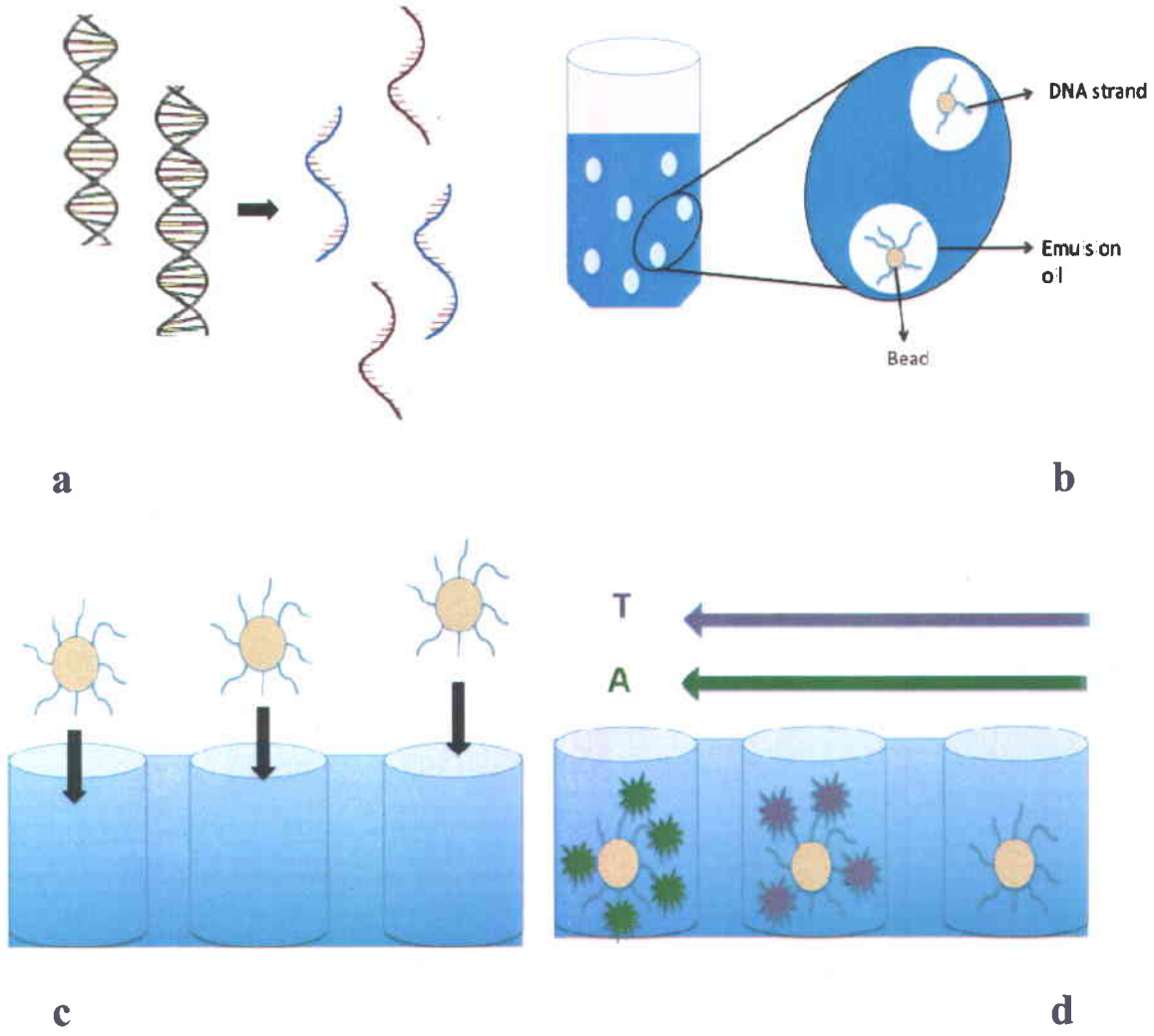

Figure 1.14 Processus de pyro-séquençage a) séparation des fragments individuels d'ADN attachés à une perle; b) perle couverte en huile d'émulsion où l'amplification de PCR a lieu; c) le placement de chaque perle dans un puits sur une plaque à plusieurs puits; d) lavage de bases sur la plaque pour déterminer la séquence d'ADN individuel de chaque souche capturée sur une perle.

Malgré que la technologie de pyro-séquençage progresse rapidement, une contrainte est son amplification de reads plus courts (des séquences plus courtes) en comparaison avec le clonage par Séquençage Sanger. Le contrôle de qualité élimine des reads contenant moins de 150 paires de base. Comparativement les séquences de de clonage par Séquençage Sanger ont un minimum de 500 paires de base, ce qui a donné des identités microbiennes plus précises, et donc cette méthode est toujours utile en ce moment. Deux libraires de clonage bactérien ont été effectués dans le cadre de cette étude pour comparer les identités bactériennes entre deux méthodes.

1.4.3. Expériences d'incubation

La réponse des taux de production de GES des mares de dégel et la communauté bactérienne à une température accrue ont été déterminée par des incubations sur 16 jours à la température moyenne de l'été (Juin - Aout) mesurée actuellement à l'île Bylot (4.6°C) (Fig. 1.15) et la température augmentée de 5°C (9°C) pour stimuler l'augmentation de température prévue pour les régions polaires à la fin du 21ème siècle (IPCC AR4 WG1, 2007). Une incubation d'une durée de 16 jours a été choisie sur la base d'une incubation précédente sur 28 jours, où la production de CO_2 a atteint un plateau après 18 jours (Figure 1.16).

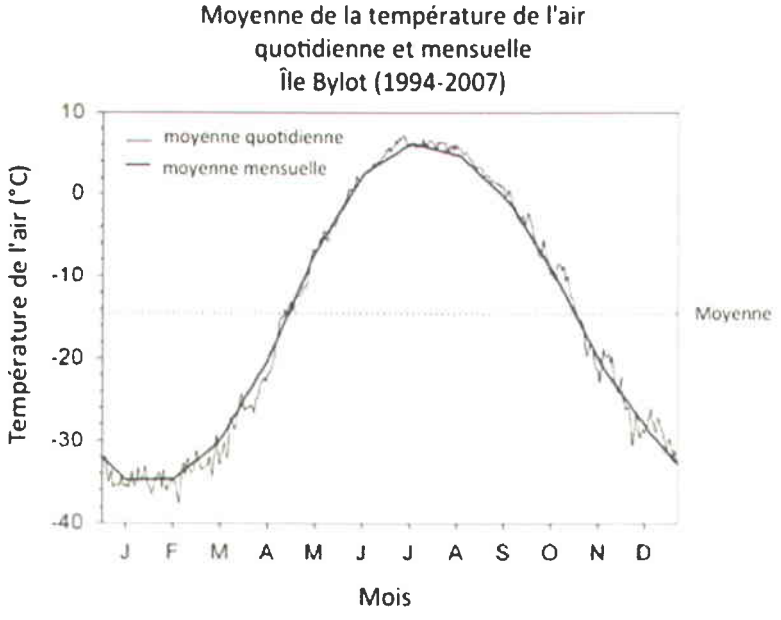

Figure 1.15 Les températures moyennes mensuelles et quotidiennes de l'île Bylot. Graph de Ecological studies and environmental monitoring at Bylot Island, Sirmirlik National Park (http://www.cen.ulaval.ca/bylot/intro.htm).

Les mesures de GES et des communautés microbiennes sédimentaires sont investiguées ici, étant donné que c'est où la majorité des méthanogènes et des méthanotrophes a été identifiée selon les résultats du chapitre 1 & 2. Les communautés bactériennes ont été identifiées par le pyroséquençage de 16S rARN ADN et ARN pour comparer les communautés totales et le potentiel de la synthèse des protéines respectivement. L'amplification de l'ADN et l'ARN archée a été tentée plusieurs fois sans succès. L'amplification qui n'a pas fonctionnée peut probablement être attribuée à la distribution spatiale ou l'abondance étant donné que ça a été essayé avec plusieurs échantillons de sédiment et que BYL38 est plus grand producteur de CH_4. Une interférence en raison de la matière organique (MO) pourrait être possible parce que BYL38 a le plus de MO comparé aux autres mares. Idéalement une autre expérimentation avec des échantillons pris pour l'identification microbienne de la mare *allongée* BYL27 aurait été utile, mais aucun tel échantillonnage de l'Arctique n'a été possible.

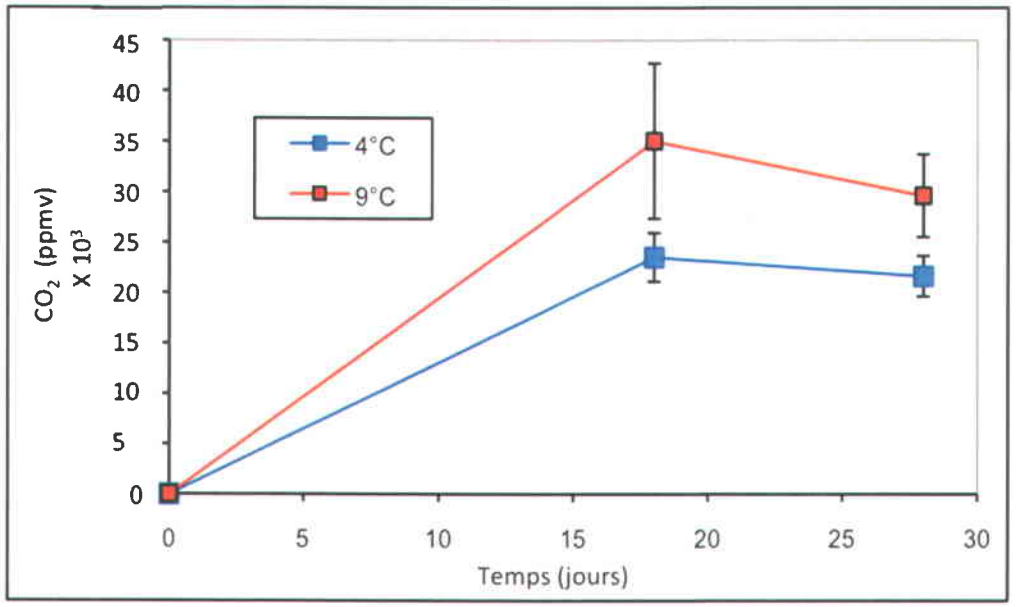

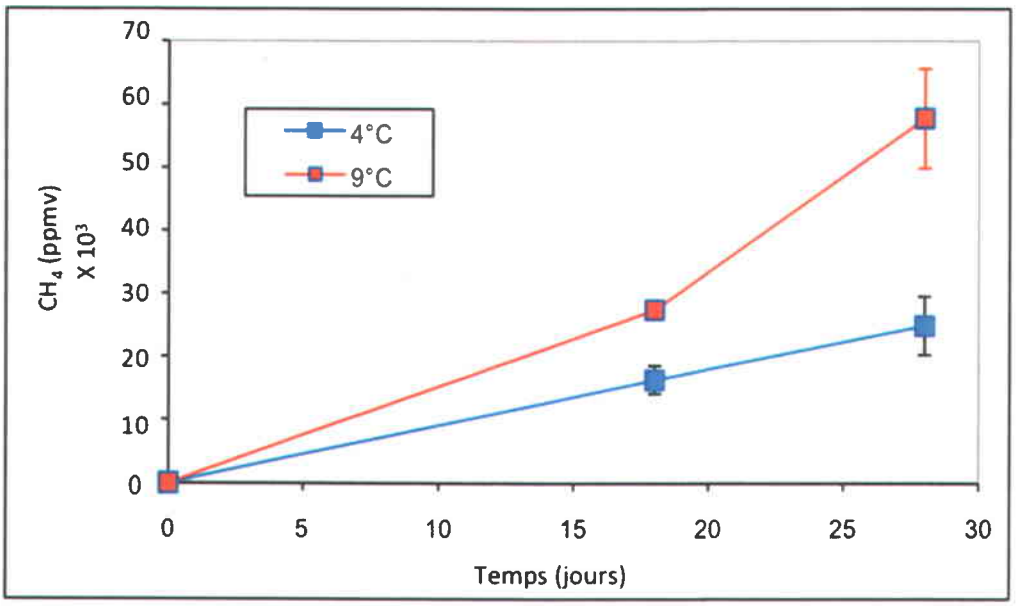

Figure 1.16 Des résultats de l'expérimentation préliminaire de la production GES à 4°C et à 9°C, indiquant un plateau de production de CO_2 autour de 18 jours et une production continue de CH_4.

1.5 Résultats et discussion

Cette section comprend un résumé des résultats les plus significatifs. Pour plus de résultats, et des figures et tableaux appuyant ces résultats et cette discussion, veuillez consulter les articles correspondants qui suivent aux chapitres 2, 3 et 4.

1.5.1 Article 1

Les concentrations de GES dissous à la surface de l'eau et les estimations de flux correspondants recueillies pour les séries compilées de mares de dégel de 2009 à 2011 (n = 91) ont été significativement plus élevées dans les mares *allongées* comparés aux mares polygonales (t-test, df = 90, $p < 0.001$). Cette séparation hautement significative entre les formations *allongées* et polygonales est marquante considérant la grande variabilité dans les flux de CO_2 (-8.1 à 76.9 mmol m^{-2} d^{-1}) et de CH_4 (0.02 to 6.3 mmol m^{-2} d^{-1}) sur 3 ans.

Deux mares polygonales testées sur 26 heures montraient respectivement des variations (coefficient de variation) diurnes de GES dissous de 18 et 25% dans le cas du CO_2, et de 17 et 21% pour le CH_4. Les flux correspondants estimés par le modèle basé sur le vent (coefficient d'échange gazeux de Cole et Caraco 1998) indiquent que les mesures de flux variaient au maximum par 25% au cours de la journée. Pour ce qui est de l'ébullition mesurée dans les deux mares polygonales, respectivement 27 et 82% des émissions totales en CH_4 provenaient de l'ébullition. Ces valeurs illustrent la grande variabilité des taux diffusifs et d'ébullition pouvant exister dans les petites mares de dégel sur l'île Bylot.

La source de C pour la production de GES émis sous forme de bulles a été catégorisée comme moderne (les derniers ~60 ans), avec des signatures $\Delta^{14}C$ de -1.1 à 114.9 ‰. Par contre, l'ébullition de CH_4 de deux mares *allongées* (n = 3 mesures) contenait une fraction significativement plus élevée de C ancien comparé aux deux mares polygonales (n = 7 mesures; $p = 0.002$). Les signatures d'isotopes stables du CO_2 et CH_4 indiquent que le CH_4 a été produit par méthanogénèse acétoclastique, et ainsi que le substrat d'acétate est abondant dans l'écosystème, au moins lors des mesures estivales. La méthanogénèse hydrogénotrophique, utilisant le CO_2 et le H_2, domine généralement lorsque le C est limitant (Hornibrook *et al.,* 2000). La dominance de MA a été observée tant pour les mares polygonales

qu'*allongées*. Cette tendance est différente que celle observée dans d'autres écosystèmes arctiques (Brosius et al., 2012).

Tandis que les isotopes stables indiquent une dominance par la MA (juin-juillet), les résultats suggèrent que la communauté des Archées des sédiments de surface était composée à la fois d'unités taxonomiques opérationnelles (UTOs, définis au niveau de similarité de 97%) MH et de UTOs MA (en proportion similaire). Étant donné que le pyro-séquençage a été effectué sur l'ADN, il inclut les microbes inactifs ainsi que ceux actifs. Ce résultat indique qu'à un certain moment dans l'année, les conditions étaient favorables pour bâtir une biomasse significative d'UTOs MH, et donc que l'hydrogénotrophie existe (ou a existé) dans cet écosystème. Par ailleurs, le pyro-séquençage indique que la communauté des Archées des sédiments de surface était dominée par des méthanogènes, représentant 88 à 95% des séquences. Les autres UTOs du domaine des Archées étaient représentées par le phylum Euryarchaeota, surtout d'un groupe euryarchaéotal aléatoire (TMEG), et du groupe crénarchaéotique aléatoire (MCG).

En conclusion, les mares *allongées* représentent une source de CH_4 plus grande et potentiellement produite à partir d'un pool de C plus ancien comparées aux mares polygonales, et elles contiennent des communautés méthanogéniques capables d'utiliser diverses sources de C, augmentant le risque d'émissions accrues de CH_4 sous les conditions changeantes du climat.

1.5.2 Article 2

Les communautés de bactéries des sédiments et de l'eau étaient très différentes, même au sein d'une mare donnée, avec peu d'UTOs partagées. Une analyse en composantes principales sur les propriétés physicochimiques (COD, propriétés optiques de la MOD, O_2, pH, ions, nutriments et température) a expliqué 53% de la variance entre les mares (n = 19) et a distinctement séparé les mares polygonales des mares *allongées*, correspondant au cloisonnement noté dans les communautés bactériennes sédimentaires mais pas dans le cas des communautés bactériennes de l'eau. Les communautés bactériennes des sédiments présentaient une richesse spécifique plus élevée, avec une faible diversité (équitabilité des valeurs), par comparaison avec les communautés de l'eau.

Autre détail intéressant, nous avons détecté une relation négative significative entre les concentrations de CH_4 dissous et le nombre de séquences des méthanotrophes des sédiments ($r = -0.895$, $p = 0.040$), mais aucune corrélation significative avec les méthanogènes, indiquant un fort contrôle des émissions de CH_4 par les consommateurs de CH_4, et ce malgré la faible profondeur de cet écosystème. Le degré d'oxydation du méthane variaient entre les mares, tel qu'indiqué par les signatures $\delta^{13}C\text{-}CO_2$ variant de -13 à -37‰. Cette signature isotopique était aussi correlée au nombre de séquences des méthanotrophes ($r = -0.927$, $p = 0.024$).

De ces résultats, nous pouvons spéculer que les différences de concentration de GES dans la colonne d'eau sont régit par les facteurs physicochimiques qui sélectionnent différents assemblages de producteurs et de consommateurs de CH_4 dans les sédiments, alors que les régimes thermiques et la turbulence variable dans les mares influencent le taux auquel les GES sont relâchés vers l'atmosphère.

1.5.3 Article 3

Au cours d'une incubation de 16 jours des sédiments provenant de 2 mares polygonales et 2 mares *allongées*, les taux de production de CO_2 et de CH_4 ont tous deux significativement augmenté à 9°C par rapport à 4°C ($p \leq 0.05$). Les mares *allongées* avaient un taux de production de CO_2 significativement plus élevé que les mares polygonales ($p = 0.002$), mais pas un taux de production plus élevé en CH_4 ($p = 0.606$). Sous les conditions expérimentales avec peu d'O_2 et dépourvues en lumière, où la photosynthèse ne pouvait se produire, la production de CO_2 inférieure des mares polygonales peut être attribuée à une respiration microbienne limitée. Ce résultat supporte les observations *in situ:* le CO_2 était sous-saturé dans les mares polygonales et sursaturé dans les mares *allongées*, indiquant une respiration microbienne inférieure dans les mares polygonales et/ou une plus grande consommation en CO_2 dans cet écosystème riche en tapis photosynthétiques cyanobactériens, représentant un puits de CO_2 atmosphérique.

Par comparaison, les résultats sur la production de CH_4 provenant de l'expérience d'incubation ne sont pas *a priori* compatibles avec les tendances observées *in situ*. Expérimentalement, les mares polygonales montraient une production de CH_4 supérieure ou similaire à celle des mares *allongées*, alors qu'*in situ,* les émissions de CH_4 des mares polygonales étaient en moyenne 3.6 fois inférieures à celles de mares *allongées*. Par contre, les conditions expérimentales, sans lumière pour la photosynthèse et sans mélange thermique résultant en de très faibles concentrations en O_2, peuvent certainement avoir pu inhibé l'oxydation du CH_4 par les méthanotrophes et l'oxydation chimique. En effet, une abondance faible et constante des taxons méthanotrophes (4,2-4,8%) était observée tout au long de l'expérience. Par conséquent, il semble que les mares polygonales et *allongées* avaient un taux de production de CH_4 similaire, mais l'activité *in situ* des méthanotrophes dans les mares polygonales (riches en O_2 dû au mélange thermique et à l'activité photosynthétique plus élevés) a réduit ses émissions, ce qui ne se produisait pas sous les conditions expérimentales. Les Archées méthanogènes n'ont pas été séquencées dans cette expérience (échec d'amplification), mais un symbiote méthanogène, *Geobacteraceae*, était plus abondant à 9°C qu'à 4°C à la fois dans l'ADN et l'ARN. L'occurrence de l'augmentation de la production de CH_4 et une augmentation d'un symbiote méthanogène suggèrent ensemble que l'activité des taxons méthanogènes a probablement aussi augmenté à 9°C.

La mare *allongée* BYL38 avait des communautés bactériennes moins différentes entre les échantillons *in situ* et T1 qu'entre T1 et T16 (analyse des similitudes ANOSIM; r=-1, p=1). Un positionnement non métrique multidimensionnel (NMDS en anglais; voir les résultats du chapitre 3 pour la figure) confirme la forte similarité au sein des communautés d'ADN *in situ* et T1, ce qui suggère que les manipulations des échantillons de sédiments pour établir l'expérience n'ont pas affecté de manière excessive la communauté bactérienne totale. Après 16 jours d'incubation, il y avait en moyenne 30,9% de différence entre les communautés à 4°C et à 9°C. La majorité de la dissemblance (86,5%; SIMPER) a été attribuée aux phyla associés à la dégradation du C, qui contribuent aussi à plus de 64% de la communauté totale. La communauté ARN responsable de la dégradation du C avait une abondance relative inférieure à 9°C (65%) qu'à 4°C (71 %), accompagnée d'une augmentation de la diversité à 9°C. En fait, la composition des communautés ARN responsables de la dégradation du C était significativement différente entre les températures (p=0.009), mais la composition des communautés ADN ne l'était pas (p= 0.096). Plus précisément, la communauté ARN à 9°C a diminué en Bacteriodetes et augmenté en Alphaproteobacteria, Betaproteobacteria, Firmicutes, Acidobacteria, Verrucomicrobia, et

Actinobacteria. Cette communauté responsable de la dégradation du C plus diversifiée à une température plus élevée pourrait permettre la dégradation d'un pool plus large de C, éventuellement de moindre qualité, ce qui expliquerait la production plus élevée en CO_2 et CH_4 causée par un changement dans la composition des communautés plutôt qu'une augmentation de la productivité.

1.6. Limitations et travaux futurs

Des limitations causées par l'éloignement de l'échantillonnage en Arctique ont été rencontrées. Par exemple, les entonnoirs étaient trop larges pour être installés dans les mares *allongées*, limitant les mesures de flux d'ébullition aux mares polygonales. D'ailleurs l'accès à la station de recherche a été limitée à la période fin juin et juillet contraignant une investigation complète des émissions de GES pour l'ensemble de l'été (début juin à fin aout) et une comparaison entre les flux dissous et d'ébullition pour ces deux types de mares, pourtant nécessaire dans le cas de phénomènes aussi variables tel que démontré par plusieurs études.

Considérant la variabilité remarquable des GES et des propriétés physicochimiques des petites mares de dégel arctiques, l'échantillonnage d'un plus grand nombre de mares aurait été bénéfique. Ceci bien sûr est limité logistiquement par le temps d'échantillonnage et la main-d'œuvre disponible en Arctique. Deux cycles d'échantillonnage de GES de 26 heures ont été effectués pour les mares polygonales, rendant compte d'une partie de la variabilité temporelle, mais avec cet échantillonnage limité, aucune conclusion majeure ne peut être tirée. L'instrumentation des mares (par ex. mesures automatisées du CO_2, CH_4, O_2, température) serait souhaitable étant donné le niveau de difficulté associé à un échantillonnage à haute fréquence dans le Nord.

L'approche moléculaire ne nous a pas permis d'amplifier avec succès les Archées des sédiments de surface de la mare *allongées* BYL38, malgré diverses tentatives et une extraction d'ADN phénol:chloroforme, mais elles sont surement présentes en raison de la très haute production de CH_4 mesurée. BYL38 était une mare clef étudiée largement dans les années précédentes et lors de cette thèse. C'était aussi cette mare que nous avons choisie dans les expériences d'incubation pour le séquençage, et donc la raison pourquoi les Archées méthanogènes n'ont pas été présentées. L'application d'autres techniques de purification de l'ADN pourraient peut-être mieux fonctionner dans le cas de mares fortement chargées en

matière organique, potentiellement la cause de l'échec de cette amplification. De plus, l'identification de méthanogènes dans les sédiments à des profondeurs de plus de 5 cm pourrait être utile, étant donné que les communautés méthanogènes peuvent aussi varier avec la profondeur (Galand *et al.*, 2002), et la production de CH_4, surtout l'ébullition, peut avoir lieu plus profondément.

Les données recueillies et présentées ici ont généré plusieurs idées pour des travaux ultérieurs. La présence tant de MA que de MH révélée par les outils moléculaires, et comparée aux signatures isotopiques indiquant que seulement les MA étaient actives lors de l'échantillonnage, suggère que l'hydrogénotrophie existe dans cet écosystème mais n'était pas active au moment où nous avons échantillonné le CH_4. Par contre, une autre explication possible pourrait être un jeu d'amorces insuffisant laissant certaines archées MA non amplifiées et favorisant de façon biaisée les MH. Par exemple, Conrad *et al.* (2007) n'a pas trouvé beaucoup de séquences MA dans un lac germanique (7% pour les sédiments supérieurs et aucun pour les inférieurs) même si les signatures isotopiques indiquaient 58% et 45% d'acétotrophie dans les sédiments supérieurs et inférieurs respectivement. Les auteurs ont reconnu la possibilité que le PCR quantitatif, l'électrophorèse en gel de gradient dénaturant (DGGE) et les outils de clonage utilisés (Ar109f - Ar915r) n'ont pas réussi à trouver toutes les archées MA dans leurs échantillons. Il est à noter cependant que notre étude a utilisé un jeu d'amorces différent que celui de l'étude de Conrad pour l'amplification de nos échantillons (969f -1406r). L'utilisation de différents jeux d'amorces d'archées semble aussi avoir produit des biais dans les séquences amplifiées résultantes dans l'étude de Comeau *et al.* (2012).

Malgré le fait que ces approches s'améliorent continuellement, des biais de séquençage par PCR sont communs, particulièrement pour les Archées, peut-être étant donné qu'on ne les connait pas depuis aussi longtemps. Elles ont été proposées comme faisant partie d'un domaine distinct dans les années 1990 (Woese *et al.*, 1990), mais c'est seulement lorsque le génome complet des Archées a été séquencé en 1996 (Bult *et al.*, 1996) que cette proposition a été acceptée dans le milieu scientifique. De plus, elles ont surtout été considérées comme des extrémophiles jusqu'à 2004 (Venter *et al.*, 2004), ce qui a entravé leur exploration. Ainsi la probabilité que des amorces ne ciblent pas toutes les Archées présentes pourrait être élevée, alors que les amorces spécifiques des bactéries ont été améliorées depuis 1990 (Ward *et al.*, 1990; Watanabe *et al.*, 2001; Nadkarni *et al.*, 2002). La démonstration de cette hypothèse exigerait cependant beaucoup plus de travaux moléculaires en raison de la nécessité de

développer de nouvelles amorces pour les Archées non-cultivées et non-identifiées. Avec l'utilisation de techniques autres que le clonage (c.-à-d. le pyro-séquençage) et disponibles pour le séquençage, de nouvelles amorces ciblant une gamme plus large d'Archées sont susceptibles d'apparaitre, et ainsi améliorer nos connaissances actuelles sur ces microorganismes jouant un rôle fondamental dans les écosystèmes.

Les expériences d'incubation ont aussi généré des questions intéressantes. L'augmentation continuelle de la production de CH_4 dans les microcosmes au fil du temps est-elle uniquement fonction de l'absence d'augmentation de l'abondance relative des méthanotrophes (ADN et ARN) sous les températures accrues, ou est-elle une réponse combinée avec l'augmentation du potentiel de synthèse des protéines méthanogéniques? Quoiqu'une augmentation d'activité par les méthanogènes devrait augmenter la production de CH_4 et ainsi le substrat pour les méthanotrophes. En fait, le faible pourcentage de méthanotrophes au départ (T1) suggère que «l'effet de bouteille» (*bottle effect*) a généré des conditions chimiques qui leur étaient défavorables (par ex. peu d'O_2 ou faible disponibilité de certains substrats), ou certains changements dans la composition de certaines autres bactéries impliquées dans le cycle du méthane. Ici les groupes fonctionnels devront être quantifiés par PCR quantitatif (Q-PCR) ou Hybridation in situ fluorescente (FISH) afin de différencier l'importance entre le potentiel de synthèse des protéines et l'abondance entre les méthanotrophes et les méthanogènes. L'utilisation de 2% de fluorure de méthyl (CH_3F) comme inhibiteur de la méthanogénèse acétoclastique (Janssen & Frenzel 1997), en comparaison avec des incubations non-inhibées, pourrait apporter des pistes de compréhension et faciliter la détermination des différents processus qui influencent la disponibilité des substrats.

1.7. Conclusions et contributions scientifiques

Récemment, quelques articles sur les cycles du C et les émissions de GES en Arctique ont été publiés, mais la plupart étaient axés sur les grands lacs thermokarstiques. Dans cette thèse j'ai étudié l'importance des petites mares de dégel (incluant les mares thermokarstiques telles que les mares *allongées*) comme des émetteurs de GES, ainsi que les processus impliqués dans les cycles de GES. Même si ces mares sont très nombreuses dans le paysage arctique, cette classe spécifique de systèmes aquatiques est généralement insuffisamment étudiée en raison de leur petite taille, nécessitant un échantillonnage spécifique. Cet échantillonnage a été accompli par l'investigation des liens complexes entre les émissions de GES, les communautés

microbiennes et les sources de C. Chacun de ces aspects est nouveau en soi pour cet écosystème sous étudié, mais de plus, cette thèse avait l'originalité de combiner ces trois aspects pour en arriver à des conclusions plus intégratives.

Un point fort de la thèse est la série de données sur les concentrations de GES et les flux calculées correspondants, mettant en évidence que les mares *allongées* sont des émetteurs significativement plus grands que les mares polygonales. Ces données soutiennent que les mares *allongées* sont une source non comptabilisée de CH_4 dans l'extrême Nord canadien, avec le potentiel de devenir plus abondantes dans les paysages en coins de glace à mesure que le climat se réchauffe et que la couche de pergélisol active s'approfondit. Ces informations permettront une meilleure compréhension de la variabilité observée des émissions de GES des zones pergélisolées de l'Arctique sur la base de la géomorphologie des mares de dégel, et contribueront à une base de données plus précise pour les modèles du climat futur. D'autre part, même si le nombre de mares où les communautés microbiennes ont été étudiées est limité, un lien fort entre les concentrations de GES et la communauté microbienne a été mis en évidence et permet d'expliquer pourquoi les mare *allongées* sont prédisposées à une production plus élevée de GES.

De façon générale, la communauté microbienne des sédiments de surface des mares de dégel de l'île Bylot s'est avérée unique par rapport aux autres environnements arctiques par ses communautés d'archées méthanogéniques et de bactéries méthanotrophiques. En fait, les communautés bactériennes de sédiment de surface étaient distinctes entres les mares polygonales et *allongées*, mais les communautés méthanogéniques des sédiments de surface ne l'étaient pas. Ces dernières incluaient de façon substantielle la méthanogénèse acétoclastique (MA). Ceci est contraire aux travaux antérieurs présentant la méthanogénèse hydrogénotrophique (MH) comme la voie dominante de l'Arctique. Les mares polygonales et *allongées* de l'île Bylot possédaient des méthanogènes capables des deux voies métaboliques en même temps, avec une dominance de la MA durant l'été indiquant aucune limitation de substrat. Les deux types de mares ont le potentiel d'émettre une production équivalente de CH_4, mais dans le cas des mares polygonales, la communauté bactérienne inclut la présence de méthanotrophes pour réguler leurs émissions de CH_4 vers l'atmosphère.

La communauté méthanotrophique des bactéries des sédiments de surface incluait aussi des taxons rares pour les environnements arctiques, incluant les méthanotrophes *Verrucomicrobia,* initialement identifiées dans les sources thermales du parc national Yellowstone, ne permettant plus une classification unique des méthanotrophes comme type I ou II, tel que fait antérieurement pour les écosystèmes arctiques. Pour les mares de dégel, il semble y avoir un lien entre les méthanotrophes des sédiments de surface et les cyanobactéries étant donné leur production d'oxygène. Ainsi, une plus grande abondance relative des méthanotrophes et des cyanobactéries a été observée dans les mares polygonales par comparaison avec les mares *allongées*. En appui avec cette tendance, les données $\delta^{13}C$ du CO_2 et du CH_4 ainsi qu'une relation significative entre la concentration d'oxygène dans l'eau de surface et les valeurs de $\delta^{13}C$ indiquent que le CH_4 diffusif des mares polygonales est plus susceptible à l'oxydation. La présence des méthanotrophes est très pertinente parce qu'elles ont été identifiées dans la régulation des émissions de CH_4.

La communauté des mares *allongées* a démontré une réponse complexe à une hausse de la température (+5°C), qui correspond probablement à la réalité du réchauffement climatique de l'Arctique dans un futur rapproché. Alors qu'une production de GES significativement plus élevée a eu lieu à 9°C qu'à 4°C, la production in situ de CH_4 des mares polygonales pourraient être régie par les méthanotrophes. Les dégradateurs de C ont démontré une baisse d'activité (ARN) à +5°C à travers une réduction des Bacteroidetes et une augmentation de multiples Phyla, incluant les Acidobacteria, qui ont été reconnues comme des mobilisateurs de C récalcitrant (Fierer *et al.*, 2007). Étant donné qu'une jeune (≤ 60 yrs) source de C, souvent caractérisée comme plus labile, soutient actuellement la production de GES dans les mares de dégel à l'île Bylot, une augmentation d'Acidobacteria pourrait permettre l'utilisation d'une source de C récalcitrante suite à l'épuisement de la source de C labile. Par conséquent, les changements futurs de la communauté responsable pour la dégradation du C pourrait mener à une production accrue de GES si l'utilisation d'un pool de C plus vieux et plus récalcitrant devient disponible, mais seulement si limité par le C labile.

Le résultat que les mares *allongées* de l'île Bylot présentent une érosion de la tourbe environnante (vieux dépots pouvant dater jusqu'à 3670 ans BP) et des émissions élevées de GES ne provenant pas clairement d'une vieille source de C, soutien l'importance de considérer davantage la labilité des différentes source de C et le rôle fondamental des communautés microbiennes dans ce processus. Une préférence microbienne actuelle au C fixé récemment par

les plantes aquatiques ainsi qu'un Arctique verdissant (Epstein *et al.*, 2013) pourraient donc promouvoir le transport et l'enfouissement du C libéré par le dégel du pergélisol et mobilisé vers d'autres endroits (Vonk et al. 2013). À ma connaissance, mon étude est la première du genre qui relie de façon détaillée les différents processus impliqués dans le cycle du C des petites mares de dégel aux communautés microbiennes en se servant d'outils moléculaires, d'isotopes stables et de datation au ^{14}C, représentant ainsi une contribution significative au domaine. Les résultats de cette thèse justifient la pertinence d'étudier les processus microbiens pour mieux prévoir les émissions futures de GES. C'est une illustration claire de la nécessité de mieux connaitre les assemblages microbiens, étant donné leur grande diversité dans l'Arctique, et leur réponse potentiellement complexe aux changements climatiques.

LES ÉMISSIONS DE GAZ À EFFET DE SERRE ET LES COMMUNAUTÉS MICROBIENNES DES MARES ASSOCIÉES AU DÉGEL DU PERGÉLISOL DANS L'ARCTIQUE

ARTICLES

2 Small thaw ponds: An unaccounted source of methane in the Canadian high Arctic

Les petites mares de dégel: une source non-comptabilisée de méthane dans le haut Arctique canadien

Karita Negandhi[1], Isabelle Laurion[1], Michael J. Whiticar[2], Pierre E. Galand[3,4], Xiaomei Xu[5], Connie Lovejoy[6]

[1] Centre for Northern Studies (CEN) and Institut national de la recherche scientifique, Centre Eau Terre Environnement, Quebec, Canada
[2] School of Earth and Ocean Sciences, University of Victoria, Victoria, British Columbia, Canada
[3] UPMC Universite´ Paris 06, (UMR 8222, LECOB), Observatoire Oceanologique, Banyuls-sur-mer, France
[4] CNRS, UMR 8222, LECOB, Observatoire Oce´anologique, Banyuls-sur-mer, France
[5] Department of Earth System Science, University of California Irvine, Irvine, California, United States of America
[6] De´partement de biologie, Institut de Biologie Inte´grative et des Syste`mes, Universite´ Laval, and Takuvik (CNRS, UMI 3376), Quebec, Canada

Les données présentées dans cet article permettent une compréhension approfondie de la production de méthane dans les petites mares de dégel. Les données interdisciplinaires ont été recueillies, traitées, analysées, et interprétées par K. Negandhi sous la supervision d'Isabelle Laurion et Connie Lovejoy. Les échantillons pour les isotopes stables et la datation ^{14}C ont été analysés dans des laboratoires spécialisés, et les données de 2009 ont été recueillies par des collègues mais analysés par K. Negandhi. La première version de la publication a été synthétisée et rédigée par K. Negandhi, suivie de la participation des co-auteurs pour une contribution spécifique à leur domaine de compétence respectif. Après, tous les co-auteurs ont apporté leurs commentaires et suggestions, une version finale a été préparée par K. Negandhi et soumise le 16 mai 2013. Avis d'acceptation reçu le 10 Septembre 2013, avec une date de publication le 13 novembre 2013 dans la revue PLoS ONE 8(11):e78204 doi:10.1371/journal.pone.0078204.

Résumé

Le dégel du pergélisol dans la toundra de l'Arctique canadien conduit à l'érosion de la tourbe et à son effondrement dans les dépressions étroites et peu profondes qui s'emplissent d'eau (nommées mares *allongées*) et qui bordent les mares polygonales, plus couramment étudiées. Nous avons comparé la production de méthane entre les mares *allongées* et les mares polygonales en utilisant des ratios d'isotopes stables et des signatures au ^{14}C, et étudié les communautés méthanogènes potentielles par séquençage à haut débit du gène 16S ARNr des Archées. Nous avons constaté que les mares *allongées* avaient des émissions de méthane et de dioxyde de carbone significativement plus élevées, et produites à partir d'une fraction légèrement plus grande du carbone ancien, par rapport aux mares polygonales. La signature isotopique du méthane indique une production par méthanogénèse acétoclastique durant l'été, mais les gènes provenant d'Archées qui font la méthanogénèse acétoclastique et hydrogénotropique ont tous deux été détectés. Nous concluons que les mares *allongées* représentent une source de méthane potentiellement plus élevée en C ancien, et qu'elles contiennent des communautés méthanogènes capables d'utiliser diverses sources de carbone, accentuant le risque d'augmenter le dégagement de méthane sous un climat plus chaud.

Mots-clés: méthanogènes, carbone, ébullition, mares thermokarst, gaz à effet de serre

Abstract

Thawing permafrost in the Canadian Arctic tundra leads to peat erosion and slumping in narrow and shallow runnel ponds that surround more commonly studied polygonal ponds. Here we compared the methane production between runnel and polygonal ponds using stable isotope ratios, ^{14}C signatures, and investigated potential methanogenic communities through high-throughput sequencing archaeal 16S rRNA genes. We found that runnel ponds had significantly higher methane and carbon dioxide emissions, produced from a slightly larger fraction of old carbon, compared to polygonal ponds. The methane stable isotopic signature indicated production through acetoclastic methanogenesis, but gene signatures from acetoclastic and hydrogenotrophic methanogenic Archaea were detected in both polygonal and runnel ponds. We conclude that runnel ponds represent a source of methane from potentially older C, and that they contain methanogenic communities able to use diverse sources of carbon, increasing the risk of augmented methane release under a warmer climate.

Key words: methanogens, ebullition, carbone, thermokarst ponds, greenhouse gases

2.1 Introduction

In arctic regions, the acceleration of permafrost thaw and deepening of the seasonal active layer leads to thaw pond formations due to the organic and ice-rich ground subsiding (Allard & Fortier 2004; Rowland *et al.*, 2010). These thaw ponds are also sometimes referred to as thermokarst lakes, since they superficially resemble ponds formed by the dissolution of limestone (karst). Two main geomorphological forms are commonly found in continuous permafrost regions of Eastern Canada: (i) small, shallow, narrow runnel ponds formed over melting ice wedges where peat slumping occurs, and (ii) more stable, slightly larger and deeper, polygonal ponds, which are naturally linked to the active layer freeze-thaw cycles, and can be colonized by aquatic plants and microbial mats (Figure 2.1). Greenhouse gas (GHG) emissions from thermokarst ecosystems are highly variable (Tank *et al.*, 2009; Laurion *et al.*, 2010; Abnizova *et al.*, 2012) and often not considered in large-scale GHG studies and global carbon cycling models since small ponds cannot be seen with remote sensing tools (Tranvik *et al.*, 2009; Muster *et al.*, 2012]. These ponds have the potential to be significant GHG emitters contributing to a positive carbon-climate feedback (Zimov *et al.*, 1997; Wagner *et al.*, 2005; Zona *et al.*, 2008), attributed to the mobilization of old stored carbon (C) stocks released back into the atmosphere (Grosse *et al.*, 2011; Schuur *et al.*, 2008; Shirokova *et al.*, 2013). In these ecosystems, microbial decomposers and methanogens have access to large quantities of allochthonous organic matter (Laurion *et al.*, 2010; Breton *et al.*, 2009). The CH_4 released from Siberian thaw lakes is significant and originates from microbial utilization of C stocks deposited thousands of years ago (Zimov *et al.*, 1997; Walter *et al.*, 2008). In the eastern Canadian Arctic, C deposition dates from the Holocene (Fortier & Allard 2004), but microbial utilization is unknown.

The conversion of organic C previously locked in permafrost to GHG is highly dependent on its lability to microbial degradation (Schuur *et al.*, 2008; Berggren *et al.*, 2010; Guillemette and Del Giorgio 2011). For instance, fresh labile organic matter favors acetoclastic methanogenesis (AM) (Hornibrook *et al.*, 1997), where the organic substrate (i.e. acetate, methanol, methylated substrates, etc.) is cleaved and the methyl group is reduced to CH_4. Comparatively, more recalcitrant compounds leached from peat favors the hydrogenotrophic pathway (HM) (Penning & Conrad 2007), which utilizes H_2 to reduce CO_2. Therefore, the available substrate selectively determines the methanogenic community and CH_4 production rate.

Once CH_4 is produced through AM or HM pathways, at the bottom of lakes and ponds, it is transported through the water column to the atmosphere by diffusion and ebullition. Ebullition transport can be classified as background, point sources or hotspots. In Siberian thermokarst lakes these three sources accounted for 25, 58, and 12% respectively, with the remaining 5% of total emissions attributed to diffusion (Walter *et al.*, 2007). Diffusion is generally considered less important than ebullition (Michmerhuizen *et al.*, 1996; Bastviken *et al.*, 2004). However, diffusion and ebullition rates are variable in aquatic systems and relative contribution of these sources has not been investigated in other Arctic thermokarst systems where geomorphology varies considerably. There are no previous reports from runnel type ponds and their potential contribution to atmospheric GHG is not known.

The objective of our study was to evaluate the release and potential for GHG emissions in the poorly studied runnel ponds compared with polygonal ponds of northeastern Canada. These ponds have the potential to form in ice and organic rich soils of permafrost and glaciated-influenced landscapes, covering ca. 9.6 million km^2 of the global northern landscape (Smith *et al.*, 2007). The methanogenic pathways and C age were investigated through stable isotopic signatures and radiocarbon dating of dissolved and bubbling GHG. Archaeal community composition in the sediments was analyzed with high-throughput 16S rRNA gene pyrosequencing. We found that runnel ponds were supersaturated in CO_2 and had more than 3 folds greater CH_4 emissions than polygonal ponds, which were a CO_2 sink. Higher CH_4 emission is likely explained by a higher supply of organic matter under more hypoxic conditions, where CH_4 oxidation is less likely to occur. The methanogenic community included genera capable of both AM and HM, indicating that methanogens could potentially use different carbon substrates and thus acclimate to changing conditions, for example vegetation cover or hydrology, under a warmer climate.

2.2 Methods

2.2.1 **Study Site**

Samples were collected at Sirmilik National Park, Bylot Island, Nunavut (73°09'N, 79° 58'W; Figure 2.1) in the continuous permafrost region of Canadian Arctic, with an active layer depth between 40 and 60 cm (D. Fortier, pers. comm.). Required permits to carry out sampling were approved by the Parks of Canada Agency for Sirmilik National Park (Research and Collection Permit) and the Nunavut Research Institute (Nunavut Science License). The Bylot SILA station recorded a mean annual air temperature of -14.5°C, with summer temperatures from June to August averaging 4.5°C and winter temperatures from December to January averaging -32.8°C. Precipitation between June and August (1994-2007) was about 94 mm. Thaw ponds and lakes covered 4.2% of the ~65 km^2 pro-glacial river valley in 2010, as obtained from a high resolution image from WorldView-1, with runnel ponds contributing approximately 44% of the surface water compared to polygonal ponds contributing 27%. Polygonal ponds form on top of low centered peat polygons, and are generally 0.5 to 1.5 m deep with an area < 500 m^2. Runnel ponds form over melting ice wedges, and are often shallower than 0.5 m but sometimes form long networks (Figure 2.1). Both pond types freeze to bottom in winter, and are unfrozen for approximately 110 days per year. The sum of all daily temperatures above freezing averaged 447 thawing-degree days (http://www.cen.ulaval.ca/bylot/climate-description-bylotisland.htm).

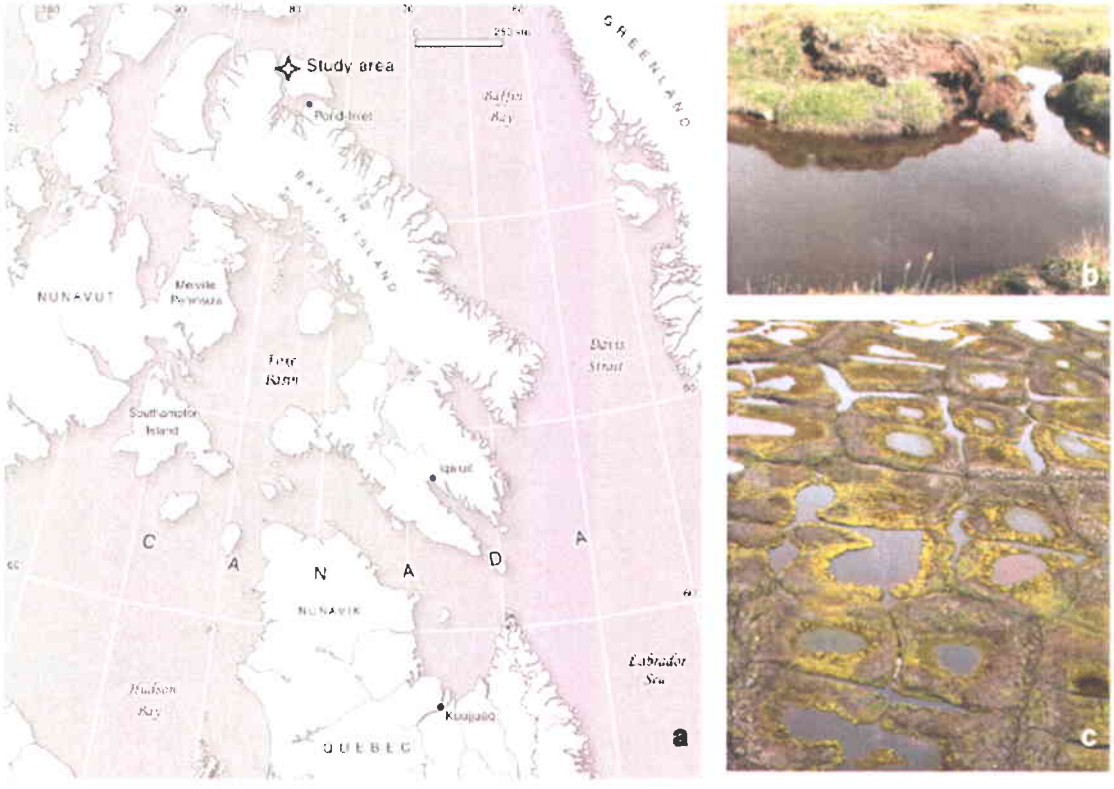

Figure 2.1 Study site description: (a) Map indicating the location of the study site on Bylot Island, Sirmilik National Park, Nunavut, Canada, (b) collapsed peat polygon ridges forming runnel ponds, and (c) landscape combining runnel and polygonal ponds.

2.2.2 Sampling

In July 2009, 34 ponds were sampled for dissolved GHG concentrations and flux estimation, with 19 sampled for carbon and hydrogen stable isotope ratios (Table 2.1), and 4 ponds (2 polygonal and 2 runnel ponds) for archaeal diversity assessment via pyrosequencing (BYL1, 22, 24, 27; Table 2). These 4 ponds were selected to represent a range of physiochemical properties, which were measured in previous years. In July 2010, 14 ponds from the 2009 series were re-sampled for dissolved GHG concentrations and flux estimations. In 2011, from mid June to mid July, dissolved GHG concentrations and flux estimates were obtained from a total of 43 ponds, including 15 from the 2009 series. In addition, ebullition samples were taken from 4 ponds (2 polygonal ponds; BYL1 and 80 and 2 runnel ponds; BYL27 and 38) for stable isotopes and $\Delta^{14}C$ analysis, and ebullition rates were measured from the two polygonal ponds, which were deep enough to install the funnels needed for rate measurements. Ebullition flux was not measured from runnel ponds because the funnels were too wide to be correctly installed in the shallow and

narrow ponds, exemplifying the difficulties in Arctic sampling. Also in 2011, GHG dissolved flux was measured approximately every 2 h over 26 h on 2 polygonal ponds (BYL1 and BYL80) to examine the daily variations in GHG dissolved concentrations.

Table 2.1 Compilation of thaw ponds samples collected each year. Polygonal ponds (P); runnel ponds (R); dissolved organic carbon (DOC); organic carbon (OC); Greenhouse gases (GHG, including CO2 and CH4); ebullition is GHG released as bubbles; production pathway indicates CH4 produced by acetoclastic methanogenesis (AM) or hydrogenotrophic methanogenesis (HM); temperature (temp). Note that most samples were collected in 2009, with diurnal, ebullition and sediment OC collected in 2011, which was the only occasion when appropriate sampling gear was available.

		Year	Total ponds (POL;RUN)	Method
Dissolved GHG	GHG flux	2009 - 2011	92 (33; 58)	Dissolved concentrations
	Production pathway	2009	19 (9; 10)	Stable isotopes
	Diurnal variations	2011	2 (2 POL)	Hourly flux measures
Ebullition	Ebullition flux	2011	2 (2 POL)	Funnel traps
	Production pathway	2011	4 (2; 2)	Stable isotopes
	C-source (age)	2011	4 (2; 2)	^{14}C dating
Diversity	Methanogenic community	2009	4 (2; 2)	Archaeal pyro-sequencing
Environment	Limnology	2009	4 (2; 2)	Nutrients, pH, temp, O_2, DOC
	C-source (amount)	2011	17 (9; 8)	Sediment OC

2.2.3 Limnological characteristics

Surface water pH was measured with a 600R multi-parametric probe (Yellow Spring Instrument). The surface temperatures of one polygonal (BYL1) and one runnel pond (BYL24) were continuously recorded from July 2008 to July 2009 (thermistors, HOBOware™ U12, Onset). Pond water filtered through 0.2 µm pre-rinsed cellulose acetate filters (Advantec) was used for dissolved organic carbon (DOC) concentrations (Shimadzu TOC-5000A carbon analyzer calibrated with potassium biphthalate). Soluble reactive phosphorus (SRP) and major ions were measured on filtered samples (Laurion *et al.*, 2010). Unfiltered water samples were fixed with H_2SO_4 (0.15% final concentration) for total phosphorus (TP) and total nitrogen (TN) quantification as in (Stainton *et al.*, 1977). In 2011, 5 mL of surface sediment were collected for total organic carbon content (TOC) and processed with 0.1 mol L^{-1} of sulfuric acid on an elemental analyzer (CHNS-932, LECO Instruments) (Chappaz *et al.*, 2008).

2.2.4 Diffusive flux

Dissolved CO_2 and CH_4 concentrations in surface waters were obtained by equilibrating 2 L of water with 20 mL of ambient air for 3 minutes. Most sampling occurred between 9 am and 4 pm. The resulting headspace was injected into glass vials (BD 3 mL Vacutainers, or Labco 5.9 mL Exetainers), helium flushed and vacuumed (Hesslein *et al.*, 1991). Samples were analyzed by gas chromatography (Varian 3800 with COMBI PAL head space injection, CP-Poraplot Q 25 m 3 0.53 mm column, flame ionization detection), and dissolved gas concentration calculated using Henry's Law:

$$C = K_H \times pGas$$

where K_H is Henry's constant adjusted according to ambient water temperature, and pGas is the partial pressure of CO_2 or CH_4 in the headspace. Dissolved GHG flux (F_d) was calculated as:

$$F_d = k\left(C_{sur} - C_{eq}\right)$$

where C_{sur} is the gas concentration in surface water, C_{eq} is the gas concentration when in equilibrium with the atmosphere at ambient temperature (global atmospheric concentrations were used), and k is the gas exchange velocity calculated as:

$$k = k_{600}\left(\frac{Sc}{600}\right)^{-0.5}$$

where Sc is the Schmidt number calculated from empirical third-order polynomial fit to water temperature and corrected at 20°C. The gas exchange coefficient k_{600} of Cole and Caraco (1998) was used as a first approximation:

$$k_{600} = 2.07 + 0.215 \times U_{10}^{1.7}$$

where U_{10} is the wind speed at 10 m above ground. However, this gas transfer model is not adequate for small aquatic systems (small fetched) where turbulence is controlled by heat exchange rather than wind (MacIntyre *et al.*, 2010). Therefore, a correction factor (× 0.2458) was applied, obtained from a series of simultaneous CO_2 flux measurements from a floating chamber connected to an EGM-4 (PP-Systems) performed at the same time as surface gas concentrations were collected (Laurion *et al.*, 2010) (data from 2007 to 2010, n=57, r^2=0.689, p<0.001; unpubl. data).

2.2.5 Ebullition

Ebullition flux and bubble characterization (composition, $\delta^{13}C$ and δD, and ^{14}C dating; see below) were obtained from submerged funnels. Bubble samples were collected in pre-combusted (500°C for 2h), miliQ-rinsed, 125 mL glass bottles, helium flushed and vacuumed, with butyl rubber caps. Funnels were installed in polygonal ponds BYL1 and 80 from 18 June to 13 July 2011. Ice was present at the bottom of BYL80 from 18 to 22 June, while no ice was present in BYL1. Ebullition flux (F_e) was obtained from passive accumulation of gas in funnels, and calculated as:

$$F_e = (pGas \times V)/(A \times MV \times time)$$

where V is the gas volume collected, A is the funnel area (0.3526 m^2), and MV the gas molar volume at ambient air temperature. In addition, gas was collected from 22 to 26 June from stirred sediments for stable isotopes and ^{14}C dating in ponds BYL27 and 38, since ebullition rate did not provide sufficient gas and funnels were too large for proper installation in shallow and narrow runnel ponds.

2.2.6 Stable isotopes

Stable isotopes of C and H in CO_2 and CH_4 ($\delta^{13}CO_2$, $\delta^{13}CH_4$, and δD_{CH4}) were analyzed at the Biochemistry Laboratory of the School of Earth and Ocean Sciences (University of Victoria, Canada). Gas samples in Wheaton bottles were analyzed for $\delta^{13}CH_4$ by introducing the gas onto a GSQ PLOT column (0.32 mm ID, 30 m) using a Valco 6-port valve and sample loop. After chromatographic separation, the CH_4 passes through an oxidation oven (1030°C), a Nafion water trap, and open-split interface to a Continuous Flow-Isotope Ratio Mass Spectrometer (CF-IRMS). The $\delta^{13}CO_2$ was measured similarly, but without the combustion oven. Precision for the □□$^{13}CH_4$ and □$^{13}CO_2$ analyses was ± 0.2‰. Hydrogen isotope ratios of CH_4 (□D_{CH4}) were measured by a TC/EA pyrolysis unit (1450°C) interfaced to a CF-IRMS. Precision for the □D_{CH4} analyses was ± 3‰, relative to VSMOW.

2.2.7 $\Delta^{14}C$ analysis

Methane and CO_2 were separated by a continuous flow line consisting of purification and combustion traps (Xu *et al.*, 2012) as follows: first, CO_2 was frozen in liquid nitrogen (LN_2), second, carbon monoxide (CO) was oxidized to CO_2 in a 300°C CuO furnace and frozen in a second LN_2 trap, finally, non-condensable CH_4 was oxidized to CO_2 in a CuO furnace at 975°C (Lindberg/Blue M Tube Furnace, Thermo Scientific). The resulting CO_2 and H_2O from CH_4 combustion were further separated cryogenically on the vacuum line. Purified CO_2 was graphitized using the sealed tube zinc reduction method (Xu *et al.*, 2007). The ^{14}C analysis was conducted at the Keck Carbon Cycle AMS (KCCAMS) facility at the University of California, Irvine (UCI), on a compact accelerator mass spectrometer (AMS) system from National Electrostatics Corporation (NEC 0.5MV 1.5SDH-2 AMS), with a modified NEC MC-SNIC ion-source (Southon & Santos 2004; 2007). The in-situ simultaneous AMS $\delta^{13}C$ measurement allowed for fractionation corrections occurring inside the AMS system and during graphitization, significantly improving the precision and accuracy, with a day-to-day analysis relative error of 2.5 to 3.1‰ based on secondary standards, and including extraction, graphitization and AMS measurement.

2.2.8 Archaeal diversity

Surface water was filtered sequentially through a 3 µm pore size polycarbonate filter and a 0.2 µm Sterivex unit (Millipore). Filters were immersed in buffer (40 mM EDTA; 50 mM Tris at pH 8.3; 0.75 M sucrose), stored in liquid nitrogen in the field (≤ 2 weeks), and then stored at -80°C until extraction. Cellular DNA was extracted from both filters, with a phenol:chloroform:Indole-3-Acetic Acid (25:24:1) and chloroform:Indole-3-Acetic Acid (24:1) separation and DNA quantified by spectrophotometry (Nanodrop ND-1000). Surface sediment samples were collected using a cut 60 mL sterile plastic syringe to depth of around 6.5 cm, placed in sterile plastic bags and homogenized. A sub-sample of 3 mL was squeezed from the bag into 5 mL cryotubes with buffer and stored as above. DNA was extracted using the MO BIO Kit (RNA Powersoil total RNA isolation kit #12866-25 and DNA elution accessory kit #12867-25) allowing both RNA and DNA to be extracted at the same time, but only DNA was sequenced for this study. Once extracted the DNA was quantified as above.

A PCR reaction mixture of 1X HF buffer (NEB), 200 µM dNTP (Feldan Bio), 0.4 mg mL^{-1} BSA (Fermentas), 0.2 µM of each 454 primer (969F: ACGCGHNRAACCTTACC and 1401R: CRGTGWGTRCAAGGRGCA) (Comeau *et al.*, 2011), 1 U of Phusion High-Fidelity DNA polymerase (NEB), and 0.1-1 µL of template DNA for sediment samples, or 2 µL for water samples. Three separate DNA concentrations were used for each sample, from 1X to 2.22X, to reduce PCR bias. Amplification cycles included denaturing at 98°C for 30s, 30 cycles of denaturing at 98°C for 10s, annealing at 55°C for 30s, extension at 72°C for 30s, and a final extension at 72°C for 5 min. For each sample, the triplicate reactions were pooled together for purification (QIAquick PCR purification kit; QIAGEN) and quantification (Nanodrop ND-1000). The resulting sample coded amplicons were mixed in equal proportions and sequenced on a Roche 454 GS-FLX Titanium platform at Université Laval Plateforme d'analyses Génomiques. Raw reads were submitted to NCBI Sequence Read Archive ,SRA) under the accession number SRA039814, with a Sequence Read Experiment (SRX) number SRX319084. Resulting reads were subjected to pyrotag pre-processing, quality control, and taxonomic analyses (Comeau *et al.*, 2011). Low-quality reads were identified and removed if they contained any non assigned nucleotides (N's), were < 150 bp not including the adaptor and sample tag-code, if they exceed the expected amplicon size, and if the Forward primer sequence was incorrect. The remaining reads were then trimmed if there were nucleotide bases after the reverse primer. Next, reads were aligned using mother (Schloss et al. 2009; Schloss 2009) against SILVA reference alignments, and then manually checked to remove misaligned reads. The number of reads after processing ranged from 1921 to 2105, and for downstream analysis was randomly resampled to 1921 reads. The SILVA database (version 108) was used for archaeal identifications, including additional previously generated clone library sequences (Pouliot *et al.*, 2009, Galand *et al.*, 2006; Comeau *et al.*, 2012) from the C. Lovejoy laboratory.

2.3 Results

2.3.1 Pond limnological properties

Within the four ponds targeted for the archaeal diversity study, runnel ponds, which are subjected to more peat leaching and erosion, had higher concentrations of DOC, nutrients (TN, SRP and TP) and iron (Table 2.2). Polygonal ponds showed no sign of recent erosion, with thick

cyanobacteria-dominated microbial mats on the bottom, and lower concentrations of DOC, nutrients and ions. The organic carbon (OC) content of surface sediment was highly variable, ranging between 1.0 and 25.1% among the series of sampled ponds (n=26, 2011), and with no significant difference (paired t-test) between polygonal ponds (8.4 ± 6.6%) and runnel ponds (6.4 ± 3.9%). Over the year, pond ice and water temperatures ranged between -26.7 and +21.4°C (averaging -7.6°C; Figure 2.2). The temperature records showed that ponds remained frozen from ~25 September to 4 June.

Table 2.2 Surface water physicochemical properties of the four ponds sampled for archaeal communities between 19 and 26 July 2009, including dissolved organic carbon (DOC, mg L-1), soluble reactive phosphorus (SRP, mg L-1), total phosphorus (TP, mg L-1), total nitrogen (TN), nitrate (NO3), sulfate (SO4), iron (Fe) all in mg L-1, pH, and dissolved CO2 and CH4 concentrations, both in mM.

POND	DOC	SRP	TP	TN	NO_3	SO_4	Fe	pH	CO_2	CH_4	OC
Polygonal ponds											
BYL1	8.4	<0.2	15.6	363	0.05	1.47	0.299	8.7	6.3	1.0	4.6
BYL22	8.1	<0.2	25.5	371	0.04	0.85	0.557	7.2	25.0	1.9	5.3
Runnel ponds											
BYL24	11.5	1.0	25.5	398	0.04	0.67	1.012	7.1	33.0	3.4	6.5
BYL27	11.8	0.5	26.3	822	0.06	1.56	0.905	6.6	78.8	2.6	17.8

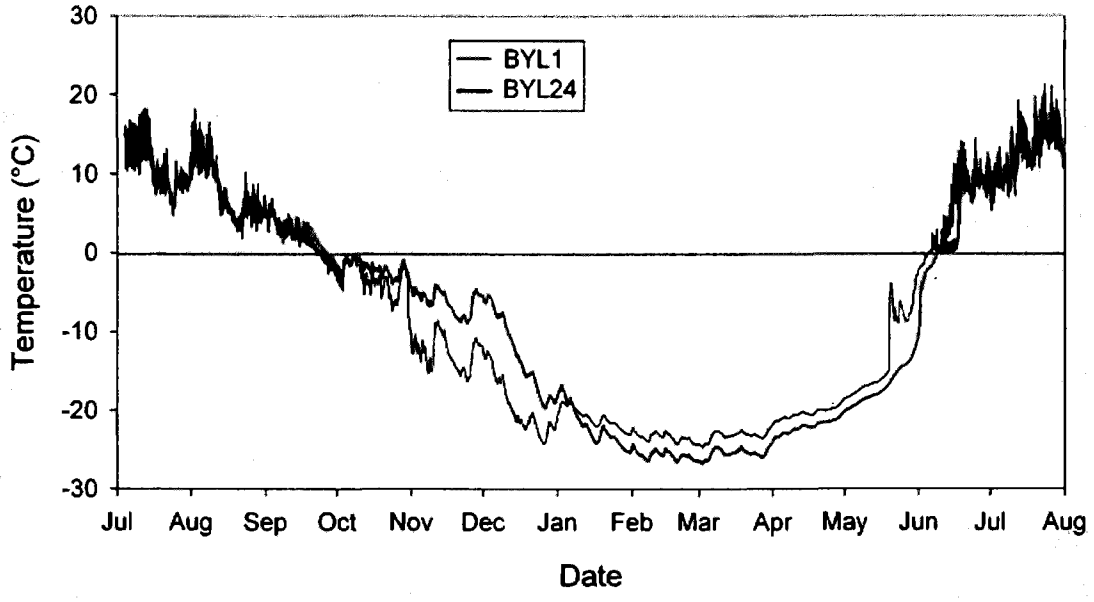

Figure 2.2. Seasonal melting and freezing: Surface water temperature for one polygonal pond (BYL1) and one runnel pond (BYL24), from July 2008 to July 2009.

2.3.2 GHG concentrations, fluxes and isotopic signatures

Surface water GHG concentrations collected in the compiled series of thaw ponds (from 2009 to 2011, n = 91) showed a significantly higher concentration of CH_4 in runnel compared to polygonal ponds (t-test, df= 90, p = 0.003). Only runnel ponds were supersaturated in CO_2 (averaging 119 ± 124 µM, compared to polygonal ponds 9.6 ± 8.9 µM) but all ponds were supersaturated in CH_4 (4.1 ± 4.7 and 1.3 ± 1.7 µM, in runnel and polygonal ponds respectively). Runnel ponds also had significantly higher CO_2 and CH_4 fluxes compared to polygonal ponds ($p \leq 0.0001$; Figure 2.3) but the diffusive flux of CO_2 (-8.1 to 76.9 mmol m^{-2} d^{-1}) and CH_4 (0.02 to 6.3 mmol m^{-2} d^{-1}) varied greatly over the 3 sampled summers. In the two ponds (BYL80 and BYL1) that were tested over 26 hours, diurnal dissolved GHGs varied by 18 and 25% for CO_2, and 17 and 21% for CH_4. The corresponding fluxes likely varied by no more than 25%

throughout a day as estimated using a wind-based model incorporating the wind speed over the preceding 2h,where the coefficient of variation was 45% for the wind speed. In the same two polygonal ponds (BYL1 and BYL80), eight separate measurements of CH_4 ebullition fluxes showed that despite the variability within ponds, fluxes were always greater in BYL80 than in BYL1 (t-test, df = 7, p = 0.02, Table 2.3). Ebullition flux was lower than diffusive flux in BYL1 (representing on average 27% of total CH_4 emission) and higher than diffusive flux in BYL80 (82% of total emission). The diffusive flux values used in this comparison were from approximately the same period in 2011, but ebullition was calculated over up to 32 h of bubble collection, while diffusive flux was always estimated from one discrete gas sample. The CH_4 concentration in bubbles was also variable (1.5-32% by volume).

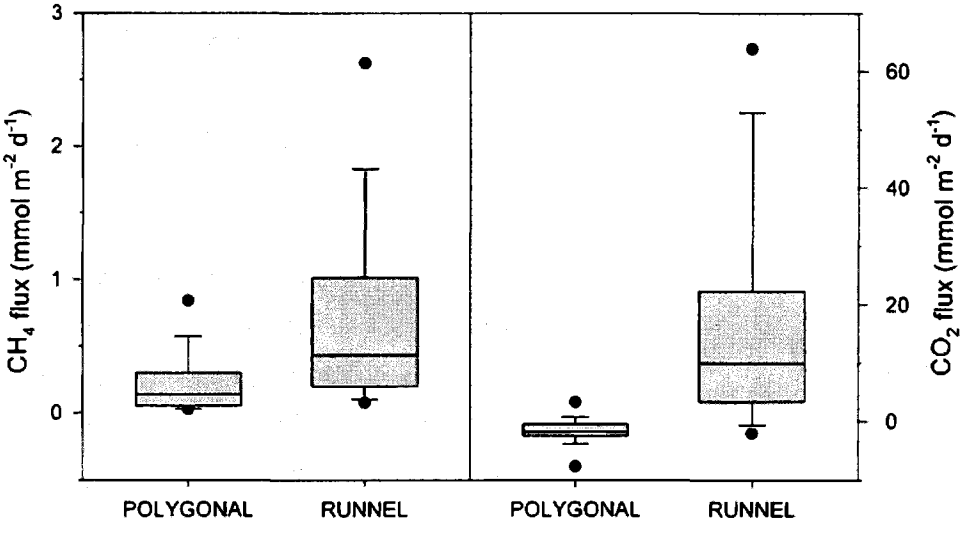

Figure 2.3 Diffusive greenhouse gas flux from polygonal and runnel ponds. Data collected from summer 2009, 2010 and 2011, including 33 measurements from polygonal ponds and 58 from runnel ponds. The diffusive flux was calculated using the windbased model of Cole and Caraco [41], but estimations were corrected with a regression equation comparing floating chamber CO_2 flux to wind-based flux (see Methods).

Table 2.3 Methane emission ranges (median value in parenthesis) through diffusion (N= 4) and ebullition (N= 8) from two polygonal ponds (BYL1 and BYL80), and diffusive flux from 12 other polygonal ponds and 14 other runnel ponds located on the same site measured from 18 June to 16 July 2011.

	Diffusive flux[1]	Ebullition flux[2]
	mmol m^{-2} d^{-1}	
BYL1	0.04 – 0.37 (0.10)	0.01 – 0.07 (0.04)
BYL80	0.05 – 0.77 (0.08)	0.18 – 2.13 (0.91)
POLYGONAL PONDS	0.02 – 0.25 (0.06)	!
RUNNEL PONDS	0.02 – 0.98 (0.30)	–

[1]Diffusive flux was calculated using the wind-based model of Cole and Caraco[41], but estimations were corrected with a regression equation comparing floating chamber CO_2 flux to wind-based flux (see Methods).
[2]Ebullition flux was calculated from the gas collected with a submerged funnel over periods of 21 to 121 h.

Overall the $\Delta^{14}C$ signatures of the GHG released from both polygonal and runnel ponds through ebullition (-1.1 to 114.9 ‰) were categorized as modern (within the last ~60 years). However, ebullition CH_4 from two runnel ponds (n=3) contained a higher fraction of old C compared to the two polygonal ponds (n=7; p = 0.002; Figure 2.4). Both C and H stable isotopic signatures indicate that all CH_4 emitted by diffusion and ebullition during summer was produced from AM (Figure 2.5a). The possibility of HM, as seen in Figure 3b, was ruled out with the inclusion of δD-CH_4 signature. There was no significant difference in the $\delta^{13}C$-CO_2 or $\delta^{13}C$-CH_4 values between the polygonal and runnel ponds (Table 2.4), supporting the idea of similar methanogenesis production pathways (AM). However, there were indications that the CH_4 emitted by diffusion was more susceptible to oxidation in the polygonal ponds (Figure 2.5b). In fact, there was a significant relationship between the oxygen concentration at the surface of ponds and $\delta^{13}C$-CH_4 (r^2=0.337; p = 0.009). Comparatively, CH_4 emitted through ebullition showed no signs of oxidation.

Table 2.4 Range (median) of d13CO2, d13CH4, and dDCH4 values for diffusion and ebullition gas samples, also given separately for polygonal and runnel thaw ponds.

	$\delta^{13}CO_2$ (‰ vs. VPDB)	$\delta^{13}CH_4$ (‰ vs. VPDB)	δD_{CH4} (‰ vs. VSMOW)
Diffusion (n=17)	-36.6 to -12.7 (-17.9)	-59.8 to -39.9 (-48.6)	-368.5 to -304.14 (-342.30)
Polygonal (n=7)	-21.4 to -15.4 (-18.3)	-53.8 to -41.5 (-47.2)	-347.75 to -304.17 (-330.94)
Runnel (n=10)	-36.6 to -12.7 (-17.6)	-59.8 to -39.9 (-50.0)	-368.50 to -319.53 (-350.24)
Ebullition (n=10)	-16.1 to -0.1 (-7.2)	-61.7 to -54.8 (-58.8)	-408.8 to -338.1 (-372.9)
Polygonal (n=7)	-8.8 to -0.1 (-4.8)	-61.7 to -57.4 (-60.0)	-381.7 to -338.1 (-363.1)
Runnel (n=3)	-16.1 to -10.0 (-13.0)	-57.3 to -54.8 (-55.9)	-408.8 to -388.4 (-396.0)

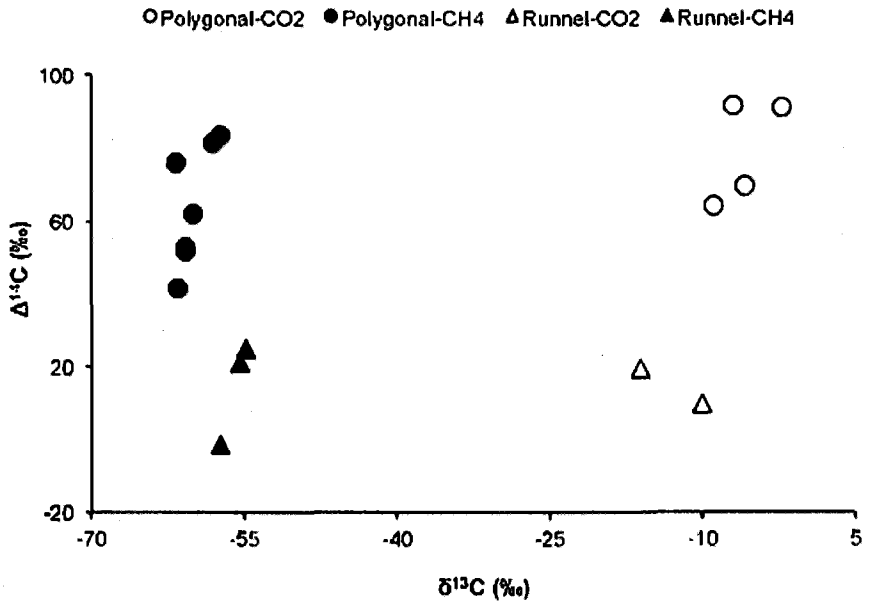

Figure 2.4 CH_4 and CO_2 carbon source and age: Radiocarbon signature ($\Delta^{14}C$) plotted against $\delta^{13}CH_4$ and $\delta^{13}CO_2$ showing: 1) that as the fraction of young carbon becomes higher for both CH_4 and CO_2, the $\delta^{13}C$ signatures become more divergent indicating a decoupling in carbon source; 2) the runnel ponds CH_4 contains a higher fraction of old carbon.

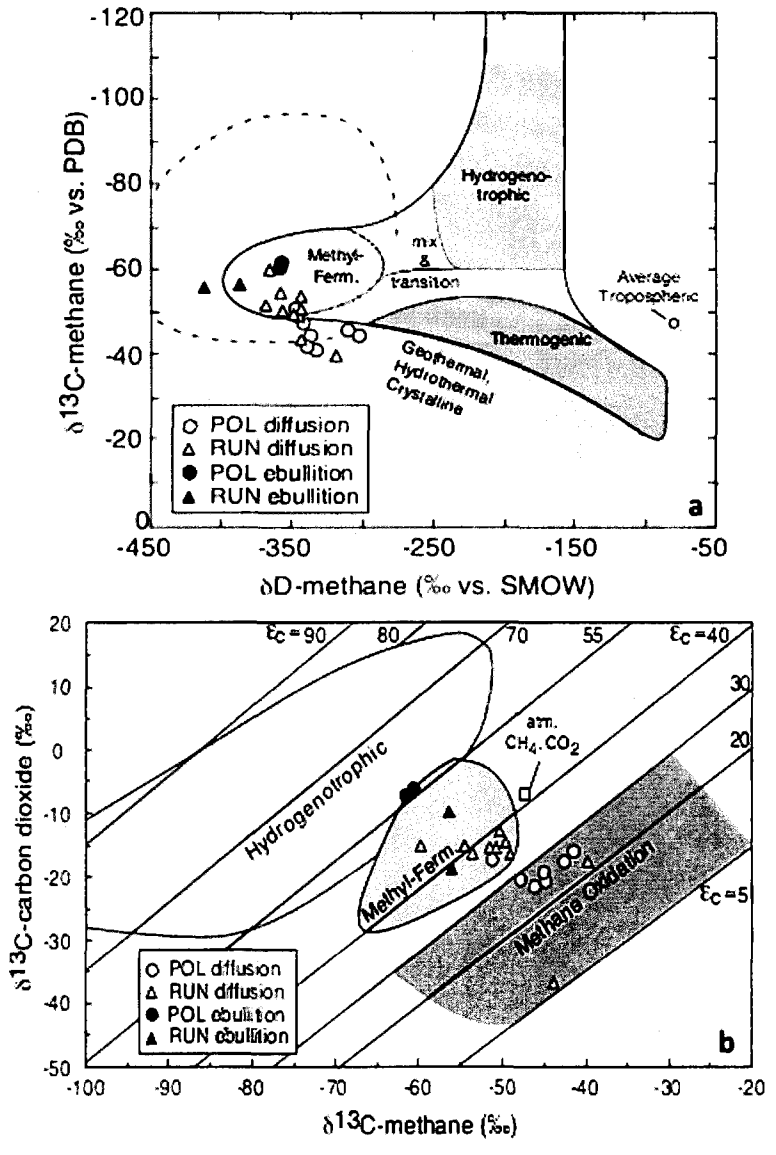

Figure 2.5 Methane production pathway through stable isotopes: (a) $\delta^{13}CH_4$ against δD_{CH4} signatures of diffusive (2009) and ebullition (2011) CH_4, indicating that acetoclastic methanogenesis (AM) is the dominant pathway in polygonal and runnel thaw ponds for samples collected in June/July. (b) $\delta^{13}CO_2$ against $\delta^{13}CH_4$ in thaw ponds showing the predominance of acetoclastic methanogenesis (AM) and the methanotrophic oxidation level for dissolved and ebullition CH_4.

2.3.3 Archaeal assemblages

There was a predominance of methanogen 16S rRNA sequences in surface sediment archaeal communities in the 4 ponds (88 – 95% of the sequences). In contrast, the methanogens represented only 40% of the sequences in the water community of one polygonal pond where we were able to amplify the 16S rRNA gene. We also failed to amplify sediment DNA from one runnel pond (BYL38). The poor PCR success may have been due to a lack of Archaeal template present in the water samples, but is unexplained for BYL38 sediment sample. The water sample archaeal communities were dominated by sequences belonging to the uncultured clusters LDS and RCV (Figure 2.6), and no anaerobic methanotrophic archaea were detected. The sediment non-methanogenic OTUs (5 – 12% of the sequences) belonged to the phylum Euryarchaeota, mainly of a terrestrial miscellaneous euryarchaeotal group (TMEG), and from the miscellaneous crenarchaeotic group (MCG). As there are no cultivated representatives of these groups, the metabolism of these environmental clusters is not known.

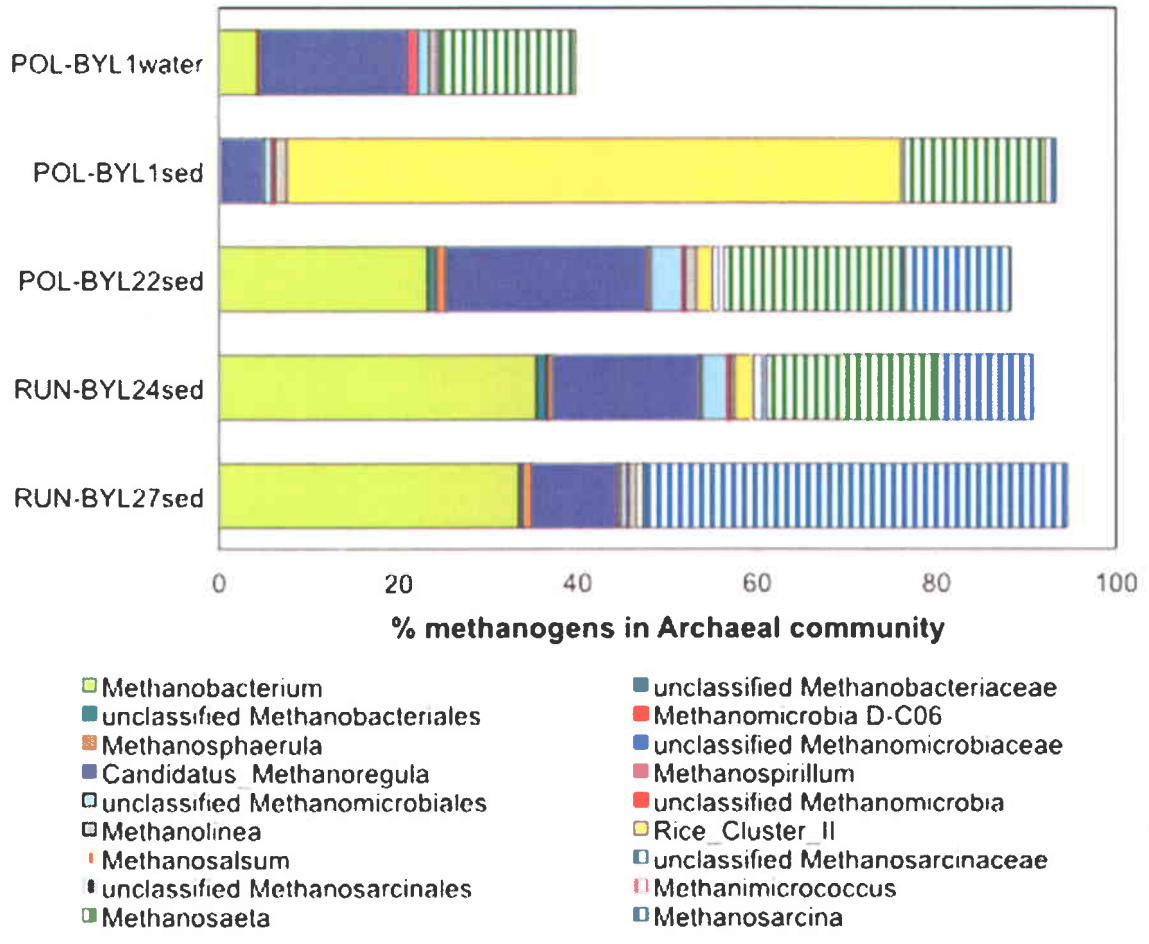

Figure 2.6 Archaeal methanogenic community of thaw ponds: Methanogen taxa retrieved from the sediment of four Arctic thaw ponds and from one water sample. Checkered symbols represent AM and solid are HM.

Altogether the majority of Archaea operational taxonomic units (OTUs) from surface sediments were classified into the four known methanogenic genera (*Methanobacterium,* Candidatus *Methanoregula, Methanosarcina* and *Methanosaeta*) and one uncultured group (Rice cluster II, RC II) within the deeply branching *Methanomicrobiales* (Figure 2.6). Overall, the polygonal pond sediments were dominated by archaeal sequences belonging to HM (*Methanobacterium*, *Methanoregula*) representing from 63 to 82% of the putative methanogen sequences, while runnel ponds were either dominated by HM (65%, BYL24) or by AM (*Methanosarcina, Methanosaeta*) (51%, BYL27). The most abundant *Methanobacterium* that represented one third of all archaeal sequences in both runnel ponds was identified closest to *Methanobacterium lacus*, a newly described strain that utilize H_2/CO_2 and methanol/H_2 as substrates (Borrel *et al.*, 2011). The most abundant *Methanosarcina* OTUs were 99% similar to *Methanosaeta concilii* (Barber *et al.*, 2011), and to *Methanosarcina mazei* (Deppenmeier *et al.*, 2002) both known to be

acetoclastic methanogens. The most abundant *Methanoregula* OTU was 98% similar to *Methanoregula boonei*, a hydrogenotroph. The polygonal pond BYL1 had a high percentage of RC II and a lower percentage of *Methanosarcina* compared to the other 3 ponds.

2.4 Discussion

The Bylot Island pro-glacial river valley's ice-wedge tundra terrain was covered by a network of ponds and was similar to the landscape of Samoylov Island, Eastern Siberia (Muster *et al.*, 2012). Our results clearly show that in addition to being a source of CO_2, as opposed to a sink, runnel ponds represented a larger source of CH_4 than polygonal ponds. Runnel ponds accounted for 44% of the open water in the valley, but contributed to 83% of the total CH_4 emissions that included lake emissions from a 3-year diffusive rate database. Our data suggest that CH_4 emissions from thawing permafrost could be strongly underestimated if measured only from the more frequently studied polygonal ponds (Grosse *et al.*, 2008; Sachs *et al.*, 2008; Tank *et al.*, 2009; Abnizova *et al.*, 2012). The smaller emissions from polygonal ponds may be due to more activity by the methanotroph community, and we note that stable isotopes were consistent with more CH_4 oxidation in polygonal ponds (Figure 2.5b).

Methane diffusion rates measured from runnel ponds (on average 0.76 mmol m^{-2} d^{-1}) were in the same range as reported from the thermokarst lakes in Siberia (Zimov *et al.*, 2001; Walter *et al.*, 2010], but relatively small compared to peatland ponds from the Hudson Bay lowland (Hamilton *et al.*, 1994), which were up to 48 mmol CH_4 m^{-2} d^{-1}. However, comparing flux estimates among studies of smaller aquatic systems is difficult due to several factors that are rarely considered, such as gas collection method, gas transfer model and flux calculation, time of day, season, latitude, water body size and depth, catchment geomorphology, and finally the presence or absence of thermokarst slumping. Here, we applied a correction factor (×0.2458; see methods) based on chamber flux measurements and wind-based estimates (Abnizova *et al.*, 2012) to account for the positive buoyancy flux occurring as thermal stratification evolves during the day in small-fetched and sheltered ponds. However, during the night, diffusion is likely to increase as water mixes due to heat loss, which was not included in our estimates. Moreover, estimates of CH_4 flux with gas exchange velocity based on Fick's law, and pure diffusive gas transfer such as for CO_2, do not take into account micro-ebullition. For these reasons, our runnel pond diffusive flux estimations may be conservative.

For the two polygonal ponds, which were measured repeatedly, the maximal ebullition rate reached 2.13 mmol m^{-2} d^{-1}, decreasing by ~1 order of magnitude over a few weeks. This was similar to the diffusive rates that were up to 0.77 mmol m^{-2} d^{-1} in the two ponds. This maximal ebullition rate was within the lowest range of values compiled by Walter et al. (2010) (see their Table 1) for northern aquatic systems (their *Arctic* class), and much less than for Siberian thermokarst lakes, which reached 1563 mmol m^{-2} d^{-1}. The high rates from Alaska and Siberia are from emissions categorized as point sources and hotspot ebullition, occurring in lakes with taliks and much thicker peat deposits. Taliks form under thermokarst lakes that are deep enough to have a layer of water and sediment or soil, which remains unfrozen in winter. These conditions are unlikely to occur under the shallow Bylot Island thaw ponds since they freeze to the bottom in winter, partly explaining their lower ebullition rates. Unfortunately ebullition measurements were only taken from polygonal ponds where funnels could be installed. However, considering that diffusive fluxes were on average 3.5 times higher in the runnel ponds, ebullition fluxes and overall CH_4 production were also likely to be greater in the runnel ponds.

A larger fraction of old C would also be available for microbial degradation in the runnel ponds compared to polygonal ponds because of peat erosion down to the thickness of the ~half meter active layer on Bylot Island. The base of the peat deposit, which is about 2 m thick, was aged at 3670 ± 110 BP (Fortier & Allard 2004). Discrete background ebullition samples collected from June to July 2011 showed little evidence of high release of this old stored C in the form of GHG from the two runnel ponds sampled. Runnel ponds however, exhibited a higher fraction of older C in CO_2 and CH_4 compared to polygonal ponds (Fig. 2.5). The utilization and release of a larger fraction of older C through point source ebullition could still occur at this site at certain times over the thaw cycle. For example, ebullition from point sources released much older C in Siberian and Alaskan thermokarst lakes, despite modern age C reported for background ebullition (Walter *et al.*, 2008).

Permafrost peat provides substrate for aquatic microbes (Roehm *et al.*, 2009), but the preferential use of modern C recently fixed from the atmosphere could be favored because of the greater lability of this pool (Guillemette & Del Giorgio 2011). In the case of the cyanobacterial mat-covered polygonal ponds on Bylot Island, the negative CO_2 flux most likely resulted from high photosynthetic rates in the mats, and the modern dates for CH_4 suggest that abundant labile compounds coming from a modern autochthonous pool could be the main C supply for

microbial activity, including methanogenesis. However, in more humic runnel ponds influenced by peat lixiviation, an older C signature in the CH_4 than what we found was expected. The predominance of AM and the high OC content of surface sediment (1.0 - 25.1%) indicate that both pond types were C-rich (Hornibrook *et al.*, 1997; Penning and Conrad 2007). These OC values were mostly greater than values reported in Siberian permafrost soils, for example in the Lena Delta 4 - 5% of OC is within the top 50 cm (Wagner *et al.*, 2007), which is similar to values from Northeast Siberia (Zimov *et al.*, 2006). The reasons for the high OC in surface sediment of small ponds lacking taliks could be due to slow microbial degradation rates linked to seasonal re-freezing. If this were the case, then a longer melt season could result in greater CH_4 emissions.

The sum of two methanogen genera adapted to high substrate levels was higher in runnel ponds than in polygonal ponds. These two genera have different CH_4 production pathways, *Methanobacterium* with the HM pathway (Karadagli & Rittmann 2007), and *Methanosarcina* with the AM pathway (Sakai *et al.*, 2009) (Figure 2.6), suggesting community adaptability. The main methanogens in thaw ponds were *Methanosarcina*, *Methanosaeta*, *Methanobacteriaceae*, *Methanomicrobiales,* and RC II, which is similar to the community retrieved from Svalbard peatlands and wetlands (Høj *et al.*, 2006; Høj *et al.*, 2008). Most of the descriptive studies to date on freshwater Arctic archaeal communities are from clone libraries, and at most three Orders out of the five known Orders of methanogens were found from a single site (Kobabe *et al.*, 2004; Metje and Frenzel 2007; Pouliot *et al.*, 2009; Barbier *et al.*, 2012). For instance, in 19 freshwater lakes, Borrel and colleagues [2011] reported 468 archaeal 16S rRNA sequences from clone libraries. *Methanomicrobiales* and *Methanosarcinales* dominated these lakes, with occasional sequences belonging to the *Methanobacteriales* (Borrel *et al.*, 2011). The higher number of methanogen Orders and presence of AM and HM pathways from Bylot Island may be a consequence of the high OC content in the ponds. Alternatively our high throughput sequencing approach with a minimum 1921 final reads per sample may have recovered the additional Orders.

Substrate availability for CH_4 production from acetate or CO_2 is likely to change seasonally due to the timing of ice melt and primary production, generating changes in the methanogen community structure (Høj *et al.*, 2006). For example, in Finnish boreal mires, there was a clear shift in the methanogen community over the arctic summer, with AM (*Methanosarcina* spp.) found only during early and mid summer (Juottonen, 2008). On Bylot Island, both AM and HM

methanogens were retrieved from the sediments. However, the isotopic signatures of CH_4 indicated that only AM was active in July (Figure 2.5a) suggesting that the HM biomass had built up earlier. These results also show that AM can be a significant summer production pathway in Arctic permafrost regions, as opposed to other thermokarst systems where only HM was thought to be significant (Brosius *et al.*, 2012). A methanogenic community composed of both AM and HM taxa will likely respond to wider temperature ranges and possible substrate changes that occur under climate stress, and both pathways should be considered in C budget estimates.

Thaw ponds contained reads with matches to methanogenic groups capable of both hydrogenotrophic and acetotrophic CH_4 production, providing the potential for community compensation under changing ambient conditions. However, the small size and great variability in shapes, limnology and microbial ecology of the ponds represent a challenge for scaling up their importance for global C cycling, especially since these ponds are primarily found in remote regions where logistic constraints are great. But considering that they have the potential to develop in permafrost and glaciated-influenced landscapes covering 9.6 millions of km^2 in circumpolar regions (Smith *et al.*, 2007), these small systems certainly deserve more attention. As the Arctic warms and permafrost recedes, the abundance of tundra ponds, especially runnel ponds generated by thaw slumping, is likely to increase. The higher CH_4 emissions measured from runnel ponds, and their potential to contain organic carbon deposited thousands of years ago qualify them as a positive feedback system contributing to climate dynamics.

Acknowledgements

We thank P.-G. Rossi, V. Gélinas, P. N. Bégin, C. Girard, L. Boutet, and G. Deslongchamps for their efficient help in the field and laboratory, A. Comeau for his precious help at the molecular laboratory and for pyrosequencing data processing, We also thank G. Gauthier for sharing his logistics allocation.

3 Arctic thaw pond morphology influences bacterial communities and associated greenhouse gas emissions

Influence des communautés fonctionnelles de bactéries sur les émissions de gaz à effet de serre par les petites mares de dégel du haut Arctique canadien

Karita Negandhi[1], Isabelle Laurion[1*], Connie Lovejoy[2]

[1]Centre Eau Terre Environnement and Centre for Northern Studies (CEN), Institut national de la recherche scientifique, Quebec, QC Canada

[2]Département de biologie, Institut de Biologie Intégrative et des Systèmes, and Takuvik, Université Laval, Quebec, QC Canada

Ce deuxième article complète le premier article en identifiant les communautés bactériennes et leurs rôles fonctionnels distincts relatifs au cycle des GES dans les mares polygonales et *allongées*. Les données moléculaires et physico-chimiques été traitées, analysées et interprétées sous la supervision de Connie Lovejoy et Isabelle Laurion. K. Negandhi a écrit la première version de l'article, suivi par des commentaires et suggestions formulées par les deux co-auteurs. L'article a été soumis à la revue *Polar Biology* le 5 Décembre 2013. Nous avons reçu les commentaires de l'éditeur le 31 mars 2014 et nous allons produire une version révisée de l'article avant le 31 mai tel que demandé.

Résumé

Le dégel du pergélisol dans un paysage Arctique modelé par les polygones de tourbe et les coins de glace résulte en la formation de nombreuses mares. Ces mares émettent du dioxyde de carbone (CO_2) et du méthane (CH_4) d'origine biologique. Ces émissions de gaz à effet de serre (GES) sont variables, pour des raisons qui ne sont pas bien comprises, mais elles sont vraisemblablement liées à un équilibre entre les producteurs et les consommateurs de GES dans les sédiments et la colonne d'eau, ainsi qu'aux propriétés physiques de l'eau (turbulence) contrôlant le taux d'échange des gaz avec l'atmosphère. Dans ce chapitre, nous avons étudié la diversité bactérienne des mares polygonales et des mares *allongées*, deux types distincts de mares couramment trouvés en zone de pergélisol continu. En utilisant une combinaison de séquences d'ARNr 16S Sanger et des séquences d'amplification à haut débit, nous avons constaté que les communautés bactériennes dans l'eau de surface sont clairement dominées par des hétérotrophes et sont similaires dans les deux types de mares, en dépit des propriétés physiques et chimiques de la colonne d'eau différentes. Toutefois, les communautés des sédiments de surface dans les deux types de mares étaient significativement différentes. Les sédiments des mares polygonales étaient colonisés par des hétérotrophes (46-29%) qui consomment la matière organique et produisent du CO_2, des cyanobactéries (20-27%) qui utilisent du CO_2 et produisent de l'O_2, et des méthanotrophes (11-20%) qui consomment du CH_4 et ont besoin d'oxygène. En revanche, les cyanobactéries étaient absentes des sédiments des mares *allongées,* qui étaient colonisées par des hétérotrophes (65-81%), des bactéries pourpres non-sulfureuses (5-21%) qui ne produisent pas d'O_2, et une quantité moins importante de méthanotrophes (1-5%). La plus faible proportion des séquences de méthanotrophes dans les mares *allongées* suggère un lien avec la géomorphologie, et fournit un outil potentiel de prédiction des émissions de GES en fonction de la morphologie du paysage.

Mots-clés: communautés méthanotrophes, carbone, thermokarst, pergélisol, méthane

Abstract

Permafrost thawing in the Arctic results in a polygonal patterned landscape and the formation of numerous thaw ponds. These ponds emit biologically produced carbon dioxide (CO_2) and methane (CH_4). These greenhouse gases (GHG) emissions are variable, for reasons that are not well understood, but related to a balance between GHG producers and consumers, as well as to physic-chemical properties of the water controlling exchange rates with the atmosphere. Here we investigated the bacterial diversity of polygonal and runnel ponds, two geomorphologically distinct pond types commonly found in the Arctic. Using a combination of 16S rRNA Sanger sequences and high throughput amplicon sequences, we found that bacterial communities in overlying water were clearly dominated by hetertrophs and were similar in both pond types, despite their variable physical and chemical properties. However, surface sediment communities in the two pond types were significantly different. Polygonal pond sediment was colonized by heterotrophs (46 – 29%) and Cyanobacteria (20 – 27%), which take up CO_2 and produce O_2, and methanotrophs (11 – 20%) that consume CH_4 and require oxygen. In contrast, Cyanobacteria were effectively absent from the surface sediment of the runnel ponds that in addition to heterotrophs (65 – 81%) were colonized by purple non-sulfur bacteria (5 – 21%), which do not produce O_2, and by fewer methanotrophs (1 – 5%). The defavorisation of methanotrophs in the runnel ponds suggests links between geomorphology and bacterial communities and provides a potential tool for predicting future GHG emissions based on landscape morphology.

Key words: methanotrophic communities, carbon, thermokarst, permafrost, methane

3.1 Introduction

The onset of warmer temperatures in the Arctic and the associated permafrost thawing has led to the formation of shallow lakes and ponds, some of them featuring thermokarst slumping. The importance of these thawing permafrost areas, in terms of global greenhouse gases (GHG) emissions, is currently subject to debate (Gao *et al.*, 2013), but these ponds are potentially a mechanism for climate warming positive feedback. This is because Arctic permafrost contains about 40% of the worlds near surface labile carbon (C) (McGuire *et al.*, 1995), part of which is from an old peatland storage that could be released back to the atmosphere in the form of GHG (Billings *et al.*, 1998). In similar systems dissolved organic carbon (DOC) originating from degrading permafrost mires significantly increases bacterial C consumption, and thus influences land-atmosphere C balances (Roehm *et al.*, 2009; (Vonk *et al.*, 2013). Moreover, aquatic photolysis of this recently mobilized pool of C can accelerate the microbial turnover and the production of GHG, especially within shallow ponds that are exposed to the intense Arctic sunlight in summer (Laurion *et al.*, 2013). Arctic wetlands are considered as the largest, natural, solitary contributor to atmospheric CH_4, and were estimated to account for ~25% of global annual emissions (Fung *et al.*, 1991; Bousquet *et al.*, 2006). Permafrost C cycling within small thaw ponds significantly influences their GHG emissions (Abnizova *et al.*, 2012) and the proportion of old C stocks fueled through microbial activity, and this ecosystem should be included in global estimations.

The limnological and geomorphological characteristics of thaw lakes generate large differences in GHG cycling and emission dynamics (Christensen *et al.*, 2007). This is evidenced by the shallow thaw ponds of Bylot Island, Canada, with summer GHG flux varying over 4 orders of magnitude (Laurion *et al.*, 2010; Negandhi *et al.*, 2013). Siberian and Alaskan lakes have been estimated to emit anywhere between 6.6 to 64 Tg CH_4 yr^{-1} (Walter *et al.*, 2006). These variable emission rates measured during early spring and summer throughout the Arctic can be explained by a wide range of microbial assemblages and physicochemical conditions, in addition to seasonality and methodological uncertainties (Zimov *et al.*, 2001;Wagner *et al.*, 2005; Zona *et al.*, 2008; Walter *et al.*, 2010).

Given the biological reactivity of carbon, and the specialization of different bacterial groups within the carbon cycle (Strickland *et al.*, 2009), understanding environmental factors that select for bacterial communities and their functional guilds across the landscape (Green *et al.*, 2008)

should provide a link between physical and trophic characteristics of thaw ponds and the variability in GHG emissions. Microbial functions broadly involved in CO_2 and CH_4 cycling include heterotrophs, phototrophs, methanotrophs, and methanogens. The relative proportions of these microbial functional groups could easily influence the GHG emissions across Arctic landscapes.

Overall there are large uncertainties in our understanding of the communal role of aquatic microbes in GHG cycling. Therefore a pressing need exists to identify how microbial communities contribute to the production and consumption of CO_2 and CH_4 to better understand future GHG emission scenarios (Bardgett *et al.*, 2008). The goal of the present study was to investigate the bacterial community of Arctic thaw ponds that contribute to GHG cycling, while the methane producers (Archaea) were examined in a companion study (Negandhi *et al.*, 2013). Bacterial assemblages from five thaw ponds, located in the continuous permafrost region of eastern Canada and featuring varying limnological and geomorphological conditions, were investigated through 16S rRNA gene pyrosequencing in waters and sediments. Our aim was to identify the influence of pond geomorphology and its associated environmental and physical properties on bacterial communities. These bacterial communities were categorized into functional guilds to identify the controlling factors regulating GHG emissions from polygonal and runnel thaw ponds.

3.2 Material and Methods

3.2.1 Study Site and limnological variables

Samples were collected in the continuous permafrost region of eastern Canada, in the Sirmilik National Park, on Bylot Island, Nunavut (73°09'N, 79° 58'W). The active layer depth is between 40 and 60 cm at the study site in the valley of glacier C-79 (Fortier & Allard 2004); D. Fortier pers. comm.). The 1-2 m deep thaw ponds were categorized by their geomorphologic shapes associated with the thawing permafrost: polygonal ponds formed on top of low centered polygons, and runnel ponds formed over melting ice wedges. In general, polygonal ponds are more physically stable systems colonized by thick microbial mats (Vézina and Vincent 1997), while thermokarst slumping and peat erosion characterize the runnel ponds. Larger bodies of

water or lakes (kettle and thermokarst lakes) are also present at the sampling site. These lakes are a few meters deep (~3-5 m).

In July 2009, we sampled a total of 17 ponds (5 for bacterial communities) and 2 lakes for dissolved GHG concentrations and limnological characteristics. Temperature, conductivity, dissolved O_2, and pH were measured with a 600R multi-parametric probe (Yellow Spring Instrument). Continuous surface temperature was recorded hourly with HOBOware™ U12 thermistors placed at 10 cm below the air-water interface in two ponds (polygonal BYL1 and runnel BYL24) from July 2008 to July 2009. Additionally, temperature profiles soon after ice melt were recorded with the YSI probe in June 2011. Dissolved organic carbon (DOC) concentrations were measured with a Shimadzu TOC-5000A carbon analyzer. Colored dissolved organic matter (CDOM) optical properties (a_{320} and $S_{275-295}$ defined by (Helms *et al.*, 2008) were obtained by filtering water through pre-rinsed 47 mm diameter, 0.2 μm pore size cellulose acetate filters (Advantec Micro Filtration System), then scanned from 200 to 800 nm on a Cary 100 spectrophotometer (Varian). Water samples for soluble reactive phosphorus (SRP) and anions were pre-filtered as above and measured as in Laurion *et al.* 2010. Similarly, major cation samples were also filtered as above in addition to being fixed with HNO_3. Total phosphorus (TP) and total nitrogen (TN) were quantified from unfiltered water samples fixed with H_2SO_4 following Stainton *et al.*, 1977. Particulate material used to estimate chlorophyll *a* (Chl *a*) was filtered onto 0.7 μm nominal pore size glass fiber filters (Advantec MFS), the pigments extracted with 95% aqueous MeOH, and the Chl *a* concentrations determined by high-pressure liquid chromatography using the method adapted by Bonilla et al. (2005).

Dissolved CO_2 and CH_4 gas concentrations in surface pond water were determined by the equilibration of 2 liters of water into 20 mL of ambient air for 3 min. The resulting headspace was injected into duplicate vials (BD 3 mL Vacutainers, or Labco 5.9 mL Exetainers) that had been previously flushed with helium and evacuated. Gas samples were analyzed by gas chromatography (Varian 3800 with a COMBI PAL head space injection system and a CP-Poraplot Q 25 m 3 0.53 mm column and flame ionization detector). Dissolved gas concentration was calculated using Henry's Law, and further used to estimate gas flux at the pond interface using the gas exchange coefficient from the empirical model of Cole and Caraco (Cole *et al.*, 1998) and corrected as detailed by Negandhi *et al.* (2013). Wind speed for estimating gas flux was obtained from the SILA meteo station of the Centre for Northern Studies located < 500 m from the ponds. To identify a possible distinguish between polygonal and runnel pond

physicochemical properties, a principal component analysis (PCA) statistical analysis of was performed on PAST (Hammer *et al.*, 2001). Dissolved GHG cnoncentrations were not utilized in the PCA since they are they would be a consequence. Separate t-tests were performed on the GHG concentrations between pond types.

3.2.2 Diversity and community composition

Surface sediments and surface water of 5 ponds (BYL1, 22, 24, 27, 38; n=10) were selected for high throughput pryosequencing targeting the 16S V6-8 region of the 16S rRNA gene (Comeau *et al.*, 2011). From these 5 ponds, one polygonal (BYL1) and one runnel pond (BYL38) were selected for the taxonomic characterization of surface water Bacteria communities via cloning and Sanger sequencing of the bacterial 16S rRNA gene. Water samples collected just below the surface were filtered sequentially through a 3 µm pore size polycarbonate (PC) filter and a 0.2 µm Sterivex unit (Millipore). Both filters were preserved in buffer (40 mM EDTA; 50 mM Tris at pH 8.3; 0.75 M sucrose), frozen in liquid nitrogen (≤ 2 weeks), and stored at -80°C upon arrival at the lab, until DNA extraction using phenol:chloroform:Indole-3-Acetic Acid (25:24:1) and chloroform:Indole-3-Acetic Acid (24:1) (Massana *et al.*, 1997). Surface sediment samples were obtained from ~6.5 cm long cores using a sterile cut 60 mL polycarbonate syringe. The cores was placed into sterile plastic bags and homogenized, 3 mL sub-samples were then put into 5 mL cryotubes with buffer and frozen as above. Sediment sample DNA was extracted using the MO BIO Kit (RNA powersoil total RNA isolation kit #12866-25 and DNA elution accessory kit #12867-25).

3.2.3 Clone Libraries

Extracted DNA was amplified by polymerase chain reaction (PCR) using bacteria specific primers 8F (5′-AGAGTTTGATCCTGGCTCAG-3′) and a universal reverse primer 1492R (5′-GGTTACCTTGTTACGACTT-3′) (Galand *et al.*, 2008). The PCR reaction mixture consisted of 5 µL 10X Mg buffer (Feldan), 1 µL 200 µM dNTP (Feldan Bio), 1 µL 0.4 mg mL^{-1} BSA (Fermentas), 0.25 µL 1.25 U Taq polymerase (Feldan), 1.5 µL of both 0.3 µM primers (Invitrogen), 0.1 – 1 of template DNA for both size fractions, and the addition of distilled H_2O for a total of 50ml. Amplification cycles included denaturation at 94°C for 3 min, 30 cycles at 94°C for 1 min, 55°C for 1 min, 72°C for 1 min, and a final extension at 72°C for 7 min. PCR products

were purified (QIAquick PCR purification kit; QIAGEN), quantified spectrophotometrically (Nanodrop ND-1000), and the two size fractions were then combined in equal quantities. An overhanging 3'-A post amplification was performed with the following mixture: 45 µL purified PCR product, 5 µL 10x buffer (Feldon), 1 µL 10 mM dATP (Feldon), 0.2 µL Taq polymerase (Feldan), and incubated at 72°C for 10 min. Amplicons were then cloned using the TOPA TA cloning kit (Invitrogen) following the manufacturers recommendations. Positive colonies were sequenced in both directions using the T7 promoter of the M13 vector at the Centre Hospitalier de l'Université Laval (CHUL, QC, Canada). Final sequences (≥1,400 bp) compiled and edited using BioEdit© (Hall, 1999) were subjected to a Basic local alignment tool search (BLASTx) against GenBank National Center for Biotechnology Information (NCBI). Sequences with at least the 97% similarity were grouped as operational taxonomical units (OTUs) and submitted to GenBank under the accession numbers KF650376-396 for BYL1 water, and KF650397-425 for BYL38 water.

3.2.4 Pyrosequencing

High-throughput 16S rRNA gene pyrosequencing for bacteria was performed as in Comeau et al. (2011). Briefly, a PCR reaction mixture consisting of 1X HF buffer (NEB), 200 µM dNTP (Feldan Bio), 0.4 mg mL^{-1} BSA (Fermentas), 0.2 µM of each primer (969F: ACGCGHNRAACCTTACC and 1406R: ACGGGCRGTGWGTRCAA, Invitrogen; see Comeau et al. 2011 for primer design), 1 U of Phusion High-Fidelity DNA polymerase (NEB), 0.01 – 1 µL of template DNA for water samples, or 0.01 – 0.5 µL for sediment samples, and the addition of distilled H_2O for a total of 50ml. Triplicate reactions for each sample were performed with DNA concentrations between 1X – 2.22X. Amplification cycles included denaturing at 98°C for 30s, 30 cycles at 98°C for 10s, 55°C for 30s, 72°C for 30s, and 72°C for 5 min. Resulting triplicate PCR products for each sample were pooled together for purification (QIAquick PCR purification kit; QIAGEN) and quantification (Nanodrop ND-1000). The equally mixed coded amplicons were sequenced on a Roche 454 GS-FLX Titanium platform at Université Laval Plate-forme d'analyses Génomiques. Raw reads were submitted to NCBI Sequence Read Archive (SRA) under accession number SRA039814, and the corresponding Sequence Read Sample (SRS) numbers 476754 for sediment and 476588 for water. Before the taxonomical analyses, reads were subjected to pyrotag pre-processing and quality control (as in Comeau *et al.*, 2011). A round of elimination was based on the presence of any non-assigned nucleotides (N's), length <

150 bp, amplicon size larger than expected, and the existence of an incorrect Forward primer sequence. In addition, any existing bases beyond the reverse primer were trimmed. Next, reads were aligned against SILVA reference alignments using Mothur (Schloss *et al.*, 2009), followed by a manual check to remove misaligned reads. Before further analysis was performed, the remaining reads were randomly resampled to 2075 per sample. The SILVA database (version 108) was used for bacterial identifications, which included additional previously generated clone library sequences (Comeau *et al.*, 2012) from the C. Lovejoy laboratory. Resulting identified taxa were then assigned to known functional groups based on literature searches. Functional groups were confirmed down to the Genus level when information was available. Bacteria without known functions were categorized as unknown function.

Water sample BYL1 and BYL38 representative abundant OTUs reads and clone library sequenced were combined for an alignment made on MUSCLE (Edgar, 2004) followed by a trimming to similar lengths. A minimum block or sequence length of 10 parameters was used with any gaps removed using Gblocks (v0.91b) (Castresana 2000). A maximum likelihood tree was produced using PhyML program and an approximate likelihood ratio test for branch values (v3.0 aLRT) (Guindon and Gascuel 2006; Anisimova and Gascuel 2006).

3.3 Results

3.3.1 Physiochemical properties

Thaw pond depth ranged from ~0.5 to 1.5 m and ponds froze to the bottom in winter. Water temperature over a complete year cycle ranged between -26.7 and 21.4°C (averaging -7.5°C), with surface temperature remaining below zero from ~25 September 2008 to 4 June 2009. From this cycle, we estimated that open water conditions last about 111 days. Runnel ponds were thermally stratified soon after ice melt and for a large part of the summer, whereas the polygonal ponds were mixed from top to bottom over most of the summer (Table 3.1).

Table 3.1 Temperature profiles from a polygonal pond (BYL1) and a runnel pond (BYL38).

	Depth (m)	Temperature (°C)	
		BYL1	BYL38
July 2009	0	15	14
	0.4	15	5
	0.8	14	3
June 2011*	0	14	14
	0.4	14	5
	0.6	-	4

*2011 profiles were done soon after ice melt and hence have a shallower depth as the ice was still present on the pond bottom

The average pH of pond water at time of sampling was 8.35 for polygonal ponds (n=8), 6.69 for runnel ponds (n=9), and 7.34 for lakes (n=2). Soluble reactive phosphorus (SRP) was below detection limit (DL) in polygonal ponds, but above DL in 7 of the 9 runnel ponds sampled (averaging 0.8 μg L^{-1}), and above DL in one lake (0.65 μg L^{-1}). There was more variability in total phosphorus (TP), with average concentrations of 18.6 μg L^{-1} for polygonal ponds, 37.8 μg L^{-1} for runnel ponds, and 10.6 μg L^{-1} for lakes. A similar trend in total nitrogen (TN) was seen with average concentrations of 0.4 μg L^{-1} for polygonal ponds, 0.8 μg L^{-1} for runnel ponds, 0.2 μg L^{-1} lakes. Water column Chl *a* concentrations averaged 2.4 μg L^{-1} in polygonal ponds, 4.4 μg L^{-1} in runnels ponds and 1.5 μg L^{-1} in the two lakes. There were statistically significant differences in C quantity and quality (DOC, a_{320}, and $S_{275-295}$) between polygonal and runnel ponds (Table 2). Dissolved organic matter (DOM) concentrations were higher in runnel ponds (DOC and a_{320}), while there was more labile carbon in polygonal ponds with the larger $S_{275-295}$. Runnels ponds also clearly showed higher concentrations in GHG than polygonal ponds (Table 3.2). In fact, CO_2 was largely below saturation in polygonal ponds.

Table 3.2 Averages (± standard deviation) from 2009, showing differences in dissolved organic matter (DOM), expressed as the concentration in dissolved organic carbon (DOC, mg L^{-1}) and the absorption coefficient of DOM at 320 nm (a_{320}, m^{-1}), its lability, expressed by DOM absorption slope calculated between 275 and 295 nm ($S_{275-295}$; more labile DOM = higher S-values), and in dissolved GHG concentrations between polygonal ponds and runnel ponds.

	DOM		DOM lability	GHG	
	DOC (mg L^{-1})	a_{320} (m^{-1})	$S_{275-295}$ (nm^{-1})	CO_2 (μM)	CH_4 (μM)
Polygonal (n=8)	9.5 (1.1)	16.4 (2.8)	0.0196 (0.0014)	9.9 (7.1)	2.2 (1.3)
Runnel (n=9)	13.2 (2.7)	45.3 (16.6)	0.0150 (0.0015)	127.3 (94.7)	7.0 (3.3)
T-test p-values	0.0192	0.0028	0.0018	0.0174	0.0194

When factoring in carbon characteristics (DOC, a_{320}, and $S_{275-295}$), nutrients and major ions (SRP, TP, TN, NOx, SO_4, Ca, Fe, K, and S), temperature, O_2, pH and Chl *a*, the thaw ponds grouped by geomorphological shapes (Figure 3.1), with the combined physicochemical properties explaining 64% of the differences. The two lakes also tended to group with the polygonal ponds.

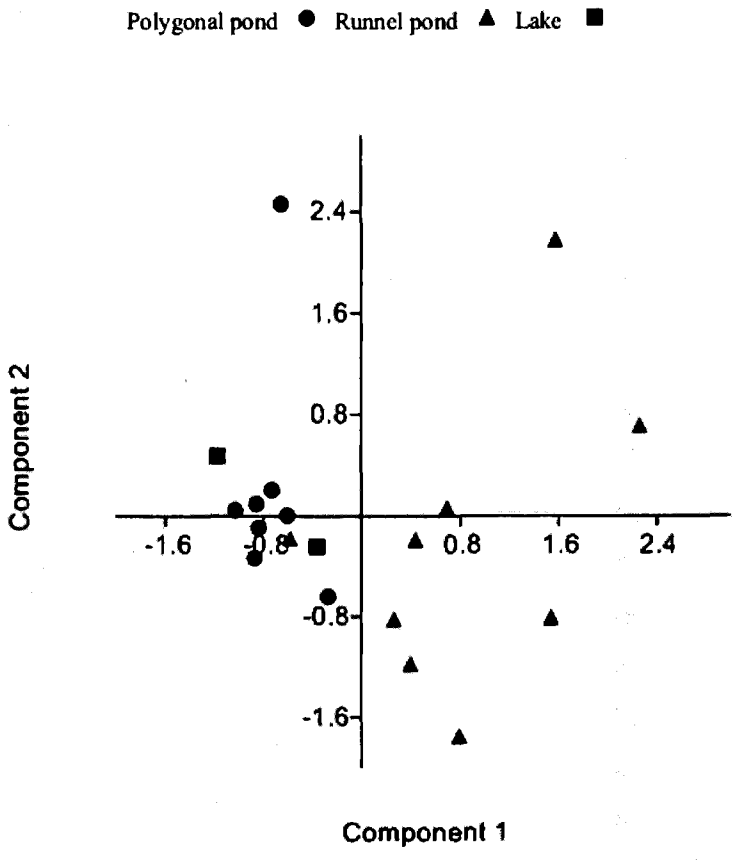

Figure 3.1 Principal component analysis of thaw pond physiochemical properties (nutrients, temperature, O_2, pH, Chl *a*, DOC, a_{320}, and $S_{275-295}$) explaining a total of 64% of the variability, with polygonal ponds grouping together with two larger lakes also sampled at the same site, and separating from most runnel ponds along axis 1 (46% of variability)

3.3.2 Bacterial community

The bacterial community composition obtained with the clone library sequencing and pyrosequencing were correlated ($r > 0.7$; $P \leq 0.03$) for the two pond water samples where cloning was performed, along with similar distributions of clone sequences and pyrosequencing reads in a neighbor joining phylogenetic tree (Figure 3.2). In polygonal pond BYL1, the unclassified *Chitinophagaceae* reads from pyrosequencing were identified as *Ferruginibacter alkalilentus*, and the unclassified *Micrococcineae* reads were identified as *Sporichthya polymorpha* (Figure 3.2a) using the longer reads from clone library sequences. Similarly, in both polygonal and runnel ponds, *Polynucleobacter* pyrosequencing reads were identified as *Polynucleobacter necessarius* (Figure 3.2b). *P. necessarius* was a dominant taxa from the surface water of runnel pond BYL38.

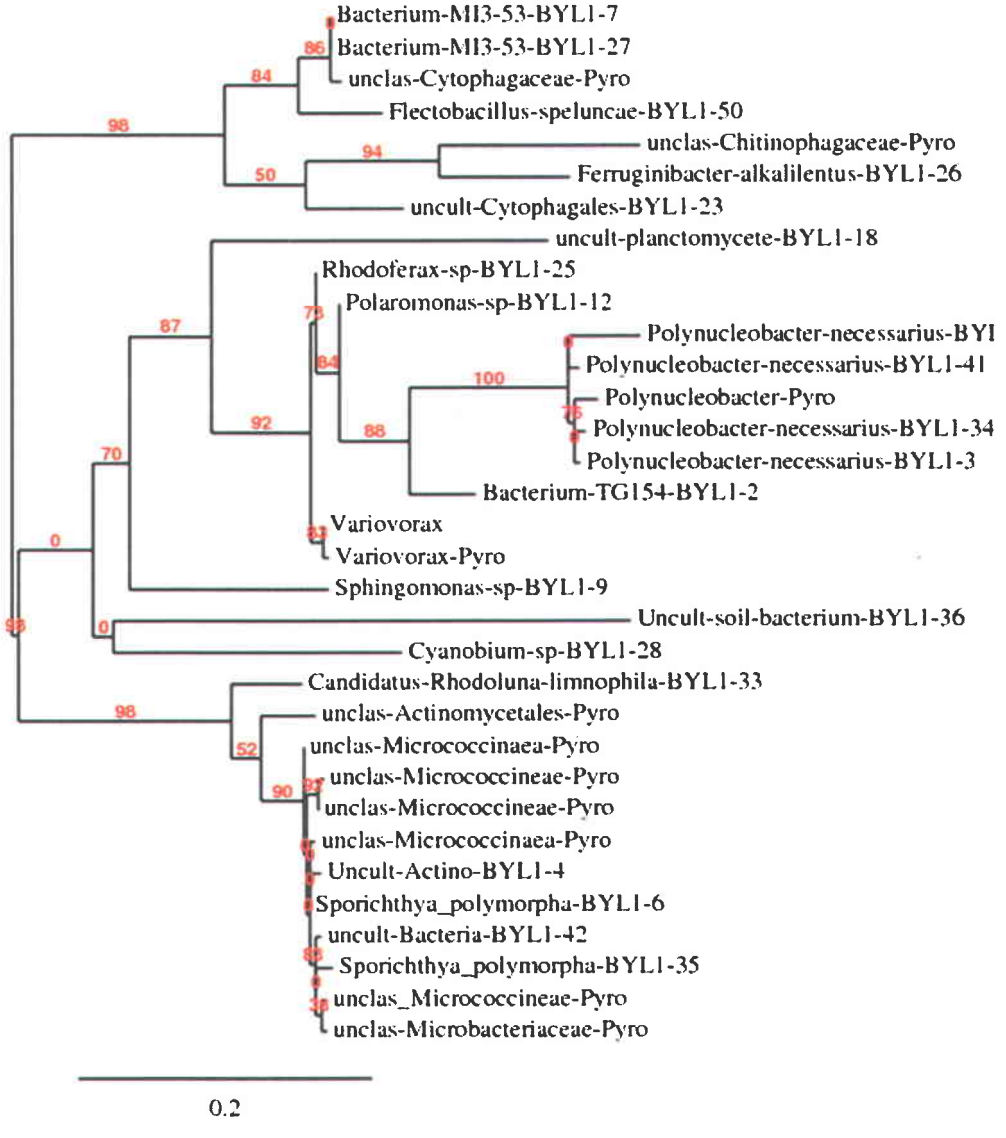
Bacterium-MI3-53-BYL1-7
Bacterium-MI3-53-BYL1-27
unclas-Cytophagaceae-Pyro
Flectobacillus-speluncae-BYL1-50
unclas-Chitinophagaceae-Pyro
Ferruginibacter-alkalilentus-BYL1-26
uncult-Cytophagales-BYL1-23
uncult-planctomycete-BYL1-18
Rhodoferax-sp-BYL1-25
Polaromonas-sp-BYL1-12
Polynucleobacter-necessarius-BYI
Polynucleobacter-necessarius-BYL1-41
Polynucleobacter-Pyro
Polynucleobacter-necessarius-BYL1-34
Polynucleobacter-necessarius-BYL1-3
Bacterium-TG154-BYL1-2
Variovorax
Variovorax-Pyro
Sphingomonas-sp-BYL1-9
Uncult-soil-bacterium-BYL1-36
Cyanobium-sp-BYL1-28
Candidatus-Rhodoluna-limnophila-BYL1-33
unclas-Actinomycetales-Pyro
unclas-Micrococcinaea-Pyro
unclas-Micrococcineae-Pyro
unclas-Micrococcineae-Pyro
unclas-Micrococcinaea-Pyro
Uncult-Actino-BYL1-4
Sporichthya_polymorpha-BYL1-6
uncult-Bacteria-BYL1-42
Sporichthya_polymorpha-BYL1-35
unclas_Micrococcineae-Pyro
unclas-Microbacteriaceae-Pyro
0.2

a

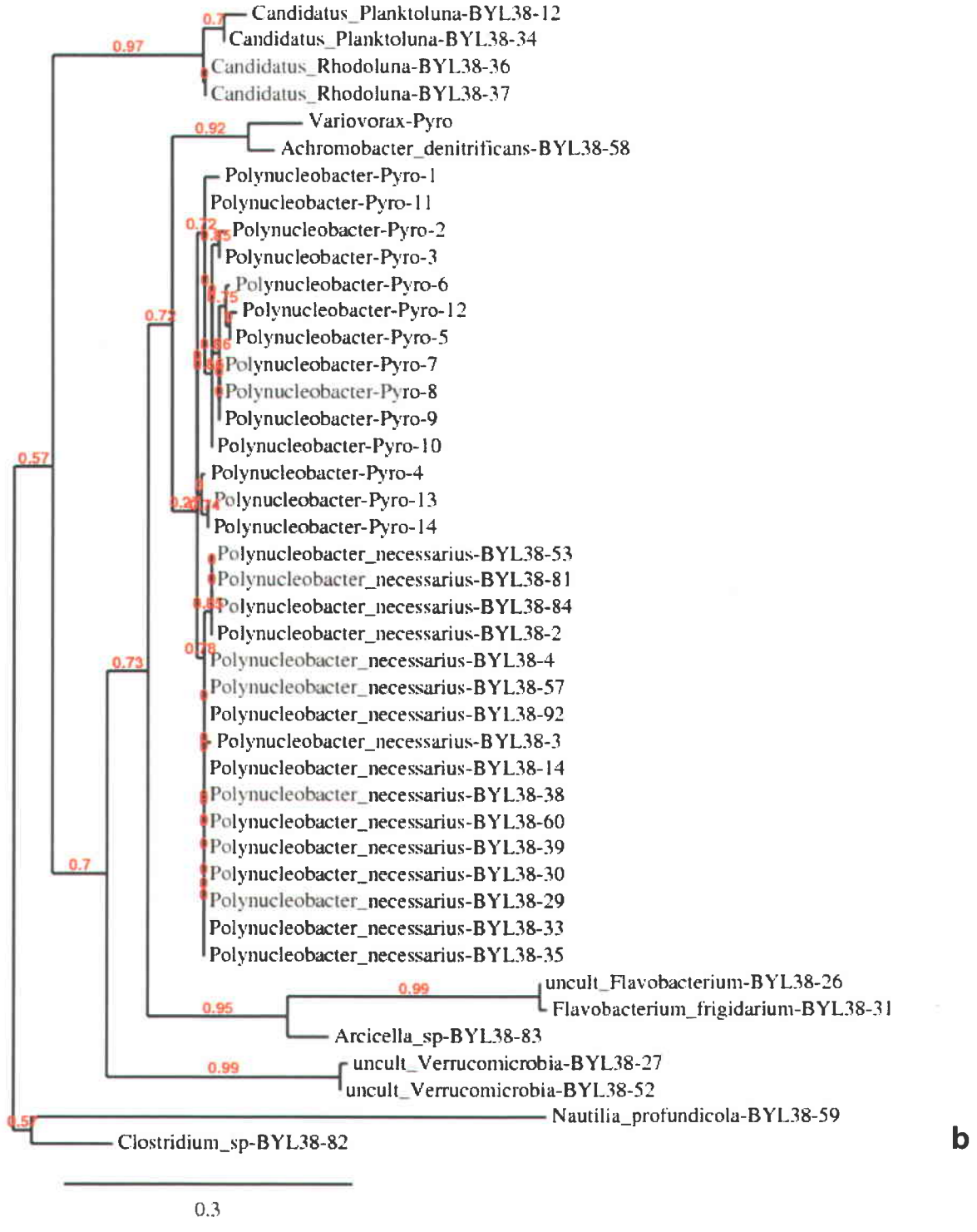

Figure 3.2 Maximum likelihood phylogenetic tree with bootstrap values at braches. Tree includes surface water bacterial communities combining clone library sequences at species level and the representative abundant pyrosequencing OTUs at genius level. Pyro reads are identified by 'pyro' at end of branch label following its BLAST identity a) Phylogenetic tree for polygonal pond BYL1 b) Phylogenetic tree for runnel pond BYL38

There was a clear separation between surface water and surface sediment bacterial communities (Figure 3.3). The water bacterial community consisted largely of heterotrophs (89 - 99%), some purple non-sulfur bacteria (1 – 3 %), methanotrophs (0 – 1%), and a few OTUs that could not be assigned to any functional group (1 – 7%) (Figure 3.4a). The heterotrophs consisted mainly of Phyla Bacteroidetes, Betaproteobacteria, and Actinobacteria (Figure 3.4b). Within the surface sediment communities, there was some grouping between runnel and polygonal ponds, along with a comparatively lower occurrence of heterotrophs (Figure 3.5). Besides heterotrophs (29 – 81%), the surface sediment bacterial functional groups included phototrophs (purple non-sulfur bacteria and cyanobacteria, 5 – 27%), methanotrophs (1 – 20%), symbionts for methanogens (1 – 4%), and some OTUs with unknown functions (9 – 15%) (Figure 3.5a). While the sediment heterotrophs make up a lower total percentage of the community compared to the water community, it includes the additional phyla of Gemmatimonas, Firmicutes, and Acidobacteria (Figure 3.5b). Compared to polygonal ponds, the runnel pond sediment had more heterotrophs, very few (if any) of the cyanobacteria, fewer methanotrophs, and two reported methanogenic symbionts genus, *Geobacter* and *Syntrophus*. A range of methanotrophs was identified (Figure 3.5c), and a negative relationship between the relative abundance of sediment methanotrophs (CH_4 oxidizers) and dissolved CH_4 concentrations in surface waters was found (r=-0.895, P=0.040) among the 5 ponds.

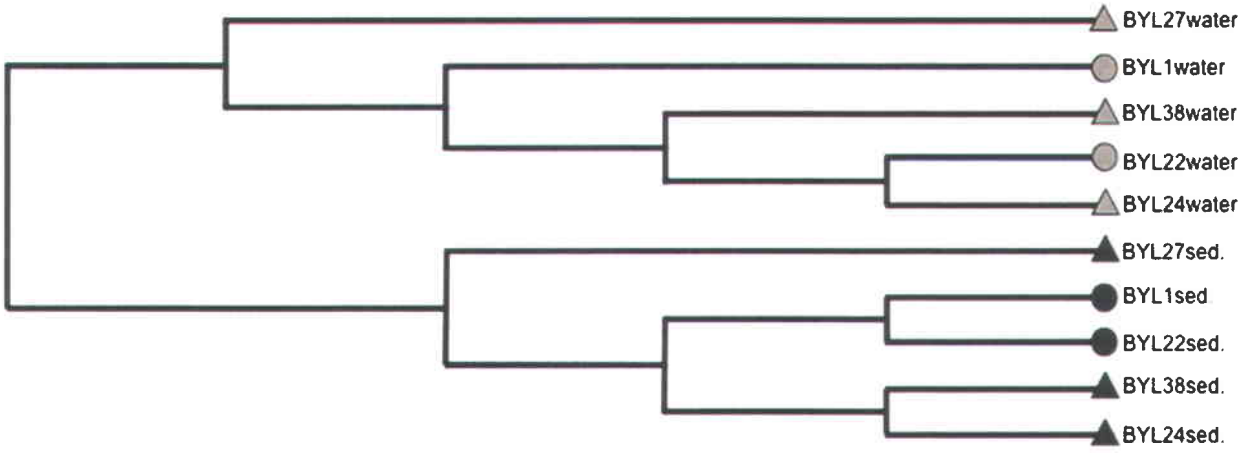

Figure 3.3 Bray-Curtis cluster of surface water and surface sediment bacterial community OTU numbers, with branch lengths proportional to the amount of differentiation (Hammer *et al.*, 2001). The bacterial communities show the occurrence of two clusters for water (n=5) and surface sediment communities (n=5). Surface sediment communities sub-cluster by pond geomorphologies, sub-cluster I containing polygonal ponds (n=2) and sub-cluster II containing runnel ponds (n=3).

● Polygonal water; ■ Runnel water; ● Polygonal sediment; ■ Runnel sediment

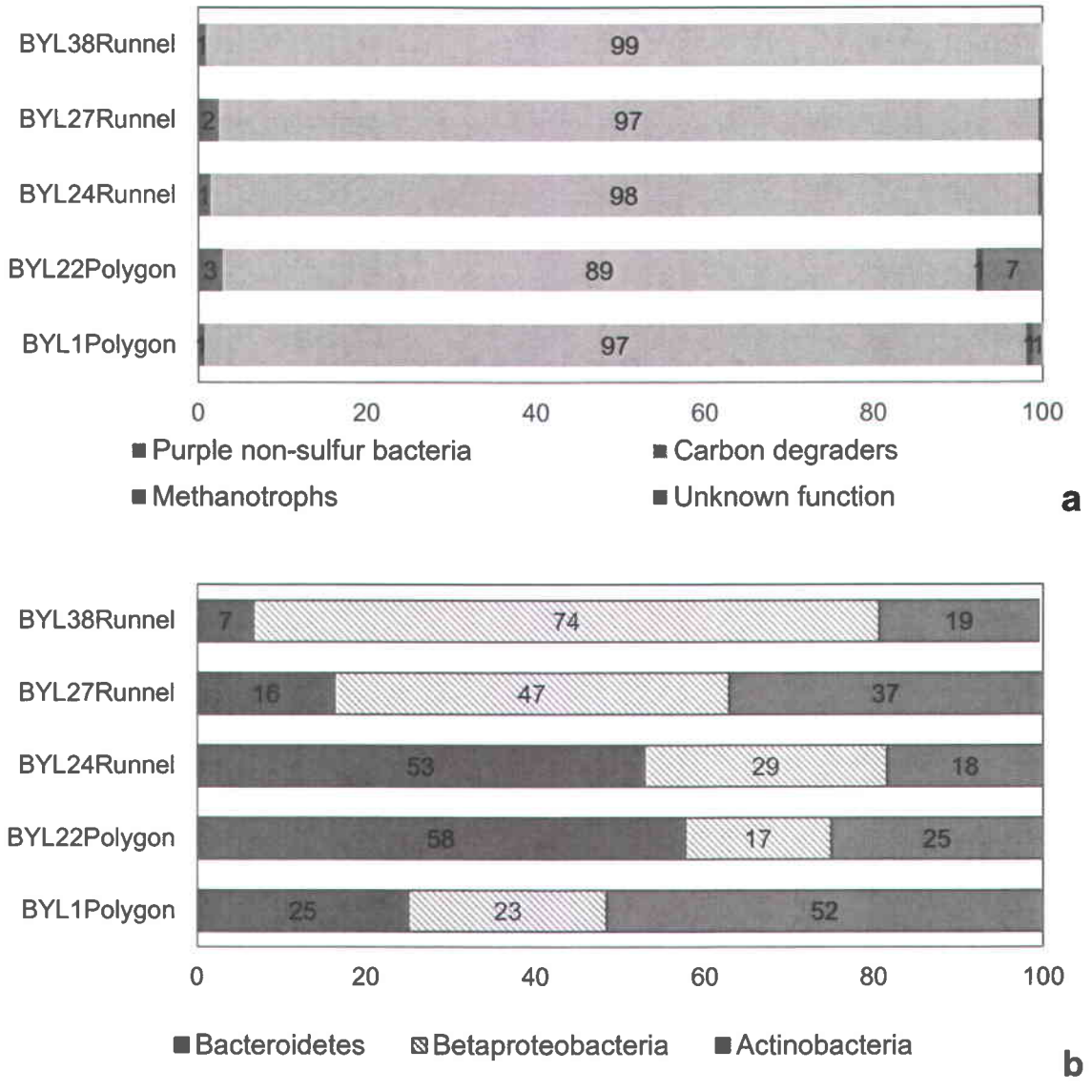

Figure 3.4 a) Percentage of the bacterial sequence functions in surface water samples; b) Percentage of the bacterial phyla contrubuting to the heterotrophs in surface water samples

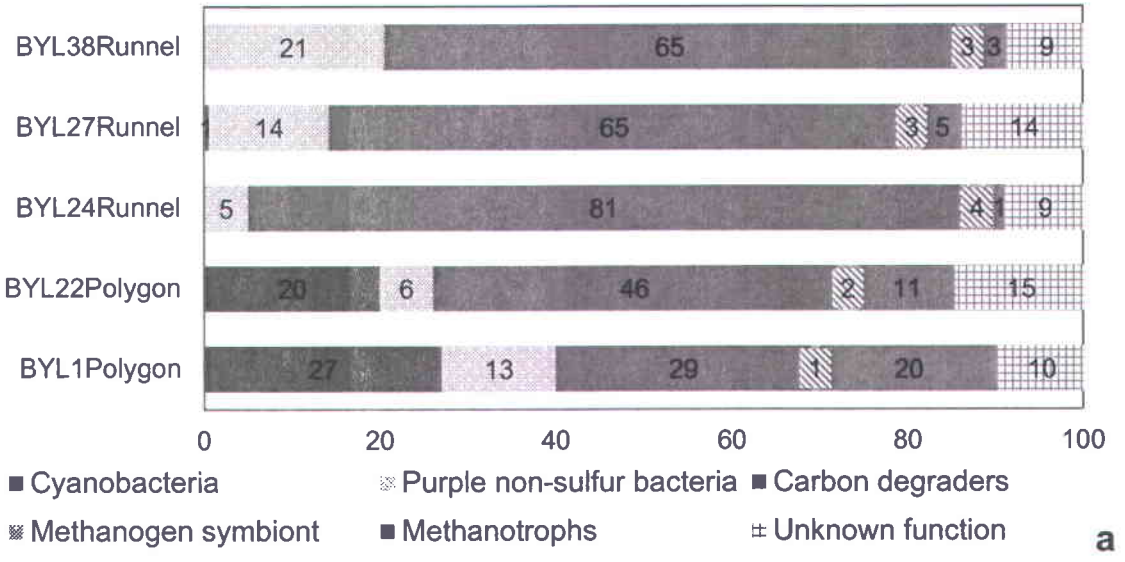
BYL38Runnel
21
65
3
3
9
BYL27Runnel
1
14
65
3
5
14
BYL24Runnel
5
81
4
1
9
BYL22Polygon
20
6
46
2
11
15
BYL1Polygon
27
13
29
1
20
10
0
20
40
60
80
100
Cyanobacteria
Purple non-sulfur bacteria
Carbon degraders
Methanogen symbiont
Methanotrophs
Unknown function

a

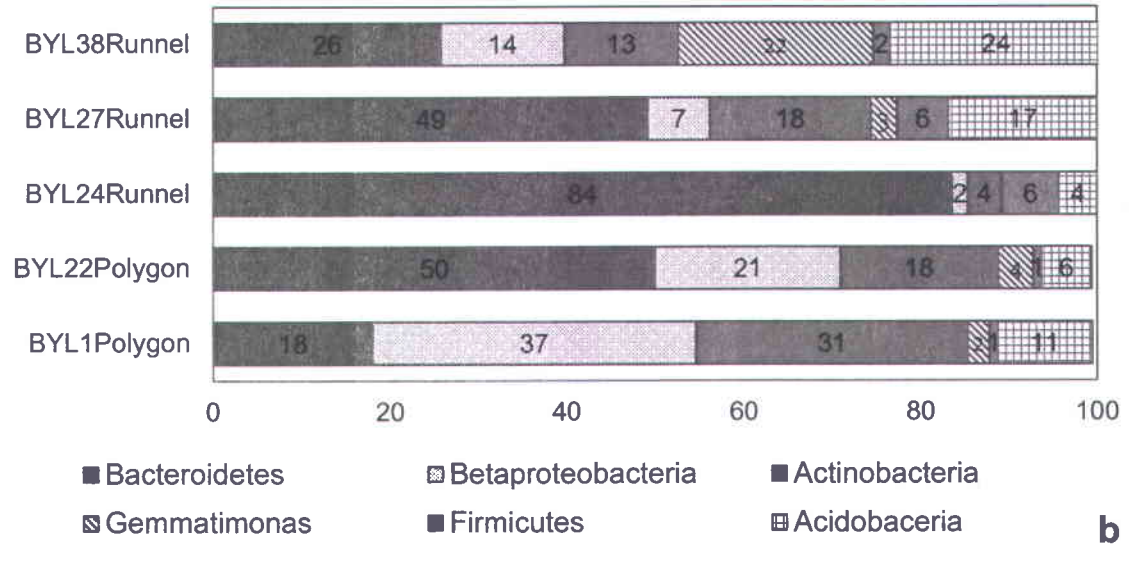
BYL38Runnel
26
14
13
22
2
24
BYL27Runnel
49
7
18
3
6
17
BYL24Runnel
84
2
4
6
4
BYL22Polygon
50
21
18
4
1
6
BYL1Polygon
18
37
31
2
11
0
20
40
60
80
100
Bacteroidetes
Betaproteobacteria
Actinobacteria
Gemmatimonas
Firmicutes
Acidobaceria

b

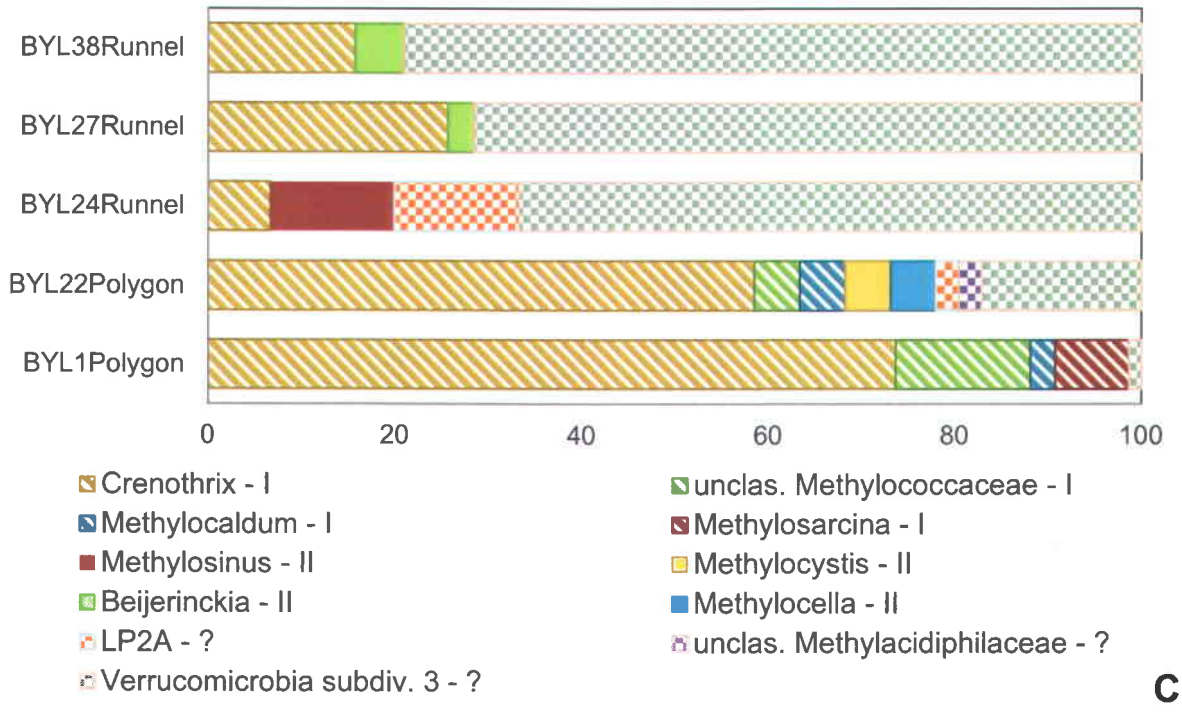

Figure 3.5 a) Percentage of the bacterial sequence functions in surface sediment samples; b) Percentage of the bacterial phyla contributing to the heterotrophs in surface sediment samples. The methanotrophs were excluded from Betaproteobacteria; c) Percentage of methanotroph genuis within surface sediments. Diagonal lines for type I, solid for type II, and checkered for phylum Verrucomicrobia with a currently unidetnified pathway

3.4 Discussion

The polygonal pond sediment bacterial communities were distinct from the runnel pond communities. The dominance of Cyanobacteria reads from the polygonal ponds was not surprising since the thick orange benthic mats and the high levels of benthic Chl *a*, up to 34.8 µg cm^2, have been reported earlier in Bylot Island polygonal ponds (Vezina *et al.*, 1997). The lower CO_2 and CH_4 emissions from polygonal ponds (averages estimated as -1.2 and +0.3 mmol m^{-2} d^{-1} respectively) compared to runnel ponds (respectively +15.7 and +1.0 mmol m^{-2} d^{-1}) could be linked to their sediment bacterial community composition (Figure 3.6). In particular, polygonal ponds had more Cyanobacterial phototrophs (Figure 3.5a) that consume CO_2 and produce O_2; water column O_2 levels were greater in the polygonal ponds, averaging 11.5 mg L^{-1} (n=8) compared to 9.2 mg L^{-1} in runnel ponds (n=9). The presence of O_2 is important for methanotrophs and could explain their higher occurrence in polygonal ponds, and therefore a

lower concentration of dissolved CH_4 (Table 3.2). The utilization of CO_2 by Cyanobacteria is also evidenced by the negative CO_2 fluxes most frequently observed in polygonal ponds.

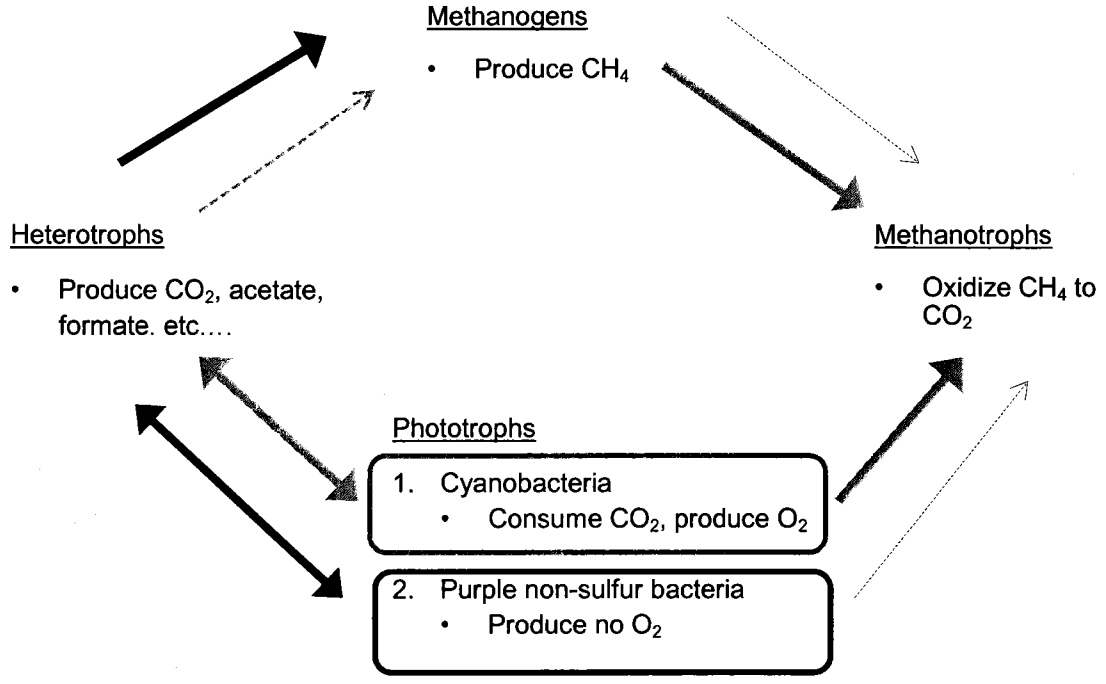

Figure 3.6 Basic relationships among bacterial functions related to GHG production and that were identified in the presented arctic thaw ponds. Black arrows and boxes represent runnel ponds; grey arrows and boxes represent polygonal ponds. Thick arrows = more important connection

Despite the lower availability of light in runnel ponds (Laurion & Mladenov 2013), these systems still harbor phototrophic bacteria, but mostly purple non-sulfur bacteria (Figure 3.5) that have low light requirements (Garcia-Contreras *et al.*, 2004). Purple non-sulfur bacteria, in the Alpha- and Betaproteobacteria, resulting in reduced sulfur compounds and not O_2 production in anaerobic environments (Basak *et al.*, 2007, van Niel, 1944), possibly impede the methanotrophs in runnel ponds (Whiticar, 1999). The larger relative abundance of heterotrophs and higher DOC in runnel ponds can also be associated to a larger production of CO_2, which would not necessarily be consumed by the versatile purple non-sulfur bacteria who can utilize multiple C sources (Pfennig, 1969).

3.4.1 Role of methanotrophs on CH_4 and CO_2 emissions

The CH_4 flux measured at the air-water interface of thaw ponds is the net contribution from methanogens minus the action of methanotrophs. While studies in subarctic regions show that methanotrophic activity can be great enough to cancel out the production of CH_4 by methanogens (Barbier *et al.*, 2012; Jaatinen *et al.*, 2005), it does not seem to be the case for the shallow ponds on Bylot Island, as CH_4 was emitted at significant rates, with estimated diffusive CH_4 flux ranging between 0.02 and 6.3 mmol m^{-2} d^{-1} (n=90; (Negandhi *et al.*, 2013). In fact, the relatively large dissolved concentrations at the surface of ponds, especially of runnel ponds (4.2 ± 4.7 µM; n=90), indicated that CH_4 was not completely oxidized and therefore methanotrophs would not be limited by its availability.

Surface water CH_4 concentrations were inversely correlated to the number of methanotroph sequences in surface sediment, but not to water methanotrophs or to sediment methanogens. This adds support to the idea that methanotrophs have an important role in regulating the release of CH_4 to the atmosphere, as suggested previously in studies of pelagic methanotrophs (Kankaala *et al.*, 2006; Barbier *et al.*, 2012). However in our study, given the few methanotrophs in surface waters (0.12 – 1.37%; Figure 3.3), methanotrophs in or near the sediment would have been responsible for lower CH_4 in the water column.

3.4.2 Benthic Arctic bacterial communities

One Phylum retrieved from Bylot Island thaw ponds, OP11, was reported in the active layer of the acidic wetlands of Axel Heiberg Island (Wilhelm *et al.*, 2011). OP11, which may be involved in sulfur cycling (Harris et al. 2004), was found at low percentages in sediment of runnel ponds BYL24 (0.53%;) and BYL27 (0.16%), along with the OP8 phylum (BYL22: 0.44%; BYL24: 0.26%). The bacterial genus *Geobacter,* a methanogen symbiont, was found in all pond sediment (0.8 – 3% of reads). This taxon has recently been found in aggregates with the methanogen *Methanosaeta*, which is also abundant in the ponds (Negandhi *et al.*, 2013). The symbiont transfers electrons to *Methanosaeta* without using H during the production of CH_4 (Morita *et al.*, 2011). A second methanogen symbiont in the genus *Syntrophus* was also found in thaw pond sediment (maximum of 1.4% of reads). *Syntrophus* bacteria are specialized as obligate syntrophic symbionts with methanogens (Zinder, 1993), where they degrade butyrate to

H_2, acetate and formate (Schink, 1997; Liu *et al.*, 2011). These two metabolically different methanogen symbionts found in both polygonal and runnel ponds are consistent with diverse CH_4 production pathway potentials in the ponds (Negandhi et al. 2013).

Microbial assemblages in polar soils reflect a variety of extreme environments. Interestingly, in the Bylot Island thaw ponds, we found variable percentages of the phyla Acidobacteria (3 - 16%) and Gemmatimonadetes (0 - 14%), which are considered acidophiles (Wilhelm *et al.*, 2011). These phyla have also been found on Ellesmere Island (Steven *et al.*, 2008; Yergeau *et al.* 2010), and are common on Axel Heiberg Island (Wilhelm *et al.*, 2011). This widespread distribution suggests that even sediments with more neutral pH levels may harbor acidophiles.

The quantity and quality of C substrates and the C degrading bacterial communities are often linked. In a study of 71 surface soils sampled throughout the USA, low C quality was correlated to the abundance of Acidobacteria (Fierer *et al.*, 2007). We found that Acidobacteria were generally more abundant in runnel ponds (Figure 3.5b) that had sediment with higher percentages of organic matter (12% in average compared to 5% in polygonal ponds; Negandhi *et al.*, 2013) but with DOC in the above water of a lower quality (lower $S_{275\text{-}295}$ associated to larger DOM molecules; Table 2) compared to in polygonal ponds. Therefore the higher percent of Acidobacteria in runnel ponds could be linked to the presence of less labile C and indicate them as initial mobilizers of less labile C sources.

3.4.3 Pelagic thaw pond bacterial community

The thermal regime and overall water temperatures were different between polygonal and runnel ponds (Table 1; Laurion & Mladenov 2013). The lower transparency of runnel ponds, together with the local micro-topography, narrow widths (1–3 m) and sheltered water surfaces that result in reduced wind fetch, promoted stratified conditions for a large part of the summer. Comparatively, temperature of the polygonal ponds water columns was homogenous in keeping with longer wind fetches. This thermal structure contributed to maintenance of hypoxia and unique chemical conditions at the bottom of runnel ponds, which resulted in distinctive sediment bacterial communities. Interestingly, although water physiochemical properties were different in both pond types, there was no noticeable effect on water bacterial communities, which were similar (Figure 3.3). A comparable result was found in Finnish lakes, where more diverse

bacterial communities were obtained from the anoxic hypolimnic waters than from the oxic surface waters (Peura *et al.*, 2012).

Surface water bacterial communities were distinct from sediment communities, suggesting that they were not originating from the sediment. Betaproteobacteria, which have been associated with high levels of nutrients (Newton *et al.*, 2011), were dominant in the water column and are characteristic of most pond waters. One of the main Betaproteobacteria genera in runnel ponds was identified as *Polynucleobacter* from clone library results (Figure 3.2). This taxon is reported to prefer allochthonous humic substances (Burkert *et al.*, 2003), which are particularly abundant in runnel ponds (Laurion & Mladenov 2013). In aquatic environments, Betaproteobacteria and Bacteriodetes are associated with substrates rich in organic C (Kirchman, 2002; Simon *et al.*, 2002) and utilize more labile C (Padmanabhan *et al.*, 2003). An abundance of these heterotrophs in the water column (≥ 50%; Fig. 4) could be associated to the overall more labile C pool of the pelagic zone exposed to the photolytic action of sunlight compared to the sediment (Laurion & Mladenov 2013).

3.4.4 Methanotrophs

Aerobic methanotrophs are often classified by their differing enzymatic methane oxidation of either RuMp (type I) or Serine (type II) pathways (Hanson *et al.*, 1996). There was no clear dominance of either type I or II methanotrophs in Bylot Island thaw ponds (Fig. 5c), especially when considering the *Verrucomicrobia* recently identified from Yellowstone National Park hot springs, which have not been confirmed to utilize either pathway (Hou *et al.*, 2008; Op den Camp *et al.*, 2009). These *Verrucomicrobia* methanotrophs were found in surface sediment of both pond types on Bylot Island, ranging from 0.2 – 2%, with higher percentages in runnel ponds.

Type I methanotrophs are reported to be dominant from other Arctic sites in Siberia, Svalbard, and Canada (Barbier *et al.*, 2012, and references therein). In our pond samples, Type I is more dominant compared to Type II, except in Runnel pond BYL24. However, the previously reported representative genera, *Methylobacter*, for Arctic Type I methanotrophs was not found in our Bylot Island ponds. These dominant type I strains reported elsewhere in the Arctic are characterized by a higher C efficiency, requiring less energy to oxidizes CH_4 than type II strains (Anthony, 1982), and prefer temperatures ranging between 0 and 10°C compared to above 15°C

for type II (He *et al.*, 2012). Bylot Island methanotrophic community containing type I, type II, and Verrucomicrobia, in an ecosystem with an average summer water temperature around 9°C (thus likely lower temperature in surface sediment), were similarly diverse to those found in temperate peat bogs (Auman *et al.*, 2000), suggesting that type II and Verucomicrobia can persist under cooler temperatures.

3.5 Conclusion

There was a clear separation between the bacterial communities of surface water and sediment in the shallow thaw ponds of Bylot Island. However, the water bacterial communities, mainly composed of heterotrophs, were not distinguishable between polygonal and runnel ponds even though the physicochemical characteristics of pond water were quite different. On the other hand, sediment bacterial communities of polygonal and runnel ponds were distinct. We propose that the geomorphology in polygonal landscapes influences thaw pond limnological properties, especially their vertical structure, exerting selection pressure on sediment microbial communities strong enough to explain the differences in GHG emissions. It is possible that diffusive CH_4 emissions are largely controlled by consumers rather than by producers, as a significant relationship was found between surface water CH_4 and methanotroph sequences but not with methanogen sequences. Further studies on a larger number of ponds and better estimates of daily and seasonal variations in CH_4, including ebullition are needed to confirm this relationship. The methanotroph communities of thaw ponds were shown to be particularly diverse, suggesting a wide range of responses to changing environmental conditions. Further studies on CH_4 consumers and producers of this widespread aquatic ecosystem are required to determine the microbial responses to the expected climate-driven changes, such as increased primary production, light availability, and organic matter quality and quantity. We found that geomorphology could be a key to predicting future GHG emissions.

Acknowledgements

We thank P.-G. Rossi, V. Gélinas, C. Girard, L. Boutet, and G. Deslongchamps for their efficient help in the field and laboratory, A. Comeau for his precious help at the molecular laboratory and for pyrosequencing data processing, G. Gauthier, the Centre for Northern Studies, the Polar Continental Shelf Project and Parks Canada for logistic support, and ArcticNet, EnviroNorth, National Science and Engineering Research Council of Canada, and International Polar Year for financial support.

4 Arctic thaw ponds response to increased temperature: DNA and RNA bacterial community and GHG production rate

La réponse des mares de dégel du haut Arctique canadien à une hausse de la température: communautés bactériennes selon l'ADN et l'ARN et taux de production de gaz à effet de serre

Karita Negandhi[1], Isabelle Laurion[1*], Connie Lovejoy[2]

[1]Centre Eau Terre Environnement and Centre for Northern Studies (CEN), Institut national de la recherche scientifique, Quebec, QC Canada

[2]Département de biologie, Institut de Biologie Intégrative et des Systèmes, and Takuvik, Université Laval, Quebec, QC Canada

Cet article présente la production de GES des mares de dégel ainsi que la communauté bactérienne associée à une mare *allongée* sous une hausse de température. K. Negandhi a effectué la collecte des échantillons, la préparation, l'incubation expérimentale, l'analyse des données et l'interprétation des résultats définitifs sous la supervision d'I. Laurion. Une première version de l'article a été rédigée par K. Negandhi et soumise à une révision pour améliorer la forme et le fond. Après d'autres révisions en cours, l'article sera soumis à une revue scientifique qui met en valeur les études des communautés microbiennes dans l'environnement.

Résumé

Le dégel du pergélisol est associé à la formation de petites mares de dégel, qui sont des producteurs substantiels de gaz à effet de serre (GES). Nous avons étudié ici la réponse de ces mares face à une augmentation de la température de 5°C au-dessus de la moyenne actuelle l'été (4,5°C). Nous avons suivi pendant 16 jours la production de GES par les sédiments, et les changements qui se reflétaient dans la structure de la communauté bactérienne par pyro-séquençage à haut débit du gène 16s de l'ARNr pour la communauté totale (ADN) et les taxons impliqués dans la synthèse des protéines (ARN). Au cours de l'incubation, les taux de production du CO_2 et du CH_4 ont augmenté de façon significative à la température plus élevée. Les conditions expérimentales mises en place pour diminuer l'activité des méthanotrophes ont révélé que c'est la consommation de méthane plutôt que le potentiel de production qui régit les émissions de méthane *in situ* des mares et selon leur classification morphologique. Une sélection pour les unités taxonomiques opérationnelles rares à 9°C (ARN) a entraîné un changement significatif dans la composition de la communauté responsable pour la décomposition du carbone organique, de même qu'une diminution de l'abondance relative du potentiel de synthèse des protéines (ARN). La réduction de la communauté de l'ARN incluait une diminution des Bacteriodetes et une légère augmentation des Betaproteobacteria, des Alphaproteobacteria, des Firmicutes, des Acidobacteria, des Verrucomicrobia, et des Actinobacteria, peut-être en permettant l'utilisation du réservoir de carbone moins labile suite à l'épuisement des composés labiles.

Mots-clés: structure de la communauté, carbone, thermokarst, pergélisol

Abstract

Thawing of permafrost is associated with the formation of thaw ponds that are substantial greenhouse gas (GHG) producers. Here we investigated GHG production in thaw pond sediment under air temperatures of 9°C, which is above the present summer average of 4.5°C. In the same incubations we tracked changes in total bacterial community structure using high throughput pyro-sequencing of a variable region of the 16s rRNA gene (DNA) and identified taxa most likely involved in protein synthesis by similarly sequencing 16S rRNA. Over the 16 days incubation, CO_2 and CH_4 production rates significantly increased at the higher temperatures. Experimental conditions that were designed to depress methanotrophic activity, revealed methane consumption rather than production potentially regulates *in situ* methane emissions from the polygonal thaw ponds. A selection for rare operational taxonomic units (OTUs) at 9°C in the RNA community were responsible for a significant community composition change among organic carbon decomposers. The community composition change comprised of a, relative decrease in the taxa from rRNA at 9°C compared to 4 °C through a decrease in Bacteriodetes (15%) and a slight increases in Betaproteobacteria (1.9%), Alphaproteobactera (0.5%), Firmicutes (3%), Acidobacteria (2%), Verrucomicrobia (1%), and Actinobacteria (1%), possibly allowing for the use of less labile C pool after the utilization of more labile compounds.

Key words: carbon, permafrost, community structure, thermokarst

4.1 Introduction

Arctic permafrost regions can be diversely characterized by their vegetation, geology, paleohistory and climate, and the microbial ecology within these permafrost environments likely varies accordingly (Graham *et al.,* 2011). In particular, due to their significant GHG emissions, permafrost environments favorable to the development of thaw ponds and lakes are of concern (Abnizova *et al,*. 2012; Laurion *et al.*, 2010; Wagner *et al.*, 2005; Walter *et al.*, 2006; Zimov *et al.*, 1997; Zona *et al.*, 2008). Of specific interest, are the large quantities of stored carbon (C) released when permafrost thaws. This previously unavailable C becomes available to microbes that produce greenhouse gases (GHG) (Tarnocai *et al.*, 2009; Schuur *et al.*, 2009), which has implications for global C budgets. The mobilization of permafrost C can be investigated experimentally by following microbial responses to increased temperatures, which are experienced while this additional stored C releases from the thawing permafrost. An understanding of the thaw pond microbial community response to temperature and available C sources will contribute to predicting future GHG emissions and constrain current permafrost biogeochemical models (Riley *et al.*, 2011).

The capacity of permafrost microbes, living under perennially cold temperatures, to adapt to warming, contributes to uncertainties in their biogeochemical response to changing conditions. For instance, permafrost bacterial activity has been reported as low as -20°C (Vishnivetskaya *et al.*, 2006), and specifically CH_4 production at -17°C (Gilichinsky & Rivkina *et al.*, 2011). The predicted increase in global temperature by the end of the 21st century ranges from 1.1 to 6.4°C, averaging 3.75°C (Solomons *et al.*, 2007), however the Arctic is more susceptible to climate change and warming more rapidly (Serreze *et al.*, 2000), with a predicted range of 2 to 9°C temperature increase, depending on model and forcing scenarios (IPCC, 2007).

Under warmer temperatures, microbial communities living in thaw pond sediment could respond in a number of ways affecting C cycling outcomes. Microbial decomposition of C could intensify, which would be lead to increased production in CO_2 and CH_4 (Cox *et al.*, 2000; Davidson and Janssens, 2006). However, the increased activity could result in C depletion over time, reversing any initial increase in GHG production (Kirschabaum, 2004). Alternatively, an increase in temperature could result in internal physiological changes of cells, leading to reduced microbial growth efficiency and lowered biomass and eventual decline in degradative C enzymes (Steinwig *et al.*, 2008; Conant *et al.*, 2011). Apart from biomass reduction, increased activities

and reduced growth efficiencies, at warmer temperature, could result in a change in community composition (Bradford *et al.*, 2008). A community change would influence GHG emissions through for example; enhanced utilization of more recalcitrant C sources (David & Janssens 2006). Furthermore, a community change could impact the balance between GHG producers and consumers; methanotrophs have previously been identified as controlling CH_4 emissions in thaw ponds (Negandhi *et al.*, submitted) and other freshwater lakes (Kankaala *et al.*, 2006) and an increase in CH_4 consumption by methanotrophs could result in lower than expected CH_4 emissions.

Identifying the bacterial community from DNA provides a measure of the present community, however numerous bacteria clades and groups simultaneously respond to increased temperatures and identifying which taxonomic groups are most sensitive to changes can provide information on the eventual community that will thrive under higher temperatures. The 16S rRNA gene is most frequently used to identify different bacterial groups (Sogin et al 2006) and by targeting this gene using DNA as a template the current community can be identified. Since rRNA is incorporated into ribosomes using RNA as a template for the same genetic marker, it provides information on what taxa are involved in protein synthesis. By examining both the rDNA and rRNA at the same time, the communal bacterial response can be inferred. For instance, specific taxonomical groups with high rDNA signatures and low rRNA signatures could indicate a high abundance with low activity. Comparatively, low rDNA signatures and high rRNA signatures could indicate low abundance and high activity (Moesseneder et al. 2004).

Here we investigated GHG production rate and the changes in bacterial communities from thaw pond sediment, in response to increased temperatures. Polygonal pond and runnel pond CO_2 and CH_4 production rates were also measured under increased temperature at 4 and 9 °C. Bacterial communities *in situ* and at the start of incubations (T1) were identified from DNA and over 16 days community composition changes were investigated using RNA as a template and compared to those from DNA.

4.2 Methods

4.2.1 Study Site

Samples were collected at Sirmilik National Park, Bylot Island, Nunavut (73°09'N, 79° 58'W), which is in the continuous permafrost region of the Canadian Arctic. The active layer depth in 2010 was between 40 and 60 cm (D. Fortier pers. comm.). The sampled ponds were 1-2 m deep and can be categorized into two geomorphic shapes associated with the thawing permafrost. Firstly are polygonal ponds formed on top of low centered polygons, and the secondly are runnel ponds formed over melting ice wedges. In general, polygonal ponds are more stable environments with thick cyanobacterial mats at the bottom, while runnel ponds have more erosion due to permafrost slumping and these are also called thermokarst ponds. Thermokarst ponds are a phenomenon associated to climate change and accelerated permafrost thawing.

In July 2010, surface sediment samples from two polygonal ponds (BYL1 & 22) and two runnel ponds (BYL24 & 38) were collected for incubation experiments (n=4), representing a categorization of physiochemical properties (Table 4.1). Runnel pond BYL38 was further sampled for bacterial community changes throughout the incubation experiment. BYL38 was chosen due to its previously recorded particularly high *in situ* GHG emissions (Laurion *et al.*, 2010). Runnel ponds in general have significantly higher GHG emissions compared to polygonal ponds (Negandhi *et al.*, 2013).

Table 4.1 Physiochemical properties of the thaw ponds sampled on Bylot Island. The four ponds present a categorization of properties between polygonal and runnel ponds with a few minor changes between 2009 and 2010. SRP – soluble reactive phosphorus; TP – total phosphorus; TN – total nitrogen; DOC – dissolved organic carbon; a_{320} – dissolved organic matter absorption at wavelength 320 nm, as an index of the quantity of colored dissolved organic matter; $S_{275-295}$ – spectral slope signature between 275 and 295 nm, an index of the molecule size of colored dissolved organic matter (larger values generally indicate smaller/more labile molecules).

Pond	Class	Yr	SRP $\mu g\ L^{-1}$	TP $\mu g\ L^{-1}$	TN $\mu g\ L^{-1}$	SO_4 $mg\ L^{-1}$	DOC $mg\ L^{-1}$	a_{320} m^{-1}	$S_{275-295}$ nm^{-1}	CO_2 µM	CH_4 µM
BYL 1	Pol.	'09	<0.2	15.6	0.36	1.5	8.4	13.1	0.0199	6.3	1.0
		'10	0.5	19.0	0.5	1.06	8.7	13.2	0.0193	20.6	0.7
BYL 22	Pol.	'09	<0.2	25.5	0.37	0.85	8.1	19.6	0.0168	25.0	1.9
		'10	0.5	68.0	0.4	1.62	6.2	20.8	0.0191	35.1	1.3
BYL 24	Run.	'09	1.0	25.5	0.4	0.67	11.5	37.0	0.0153	33.0	3.4
		'10	1.6	38.0	0.4	1.81	9.6	36.3	0.0139	63.2	0.8
BYL 38	Run.	'09	1.8	71.8	0.87	3.1	12.2	72.9	0.0115	181.5	4.7
		'10	4.7	54.0	0.5	1.74	12.1	67.3	0.0122	85.4	2.7

4.2.2 Incubations

Preliminary experiments were performed the previous year in 2009 on BYL38 sediment to determine the optimal experimental setup. In these experiments over 28 days, CO_2 production plateaued after 18 days. Therefore, since our focus was on early GHG dynamics, an incubation time of 16 days was chosen for the 2010 experiments. In 2010, Incubations were started three days after collection (T1), immediately upon return from Bylot Island and arrival in Quebec City in efforts to limit the changes in the composition of the microbial community due to transporting.

On 25 July 2010, sediment samples from four thaw ponds were collected with gloved hands, placed in a sterilized ziplock bag, and mixed. A 50 ml sediment subsample was collected from the ziplock bag into a sterile Falcon tube (Fisherbrand) and poured through a funnel into pre-combusted and acid-washed glass bottles. Water from the corresponding thaw ponds was used to fill the glass bottles to the top leaving no headspace and to maintain hypoxic conditions similar to *in situ*. A butyl rubber cap was used, with a gas tight syringe to release the pressure. The same collection technique was used on all four ponds (2 polyongal and 2 runnel ponds), with a total of 72 bottles collected (n=18 per pond). This allowed for CO_2 and CH_4 to be measured 6 times within the 16-day incubation, each with 3 replicates.

At the same time of sediment collection for bottle incubations, 3 ml of sediment from runnel pond BYL38 for *in situ* DNA and RNA analysis were taken from the same ziplock bag mixture and stored in 2 ml of lysis buffer and RNA later respectively.

All 72 incubation bottles were kept at around 4°C and in the dark until we were back at the lab on 27 July 2010, where half of the bottles were incubated at 4°C and half at 9°C, both in the dark. The 4°C was maintained by incubating bottles within an electronically monitored refrigerator. Temperature of 9°C was maintained within an incubator (Fisher low temperature incubator model 307) and internal temperature recorded from a thermistor (U12, Onset). On 28 July 2010, 50 ml of water was removed and flushed with helium for 5 minutes with an exit valve, and initial GC measurements (T1) were taken. For this, 0.6 ml of gas was removed and 0.5ml was injected in the GC using a 1.0 ml syringe (SG008130 Canadian Life Science, 1MF-CTC-GT-HS-5/0.63H). For all other time points, 0.4 ml of gas was removed and 0.1 ml injected to stay within the detection level ranges. GC measurements of CO_2 and CH_4 were taken at 6 time points

(day 1, 5, 7, 9, 13 and 16). Each time point had three replicates (n=72, n=18 per pond). Sediment was dried and weighed for each sample. The dry weight for each sample (averaged 21.4g at 4°C and 20.8g at 9°C) was used to normalize GHG production rates.

From BYL38, DNA and RNA sediment samples for 16s rRNA bacterial pyrosequencing at the start of the incubation (T1) and at the end of the incubation (T16) were collected after their GC measurements were taken. Samples were stored at -80°C with lysis buffer and RNA later respectively until extraction. Therefore DNA and RNA samples were collected at time points *in situ*, T1, T16-4°C, and T16-9°C (n=8).

4.2.3 Pyrosequencing

DNA and RNA were extracted using the MO BIO Kit (RNA powersoil total RNA isolation kit #12866-25 and DNA elution accessory kit #12867-25) allowing both RNA and DNA to be extracted from the same sample. A reverse transcription of extracted RNA to cDNA was performed using a High Capacity Reverse Transcriptase Kit (Applied Biosystems, CA) including an equal mixture (30 µL) of RNA and a RT mixture consisting of 6 µL RT buffer, 2.4 µL dNTP, 6 µL of random primers, 3 µL of Multi-scrible reverse transcriptase, and 12.6 µL of H_2O. Amplification of DNA for high-throughput 16S rRNA gene and 16S rRNA from cDNA pyrosequencing was performed with a PCR reaction mixture consisting of 1X HF buffer (NEB), 200 µM dNTP (Feldan Bio), 0.4 mg mL^{-1} BSA (Fermentas), 1 U of Phusion High-Fidelity DNA polymerase (NEB), 0.2 µM of both primers (969F: ACGCGHNRAACCTTACC and 1406R: ACGGGCRGTGWGTRCAA, Invitrogen; see Comeau *et al.*, 2011 for primer design), and 0.01 - 0.1 µL of template DNA and 1 µLof template RNA from sediment samples. Amplification cycles included 98°C for 30s, 30 cycles of denaturing at 98°C for 10s, annealing at 55°C for 30s, extension at 72°C for 30s, and a final extension at 72°C for 5 min. For each sample, triplicate reactions performed for DNA and duplicate for RNA were pooled together for purification (QIAquick PCR purification kit; QIAGEN) and quantification (Nanodrop ND-1000). Coded amplicons were mixed equally into one tube for sequencing on a Roche 454 GS-FLX Titanium platform at Université Laval Plate-forme d`analyses Génomiques. Resulting reads were subjected to pyrotag pre-processing and quality control. Low-quality reads were removed if they contained non assigned nucleotides (N's), were < 150 bp excluding the adaptor and sample tag-code, if they exceed the expected amplicon size, and if they had an incorrect Forward primer

sequence. Additionally, bases present after the reverse primer were trimmed. Next, reads were aligned using Mothur (Schloss, 2009) against SILVA reference alignments and then manually checked to remove misaligned reads. After processing, 2321 input reads were randomly selected per sample. The SILVA database (version 108) including additional previously generated clone library sequences from the C. Lovejoy laboratory was used for taxonomical identifications.

4.2.4 Statistics

Production rates of CO_2 and CH_4 ($\mu M\ day^{-1}$) were obtained from the linear regressions of the averaged GC concentration (n=3) taken at day 1, 5, 7, 9, 13 and 16 (Excel 2010). Statistical difference in CO_2 production rates between temperature (4°C and 9°C) and between pond types (polygonal and runnel ponds) were tested by separate paired t-test. Statistical difference in CH_4 production rates between temperature (4°C and 9°C) and between pond types (polygonal and runnel ponds) were tested by separate paired t-test. All paired t-test were performed in PAST version 3.01 (Hammer et al., 2001)

Descriptive statistics (OUT #'s, Chao 1, ACE, Shannon, and Simpson) for bacterial communities were performed in MOTHUR. A Bray-Curtis cluster analysis was used to find groupings among the sampled bacterial community time points. From here, an analysis of similarity (ANOSIM) test was used to find significance values, followed by a similarity percentage test (SIMPER) to identify the relative influence attributed by bacterial groups. These test were also performed in PAST version 3.01.

4.3 Results

4.3.1 GHG production at different temperatures

Carbon dioxide and CH_4 were both produced at a significantly higher rate at 9°C than at 4°C for all four ponds ($p \leq 0.05$; Table 4.2). The response level of CO_2 and CH_4 to increased temperature was not significantly different between polygonal and runnel ponds ($p \geq 0.5$). Runnel

ponds had a significantly higher CO_2 production rate than polygonal ponds (p=0.002), but this was not the case for CH_4 (p=0.606; Table 4.2).

Table 4.2 Greenhouse gas linear production rates ($r^2 \geq 0.942$, $p < 0.001$, in µM day^{-1} g^{-1}) by thaw pond sediment of BYL38 in response to increased temperature. Diff. = Difference in production rate over 16 days between the two temperatures. The stars indicate the significance levels obtained from a paired t-test performed on CO_2 and CH_4 for the difference between temperature treatments and pond types.

		CO_2 ($x10^{-2}$)*, **			CH_4($x10^{-2}$)*		
Pond	**Class**	**4°C**	**9°C**	**Diff.**	**4°C**	**9°C**	**Diff.**
BYL1	Pol.	26.8 (3.8-17.5)	38.3 (5.0-30.1)	11.5	6.2 (0-3.1)	8.2 (0-3.8)	2.0
BYL22		25.0 (3.9-23.0)	37.2 (2.1-11.5)	12.2	3.3 (0-2.0)	4.2 (0.52-3.1)	0.9
BYL24	Run.	48.0 (3.2-34.6)	61.9 (6.9-44.6)	13.9	4.3 (0-1.6)	5.0 (0.5-2.0)	0.7
BYL38		35.6 (1.6-11.8)	42.2 (7.9-19.0)	6.6	2.0 (0-0.1)	3.9 (0.04-0.32)	1.9

* Significant difference (0.05) between temperatures
** Significant difference (0.005) between polygonal and runnel ponds production rate

4.3.2 DNA and RNA community structure

The DNA at phyla level, for all four sampling time points (*in situ*, T1, T16-4°C, and T16-9°C), were dominated (>10%) by Bacteriodetes, Proteobacteria and Actinobacteria, with smaller proportions (1 – 10%) of Acidobacteria, Firmicutes, Verrumicrobia, Gemmatimonadetes and Chloroflexi (Figure 4.1). The RNA reads at the level of phyla were similar, with some differences in proportions and more of unclassified bacteria (1.8 – 3.6%) compared to DNA (≤ 0.7%) (Figure 4.2). The RNA community was more diverse compared to the DNA community (Table 4.3; Figure 4.3).

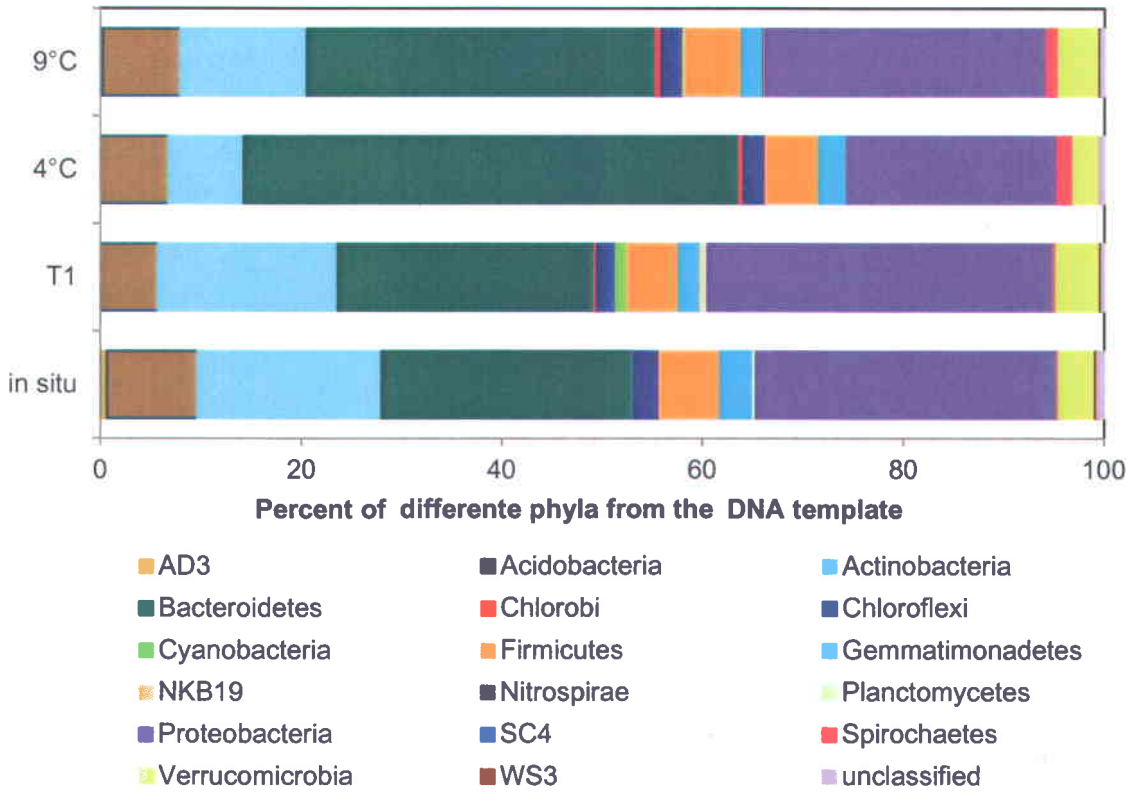

Figure 4.1 Relative abundance of bacterial phyla from DNA in thaw pond BYL38 sediment *in situ*, at start of the incubation (T1), and after 16 days of incubation at 4°C and 9°C.

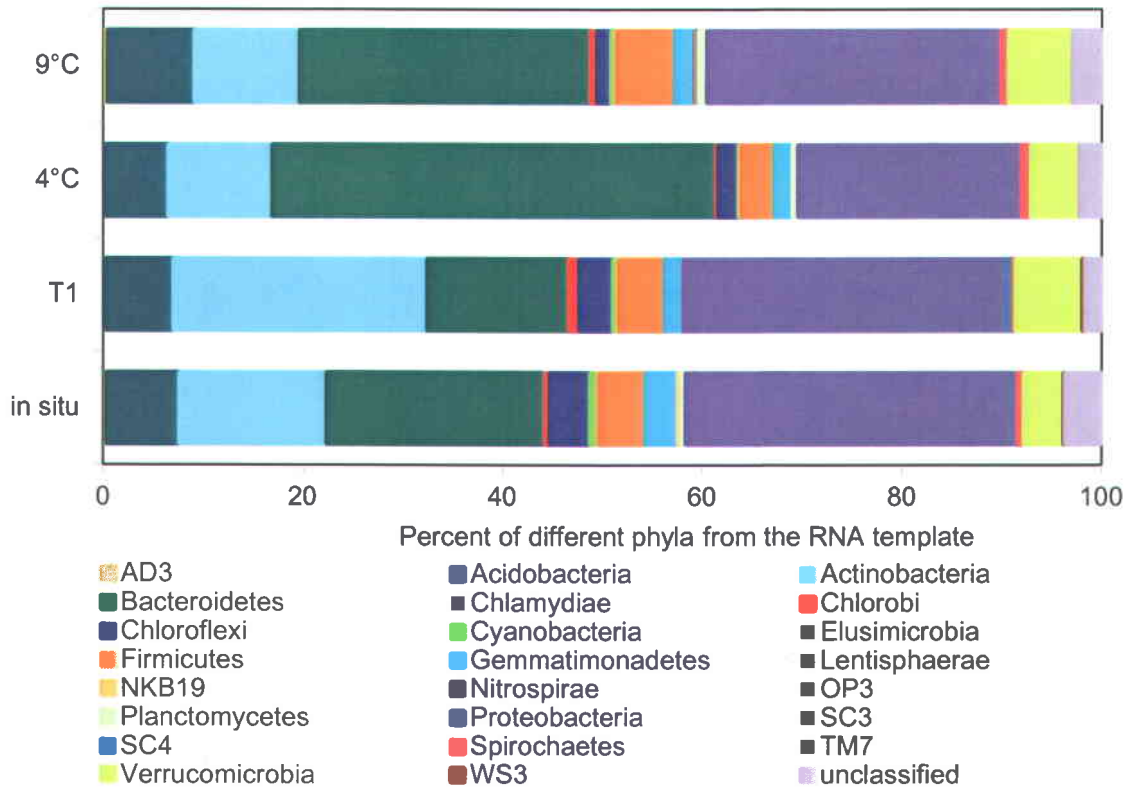

Figure 4.2 Relative abundance of bacterial phyla RNA in thaw pond BYL38 sediment *in situ*, at start of the incubation (T1), and after 16 days of incubation at 4°C and 9°C. All squares in black are Phyla not present in DNA.

Table 4.3 Descriptive statistics comparing DNA and RNA reads where each time point sample was resample to 2321 reads.

		OTUs	Chao1	ACE	Shannon	Simpson
All DNA		1240	1287	1240	6.95	0.0010
All RNA		1768	1815	1768	7.26	0.0008
DNA	*in situ*	275	285	275	5.47	0.0043
	T1	304	311	304	5.56	0.0036
	4°C	329	336	329	5.58	0.0042
	9°C	332	340	332	5.63	0.0037
RNA	*in situ*	449	454	449	5.91	0.0029
	T1	424	434	424	5.85	0.0033
	4°C	448	454	448	5.84	0.0036
	9°C	447	459	447	5.92	0.0028

The communities between *in situ* and T1 contained significantly more dissimilarity between DNA and RNA than any other time points (analysis of similarities, ANOSIM; r=-1, p=1). At time point T1, the largest differences between DNA and RNA among all sampling time points are present (Figure 4.3; bubble sizes). Bacteriodetes have the largest difference (11.4%; bubble size in Figure 4.3b), with a similar percentages at DNA-*in situ* and DNA-T1 but a decrease (8%) in RNA from *in situ* to T1. Actinobacteria also have large difference between DNA-T1 and RNA-T1 (7.5%; bubble size in Figure 4.3b) due to an increase (11%) in RNA from *in situ* to T1(Figure 4.4a-b).

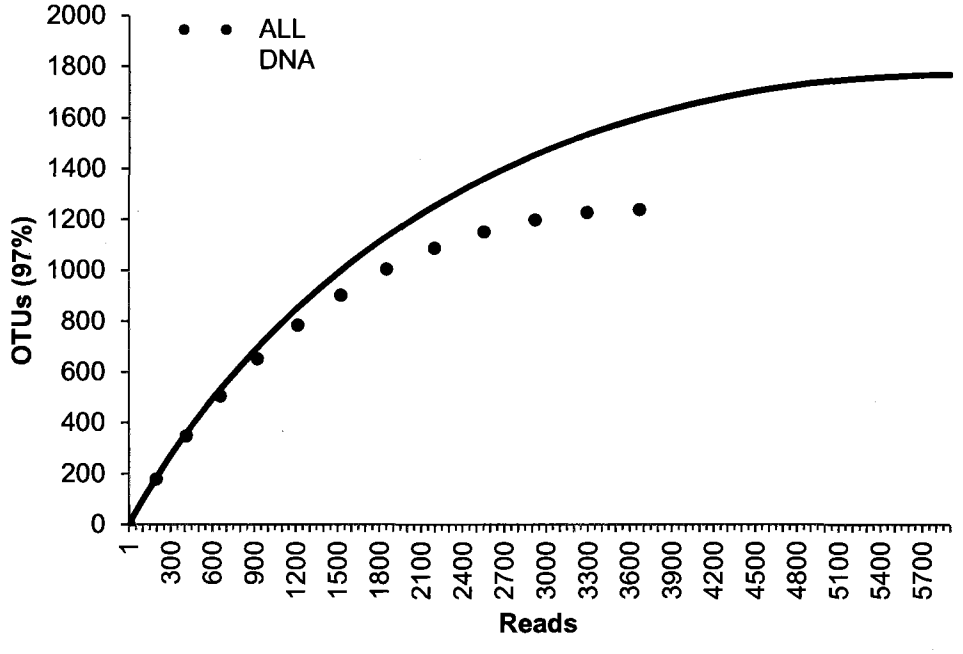

Figure 4.3 Rarefaction curves for DNA and RNA

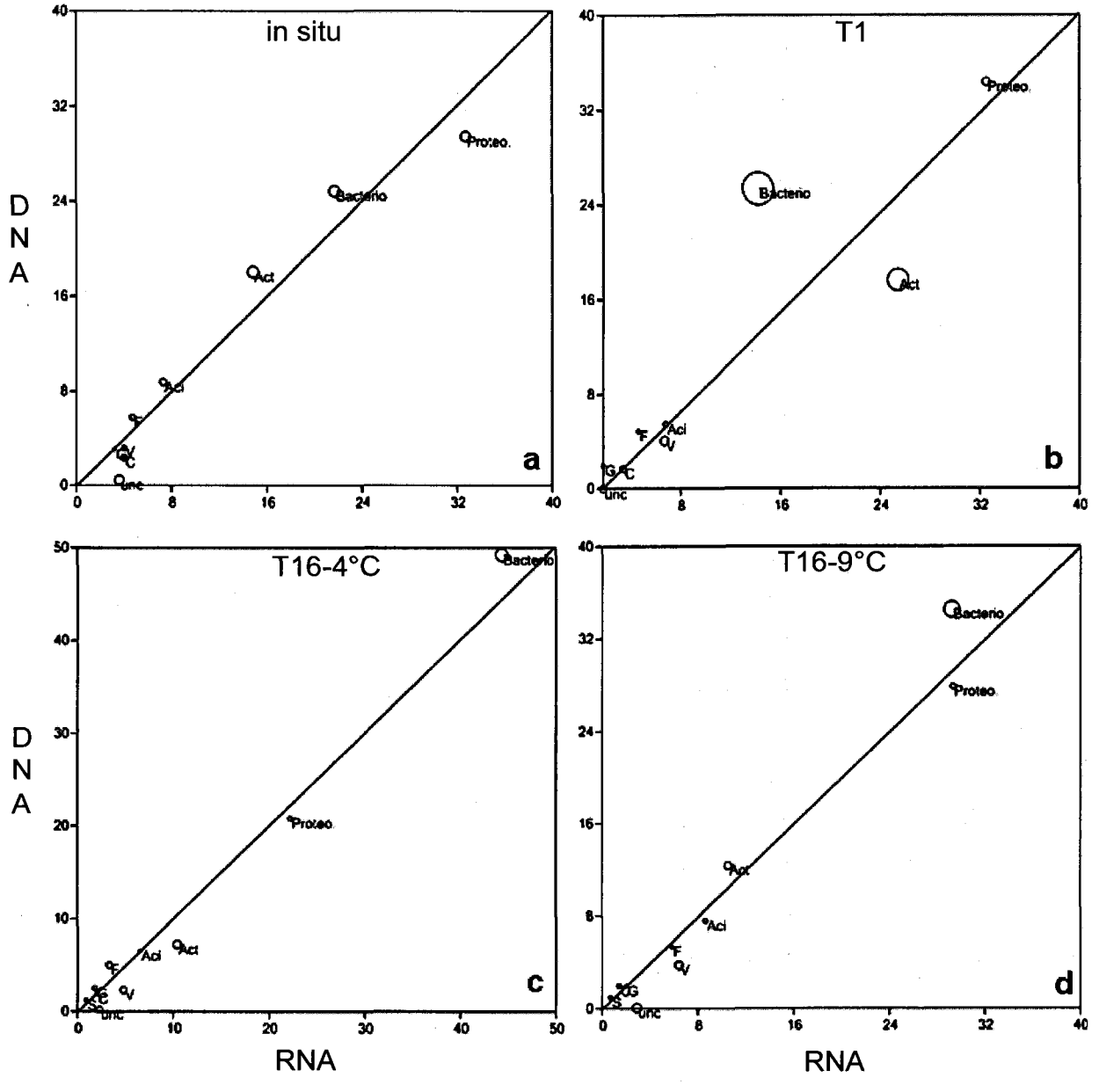

Figure 4.4 RNA-DNA comparison of abundant (>1%) Phyla at all four sampling time points. Phyla above diagonal line indicate a higher DNA percentage than RNA and vice versa for RNA. Size of circle (bubble) indicates amount of difference between RNA-DNA. a) community at *in situ,* b) community at T1, start of incubation experiment 3 days after collection, c) community after 16 days of incubation at 4°C, d) community after 16 days of incubation at 9°C. Aci.= Acidobacteria; Act=Actinobacteria; Bacterio=Bacteriodetes; C=Chloroflexi; F=Firmicutes; G=Gemmatimonadetes; Proteo=Proteobacteria; S=Spirochaetes; V=Verrucomicrobia; unc=unclassified bacteria

4.3.3 Bacterial communities at different temperatures

Communities from *in situ* and T1 were significantly different from the two communities after 16 days of incubation (ANOSIM, p=0.027, R=0.75). Attributing to this significant difference are Bacteriodetes and Actinobacteria. From T1 to T16 time points, Bacteriodetes DNA and RNA increase at 4°C (23.9%, 30.1%) and to an extent at 9°C (9.2%, 15%) (Figure 4.4 b-d). From T1 to T16 time points, Actinobacteria's DNA and RNA decrease at 4°C (10.4%, 15%) and 9°C (5.5%,14.9%) (Figure 4.4 b-d).

At the end of the 16 day incubation, both DNA-9°C and RNA-9°C were more diverse communities compared to DNA-4°C and RNA-4°C communities (Table 4.3, Figure 4.5). While cluster analysis indicated DNA and RNA communities to cluster by temperature, at 9°C the DNA and RNA communities were more dissimilar, with RNA-9°C branching the furthest away from the others and the most dissimilar (Figure 4.6).

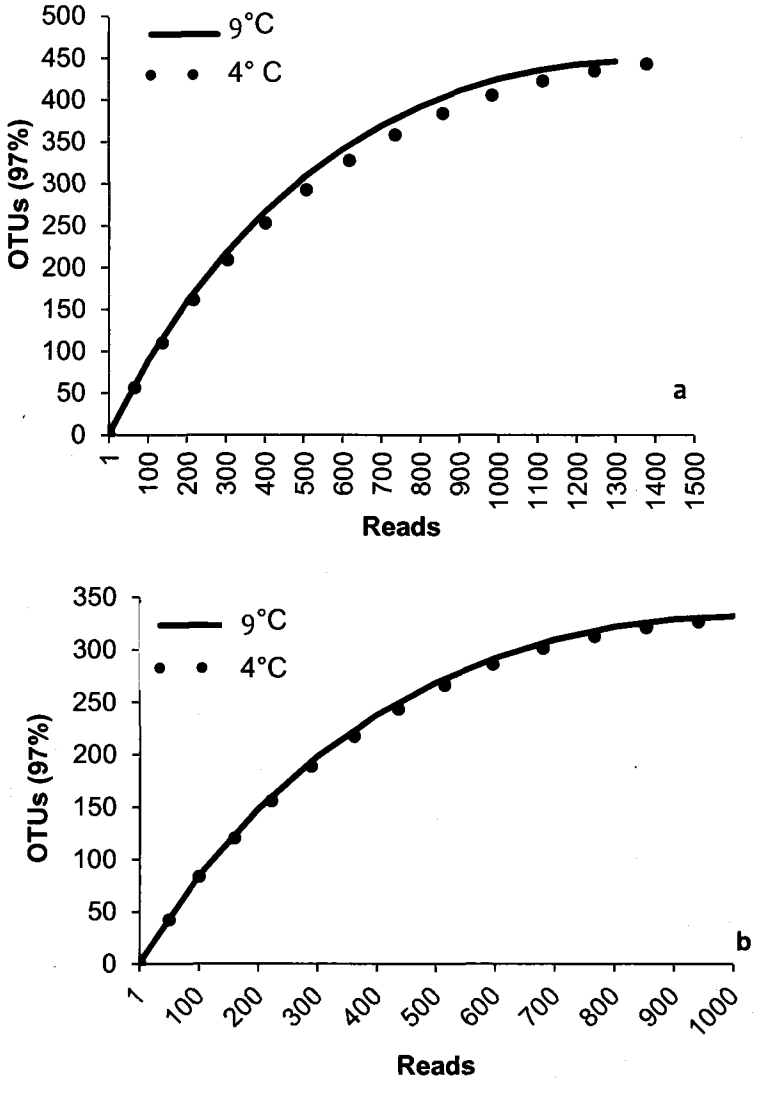

Figure 4.5 Rarefaction curves by temperature for a) RNA reads b) DNA reads.

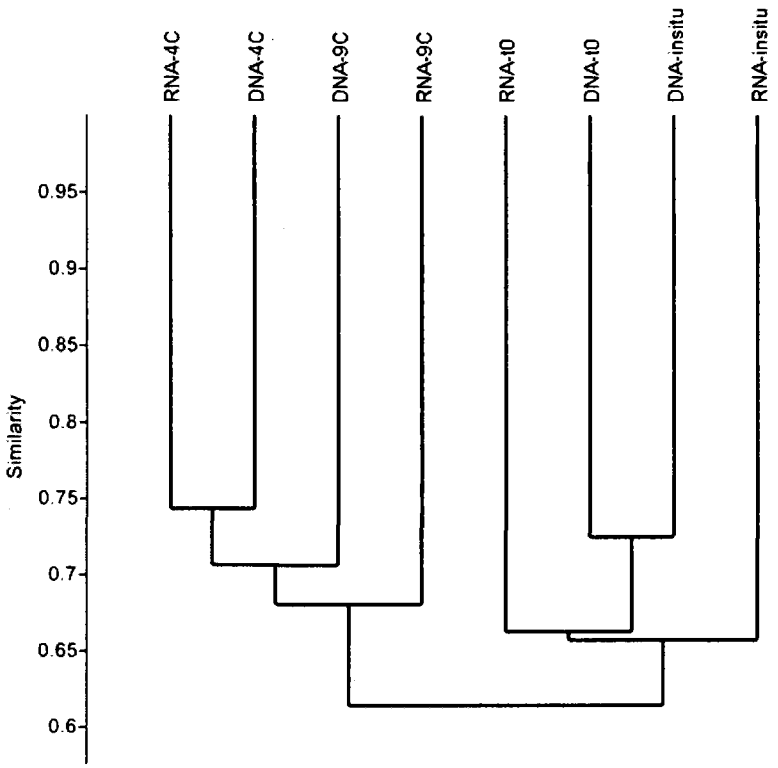

Figure 4.6 Cluster analysis using Bray Curtis for BYL38 sediment bacterial communities identified genera relative abundances among experimental time points.

Similarity percentage (SIMPER) analysis reported an average of 30.87% dissimilarity between communities by temperature, with the majority of this dissimilarity (86.5%) attributed to the six phyla: Proteobacteria, Firmicutes, Acidobacteria, Verrucomicrobia, Actinobacteria, and Bacteriodetes.

The community compositions of the 6 phyla reported by SIMPER to be contributing to a significant dissimilarity are all carbon decomposers. Interestingly there is not significant difference between the DNA communities at 4°C and 9°C (t-test, d.f.=5, p=0.096; Figure 4.7), but is in the RNA communities at 4°C and 9°C (t-test, d.f.=5, p=0.009, Figure 4.7).

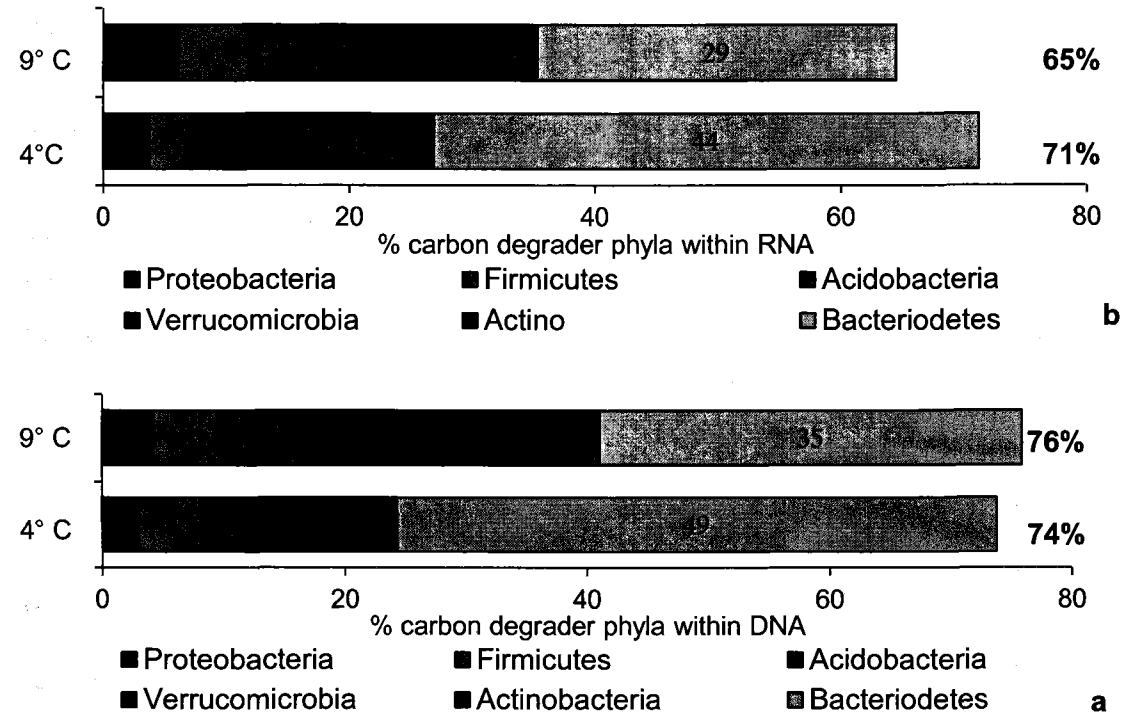

Figure 4.7 Identification of carbon degrader phyla in BYL38 sediment after 16 days of incubation at 4°C and 9°C for a) DNA and b) RNA. A significant difference in community composition of phyla between temperatures is found for RNA (p=0.009) but not for DNA (p=0.096)

The RNA derived community of carbon decomposers was relatively more abundant at 4°C (70%) than at 9°C (64%; Figure 4.7). This difference was generated through a complex bacterial community shift to result in lower relative abundance, yet more diverse community at 9°C (Table 4.3; Figure 4.7a). Specifically, differences between RNA-4°C and RNA-9°C, included fewer Bacteriodetes (15%), but higher Proteobacteria (Betaproteobacteria by 1.9%, Alphaproteobactera by 0.5%), Firmicutes (3%), Acidobacteria (2%), Verrucomicrobia (1%), and Actinobacteria (1%) for combined total difference of -6% at RNA-9°C. The total DNA carbon degrading community also became lower at 9°C than at 4°C (73% compared to 77%), emphasizing the decrease in RNA carbon degraders.

4.3.4 Bacteria at Family level

Comparing the community taxa at the family level increased the significance of dissimilarity among communities at 4°C and 9°C (SIMPER, 26.7%; ANOSIM, P=0.667,R=0.5). Plots of the DNA and RNA signatures from the specific taxa within the specifictaxa within the 6 carbon

decomposing Phyla that were shown to significantly change between temperatures distinguish specific Family's that are responding to temperature.

Acidobacteria – Soilbacteraceae (#4) and Acidobacteriaceae (#1) increased in activity (RNA) at 9°C. Unclassified Acidobacteria DS-18 (#6) was upregulated (increased in both DNA and RNA) at 9°C (Figure 4.8 a & b).

Firmicutes – Erysipelotrichaceae (#54) and Clostridiales Family XIII incertae sedis (#47) increased in activity at 9°C, while their DNA stayed similar between the two temperatures. Clostridiales Family XIII incertae sedis (#47) also had more DNA than RNA at both temperatures. Ruminococcaceae (#51) was upregulated (increased in both DNA and RNA) at 9°C (Figure 4.8 c & d).

Alphaprotebacteria & Verrucomicrobia – Unclassified verrucomicrobia RFP12 (#60) was upregulated (increase in both DNA than RNA) at both temperatures. *Verrucomicrobiaceae* (#61) increased in activity at 9°C. Then at 9°C, unclassified verrucomicrobia R76-B18 (#58) and Spartobacteriaceae (#59) have more similarity in their DNA and RNA signatures. For Spartobacteriaceae (#59), this may be due a decrease in activity at 9°C, leaving an overall trend for more RNA than DNA signatures for the phylum Verrucomicrobia. For the two Alphaproteobacteria Caulobacteraceae (#55) and Acetobacteraceae (#56), there was also a trend for more RNA signatures than DNA signatures (Figure 4.8 e & f).

Bacteriodetes – The three dominating families Bacteriodetes incertae sedis (#29), Cytophagaceae (#38), and unclassified Bacteriodetes (#42) have a very equal DNA and RNA signatures, with all three being downregultated (decrease in both DNA and RNA) at 9°C. Cryomorphaceae (#34) is also downregulated at 9°C, but maintains a higher DNA signature at both temperatures. Unclassified Bacteriodales (#33), unclassified Flexibacteraceae (#36), and Flavobacteriaceae (#35) are also less active at 9°C. Chitinophagaceae (#37) is one Bacteriodete whose activity is similar at 4°C and 9°C (Figure 4.9).

Actinobacteria – Unclassified Actinomycetales (#23) and Cellulomonadaceae (#13), have slightly higher DNA than RNA signatures. This is likely because they are being deselected for at 9°C. Conexibacteraceae (#26) has similar DNA and RNA signatures, but is only seen at 9°C indicating an upregulation at 9°C. Actionobacteria have a trend to have more RNA than DNA signatures (Figure 4.10).

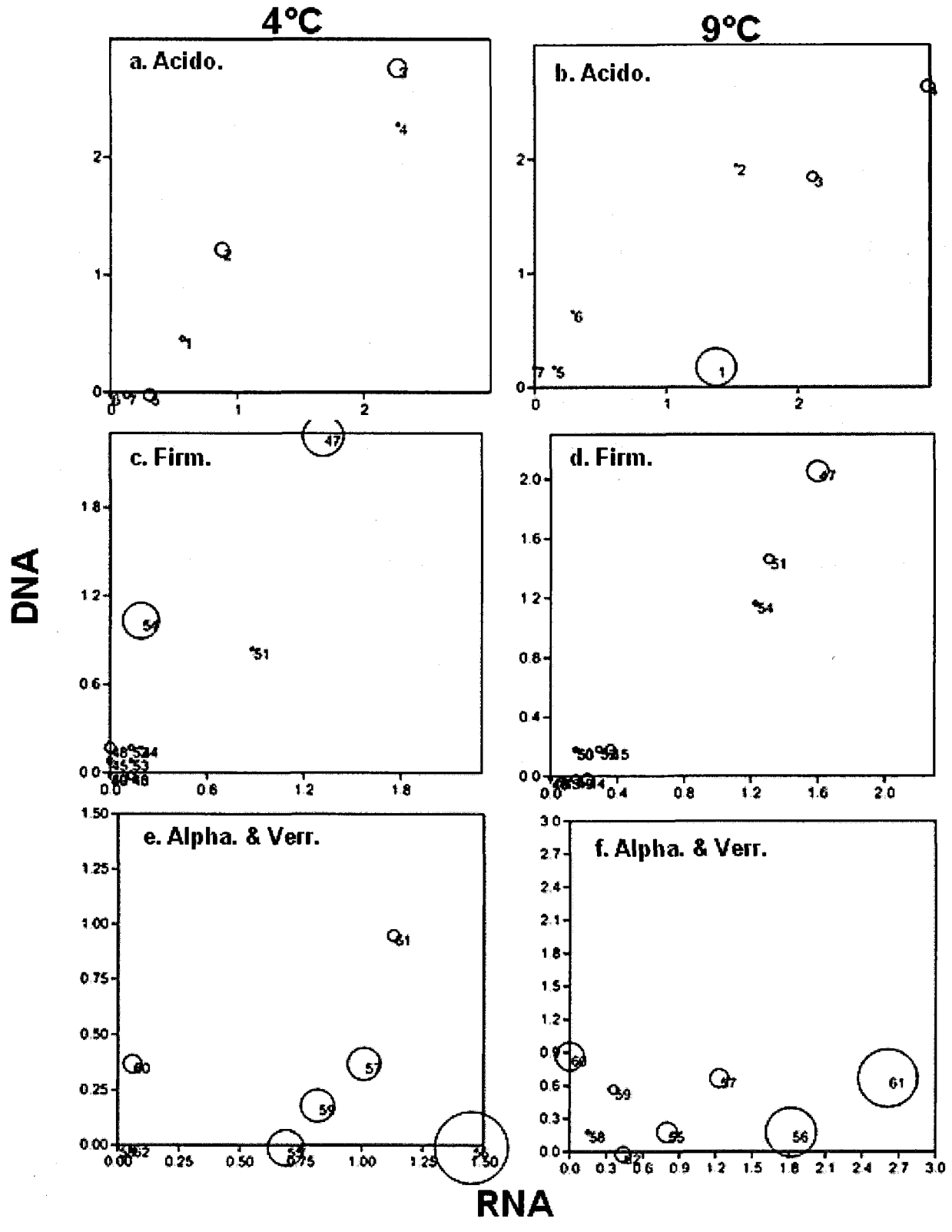

Figure 4.8 Comparision of RNA and DNA signatures at the family level found to contribute to the signifant differene in community structure between the two incubation temperatures for the phyla a & b) Acidobacteria; c & d) Firmicutes; e & f) Alphaproteobacteria and Verrucomicrobia. See table 4.4 for number code of the taxa represented. Bubble sizes represent difference in RNA-DNA

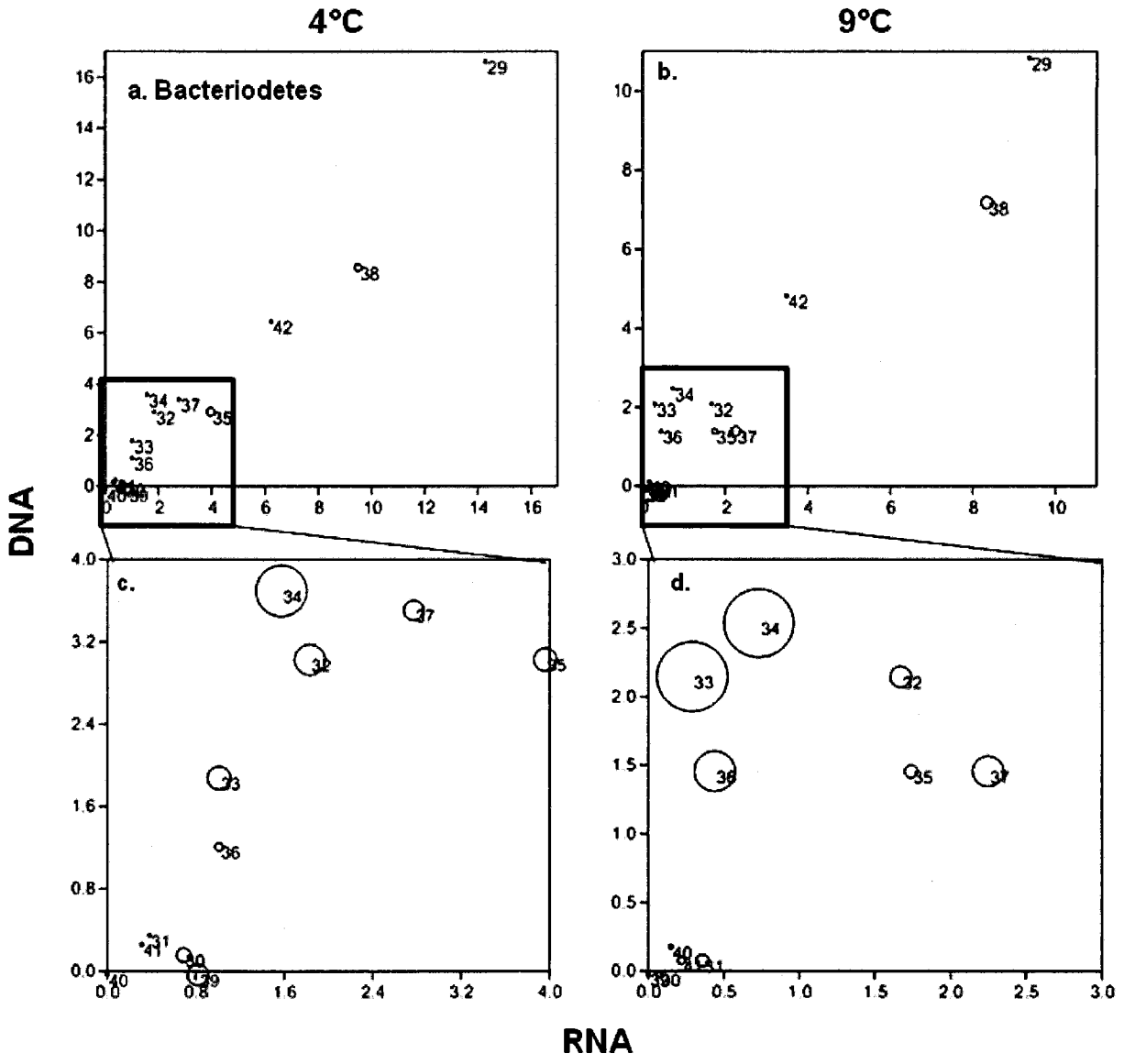

Figure 4.9 Comparision of RNA and DNA signatures at the family level found to contribute to the signifant differene in community structure between the two incubation temperatures for the phylum Bacteriodetes. a & b) plots of the the taxa within Bacteriodetes; c & d) magnification of taxa found at lower percentages. See table 4.4 for number code of the taxa represented. Bubble sizes represent difference in RNA-DNA

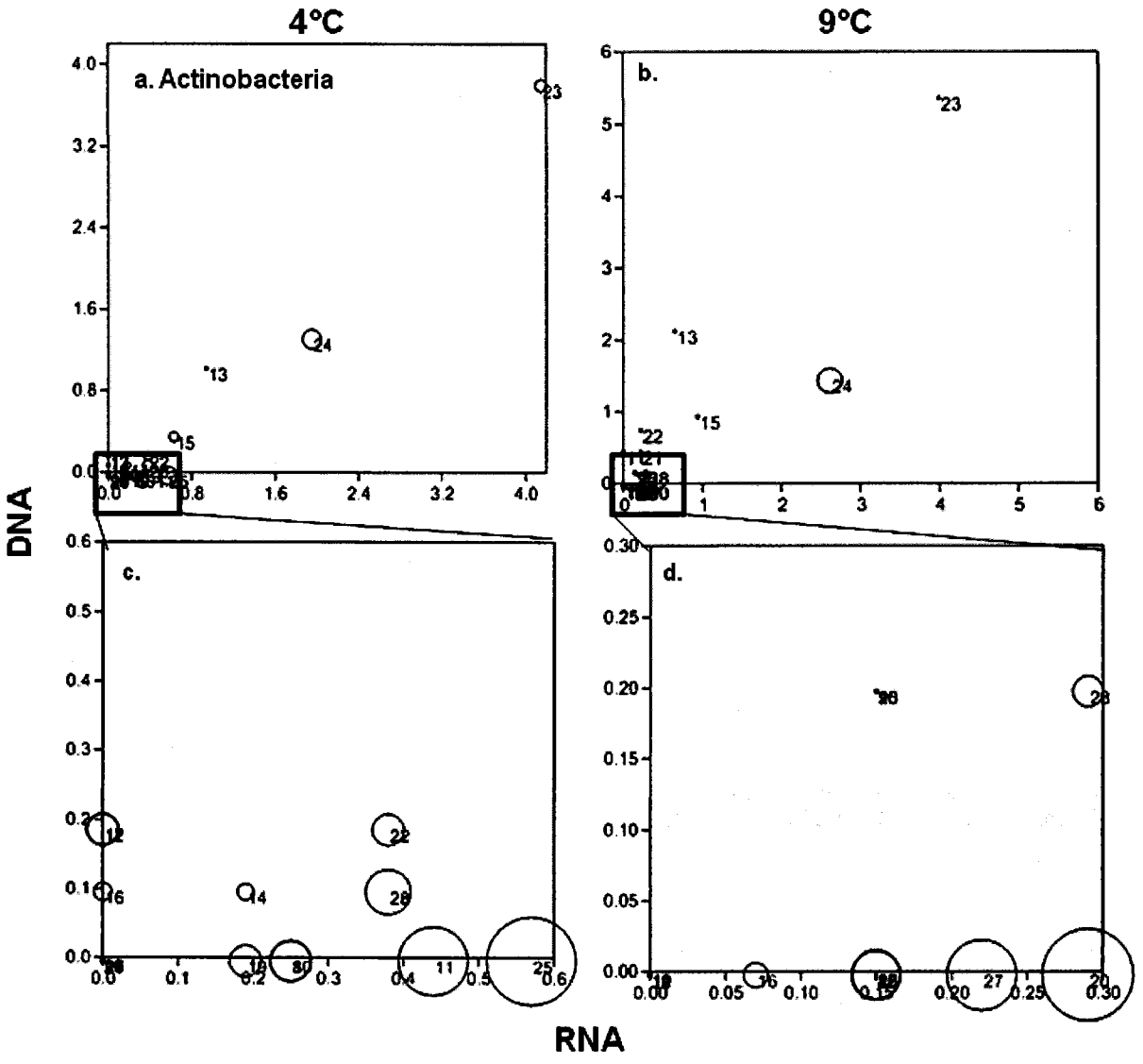

Figure 4.10 Comparision of RNA and DNA signatures at the family level found to contribute to the signifant differene in community structure between the two incubation temperatures for the phylum Actionbacteria. a & b) plots of the all the family's within Actionbacteria; c & d) magnification of taxa found at lower percentages. See table 4.4 for number code of the taxa represented. Bubble sizes represent difference in RNA-DNA

Table 4.4 Number code for Family represented in Figures 4.8 – 4.10

#	Acido.	#	Actino.	#	Bacterio.	#	Firmicutes	#	Alpha	#	Verruco.
1	Acidobacteriaceae	8	unclas. Actino 0319-7L14	29	Bacteroidetes _inc_sedis	43	unclas. Bacilli	55	Caulobacteraceae	57	Opitutaceae
2	Acidobacteriales Gp6	9	Acidimicrobineae _inc._sedis	30	Bacteroidaceae	44	Catabacteriaceae	56	Acetobacteraceae	58	unclas. verrucom.-R76-B18
3	Holophagaceae	10	Acidomicrobiales CL500-29		Marinilabiaceae	45	Clostridiaceae			59	Spartobacteriaceae
4	Solibacteraceae	11	Acidomicrobiales EB1017	32	Porphyromonadaceae	46	Clostridiales FamilyXII.IncertaeSedis			60	unclas.-verrucom.-RFP12
5	unclas. 32-20	12	Actinomycetales-ACK-M1	33	unclas. Bacteriodales	47	Clostridiales FamilyXIII.IncertaeSedis			61	Verrucomicrobiaceae
6	unclas. DS-18	13	Cellulomonadaceae	34	Cryomorphaceae	48	Eubacteriaceae			62	unclas. Verrucomicrobia
7	unclas. SJA-36	14	Frankiaceae	35	Flavobacteriaceae	49	Lachnospiraceae				
		15	Intrasporangiaceae	36	unclas. Flavobacteriales	50	Peptococcaceae				
		16	Kineosporiaceae	37	Chitinophagaceae	51	Ruminococcaceae				
		17	Microbacteriaceae	38	Cytophagaceae	52	Veillonellaceae				
		18	Micromonosporaceae	39	Flexibacteraceae	53	unclas. Clostridia				
		19	Mycobacteriaceae	40	Saprospiraceae	54	Erysipelotrichaceae				
		20	Nocardioidaceae	41	unclas. Sphingobacteriales						
		21	Propionibacteriaceae	42	unclas. Bacteriodetes						
		22	Sporichthyaceae								
		23	unclas. Actinomycetales								
		24	Coriobacteriaceae								
		25	unclassified MC47								
		26	Conexibacteraceae								
		27	unclas. Solirubrobacterales								
		28	unclas. Actinobacteria								

4.4 Discussion

In situ observations over the last few years at this site reveal a trend, with runnels being supersaturated in both CO_2 and CH_4, and polygonal ponds supersaturated only in CH_4 due to microbial mat photosynthesis reducing CO_2 below saturation levels (Breton *et al.*, 2009; Laurion *et al.*, 2010). Daily variations from the two ponds revealed that fluxes varied no more than by 25% for both CO_2 and CH_4, with runnel ponds having 3 folds higher CH_4 emissions (Negandhi *et al.*, 2013). The experimental set-up eliminated factors such as thermal mixing, meteorological conditions, and water surface turbulence, isolating microbes from any exchange with atmospheric O_2 and CO_2. The absence of atmospheric O_2 and CO_2 exchange is therefore reflected below when comparing *in situ* trends with our experimental results.

Significantly more CO_2 and CH_4 were produced at the higher temperature (+5°C above ambient) for all four thaw ponds. At both temperatures, runnel pond sediment produced almost twice as much CO_2 compared to polygonal pond sediment, consistent with *in situ* observations. These results corroborate with the idea that polygonal ponds can act as a sink for CO_2 atmospheric sink (Laurion *et al.*, 2010; Negandhi *et al.*, 2013).

However, CH_4 production in the incubation experiment was not consistent with the polygonal and runnel pond *in situ* GHG trends. Runnel pond BYL38, which has the highest *in situ* surface water dissolved CH_4 concentration among the four ponds, had the lowest CH_4 production rate during the incubation experiment. Runnel pond BYL24 also exhibited the same trend as BYL38, with a lower CH_4 production rate than from polygonal pond BYL1, and opposite to *in situ* trends. The experimental conditions of anoxia and inhibition of photosynthesis, due to an absence of light, feasibly inhibited methanotrophic oxidation of CH_4. The polygonal ponds increased CH_4 production rates accentuates the balance between methanotrophs and methanogens, as their lower *in situ* CH_4 emissions is possibly due to methanotrophic consumption of CH_4, as opposed to methanogenic production potential.

The increase in CH_4 production with temperature cannot be attributed to a decrease in methanotrophs since their contribution to the communities estimated from the 16S rRNA reads originating from DNA and RNA did not change with increased temperature (Annexe Figure S1). The results rather suggest that Arctic thaw pond methanogens were sensitive to an increase in temperature, at least under the incubation conditions. Increased CH_4 production with

temperature has been reported. Higher temperatures can lower the activation energy required for CH_4 production (VanBodegon and Stams 1999; Fey and Conrad 2000). Temperature can also influences the decomposition of organic materials by heterotrophic bacteria and hence change the methanogenic community composition depending on the available substrates. (Schütz et al., 1990; Chin *et al.*, 1999). Unfortunately the methanogens could not be assessed in the presented study because of unsuccessful amplification of Archaea within this one thaw pond, BYL38. However, the bacterial community shows support for increased methanogenic activity. There was a 3.6% and 0.6% higher percentage of Geobacteraceae in DNA and RNA respectively (Annexe Figure S3) at 9°C than at 4°C. This is a family with several Genera that are symbionts of *Methanosaeta concilli*, an acetogenic methanogen that has been found in these arctic thaw ponds (in other thaw ponds of the same site where Archaea amplification was successful; see Negandhi *et al.*, 2013). This of course does not take into account any possible increase in hydrogenotrophic methanogens, whose DNA has been found in these thaw ponds (Negandhi et al. 2013) and are also known to possibly increase with temperature (Høj et al., 2008). These inconclusive results place importance for further research onto the ratio of change between methanogens and methanotrophs with temperature in permafrost environments.

4.4.1 DNA and RNA communities among time points and temperature

There was a considerable overlap between the DNA and RNA communities, with all abundant OTUs found in both DNA and RNA. These results are similar to other studies comparing DNA and RNA communities from soils and sediment (Baldrian *et al.*, 2012; Koizumi *et al.*, 2003; Prosser *et al.*, 2010), indicating a stable and active core community (Bretter et al. 2012). Therefore the large discrepencies in DNA and RNA at T1 likely indicate a community reacting to bottle conditions, with larger bubble sizes indicating Phyla that were reacting (Figure 4.4b). Specifically, Bacteriodetes at T1 had higher DNA than RNA, indicating a reduction in activity, and Actinobacteria had higher RNA than DNA indicating an increase in activity due to possible confined environment of the bottle conditions on a very short time scale of 3 days.

After 16 days of incubation, DNA and RNA communities subjected to 4°C and 9°C grouped by temperature, with DNA and RNA communities at 4°C being very similar (Figure 4.5). The slight temperature increase already imposed on at 4°C, induced a high dominance taken over by Bacteriodetes. At 4°C, the community is actually less diverse compared to the *in situ* community. Comparatively, the community at 9°C is more diverse than the community at 4°C and *in situ*. The

RNA-9°C community separated from the DNA-9°C (Figure 4.6). Rarefaction curves confirm this with an increase presence of rare OTUs for RNA-9°C. Together these results indicate that at 9°C selection for an increased expression of rare OTUs within the RNA community occurred, suggesting that with more time the DNA-9°C community would further separate from the 4°C communities.

The continual diversity increase would likely be through an increase in rare OTUs associated with Verrucomicrobia, Acidobacteria, unclassififed bacteria, and Proteobacteria due to their higher RNA (activity) than DNA percentages (Figure 4.4d; fall below the line), and also a continual decrease in Bacteriodetes with a higher DNA than RNA percentage (Figure 4.4; falls above the line). Bacteriodetes at the phylum level consistently had a higher percentage of DNA than RNA at all time points (Figure 4.4 a-d). Previous bacterial communities have found the opposite of higher RNA than DNA, but these were in planktonic environments (Cortell and Kirchman 2000; Eilers et al. 2000). This is likely due to different taxa within the phylum Bacteriodetes having different traits that are being selected upon. For instance, at both temperatures the main three families including Bacteriodetes incertae sedis, Cytophagaceae, and unclassified Bacteriodetes had similar DNA to RNA ratios (Figure 4.9a-b), while Cryomorphaceae, unclassified Bacteriodales, unclassified Flexibacteraceae had higher DNA than RNA, and Flavobacteriales had higher RNA than DNA. For these families the trend in DNA to ratios was similar between temperatures, yet their contributing percentages at 4°C and 9°C were different. Chitinophagaceae was the only Bacteriodete to maintain a similar activity (RNA) at 4°C and 9°C only. This may be due to its ability to degrade more complex OM which would be left as the labile C is rapidly utilized at 9°C.

The Actinobacteria also contributed to the active community change between temperatures, which does not show up at the phylum level (Figure 4.4c-d, 4.7b), but does at the family level (Figure 4.10c-d). In fact, the majority of Actinobacterial diversity would not have been produced with DNA signatures alone. Similar to Bacteriodetes, a selection for different taxa within Actinobacteria was present, with unclassified MC47, Acidomicrobiales EB1017, and Mycobacteriaceae rRNA only present at 4°C, compared to Nocardiodaceae, Conexibacteraceae, and unclassified Soilrubrobacterales rRNA only present at 9°C. The lack of sediment replication within time points may contribute to some of these low represented taxa being present or absent. Through the use of high-throuput sequencing, lower abuntant taxa (~ < 3%) within Actionbacteria, along with Alphaproteobacteria and Verrucomicrobia, possibly have more

dicrepencies in DNA to RNA ratios and possibly more vulnerability to temperature selection pressures in Arctic thaw ponds.

4.4.2 Carbon decomposing communities

Carbon decomposers had a counter-intuitive reaction, with a slightly higher percentage in DNA at 9°C, but a lower RNA percentage at 9°C. The majority of all the bacterial communities were C decomposers (≥ 64%), with a shift towards a more diverse yet less active C degrading community occurring along with an increase in CO_2 and CH_4 production at higher temperature. The decline in C-degrading potential from RNA at 9°C coincided with other studies reporting a decrease in biomass and enzymatic activity with warming (Rinnan *et al.*, 2007; Bradford *et al.*, 2008), possibly due to internal allocation of C to respiration rather than to growth (López-Urrutia *et al.*, 2007). However, the reduced biomass at 9°C is accompanied by a community change and continual higher CO_2 production than at 4°C. Specifically, it can be attributed to a decrease in activity of the Bacteriodete (Figure 4.4 & 4.7). Similar results have been reported in a study of forest surface soil (7cm) in Michigan, where an increase in temperature resulted in higher respiration but a smaller active microbial biomass (Zogg *et al.*, 1997). Interestingly this shift was noticeable in our Arctic samples with a +5°C, compared to a +20°C in the study by Zogg *et al.* (1997). This counter-intuitive reaction in the carbon decomposing community accompanying increased GHG production can be explained by the more diverse community, selected though rare OTUs, allowing for utilization of differential C substrates.

The relative abundance differences and increased diversity in the carbon decomposing communities between RNA-4°C and RNA-9°C included a decrease in Bacteriodetes and slight increase in Acidobacteria at 9°C, suggesting a shift towards a community capable of degrading less labile C. The main source of dissimilarity (26%) between 4°C and 9°C were decreases among 34 genera of Bacteriodetes at 9°C (Figure 4.6). Bacteriodetes and Beta-proteobacteria reported to be initial mobilizers of labile C (Padmanabhan *et al.*, 2003). On the other hand, Acidobacteria are considered in some cases to be oligotrophic bacteria, which are categorized as having high substrate affinities to compete when substrates are low or less labile, and also have lower growth rates (Fierer *et al.*, 2007).

Rising temperature has increased the amount of old C used by microbes and could be attributed to a change in the microbial community (Waldrop & Firestone, 2004). The significant C degrader

community shift seen in our study is compatible with a previous Alaskan permafrost soil study where community shifts in Actionbacteria, Proteobacteria, Bacteriodetes, and Firmicutes were seen upon permafrost thaw when more C becomes available (Mackelprange et al. 2011). The shift to a more diverse C degrading community in our study possibly supports the utilization of the less labile and older C pool deposited in runnel thaw ponds upon permafrost thaw (Vonk et al. 2003). Considering the large pool of old carbon being released from the thawing permafrost, even a small increase in the decomposition of this recalcitrant pool could change the C stock over a decade (Davidson & Janssens, 2006).

4.5 Conclusions

This study demonstrated that at a warmer temperature, there is a significant increase in GHG production rate from arctic thaw pond sediment. Global climate models should take into account that warmer temperatures will increase GHG production rate in addition to expand the area covered by this overlooked aquatic system. Methanotrophic activity is attributed to reducing CH_4 emissions in polygonal ponds *in situ*, as they exhibit comparable CH_4 production potential and response level at 9°C to runnel ponds under experimental conditions where methanotrophic activity was reduced. There was an overall increase in bacterial diversity with temperature. Under warmer conditions, the major functional group of carbon decomposers decreased in activity, estimated from ribosomal RNA, and was accompanied by a community shift through an increase in rare OTUs. Many of these rare taxa within Actinobacteria, Alphaproteobacteria, and Verrucomicrobia were only identifiable by rRNA signatures and not rDNA. A more diverse community, may increase the available C pool through accessibility of a lower quality carbon, and therefore contribute to an increase in GHG production rates.

5 ANNEXE – Bibliographie

Abnizova A, Siemens J & Langer M (2012) Small ponds with major impact: The relevance of ponds and lakes in permafrost landscapes to carbon dioxide emissions. *Glob. Biogeochem. Cyc.* 26:GB2041-GB2050.

Abram JW & Nedwell DB (1978) Inhibition of methanogenesis by sulfate reducing bacteria competing for transferred hydrogen. *Arch Microbiol* 117:89-92.

Algesten G, Sobek S, Bergstrom AK, Agren A, Tranvik LJ & Jansson M (2004) Role of lakes for organic carbon cycling in the boreal zone. *Glob. Change Biol.* 10:141-147.

Alstad KP & Whiticar MJ (2011) Carbon and hydrogen isotope ratio characterization of methane dynamics for Fluxnet Peatland Ecosystems. *Org. Geochem.* 42:548-558.

Anderson O (2010) An Analysis of Respiratory Activity, Q10, and Microbial Community Composition of Soils from High and Low Tussock Sites at Toolik, Alaska. *J. Eukaryot. Microbiol.* 57:218-219.

Anesio A, Graneli W, Aiken G, Kieber DJ & Mopper K (2005) Effect of humic substances photodegradtion on bacterial growth and respiration in lake water. *Appl. Environ. Microbiol.* 71:626-6275.

Anisimova M & Gascuel O (2006) Approximate likelihood ratio test for branchs: A fast, accurate and powerful alternative. *Syst Biol.* 55:539-52.

Anthony C (1982) The biochemistry of methylotrophs. *Academic Press, Inc. London, England.*

Auguet JC, Barberan A & Casamayor EO (2009) Global ecological patterns in uncultured Archaea. *The ISME Journal*:1-9.

Auman AJ, Stolyar S, Costello AM & Lidstorm ME (2000) Molecular characterization of methanotrophic isolates from freshwater lake sediment. *Appl. Environ. Microbiol.* 66(12):5259-5266.

Baker-Blocker A, Donahue TM & Mancy KH (1977) Methane flux from wetland areas. *Tellus* 29:245-250.

Baldrian P, Kolarik M, Stursova M, Kopecky J, Valaskova V, Vetrovsky T, Zifcakova L, Snajdr J, Ridl J, Vlcek C & Voriskova J (2012) Active and total microbial communities in forest soil are largely different and highly stratified during decomposition. *ISME J* 6:248-258.

Barber R, Zhang L, Harnack M, Olson M, Kaul R, Ingram-Smith C & Smith KS (2011) Complete Genome Sequence of Methanosaeta concilii, a Specialist in Aceticlastic Methanogenesis. *J. Bacteriolog.* 193:3668-3669.

Barbier BA, Dziduch I, Liebner S, Ganzert L, Lantuit H, Pollard W & Wagner D (2012) Methane-cycling communities in a permafrost-affected soil on Herschel Island, Western Canadian Arctic: active layer profiling of mcrA and pmoA genes. *FEMS Microbiol. Ecol.* 82:1574-6941.

Bardgett RD, Freeman C & Ostle NJ (2008) Microbial contributions to climate change through carbon cycle feedbacks. *ISME J* 2:805-814.

Bartlett KB, Crill PM, Sebacher DI, Harriss RC, Wilson JO & Melack JM (1988) Methane flux from the central Amazonian floodplain. *J. Geophys, Res.* 93:1571-1582.

Basak N & Das D (2007) The Prospect of purple non-sulfur (PNS) photosynthetic bacteria for hydrogen production: The present state of the art. *World J. Microbiol. and Biotechnol.* 23:31-42.

Bastviken D, Cole J, Pace ML & Tranvik LJ (2004) Methane emissions from lakes: Dependence of lake characteristics, two regional assesments, and a global estimate. *Glob. Biogeochem. Cyc.* 8:4009-4021.

Bastviken D, Cole J, Pace ML & Van de Bogert M (2008) Fates of methane from different lake habitats: Connecting whole-lake budgets and CH_4 emissions. *J. Geophys. Res.* 113:GO2024-GO2037.

Bégin PN (2012) *Estimation des émissions de gaz à effet de serre par les milieux aquatiques à l'échelle d'une vallée glaciaire au Nunavut à l'aide de l'imagerie satellitaire. Mémoire d'initiation à la recherche.* travaux de baccalauréat (Université Laval, Québec, QC).

Bekku Y, Nakatsubo T, Kume A, Adachi M & Koizumi H (2003) Effect of warming on the temperature dependence of soil respiration rate in arctic, temperate and tropical soils. *Appl. Soil Ecol.*22:205-210.

Berggren M, Strom L, Laudon H, Karlsson J, Jonsson A, Giesler R, Bergstrom AK & Jansson M (2010) Lake secondary production fueled by rapid transfer of low molecular weight organic carbon from terrestrial sources to aquatic consumers. *Ecol. lett.* 13:870-880.

Bertilsson S & Allard B (1996) Sequential photochemical and microbial degradation of refractory dissolved organic matter in a humic freshwater system. *Arch. Hydrobiol. Adv. Limnol.* 48:133-141.

Billings SA, Richter DD & Yarie J (1998) Soil carbon dioxide fluxes and profile concentrations in two boreal forests. *Can. J. For. Res.* 28:1773-1783.

Blazewicz S, Barnard R, Daly R & Firestone MK (2013) Evaluating rRNA as an indicator of microbial activity in environmental communities: limitations and uses. *ISME J* 7:2061-2068.

Bonilla S, Conde D, Aubriot L & Perez M (2005) Influence of hydrology on phyto- plankton species composition and life strategies in a subtropical costal lagoon periodically connected with the Atlantic Ocean. *Estuaries* 28:884-895.

Borrel G, Joblin K, Guedon A, Colombet J, Tardy V, Lehours AC & Fonty G (2011) Methanobacterium lacus sp. nov., isolated from the profundal sediment of a freshwater meromictic lake. *Int. J. Sys. Evol. Micr.* 62:1625-1629.

Bousquet P, Ciais P, Miller J, Dlugokencky EJ, Hauglustaine D, et al. (2006) Contribution of anthropogenic and natural sources to atmospheric methane variability. *Nature* 443:439-443.

Bradford MA, Davies CA, Frey SD, Maddox TR, Melillo JM, Mohan JE, Reynolds JF, Treseder KK & Wallenstein MD (2008) Thermal adaptation of soil microbial respiration to elevated temperature. *Ecol. lett.* 11:1316-1327.

Breton J, Valliere C & Laurion I (2009) Limnological properties of permafrost thaw ponds in northeastern Canada. *Can. J. Fish. Aquat. Sci.* 66:1635-1648.

Brosius LS, Walter Anthony KM, Grosse G, Chanton JP, Farquharson LM, Overduin PP & Meyer H (2012) Using the deuterium isotope composition of permafrost meltwater to constrain thermokarst lake contributions to atmospheris CH_4 during the last deglaciation. *J. Geophys. Res.* 117:G01022.

Brown P, Cabarle B & Livernash R (1997) Carbon counts: estimating climae change mitigation in forestry projects. *World Resources Institute, Washington*:1997-2022.

Bult C, White O, Olsen G, Zhou L, Fleischmann R, et al. (1996) Complete Genome Sequence of the Methanogenic Archaeon, Methanococcus jannaschii. *Science* 273:1058-1073.

Burkert U, Warnecke F, Babenzien D, Zwirnmann E & Pernthaler J (2003) Members of a Readily Enriched β-Proteobacterial Clade Are Common in Surface Waters of a Humic Lake. *Appl. Environ. Microbiol.* 69(11):6550-6559.

Camill P, Lynch J, Clark J, Adams J & Jordan B (2001) Changes in biomass aboveground net primary production, and peat accumulation following permafrost thaw in the boreal peatlands of Manitoba, Canada. *Global Biogeochem. Cy.* 4:461-478.

Casper P, Maberly SC, Hall GH & Finlay BJ (2000) Fluxes of methane and carbon dioxide fram a small productive lake to the atmosphere. *Biogeochem.* 49:1-19.

Castresana J. (2000) Selection of conserved blocks from multiple alignments for their use in phylogenetic analysis. *Mol Biol Evol.* 17:540-552.
Chanton JP & Martens CS (1988) Seasonal variations in ebullitive flux and carbon isotopic compostion of methane in a tidal freshwater estuary. *Global Biogeochem. Cy.* 2:289-298.
Chappaz A, Gobeil C & Tessier A (2008) Geochemical and anthropogenic enrichments of Mo in sediments from perennially oxic and seasonally anoxic lakes in Eastern Canada. *Geochim. Cosmochim Acta* 72:170-184.
Chin K, Lukow T, Stubner S & Conrad R (1999) Structure and function of the methanogenic archaeal community in stable cellulose-degrading enrichment cultures at two different temperatures (15 and 30°C). *FEMS Microbiol Ecol* 30:313-326.
Christensen TR, Johansson T, Olsrud M, Strom L, Lindroth A, Mastepanov M, Malmer N, Friborg T, Crill P & Callaghan TV (2007) a catchment-scale carbon and greenhouse gas budget of a subarctic landscape. *Philosophical Transactions of the Royal Society A* 365:1643-1656.
Cicerone RJ & Shetter JD (1981) Sources of atmospheris methane: measurements in rice paddies and a discussion. *J. Geophys. Res.* 86:7203-7209.
Cole J & Caraco NF (1998) Atmospheric exchange of carbon dioxide in a low-wind oligotrophic lake measured by the addition of SF6. *Limnol. Oceanogr.* 43(4):647-656.
Comeau AM, Harding T, Galand PE, Vincent WF & Lovejoy C (2012) Vertical distribution of microbial communities in a perennially stratified Arctic lake with saline, anoxic bottom waters. *Scientific Reports* 2:#604.
Comeau AM, William KW, Tremblay JE, Carmack EC & Lovejoy C (2011) Arctic Ocean Microbial Community Structure before and after the 2007 Record Sea Ice Minimum. *PLoS ONE* 6(11):e27492.
Conant R, Ryan M, Agren G, Birge H, Davidson EA & al. e (2011) Temperature and soil organic matter decomposition rates – synthesis of current knowledge and a way forward. *Global Change Biol.* 17:3392-3404.
Conrad R (2005) Quantification of methanogenic pathways using stable carbon isotopic signatures: a review and a proposal. *Organ. Geochem.* 36:739-752.
Conrad R, Chan O, Claus P & Casper P (2007) Characterization of methanogenic Archaea and stable isotope frationation during methane production in the profundal sediment of an oligotrophic lake (Lake Stechlin, Germany). *Limnol. Oceanogr.* 52:1393-1406.
Cottrell MT and Kirchman DL (2000) Community composition of marine bacterioplankton determined by 16S rRNA gene clone libraries and fluorescence in situ hybridization. *Appl. Environ. Microbiol.* 66:5116-5122.
Coulthard TJ, Baird AJ, Ramirez J & Waddington JM (2009) Methane Dynamics in Peat: Importance of shallow peats and a novel reduced-complexity approach for modeling ebullition. *Carbon Cycling in Northern Peatlands*, Baird AJ, Belyea LR, Comas X, Reeve A & Slater L (Édit.) American Geophysical Union, Washington, D. C., Vol 184. p 173-187.
Cox P, Betts R, Jones C, Spall S & Totterdell I (2000) Acceleration of global warming due to carbon-cycle feddbacks in a coupled climate model. *Letters to nature* 408:184-187.
Davidson EA & Janssens IA (2006) Temperature sensitivity of soil carbon decomposition and feedbacks to climate change. *Nature* 440:165-173.
Deppenmeier U, Johann A, Hartsch T, Merkl R, Schmitz RA, Martinez-Arias R, Henne A, Wiezer A, Baumer S, Jacobi C, Bruggemann H, Lienard T, Christmann A, Bomeke M, Steckel S, Bhattacharyya A, Lykidis A, Overbeek R, Klenk HP, Gunsalus RP, Fritz HJ & Gottschalk G (2002) The genome of *Methanosarcina mazei*: evidence for lateral gene transfer between bacteria and archaea. *J. Mol. Microb. Biotech.* 4:453-461.
Deppenmeier U, Muller V & Gottschalk G (1996) Pathways of energy conservation in methanogenic archaea. *Arch Microbiol* 165:149-163.

Downing JA, Prairie YT, Cole JJ, Duarte CM, Tranvik LJ, Striegel RG, McDowell WH, Kortelainen P, Caraco NF, Melack JM & Middelburg JJ (2006) The global abundance and size distribution of lakes, ponds, and impoundments. *Limnol. Oceanogr.* 5(15):2388-2397.

Edgar R (2004) MUSCLE: multiple sequence alignment with high accuracy and high throughput. *Nucleic Acids Res.* 32:1792-1797.

Eilers H, Pernthaler J, Glöckner FO, Amann R (2000) Culturability and in situ abundance of pelagic bacteria from the North Sea. *Appl. Environ. Microbiol.* 66:3044-3051

Elmendorf S.C, Henry G. H. R., Hollister R. D., Björk R. J., Boulanger-Lapointe N., Cooper E. J., et al.(2012) Plot-scale evidence of tundra vegetation change and links to recent summer warming. *Nature Climate Change* 2:453-457.

Epstein H, Smith I & Walker D (2013) Recent dynamics of arctic and sub-arctic vegetation. *Environ Res Lett* 8:015040.

Fey A & Conrad R (2000) Effect of temperature on carbon and electron flow and on the archaeal community in methanogenic rice field soil. *Applied and Environmental Microbiology* 66:4790-4797.

Fierer N, Bradford MA & Jackson RB (2007) Toward an ecological classification of soil bacteria. *Ecology* 88:1354-1364.

Fortier D & Allard M (2004) Late Holocene syngenetic ice-wedge polygons development, Bylot Island, Canadian Arctic Archipelago. *Can. J. Earth Sci.* 41:997-1012.

Fung I, John J, Lemer J, Matthews E, Prather M, Steele LP & Fraser PJ (1991) Three-dimensional model synthesis of the Global methane cycle. *J. Geophys. Res.* 96:13033-13065.

Galand PE, Lovejoy C, Pouliot J, Garneau M & Vincent WF (2008) Microbial community diversity and heterotrophic productionin a coastal Arctic ecosystem: a Stamukhi lake and its source waters. *Limnol. Oceanogr.* 53:813-823.

Galand PE, Lovejoy C & Vincent WF (2006) Remarkably diverse and contrasting archaeal communities in a large arctic river and the coastal Arctic Ocean. *Aquat. Microb. Ecol.* 44:115-126.

Galand PE, Saarnio S, Fritze H & Yrjala K (2002) Depth related diversity of methanogen Archaea in Finnish oligotrophic fen *FEMS Microb. Ecol.* 42:441-449.

Gao X, Schlosser CA, Sokolov A, Anthony KW, Zhuang Q & Kicklighter D (2013) Permafrost degradation and methane: low risk of biogeochemical climate-warming feedback. *Envir. Res. Let.* 8:035014.

Garcia JL, Patel BKC & Ollivier B (2000) Taxonomic, phylogenetic, and ecological diersity of methanogenic archea. *Anaerobe* 6:205-226.

Gilichinsky D & Rivkina E (2011) Permafrost Microbiology.*Encyclopedia of Geobiology*. Reitner J & Thiel V (Editer) springer, Verlag.

Graham DE, Wallenstein MD, Vishnivetskaya TA, Waldrop MP, Phelps TJ, Pfiffner SM, Onstott TC, Whyte LG, Rivkina EM, Gilichinsky DA, Elias DA, Mackelprang R, VerBerkmoes NC, Hettich RL, Wagner D, Wullschleger SD & Jansson JK (2011) Microbes in thawing permafrost: the unknown variable in the climate change equation. *ISME J* 6:709-712.

Green JL, Bohannan BJM & Whitikar RJ (2008) Microbial biogeography: From taxonomy to traits. *Science* 23:1039-1043.

Grosse G, Harden J, Turetsky M, McGuire AD, Camill P, Tarnocai C, Frolking S, Schuur EAG, Jorgenson T, Marchenko S, Romanovsky V, Wickland KP, French N, Waldrop M, Bourgeau-Chavez L & Striegl RG (2011) Vulnerability of high-latitude soil organic carbon in North America to disturbance. *J. Geophys. Res.*116:2005-2012.

Grosse G, Romanovsky V, Walter K, Morgenstern A, Lantuit H & Zimov S (2008) Distribution of thermokarst lake and ponds at three yedoma sites in Siberia.551-556.

Guillemette F & delGiorgio PA (2011) Reconstructing the various facets of dissolved organic carbon bioavailability in freshwater ecosystems. *Limnol. Oceanogr.* 56:734-748.

Guindon S & Gascuel O (2003) A simple, fast, and accurate algorithm to estimate large phylogenies by maximum likelihood. *Syst Biol.* 52:696-704.

Hall TA (1999) BioEdit: a user-friendly biological sequence alignment editor and analysis program for Windows 95/98/NT. *Nucleic acids symposium series* 41:95-98.

Hamilton JD, Kelly CA, Rudd JWM, Hesslein RH & Roulet NT (1994) Flux to the atmosphere of CH4 and CO2 from wetland ponds on the Hudson Bay Lowlands (HBLs). *J. Geophy. Res.* 99:1495-1510.

Hammer Ø, Harper DAT & Ryan PD (2001) Past: Paleontological Statistics Software Package for Education and Data Analysis. *Palaeontol. Electron.* 4:art. 4: 9pp.

Hansen AA, Herbert RA, Mikkelsen K, Jensen LL, Kristoffersen T, Tiedje JM, Lomstein BA & Finster KW (2007) Viability, diversity and composition of the bacterial community in a high Arctic permafrost soil from Spitsbergen, Northern Norway. *Envirion. Microbiol.* 9:2870-2884.

Hanson RS & Hanson TE (1996) Methanotrophic bacteria. *Micobiol. Rev.* 60:439-471.

He R, Wooller MJ, Pohlmane JW, Quensenf J, Tiedjef JM & Leigh MB (2012) Shifts in identity and activity of methanotrophs in Arctic lake sediments in response to temperature changes. *Appl. Environ. Microbiol.* 78:4715-4723.

Helms JR, Stubbins A, Ritchie JD, Minor EC, Kieber DJ & Mopper K (2008) Absorption spectral slopes and slope ratios as indicators of molecular weight, sources, and photobleaching of chromophotic dissolved organic matter. *Limnol. Oceanogr.* 53:955-969.

Hesslein RH, Ruddd J, Kelly C, Ramlai P & Hallard K (1991) Carbon dioxide pressure in surface waters of Canadian lakes. *In S. C. Wilhelms and J. S, Guliver (eds),* Air-water mass transfer. Amr. Soc. Eng.:p. 413-431.

Høj L, Olsen R & Torsvik V (2008) Effects of temperature on the diversity and community structure of known methanogenic groups and other Archaea in high Arctic peat. *ISME J* 2:37-48.

Høj L, Olsen RA & Torsvik VL (2006) Archaeal communities in High Arctic wetlands at Spitsbergen, Norway (78°N) as characterized by 16S rRNA gene fingerprinting. *FEMS Microbiol. Ecol.* 53:89–101.

Holmes R, McClelland J, Raymond P, Frazer B, Peterson B & Stieglitz M (2008) Liablity of DOC transported by Alaskan rivers to the Arctic Ocean. *Geophys. Res. Let.* 35:L03402, doi:10.1029/2007GL032837).

Hornibrook ERC, Longstaffe FJ & Fye WS (1997) Spatial distrubution of microbial methane production pathways in temperate zone wetland soils: Stable carbon and hydrogen isotope evidence. *Geochim. Cosmochim Acta* 61:745-753.

Hornibrook ERC, Longstaffea FJ & Fyfea WS (2000) Evolution of stable carbon isotope compositions for methane and carbon dioxide in freshwater wetlands and other anaerobic environments. *Geochim. Cosmochim. Ac.* 64:1013-1027.

Hou S, Makarova KS, Saw JHW, Senin P, Ly BV, Zhou Z, Ren Y & al. e (2008) Complete genome sequence of the extremely acidophilic methanotroph isolate V4, Methylacidiphilum infernorum, a representative of the bacterial phylum Verrucomicrobia. *Biology Direct* 3:26.

IPCC AR4 WG1 (2007), Solomon, S.; Qin, D.; Manning, M.; Chen, Z.; Marquis, M.; Averyt, K.B.; Tignor, M.; and Miller, H.L., ed., *Climate Change 2007: The Physical Science Basis*, Contribution of Working Group I to the Fourth Assessment Report of the Intergovernmental Panel on Climate Change, Cambridge University Press, ISBN 978-0-521-88009-1 (pb: 978-0-521-70596-7).

Pouliot J, Galan PE, Lovejoy C & Warwick FV (2009) Vertical structure of archaeal communities and the distribution of ammonia monooxygenase: A gene variants in two meromictic High Arctic lake. *Environ Microbiol* 11:687-699.

Jaatinen K, Tuittila E-S, Laine J, Yrjälä K & Fritze H (2005) Methane-Oxidizing Bacteria in a Finnish Raised Mire Complex: Effects of Site Fertility and Drainage. *Microbial Ecology* 50:429-439.

Janssen PH & Frenzel P (1997) nhibition of methanogenesis by methyl fluoride – studies of pure and defined mixed cultures of anaerobic bacteria and archaea. *Appl. Environ. Microbiol.* 63:4552-4557.

Jonsson A, Maili M, Bergstrom AK & Jansson M (2001) Whole-lake mineralization of allochthonous and autochthonous organic carbon in a large humic lake (Oertraesket, N. Sweden) *Limnol. Oceanogr.* 46:1691-1700.

Juottonen H (2008) Archaea, Bacteria, and methane production along environmental gradients in fens and bogs. *(Unpublished doctoral dissertation)* (University of Helsinki, Finland).

Kankaala P, Huotari J, Peltomaa E, Saloranta T & Ojala A (2006) Methanotrophic activity in relation to methane efflux and total heterotrophic bacterial production in a stratified, humic, boreal lake *Limnol. Oceanogr.* 51(2):1195-1204.

Karadagli F & Rittmann BE (2007) A mathematical model for the kinetics of *Methanobacterium bryantii* M.o.H. considering hydrogen thresholds. *Biodegradation* 18:453-464.

Kendall C & McDonnell J (1998) *Isotope tracers om catchment hydrology.* Elsevier Science B.V, Amsterdam, First ed.

Kirchman DL (2002) The ecology of Cytophaga-Flavobacteria in aquatic environments. *FEMS Microbiol Ecol* 39:91-100.

Kirschbaum MUF (2004) Soil respiration under prolonged soil warming: are rate reductions caused by acclimation or substrate loss? *Global Change Biol.* 10:1870-1877.

Klappenbach J, Dunbar J & Schmid T (2000) rRNA Operon Copy Number Reflects Ecological Strategies of Bacteria. *Appl. Environ. Microbiol.* 79:1328-1333.

Kobabe S, Wagner D & Pfeiffer EM (2004) Characterisation of microbial community composition of a Siberian tundra soil by fluorescence in situ hybridisation. *FEMS Microbiol Ecol* 50:13-23.

Kolmonen EK, Sivonen J, Haukka K (2004) Diversity of cyanobacteria and heterotrophic bacteria in cyanobacterial blooms in Lake Joutikas, Finland. *Aquat. Microb. Ecol.* 36:201-211.

Kortelainen P, Rantakari M, Huttunen J, Mattsson T, Alm J, Juutinen S, Larmola T, Silvola J & Martikainen P (2006) Sediment respiration and lake trophic state are important predictors of large CO2 evasion from small boreal lakes *Global Change Biol.* 12:1554-1567.

Koven C, Ringeval B, Friedlingstein P, Ciais P, Cadule P, Khvorostyanov D, Krinner G & Tarnocai C (2013) *Permafrost carbon-climate feedbacks accelerate global warming* 108:14769-14774.

Kudryavtsev Ve (1978) Obshcheye merzlotovedeniya (Geokriologiya) (General permafrost science) In Russian. . *Moskva (Moscow), Izdatel'stvo Moskovskogo Universiteta, (Moscow University Editions)* Izd. 2(Edu 2):404.

Larkin M, Blackshields G, Brown N, Chenna R, McGettigan P, McWilliam H, Valentin F, Wallace I, Wilm A, Lopez R, Thompson J, Gibson T & Higgins D (2007) ClustalW and ClustalX, version 2 (2007). *Bioinformatics* 23:2947-2948.

Laurion I & Mladenov N (2013) Dissolved organic matter photolysis in Canadian arctic thaw ponds. *Envir. Res. Lett.* 8:035026.

Laurion I, Vincent WF, MacIntyre S, Retamal L, Dupont C, Francus P & Pienitz R (2010) Variability in greenhous gas emissions from permafrost thaw ponds. *Limnol. Oceanogr.* 55(1):115-133.

Liu P, Qiu Q & Lu Y (2011) Syntrophomonadaceae-affiliated species as active butyrate-utilizing syntrophs in paddy field soil. *Appl. Environ. Microbiol.* 77:3884-3887.
López-Urrutia Á & Morán XAG (2007) Resource limitation of bacterial production distorts the temperature dependence of oceanic carbon cycling. *Ecology* 88:817-822.
MacDonald NW, Zak DR & Pregitzer KS (1995) Temperature effects on kinetics of microbial respiration and net nitrogen and sulfur mineralization. *Soil Sci. Soc. Am. J.* 59:233-240.
MacIntyre S, Jonsson A, Jansson M, Aberg J, Turney DE & Miller SD (2010) Buoyancy flux, turbulence, and the gas transfer coefficient in a stratified lake. *Geophys. Res. Let.* 37:L24604.
Mackelprange R, Waldrop MP, DeAngelis KM, David MM, Chavarria KL, Blazewicz SJ, Rubin EM, Jansson JK (2011) Metagenomic analysis of a permafrost microbial community reveals response to thaw. *Nature* 480:368-371.
Margulies M, Egholm M, Altman WE, Attiya S, Bader JS, Bemben LA, et al.(2005) Genome sequencing in microfabricated high-density picolitre reactors. *Nature* 437:376-380.
Massana R, Murray AE, Preston CM & DeLong EF (1997) Vertical distribution and phylogenetic characterization of marine planktonic Archaea in the Santa Barbara Channel. *Appl. Environ. Microbiol.* 63:50-56.
Mazeas O, von Fischer JC & Rhew RC (2009) Impact of terrestrial carbon input on methane emissions from an Alaskan Arctic lake. *Geophys. Res. Let.* 36:18501-18506.
McGuire AD, Anderson LG, Christensen TR, Dallimore S, Guo L, Hayes DJ, Heimann M, Lorenson TD, MacDonald RW & Roulet N (2009) Sensitivity of the carbon cycle in the Arctic to climate change. *Ecolog. Monog.* 79:523-555.
McGuire AD, Melillo JM, Kicklighter DW & Joyce LA (1995) Equilibrium responses of soil carbon to climate change: empirical and process-based estimates. *J. Biogeogr.*22:785-796.
Metje M & Frenzel P (2007) Methanogenesis and methanogenic pathways in a peat from subarctic permafrost. *Envirion. Microbiol.* 9:954-964.
Meybeck M (1995) Global distribution of lakes. *Physics and chemistry of lakes*, Lerman A, Imboden D & Gat J (Édit.) Sringer-Verlag. p 1-35.
Michmerhuizen CM, striegl RG & McDonald ME (1996) Potential methane emission from north-temperate lakes following ice melt. *Limnol. Oceanogr.* 41(5):985-991.
Miyajima T, Wada E, Hanba YT & Vijarnsorn P (1997) Anaerobic mineralization of indigenous organic matters and methanogenesis in tropical wetland soils. *Geochim. Cosmochim. A.* 61:3739-3751.
Morita M, Malvankar N, Franks AE, Summers ZM, Giloteaux L & al. e (2011) Potential for Direct Interspecies Electron Transfer in Methanogenic Wastewater Digester Aggregates. *mBio* 2(4):e00159-00111.
Muster S, Langer M, Heim P, Westermann S & Boike J (2012) Subpixel heterogeneity of ice-wedge polygonal tundra: a multi-scale analysis of land cover and evapotranspiration in the Lena River Delta, Siberia. *Tellus B* 64:17301.
Nadkarni M, Martin F, Jacques N & Hunter N (2002) Determination of bacterial load by rea-time PCR using a broad-range (universal) probe and primer set. *Microbiology* 148:257-266.
Negandhi K, Laurion I & Lovejoy C (submitted) Arctic thaw pond morphology influences bacterial communities and associated greenhouse gas emissions *Polar Biol.*
Negandhi K, Laurion I, Whiticar MJ, Galand PE, Xu X & Lovejoy C (2013) Small thaw ponds: an unaccounted source of methane in the Canadian high Arctic. *PLoS ONE* 8:e78204.
Newton RJ & McMahon KD (2011) Seasonal differences in bacterial community composition following nutrient additions in a eutrophic lake. *Envirion. Microbiol.* 13:887-899.
O'Brien BJ & Stout JD (1978) Movement and turnover o soil organic matter as indicated by carbon isotope measurements. *Soil Biol. Biochem.* 10:309-317.

Op den Camp HJM, Islam T, Stott MB, Harhangi HR, Hynes A, Schouten S, Jetten MSM, Birkeland NK, Pol A & Dunfield PF (2009) Environmental, genomic and taxonomic perspectiveson methanotrophic Verrucomicrobia. *Envirion. Microbiol. Reports* 1(5):293-306.

Padmanabhan P, Padmanabhan S, deRito C, Gray A, Gannon D, Snape JR, Tsai CS, Park W, Jeon C & Madsen EL (2003) Respiration of 13C-labeled substrates added to soil in the feild and subsequent 16S rRNA gene analysis of 13C-labeled soil DNA. *Appl. Environ. Microbiol.* 69:1614-1622.

Penning H & Conrad R (2007) Quantification of carbon flow from stable isotope fractionation in rice field soils with different organic matter. *Org Geochem* 38:2058-2069.

Peura S, Eiler A, Bertilsson S, Nykanen H, Tiirola M & Jones RI (2012) Distinct and diverse anaerobic bacterial communities in boreal lakes dominated by candidate division OD1. *ISME J* 6:1640-1652.

Pfennig N (1969) Rhodopseudomonas acidophila, sp. n., a new species of the budding purple nonsulfur bacteria. *J. Bacteriol.* 99:597-602.

Pouliot J, Galand PE, Lovejoy C & Vincent WF (2009) Vertical structure of archaeal communities and the distribution of ammonia monooxygenase A gene variants in two meromictic High Arctic lakes. *Enivron. Microbiol.* 11:687-699.

Prairie Y & del Giorgio P (2013) A new pathway of freshwater methane emissions and the putative importance of microbubbles. *Inland Waters* 3:311-320.

Prowse TD, Wrona FJ, Reist JD, Gibson JJ, Hobbie JE, Levesque LMJ & Vincent WF (2006) Climate change effects on hydroecology of Arctic freshwater ecosystems. *Ambio* 35:350 - 358.

Riley W, Subin Z, Lawrence D, Swenson S, Torn M, Men gL & al. e (2011) Barriers to predicting changes in global terrestrial methane fluxes: analyses using CLM4Me, a methane biogeochemistry model integrated in CESM. *Biogeosciences* 8:1925-1953.

Rinnan R, Michelsen A, Bååth E & Jonasson S (2007) Fifteen years of climate change manipulations alter soil microbial communities in a subarctic heath ecosystem. *Glob. Change Biol.* 13:28-39.

Roehm CL, Giesler R & Karlsson J (2009) Bioavailability of terrestrial organic carbon to lake bacteria: The case of a degrading subarctic permafrost mire complex. *J. Geophys. Res.* 114:G03006.

Rowland JC, Jones CE, Altman G, Bryan R, Crosby BT, et al. (2010) Arctic Landscapes in Transition: Responses to Thawing Permafrost. *Eos Trans AGU* 91:229-230.

Sachs T, Wille C, Boike J & Kutzbach L (2008) Environmental controls on ecosystem-scale CH_4 emission from polygonal tundra in the Lena River Delta, Siberia. *J. Geophys. Res.* 113:2005-2012.

Sakai S, Imachi H, Sekiguchi Y, Tseng IC, Ohashi A, Harada H & Yoichi Kamagata Y (2009) Cultivation of Methanogens under Low-Hydrogen Conditions by Using the Coculture Method. *Appl. Environ. Microbiol.* 75:4892 - 4896.

Schaefer K, Lantuit H, Romanovsky V & Schuur E (2012) Policy Implication of Warming Permafrost. Édit (Unep) UNEP.

Schink B (1997) Energetics of syntrophic cooperation in methanogenic degradation. *Micobiol. Rev.* 61:262-280.

Schloss P (2009) A high-throughput DNA sequence aligner for microbial ecology studies. *PLoS ONE* 4:e8230.

Schloss PD, Westcott SL, Ryabin T, Hall JR, Hartmann M, Hollister EB, Lesniewski RA, Oakley BB, Parks DH, Robinson CJ, Sahl JW, Stress B, Thallinger GG, Horn DJV & Weber CF (2009) Introducing mothur: Open Source, Platform-independent, Community-supported Software for Describing and Comparing Microbial Communities. *Appl. Environ. Microbiol.* Microbiol. doi:10.1128/AEM.01541-09.

Schütz H, Seiler W, Conrad R (1990) Influence of soil temperature on methane emission from rice paddy fields. *Biogeochemistry* 11:77–95.
Schuur EAG, Bockheim J, Canadell JG, Euskirchen E, Feild CB & al e (2008) Vulnerability of permafrost carbon to climate chagne: implications for the global carbon cycle. *BioScience* 58:701-714.
Sekar R, PernthalerA, Pernthaler J, Warnecke F, Posch T, Amann R (2003) An improved protocol for quantification of freshwater Actinobacteria by fluorescence in situ hybridization. *Appl. Environ. Microbiol.* 69:2928-2935.
Serreze MC, Walsh JE, Chapin FSI, Osterkamp TE, Dyurgerov M, Romanovsky V, Oechel WC, Morison J, Zhang T & Barry RG (2000) Observational evidence of recent change in the northern high-latitude environment. *Climate Change* 46:159-207.
Shannon RD, White JR, Lawson JE & Gilmour BS (1996) Methane efflux from emergent vegetation in peatlands. *J.f Ecol.* 84:239-246.
Shirokova LS Pokrovsky OS, Kirpotin SN, Desmukh C, Pokrovsky BG, et al. (2013) Biogeochemistry of organic carbon, CO_2, CH_4, and trace elements in thermokarst water bodies in discontinuous permafrost zones of Western Siberia. *Biogeochem* 113:573-593.
Simon H, Grossart H-P, Schweitzer B & Ploug H (2002) Microbial ecology of organic aggregates in aquatic ecosystems. *Aquat. Microb. Ecol.* 28:175-211.
Smith M & Wise S (2007) Problems of bias in mapping linear landforms from satellite imagery. *Int.l J. Appl. Earth Obs.* 9:65-78.
Sogin ML, Morrison HG, Huber JA, Welch DM, Huse SM, Neal PR, Arrieta JM, and Herndi GJ (2006) Microbial diversity in the deep sea and the underexplored "rare biosphere". *PNAS.* 103:12115-12120.
Solomons SD, Qin D, Manning M, Chen Z, Marquis M, Averyt KB, Tignor M & Miller HS (2007) *Contribution of working group I to the fourth assessment report of the intergovernmental panel on climate change.* Cambridge University Press, Cambridge, United Kingdom and New York, NY, USA
Southon J & Santos G (2004) Ion source development at KCCAMS, University of California, Irvine. *Radiocarbon* 46:33-39.
Southon J & Santos GM (2007) Life with MC-SNICS. Part II: Further ion source development at the Keck carbon cycle AMS facility. *Nucl. Instrum. Meth.* 259:88-93.
Stainton M, Capel M & Armstrong A (1977) The chemical analysis of freshwater. *Can Fish Mar Serv, Misc Spec Publ*:25.
Steinweg J, Plante A, Contant R, Paul E & Tanaka D (2008) Patterns of substrate utilization during long-term incubations at different temperatures. *Soil Biol. Biochem.* 40:2722-2728.
Steven B, Pollard WH, Greer CH & Whyte LG (2008) Microbial diversity and activity through a permafrost/ground ice core profile form the Canadian high Arctic. *Environmental Microbiology* 10:3388-3403.
Strickland MS, Lauber C, Fierer N & Bradford MA (2009) Testing the functional significance of microbial community composition. *Environmental Research Letters* 90(2):441-451.
Striegl RG, Kortelainen P, Chanton JP, Wickland KP, Bugna GC & Rantakari M (2001) Carbon dioxide partial pressure and 13C content of north temperate and boreal lakes at spring ice melt *Limnol. Oceanogr.* 46(4):941-945.
Striegl RG & Michmerhuizen CM (1998) Hydrological influence on methane and carbon dioxide dynamics at two north-central Minnesota lakes. *Limnol. Oceanogr.* 42(7):1519-1529.
Tank SE, Lesack LFW & Hesslein RH (2009) Northern Delta Lakes as Summertime CO2 Absorbers Within the Arctic Landscape. *Ecosystems* 12:144-157.
Tarnocai C (2009) The impact of climate change on Canadian peatlands. *Canadian Water Resources Journal* 34(4):453-466.

Tokida T, Miyazaki T, Mizoguchi M, Nagata O, Takakai F, Kagemoto A & Hatano R (2007) Falling atmospheric pressure as a trigger for methane ebullition from peatland. *Glob. Biogeochem. Cyc.* 21:GB2003.

Tranvik LJ & al. e (2009) Lakes and reservoirs as regulators of carbon cycling and climate. *Limnol. Oceanogr.* 54:2298-2314.

Trumbore SE, Keller M, Wofsy SC & da Costa JM (1990) Measurements of Soil and Canopy Exchange Rates in the Amazon Rain Forest using 222Rn. *J. Geophys. Res.h Atm.*95:16,865-816,873.

Valentine DW, Holland EA & Schimel DS (1994) Ecosystem and physiological controls over methane production in northern wetlans. *J. Geophys. Res.* 99:1563-1571.

VanBodegom PM, Stams AJM (1999) Effects of alternative electron acceptors and temperature on methanogenesis in rice paddy soils. *Chemosphere* 39:167–182.

van Everdingen R & (ed) (1998 revised 2005) Multi-Language Glossary Of Permafrost and Related Ground-Ice Terms. *Boulder, CO :National Snow and Ice Data Center/World Data Center for Glaciology.*

van Niel CB (1944) The culture, general physiology, morphology, and classification of the non-sulfure purple and brown bacteria. *Bacteriol. Rev.* 8(1):1-118.

Venter J, Remington K, Heidelberg J, Halpern A, Rusch D & al. e (2004) Environmental genome shotgun sequencing of the Sargasso Sea. *Science* 304:66-74.

Vezina S & Vincent W (1997) Arctic cyanobacteria and limological properties of their environment: Bylot Island, Northwest Territories, Canada (73°N, 80°W). *Polar Biol.* 17:523-534.

Vincent WF, Hobbie JE & Laybourn-Parry J (2008) Introduction to the limnology of high latitude lake and river ecosystems. *Polar lakes and rivers: limnology of Arctic and Antarctic aquatic ecosystems.* (Eds.) W.F. Vincent and J. Laybourn-Parry. Oxford University Press, New York:1-23.

Vishnivetskaya T, Petrova M, Urbance J, Ponder M, Moyer C, Gilichinsky D & al e (2006) Bacterial community in ancient Siberian permafrost as characterized by culture and culture-independent methods. *Astrobiology* 6:400-414.

Vonk JE, Mann PJ, Dowdy KL, Davydova A, Davydov SP, Zimov N, Spencer RGM, Bulygina EB, Eglinton TI & Holmes RM (2013) Dissolved organic carbon loss from Yedoma permafrost amplified by ice wedge thaw. *Environm. Res. Lett.* 8:035023.

Wagner D (2008) Microbial Communities and Processes in Arctic Permafrost Environments. *Micriobiology of Extreme Soils*, Dion P & Nautival C (Édit.) Springer Berlin Heidelberg, Vol 13. p 133-154.

Wagner D, Gattinger A, Embacher A, Pfeiffer EM, Schloter M & Lipskis A (2007) Methanogenic activity and biomass in Holocene permafrost deposits of the Lena Delta, Siberian Arctic and its implication for the global methane budget. *Glob. Change Biol.* 13:1089-1099.

Wagner D, Lipski A, Embacher A & Gattinger A (2005) Methane fluxes in permafrost habitats of the Lena Delta: effects of microbial community structure and organic matter quality. *Enivronm. Microbiol.* 7:1582-1592.

Waldrop MP & Firestone MK (2004) Altered utilization patterns of young and old C by microorganisms caused by temperature shifts and N additions. *Biogeochemistry* 67:235-248.

Walter Anthony KM, Vas DA, Brosius L, Chapin III FS, Zimov SA & Zhuang Q (2010) Estimating methane emissions from northern lakes using ice-bubble surveys. *Limnol. Oceanogr.: Methods* 8:592-609.

Walter KM, Chanton JP, Chapin FS, Schuur EAG & Zimov SA (2008) Methane production and bubble emissions from arctic lakes: Isotopic implications for source pathways and ages. *J. Geophys. Res.* 113: G00A08 doi:10.1029/2007JG000569.

Walter KM, Smith LC & III FSC (2007) Methane bubbling from northern lakes: present and future contributions to the global methane budget. *Philos. T. Roy. Soc. A* 365:1657-1676.
Walter KM, Zimov A, Chanton JP, Verbyla D & Chapin III FS (2006) Methane bubbling from Siberian thaw lakes as a positive feedback to climate warming. *Nature* 443:71-75.
Ward DM, Weller R & Bateson M (1990) 16S rRNA sequences reveal numerous uncultured microorganisms in a natural community. *Nature* 345:63-65.
Washburn A (1980) Permafrost feature as evidence of climate change. *Earth-Science Reviews* 15:327-402.
Watanabe K, Kodama Y & Harayama S (2001) Design and evaluation of PCR primers to amplify 16S ribosomal DNA fragments used for community fingerprinting. *J. Microbiol. Methods* 44:253-262.
Westermann P, Ahring B & Mah R (1989) Temperature compensation in Methanosarcina bakeri by modulation of hydrogen and acetate affinity. *Appl. Environm.Microbiol.* 55:1262-1266.
Wetzel R (1990) Land-water interfaces: Metabolicand limnological regulators. *Int. Verein. Theor. Limnol. Verh.* 24:6-24.
Whalen SC (2005) Biogeochemistry of methane between natural wetlands and the atmosphere. *Environ. Eng. Sci.* 22:73-94.
Whiticar M (1999) Carbon and hydrogen isotope systematics of bacterial formation and oxidation of methane. *Chem. Geol.*161:291-314.
Whiticar MJ, Faber E & Schoell M (1986) Biogenic methane formation in marine and freshwater environments: CO2 reduction VS. acetate fermentation-Isotope evidence. *Geochim. Cosmochim. A.* 50:693-709.
Wilhelm RC, Niederberger TD, Greer C & Whyte LG (2011) Microbial diversity of active layer and permafrost in an acidic wetland from the Canadian High Arctic. *Can. J. Microb.* 57(4):303-315.
Woese C, Kandler O & Wheelis M (1990) Towards a natural system of organisms: proposal for the domains Archaea, Bacteria, and Eucarya. *Proc. Natl. Acad. Sci.* 87:4576-4579.
X. X, Pack MA, Stills A, Lupascu M & Czimczik CI (2012) A Rapid Method for Preparing High Concentration CH_4 Gas Samples for 14C Analysis by AMS. *Abstract in The 21th Radiocarbon Conference, Paris.*
Xu X, Trumbore SE, Zheng S, Southon JR, McDuffee KE, Luttgen M & Liu JC (2007) Modifying a sealed tube zinc reduction method for preparation of AMS graphite targets: Reducing background and attaining high precision. *Nucl. Instrum. Meth.* 259:320-329.
Yergeau E, Hogues H, Whyte LG & Greer CW (2010) The functional potential of high Arctic permafrost revealed by metagenomic sequencing, qPCR and microarray analyses. *ISME J* 4:1206-1214.
Zimov SA, Schurr EAG & ChapinIII FS (2006) Climate Change: Permafrost and the global carbon budget. *Science* 312:1612-1613.
Zimov SA, Voropaev YV, Davydov SP, Zimova GM, Davydova AI, Chapin III FS & Chapin MC (2001) Flux of methane from north Siberian aquatic systems: influence on atmospheric methane. *Permafrost Response on Economic Development, Environmental Security and Natural Resources* 76:511-524.
Zimov SA, Voropaev YV, Semiletov IP, Davidov SP, Prosiannikov SF, Chapin III FS, Chapin MC, Trumbore SE & Tyler S (1997) North Siberian lakes : a methane source fueled by Pleistocene carbon. *Science* 277:800-802.
Zinder SH (1993) Physiological ecology of methanogens. In: Ferry JG (ed) Methanogenesis: ecology, physiology, biochemistry and genetics. *Chapman & Hall, New York,* :123.
Zogg PG, Zak DR, Ringelberg DB, MacDonald NW, Pregitzer KS & White DC (1997) Compositional and functional shifts in microbial communities due to soil warming. *Soil Sci. Soc. Am. J.* 61:475-481.

Zona D, Oechel WC & Peterson KM (2008) Carbon Fluxes Across Vegetated Drained Lakes of Different ages on the Arctic Coastal Plain, Alaska. *AGU Fall Meeting Abstracts*:A421+.

6 ANNEXE – Données supplémentaires du 3e article

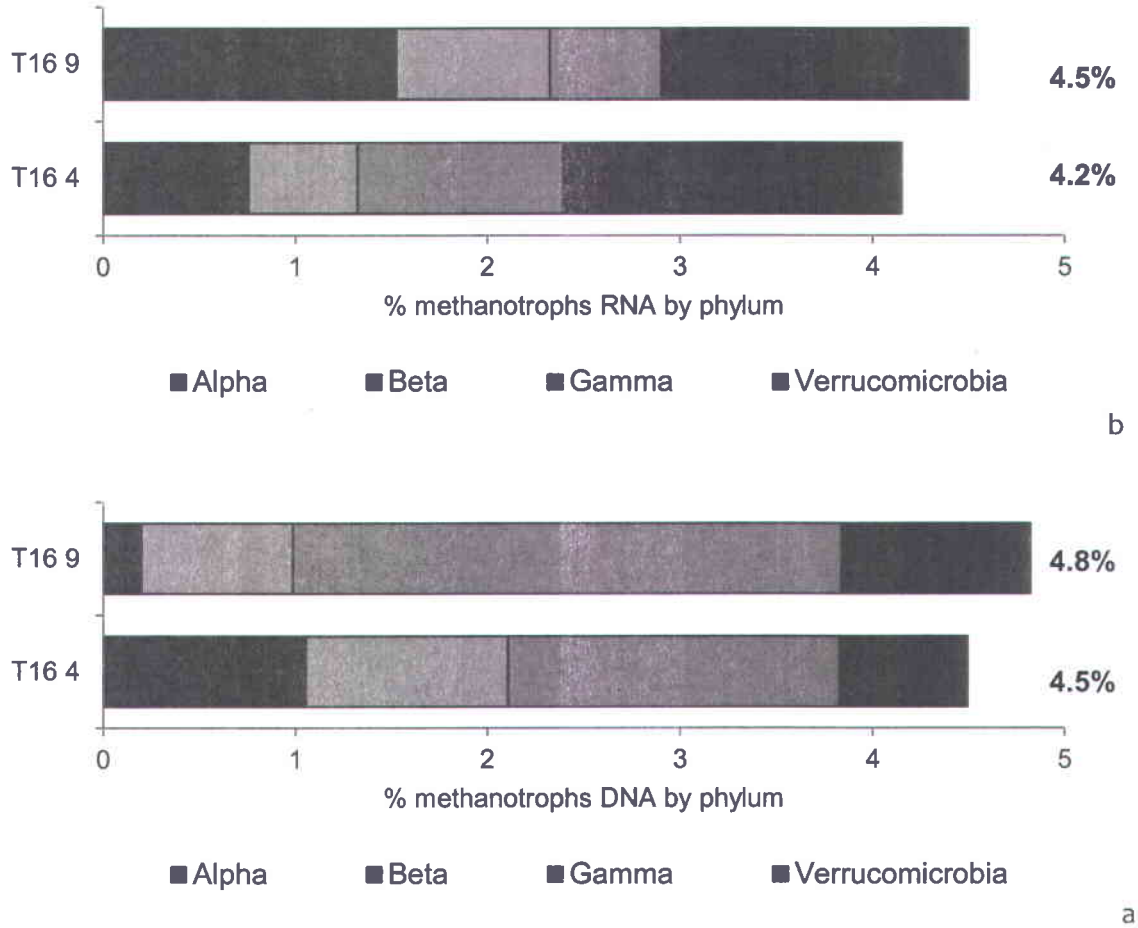

Supplementary Figure 1.

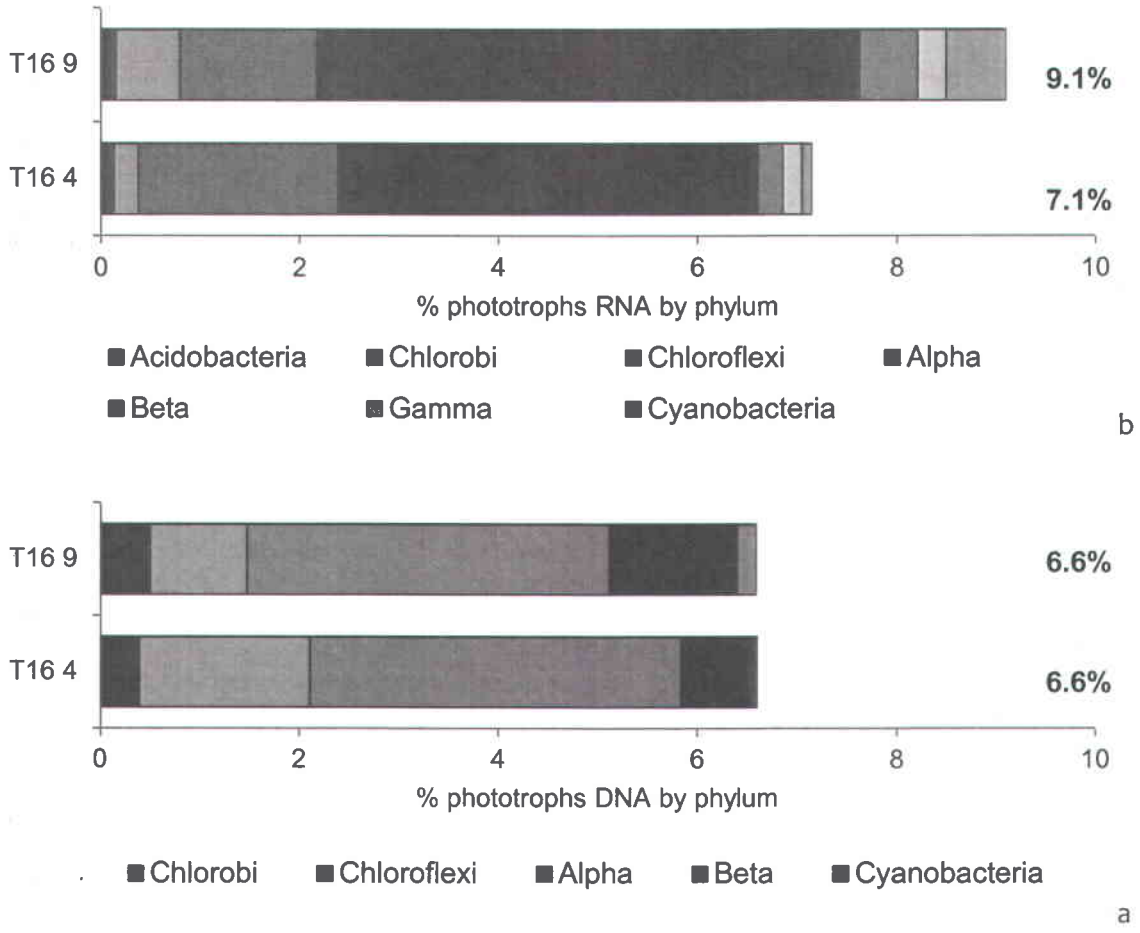

Supplementary Figure 2.

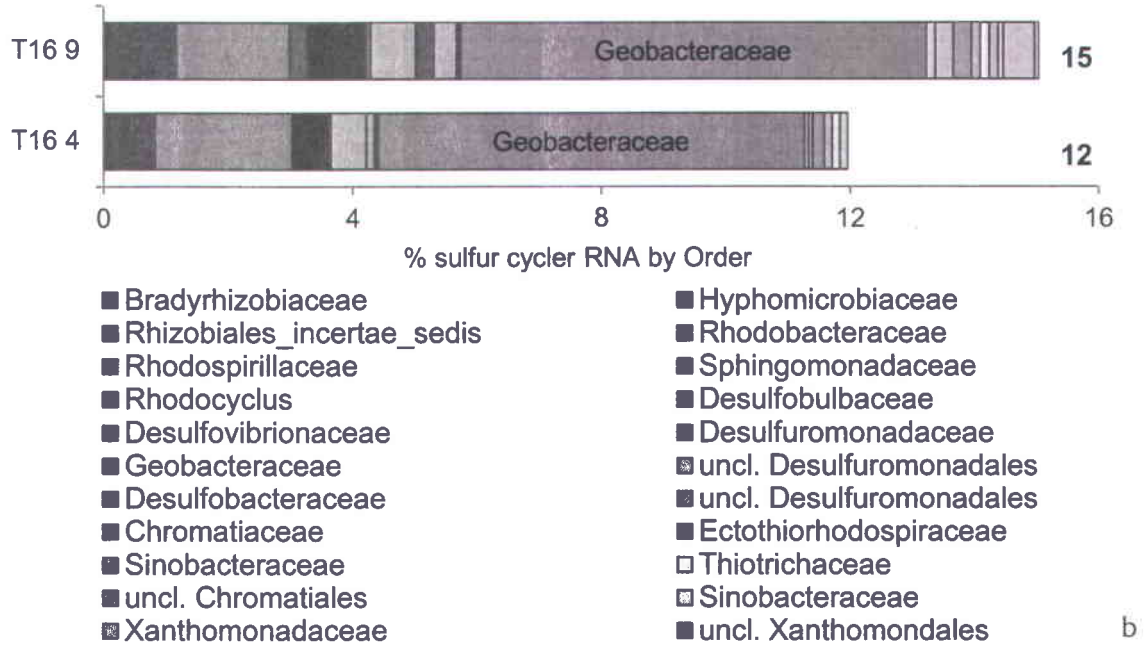

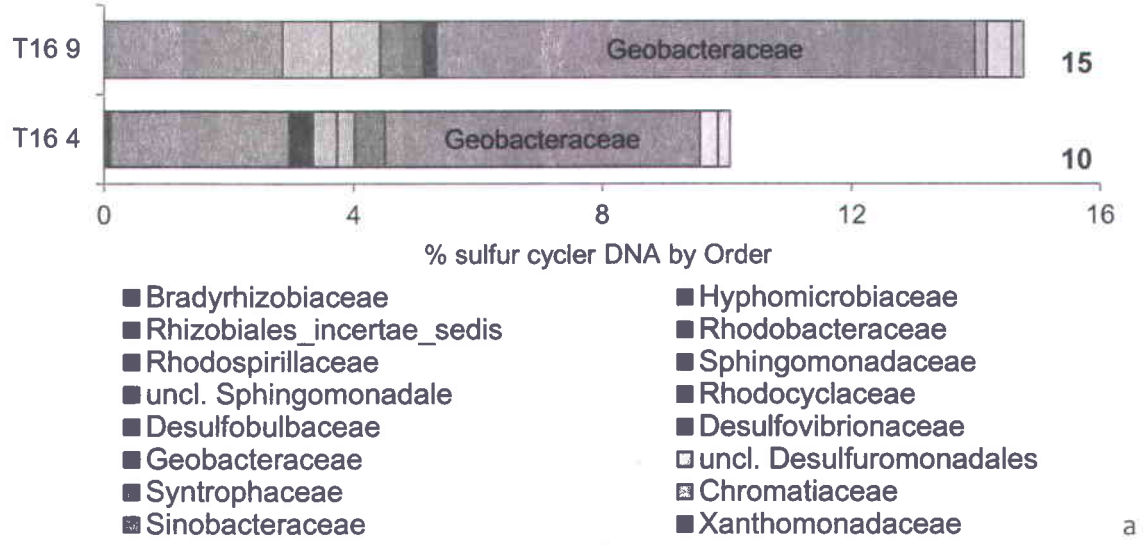

Supplementary Figure 3.

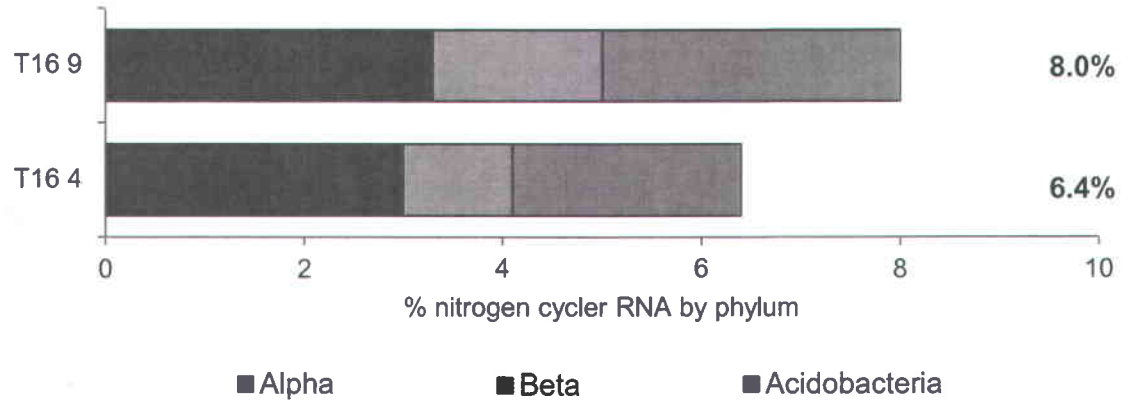

b

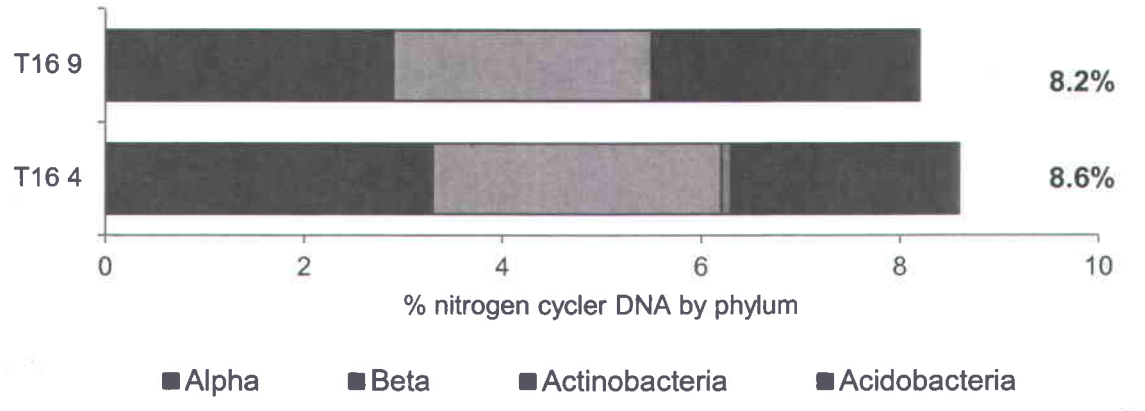

a

Supplementary Figure 4.

7 ANNEXE – Premier article publié

OPEN ACCESS Freely available online

PLOS ONE

Small Thaw Ponds: An Unaccounted Source of Methane in the Canadian High Arctic

Karita Negandhi[1], Isabelle Laurion[1], Michael J. Whiticar[2], Pierre E. Galand[3,4], Xiaomei Xu[5], Connie Lovejoy[6]*

1 Centre for Northern Studies (CEN) and Institut national de la recherche scientifique, Centre Eau Terre Environnement, Quebec, Canada, **2** School of Earth and Ocean Sciences, University of Victoria, Victoria, British Columbia, Canada, **3** UPMC Université Paris 06, (UMR 8222, LECOB), Observatoire Océanologique, Banyuls-sur-mer, France, **4** CNRS, UMR 8222, LECOB, Observatoire Océanologique, Banyuls-sur-mer, France, **5** Department of Earth System Science, University of California Irvine, Irvine, California, United States of America, **6** Département de biologie, Institut de Biologie Intégrative et des Systèmes, Université Laval, and Takuvik (CNRS, UMI 3376), Quebec, Canada

Abstract

Thawing permafrost in the Canadian Arctic tundra leads to peat erosion and slumping in narrow and shallow runnel ponds that surround more commonly studied polygonal ponds. Here we compared the methane production between runnel and polygonal ponds using stable isotope ratios, ^{14}C signatures, and investigated potential methanogenic communities through high-throughput sequencing archaeal 16S rRNA genes. We found that runnel ponds had significantly higher methane and carbon dioxide emissions, produced from a slightly larger fraction of old carbon, compared to polygonal ponds. The methane stable isotopic signature indicated production through acetoclastic methanogenesis, but gene signatures from acetoclastic and hydrogenotrophic methanogenic Archaea were detected in both polygonal and runnel ponds. We conclude that runnel ponds represent a source of methane from potentially older C, and that they contain methanogenic communities able to use diverse sources of carbon, increasing the risk of augmented methane release under a warmer climate.

Citation: Negandhi K, Laurion I, Whiticar MJ, Galand PE, Xu X, et al. (2013) Small Thaw Ponds: An Unaccounted Source of Methane in the Canadian High Arctic. PLoS ONE 8(11): e78204. doi:10.1371/journal.pone.0078204

Editor: Vishal Shah, Dowling College, United States of America

Received May 16, 2013; **Accepted** September 9, 2013; **Published** November 13, 2013

Funding: Funding for the study was primarily from the National Research and Engineering Council (NSERC) Canada, including grants to LL, CL, and MJW. Additional support was from ArcticNet, the Canadian International Polar Year (IPY), Parks Canada and The Polar Continental Shelf Project provided logistic support. XX had support from the Keck Carbon Cycle AMS Facility. The funders had no role in study design, data collection and analysis, decision to publish, or preparation of the manuscript.

Competing Interests: The authors have declared that no competing interests exist.

* E-mail: connie.lovejoy@bio.ulaval.ca

Introduction

In arctic regions, the acceleration of permafrost thaw and deepening of the seasonal active layer leads to thaw pond formations due to the organic and ice-rich ground subsiding [1–2]. These thaw ponds are also sometimes referred to as thermokarst lakes, since they superficially resemble ponds formed by the dissolution of limestone (karst). Two main geomorphological forms are commonly found in continuous permafrost regions of Eastern Canada: (i) small, shallow, narrow runnel ponds formed over melting ice wedges where peat slumping occurs, and (ii) more stable, slightly larger and deeper, polygonal ponds, which are naturally linked to the active layer freeze-thaw cycles, and can be colonized by aquatic plants and microbial mats (Fig. 1). Greenhouse gas (GHG) emissions from thermokarst ecosystems are highly variable [3–5] and often not considered in large-scale GHG studies and global carbon cycling models since small ponds cannot be seen with remote sensing tools [6–7]. These ponds have the potential to be significant GHG emitters contributing to a positive carbon-climate feedback [8–10], attributed to the mobilization of old stored carbon (C) stocks released back into the atmosphere [11–13]. In these ecosystems, microbial decomposers and methanogens have access to large quantities of allochthonous organic matter [4,14]. The CH_4 released from Siberian thaw lakes is significant and originates from microbial utilization of C stocks deposited thousands of years ago [8,15]. In the eastern Canadian Arctic, C deposition dates from the Holocene [1], but microbial utilization is unknown.

The conversion of organic C previously locked in permafrost to GHG is highly dependent on its lability to microbial degradation [12,16,17]. For instance, fresh labile organic matter favors acetoclastic methanogenesis (AM) [18], where the organic substrate (i.e. acetate, methanol, methylated substrates, etc.) is cleaved and the methyl group is reduced to CH_4. Comparatively, more recalcitrant compounds leached from peat favors the hydrogenotrophic pathway (HM) [19], which utilizes H_2 to reduce CO_2. Therefore, the available substrate selectively determines the methanogenic community and CH_4 production rate.

Once CH_4 is produced through AM or HM pathways, at the bottom of lakes and ponds, it is transported through the water column to the atmosphere by diffusion and ebullition. Ebullition transport can be classified as background, point sources or hotspots. In Siberian thermokarst lakes these three sources accounted for 25, 58, and 12% respectively, with the remaining 5% of total emissions attributed to diffusion [20]. Diffusion is generally considered less important than ebullition [21–22]. However, diffusion and ebullition rates are variable in aquatic systems and relative contribution of these sources has not been

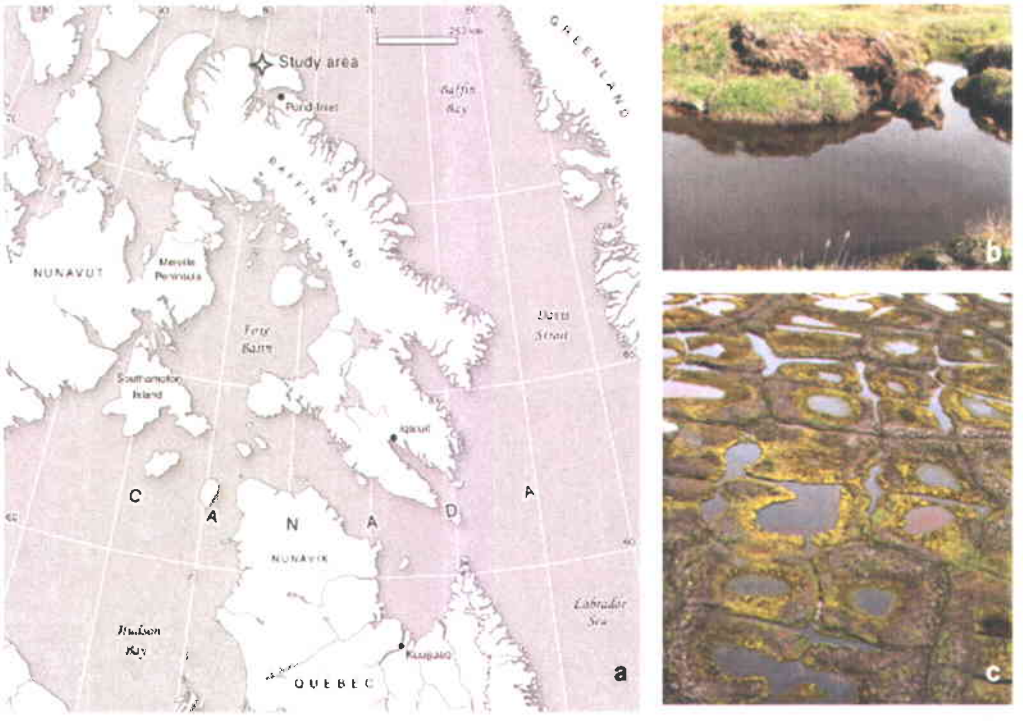

Figure 1. Study site description. (a) Map indicating the location of the study site on Bylot Island, Sirmilik National Park, Nunavut, Canada, (b) collapsed peat polygon ridges forming runnel ponds, and (c) landscape combining runnel and polygonal ponds.
doi:10.1371/journal.pone.0078204.g001

investigated in other Arctic thermokarst systems where geomorphology varies considerably. There are no previous reports from runnel type ponds and their potential contribution to atmospheric GHG is not known.

The objective of our study was to evaluate the release and potential for GHG emissions in the poorly studied runnel ponds compared with polygonal ponds of northeastern Canada. These ponds have the potential to form in ice and organic rich soils of permafrost and glaciated-influenced landscapes, covering ca. 9.6 million km^2 of the global northern landscape [23]. The methanogenic pathways and C age were investigated through stable isotopic signatures and radiocarbon dating of dissolved and bubbling GHG. Archaeal community composition in the sediments was analyzed with high-throughput 16S rRNA gene pyrosequencing. We found that runnel ponds were supersaturated in CO_2 and had more than 3 folds greater CH_4 emissions than polygonal ponds, which were a CO_2 sink. Higher CH_4 emission is likely explained by a higher supply of organic matter under more hypoxic conditions, where CH_4 oxidation is less likely to occur. The methanogenic community included genera capable of both AM and HM, indicating that methanogens could potentially use different carbon substrates and thus acclimate to changing conditions, for example vegetation cover or hydrology, under a warmer climate.

Results

Pond limnological properties

Within the four ponds targeted for the archaeal diversity study, runnel ponds, which are subjected to more peat leaching and erosion, had higher concentrations of DOC, nutrients (TN, SRP and TP) and iron (Table 1). Polygonal ponds showed no sign of recent erosion, with thick cyanobacteria-dominated microbial mats on the bottom, and lower concentrations of DOC, nutrients and ions. The organic carbon (OC) content of surface sediment was highly variable, ranging between 1.0 and 25.1% among the series of sampled ponds (n = 26, 2011), and with no significant difference (paired t-test) between polygonal ponds (8.4±6.6%) and runnel ponds (6.4±3.9%). Over the year, pond ice and water temperatures ranged between −26.7 and +21.4°C (averaging −7.6°C; Figure S1 in File S1). The temperature records showed that ponds remained frozen from ~25 September to 4 June.

GHG concentrations, fluxes and isotopic signatures

Surface water GHG concentrations collected in the compiled series of thaw ponds (from 2009 to 2011, n = 91) showed a significantly higher concentration of CH_4 in runnel compared to polygonal ponds (t-test, df = 90, p = 0.003). Only runnel ponds were supersaturated in CO_2 (averaging 119±124 µM, compared to polygonal ponds 9.6±8.9 µM) but all ponds were supersaturated in CH_4 (4.1±4.7 and 1.3±1.7 µM, in runnel and polygonal

Table 1. Surface water physicochemical properties of the four ponds sampled for archaeal communities between 19 and 26 July 2009, including dissolved organic carbon (DOC, mg L^{-1}), soluble reactive phosphorus (SRP, µg L^{-1}), total phosphorus (TP, µg L^{-1}), total nitrogen (TN), nitrate (NO_3), sulfate (SO_4), iron (Fe) all in mg L^{-1}, pH, and dissolved CO_2 and CH_4 concentrations, both in µM.

POND	DOC	SRP	TP	TN	NO_3	SO_4	Fe	pH	CO_2	CH_4	OC
Polygonal ponds											
BYL1	8.4	<0.2	15.6	363	0.05	1.47	0.299	8.7	6.3	1.0	4.6
BYL22	8.1	<0.2	25.5	371	0.04	0.85	0.557	7.2	25.0	1.9	5.3
Runnel ponds											
BYL24	11.5	1.0	25.5	398	0.04	0.67	1.012	7.1	33.0	3.4	6.5
BYL27	11.8	0.5	26.3	822	0.06	1.56	0.905	6.6	78.8	2.6	17.8

Surface sediment organic carbon content (OC as percent) samples were collected between 12 June and 15 July 2011.
doi:10.1371/journal.pone.0078204.t001

ponds respectively). Runnel ponds also had significantly higher CO_2 and CH_4 fluxes compared to polygonal ponds ($p \leq 0.0001$; Figure S2 in File S1) but the diffusive flux of CO_2 (−8.1 to 76.9 mmol m^{-2} d^{-1}) and CH_4 (0.02 to 6.3 mmol m^{-2} d^{-1}) varied greatly over the 3 sampled summers. In the two ponds (BYL80 and BYL1) that were tested over 26 hours, diurnal dissolved GHGs varied by 18 and 25% for CO_2, and 17 and 21% for CH_4. The corresponding fluxes likely varied by no more than 25% throughout a day as estimated using a wind-based model incorporating the wind speed over the preceding 2 h,where the coefficient of variation was 45% for the wind speed. In the same two polygonal ponds (BYL1 and BYL80), eight separate measurements of CH_4 ebullition fluxes showed that despite the variability within ponds, fluxes were always greater in BYL80 than in BYL1 (t-test, df = 7, p = 0.02, Table S1in File S1). Ebullition flux was lower than diffusive flux in BYL1 (representing on average 27% of total CH_4 emission) and higher than diffusive flux in BYL80 (82% of total emission). The diffusive flux values used in this comparison were from approximately the same period in 2011, but ebullition was calculated over up to 32 h of bubble collection, while diffusive flux was always estimated from one discrete gas sample. The CH_4 concentration in bubbles was also variable (1.5–32% by volume).

Overall the $\Delta^{14}C$ signatures of the GHG released from both polygonal and runnel ponds through ebullition (−1.1 to 114.9‰) were categorized as modern (within the last ~60 years). However, ebullition CH_4 from two runnel ponds (n = 3) contained a higher fraction of old C compared to the two polygonal ponds (n = 7; p = 0.002; Fig. 2). Both C and H stable isotopic signatures indicate that all CH_4 emitted by diffusion and ebullition during summer was produced from AM (Fig. 3a). The possibility of HM, as seen in Fig. 3b, was ruled out with the inclusion of δD-CH_4 signature. There was no significant difference in the $\delta^{13}C$-CO_2 or $\delta^{13}C$-CH_4 values between the polygonal and runnel ponds (Table S2 in File S1), supporting the idea of similar methanogenesis production pathways (AM). However, there were indications that the CH_4 emitted by diffusion was more susceptible to oxidation in the polygonal ponds (Fig. 3b). In fact, there was a significant relationship between the oxygen concentration at the surface of ponds and $\delta^{13}C$-CH_4 ($r^2 = 0.337$; p = 0.009). Comparatively, CH_4 emitted through ebullition showed no signs of oxidation.

Archaeal assemblages

There was a predominance of methanogen 16S rRNA sequences in surface sediment archaeal communities in the 4 ponds (88–95% of the sequences). In contrast, the methanogens represented only 40% of the sequences in the water community of one polygonal pond where we were able to amplify the 16S rRNA gene. We also failed to amplify sediment DNA from one runnel pond (BYL38). The poor PCR success may have been due to a lack of Archaeal template present in the water samples, but is unexplained for BYL38 sediment sample. The water sample archaeal communities were dominated by sequences belonging to the uncultured clusters LDS and RCV (Fig. 4), and no anaerobic methanotrophic archaea were detected. The sediment non-methanogenic OTUs (5–12% of the sequences) belonged to the phylum Euryarchaeota, mainly of a terrestrial miscellaneous euryarchaeotal group (TMEG), and from the miscellaneous crenarchaeotic group (MCG). As there are no cultivated representatives of these groups, the metabolism of these environmental clusters is not known.

Altogether the majority of Archaea operational taxonomic units (OTUs) from surface sediments were classified into the four known methanogenic genera (*Methanobacterium*, Candidatus *Methanoregula*, *Methanosarcina* and *Methanosaeta*) and one uncultured group (Rice cluster II, RC II) within the deeply branching *Methanomicrobiales* (Fig. 4). Overall, the polygonal pond sediments were dominated by archaeal sequences belonging to HM (*Methanobacterium*, *Methanoregula*) representing from 63 to 82% of the putative methanogen sequences, while runnel ponds were either dominated by HM (65%, BYL24) or by AM (*Methanosarcina*, *Methanosaeta*) (51%, BYL27). The most abundant *Methanobacterium* that represented one third of all archaeal sequences in both runnel ponds was identified closest to *Methanobacterium lacus*, a newly described strain that utilize H_2/CO_2 and methanol/H_2 as substrates [24]. The most abundant *Methanosarcina* OTUs were 99% similar to *Methanosaeta concilii* [25], and to *Methanosarcina mazei* [26] both known to be acetoclastic methanogens. The most abundant *Methanoregula* OTU was 98% similar to *Methanoregula boonei*, a hydrogenotroph. The polygonal pond BYL1 had a high percentage of RC II and a lower percentage of *Methanosarcina* compared to the other 3 ponds.

Discussion

The Bylot Island pro-glacial river valley's ice-wedge tundra terrain was covered by a network of ponds and was similar to the landscape of Samoylov Island, Eastern Siberia [7]. Our results clearly show that in addition to being a source of CO_2, as opposed to a sink, runnel ponds represented a larger source of CH_4 than polygonal ponds. Runnel ponds accounted for 44% of the open water in the valley, but contributed to 83% of the total CH_4 emissions that included lake emissions from a 3-year diffusive rate database. Our data suggest that CH_4 emissions from thawing permafrost could be strongly underestimated if measured only from the more frequently studied polygonal ponds [3,5,27,28].

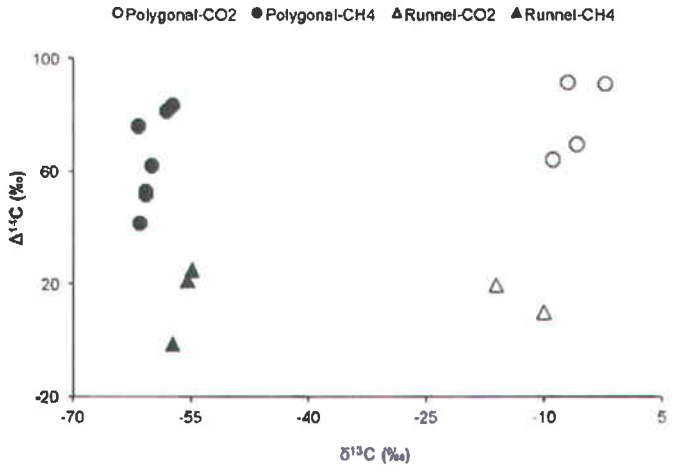

Figure 2. CH_4 and CO_2 carbon source and age. Radiocarbon signature ($\Delta^{14}C$) plotted against $\delta^{13}CH_4$ and $\delta^{13}CO_2$ showing: 1) that as the fraction of young carbon becomes higher for both CH_4 and CO_2, the $\delta^{13}C$ signatures become more divergent indicating a decoupling in carbon source; 2) the runnel ponds CH_4 contains a higher fraction of old carbon.
doi:10.1371/journal.pone.0078204.g002

The smaller emissions from polygonal ponds may be due to more activity by the methanotroph community, and we note that stable isotopes were consistent with more CH_4 oxidation in polygonal ponds (Fig. 3b).

Methane diffusion rates measured from runnel ponds (on average 0.76 mmol m^{-2} d^{-1}) were in the same range as reported from the thermokarst lakes in Siberia [29–30], but relatively small compared to peatland ponds from the Hudson Bay lowland [31], which were up to 48 mmol CH_4 m^{-2} d^{-1}. However, comparing flux estimates among studies of smaller aquatic systems is difficult due to several factors that are rarely considered, such as gas collection method, gas transfer model and flux calculation, time of day, season, latitude, water body size and depth, catchment geomorphology, and finally the presence or absence of thermokarst slumping. Here, we applied a correction factor (×0.2458; see methods) based on chamber flux measurements and wind-based estimates [4] to account for the positive buoyancy flux occurring as thermal stratification evolves during the day in small-fetched and sheltered ponds. However, during the night, diffusion is likely to increase as water mixes due to heat loss, which was not included in our estimates. Moreover, estimates of CH_4 flux with gas exchange velocity based on Fick's law, and pure diffusive gas transfer such as for CO_2, do not take into account micro-ebullition. For these reasons, our runnel pond diffusive flux estimations may be conservative.

For the two polygonal ponds, which were measured repeatedly, the maximal ebullition rate reached 2.13 mmol m^{-2} d^{-1}, decreasing by ~1 order of magnitude over a few weeks. This was similar to the diffusive rates that were up to 0.77 mmol m^{-2} d^{-1} in the two ponds. This maximal ebullition rate was within the lowest range of values compiled by Walter et al. [30] (see their Table 1) for northern aquatic systems (their *Arctic* class), and much less than for Siberian thermokarst lakes, which reached 1563 mmol m^{-2} d^{-1}. The high rates from Alaska and Siberia are from emissions categorized as point sources and hotspot ebullition, occurring in lakes with taliks and much thicker peat deposits. Taliks form under thermokarst lakes that are deep enough to have a layer of water and sediment or soil, which remains unfrozen in winter. These conditions are unlikely to occur under the shallow Bylot Island thaw ponds since they freeze to the bottom in winter, partly explaining their lower ebullition rates. Unfortunately ebullition measurements were only taken from polygonal ponds where funnels could be installed. However, considering that diffusive fluxes were on average 3.5 times higher in the runnel ponds, ebullition fluxes and overall CH_4 production were also likely to be greater in the runnel ponds.

A larger fraction of old C would also be available for microbial degradation in the runnel ponds compared to polygonal ponds because of peat erosion down to the thickness of the ~half meter active layer on Bylot Island. The base of the peat deposit, which is about 2 m thick, was aged at 3670±110 BP [1]. Discrete background ebullition samples collected from June to July 2011 showed little evidence of high release of this old stored C in the form of GHG from the two runnel ponds sampled. Runnel ponds however, exhibited a higher fraction of older C in CO_2 and CH_4 compared to polygonal ponds (Fig. 2). The utilization and release of a larger fraction of older C through point source ebullition could still occur at this site at certain times over the thaw cycle. For example, ebullition from point sources released much older C in Siberian and Alaskan thermokarst lakes, despite modern age C reported for background ebullition [15].

Permafrost peat provides substrate for aquatic microbes [32], but the preferential use of modern C recently fixed from the atmosphere could be favored because of the greater lability of this pool [17]. In the case of the cyanobacterial mat-covered polygonal ponds on Bylot Island, the negative CO_2 flux most likely resulted from high photosynthetic rates in the mats, and the modern dates for CH_4 suggest that abundant labile compounds coming from a modern autochthonous pool could be the main C supply for microbial activity, including methanogenesis. However, in more humic runnel ponds influenced by peat lixiviation, an older C signature in the CH_4 than what we found was expected. The predominance of AM and the high OC content of surface sediment (1.0–25.1%) indicate that both pond types were C-rich

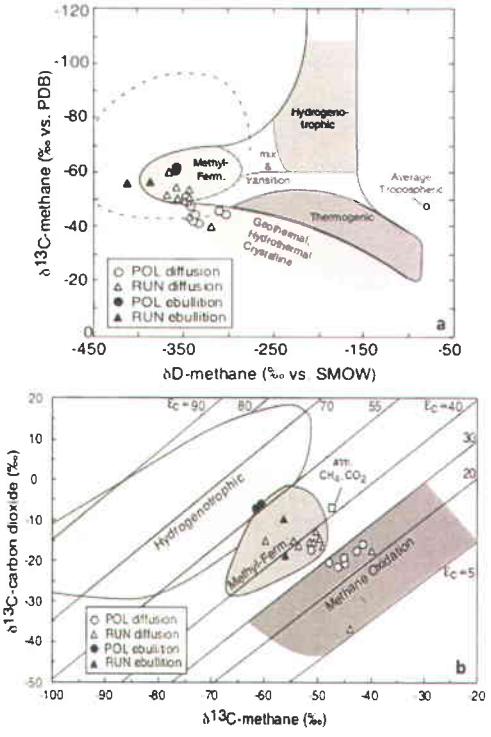

Figure 3. Methane production pathway through stable isotopes. (**a**) $\delta^{13}CH_4$ against δD_{CH4} signatures of diffusive (2009) and ebullition (2011) CH_4, indicating that acetoclastic methanogenesis (AM) is the dominant pathway in polygonal and runnel thaw ponds for samples collected in June/July. (**b**) $\delta^{13}CO_2$ against $\delta^{13}CH_4$ in thaw ponds showing the predominance of acetoclastic methanogenesis (AM) and the methanotrophic oxidation level for dissolved and ebullition CH_4.
doi:10.1371/journal.pone.0078204.g003

[18–19]. These OC values were mostly greater than values reported in Siberian permafrost soils, for example in the Lena Delta 4–5% of OC is within the top 50 cm [33], which is similar to values from Northeast Siberia [34]. The reasons for the high OC in surface sediment of small ponds lacking taliks could be due to slow microbial degradation rates linked to seasonal re-freezing. If this were the case, then a longer melt season could result in greater CH_4 emissions.

The sum of two methanogen genera adapted to high substrate levels was higher in runnel ponds than in polygonal ponds. These two genera have different CH_4 production pathways, *Methanobacterium* with the HM pathway [35], and *Methanosarcina* with the AM pathway [36] (Fig. 4), suggesting community adaptability. The main methanogens in thaw ponds were *Methanosarcina*, *Methanosaeta*, *Methanobacteriaceae*, *Methanomicrobiales*, and RC II, which is similar to the community retrieved from Svalbard peatlands and wetlands [37–38]. Most of the descriptive studies to date on freshwater Arctic archaeal communities are from clone libraries, and at most three Orders out of the five known Orders of methanogens were found from a single site [39–42]. For instance, in 19 freshwater lakes, Borrel and colleagues [24] reported 468 archaeal 16S rRNA sequences from clone libraries. *Methanomicrobiales* and *Methanosarcinales* dominated these lakes, with occasional sequences belonging to the *Methanobacteriales* [43]. The higher number of methanogen Orders and presence of AM and HM pathways from Bylot Island may be a consequence of the high OC content in the ponds. Alternatively our high throughput sequencing approach with a minimum 1921 final reads per sample may have recovered the additional Orders.

Substrate availability for CH_4 production from acetate or CO_2 is likely to change seasonally due to the timing of ice melt and primary production, generating changes in the methanogen community structure [38]. For example, in Finnish boreal mires, there was a clear shift in the methanogen community over the arctic summer, with AM (*Methanosarcina* spp.) found only during early and mid summer [44]. On Bylot Island, both AM and HM methanogens were retrieved from the sediments. However, the isotopic signatures of CH_4 indicated that only AM was active in July (Fig. 3) suggesting that the HM biomass had built up earlier. These results also show that AM can be a significant summer production pathway in Arctic permafrost regions, as opposed to other thermokarst systems where only HM was thought to be significant [45]. A methanogenic community composed of both AM and HM taxa will likely respond to wider temperature ranges and possible substrate changes that occur under climate stress, and both pathways should be considered in C budget estimates.

Thaw ponds contained reads with matches to methanogenic groups capable of both hydrogenotrophic and acetotrophic CH_4 production, providing the potential for community compensation under changing ambient conditions. However, the small size and great variability in shapes, limnology and microbial ecology of the ponds represent a challenge for scaling up their importance for global C cycling, especially since these ponds are primarily found in remote regions where logistic constraints are great. But considering that they have the potential to develop in permafrost and glaciated-influenced landscapes covering 9.6 millions of km^2 in circumpolar regions [23], these small systems certainly deserve more attention. As the Arctic warms and permafrost recedes, the abundance of tundra ponds, especially runnel ponds generated by thaw slumping, is likely to increase. The higher CH_4 emissions measured from runnel ponds, and their potential to contain organic carbon deposited thousands of years ago qualify them as a positive feedback system contributing to climate dynamics.

Methods

Study Site

Samples were collected at Sirmilik National Park, Bylot Island, Nunavut (73°09′N, 79°58′W; Fig. 1) in the continuous permafrost region of Canadian Arctic, with an active layer depth between 40 and 60 cm (D. Fortier, pers. comm.). Required permits to carry out sampling were approved by the Parks of Canada Agency for Sirmilik National Park (Research and Collection Permit) and the Nunavut Research Institute (Nunavut Science License). The Bylot SILA station recorded a mean annual air temperature of −14.5°C, with summer temperatures from June to August averaging 4.5°C and winter temperatures from December to January averaging −32.8°C. Precipitation between June and August (1994–2007) was about 94 mm. Thaw ponds and lakes covered 4.2% of the ~65 km^2 pro-glacial river valley in 2010, as obtained from a high resolution image from WorldView-1, with runnel ponds contributing approximately 44% of the surface water compared to polygonal ponds contributing 27%. Polygonal ponds form on top of low centered peat polygons, and are generally 0.5 to 1.5 m deep with an area <500 m^2. Runnel ponds form over

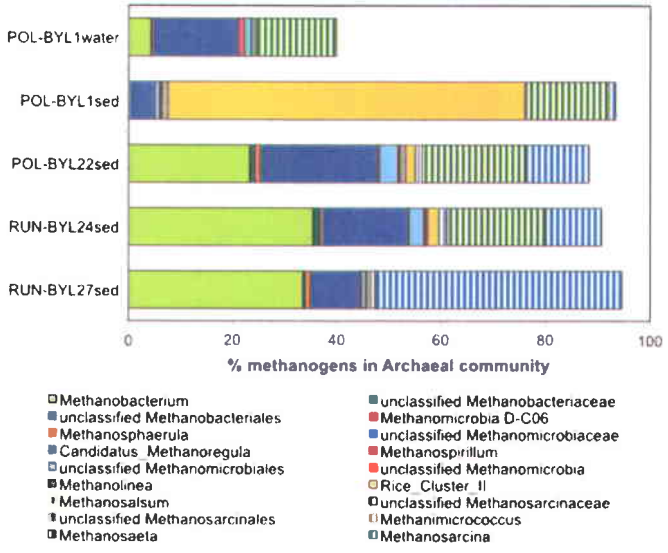

Figure 4. Archaeal methanogenic community of thaw ponds. Methanogen taxa retrieved from the sediment of four Arctic thaw ponds and from one water sample. Checkered symbols represent AM and solid are HM.
doi:10.1371/journal.pone.0078204.g004

melting ice wedges, and are often shallower than 0.5 m but sometimes form long networks (Fig. 1). Both pond types freeze to bottom in winter, and are unfrozen for approximately 110 days per year. The sum of all daily temperatures above freezing averaged 447 thawing-degree days (http://www.cen.ulaval.ca/bylot/climate-description-bylotisland.htm).

Sampling

In July 2009, 34 ponds were sampled for dissolved GHG concentrations and flux estimation, with 19 sampled for carbon and hydrogen stable isotope ratios (Table 2), and 4 ponds (2 polygonal and 2 runnel ponds) for archaeal diversity assessment via pyrosequencing (BYL1, 22, 24, 27; Table 1). These 4 ponds were selected to represent a range of physiochemical properties, which were measured in previous years. In July 2010, 14 ponds from the 2009 series were re-sampled for dissolved GHG concentrations and flux estimations. In 2011, from mid June to mid July, dissolved GHG concentrations and flux estimates were obtained from a total of 43 ponds, including 15 from the 2009 series. In addition, ebullition samples were taken from 4 ponds (2 polygonal ponds; BYL1 and 80 and 2 runnel ponds; BYL27 and 38) for stable isotopes and $\Delta^{14}C$ analysis, and ebullition rates were measured from the two polygonal ponds, which were deep enough to install the funnels needed for rate measurements. Ebullition flux was not measured from runnel ponds because the funnels were too wide to be correctly installed in the shallow and narrow ponds, exemplifying the difficulties in Arctic sampling. Also in 2011, GHG dissolved flux was measured approximately every 2 h over 26 h on 2 polygonal ponds (BYL1 and BYL80) to examine the daily variations in GHG dissolved concentrations.

Limnological characteristics

Surface water pH was measured with a 600R multi-parametric probe (Yellow Spring Instrument). The surface temperatures of one polygonal (BYL1) and one runnel pond (BYL24) were continuously recorded from July 2008 to July 2009 (thermistors, HOBOware™ U12, Onset). Pond water filtered through 0.2 µm pre-rinsed cellulose acetate filters (Advantec) was used for dissolved organic carbon (DOC) concentrations (Shimadzu TOC-5000A carbon analyzer calibrated with potassium biphthalate). Soluble reactive phosphorus (SRP) and major ions were measured on filtered samples [4]. Unfiltered water samples were fixed with H_2SO_4 (0.15% final concentration) for total phosphorus (TP) and total nitrogen (TN) quantification as in [46]. In 2011, 5 mL of surface sediment were collected for total organic carbon content (TOC) and processed with 0.1 mol L^{-1} of sulfuric acid on an elemental analyzer (CHNS-932, LECO Instruments) [47].

Diffusive flux

Dissolved CO_2 and CH_4 concentrations in surface waters were obtained by equilibrating 2 L of water with 20 mL of ambient air for 3 minutes. Most sampling occurred between 9 am and 4 pm. The resulting headspace was injected into glass vials (BD 3 mL Vacutainers, or Labco 5.9 mL Exetainers), helium flushed and vacuumed [48]. Samples were analyzed by gas chromatography (Varian 3800 with COMBI PAL head space injection, CP-Poraplot Q 25 m 3 0.53 mm column, flame ionization detection), and dissolved gas concentration calculated using Henry's Law:

$$C = K_H \times pGas$$

where K_H is Henry's constant adjusted according to ambient water temperature, and pGas is the partial pressure of CO_2 or CH_4 in the headspace. Dissolved GHG flux (F_d) was calculated as:

$$F_d = k(C_{sat} - C_{eq})$$

Table 2. Compilation of thaw ponds samples collected each year.

		Year	Number of ponds	Methods
Dissolved GHG	**GHG flux**	**2009–2011**	**33P, 58R**	**Dissolved concentrations**
	Production pathway	2009	9P, 10R	Stable isotopes
	Diurnal variations	**2011**	**2P**	**Hourly flux measures**
Ebullition	Ebullition flux	2011	2P	Funnel traps
	Production pathway	**2011**	**2P, 2R**	**Stable isotopes**
	C-source (age)	2011	2P, 2R	^{14}C dating
DNA	**Methanogens**	**2009**	**2P, 2R**	**Pyrosequencing**
Environment	Limnology	2009	2P, 2R	Nutrients, ions, pH, temp, O_2, DOC
	C-source (amount)	**2011**	**9P, 8R**	**Sediment OC**

Polygonal ponds (P), runnel ponds (R); dissolved organic carbon (DOC); organic carbon (OC); Greenhouse gases (GHG, including CO_2 and CH_4); ebullition is GHG released as bubbles; production pathway indicates CH_4 produced by acetoclastic methanogenesis (AM) or hydrogenotrophic methanogenesis (HM); temperature (temp). Note that most samples were collected in 2009, with diurnal, ebullition and sediment OC collected in 2011, which was the only occasion when appropriate sampling gear was available.

doi:10.1371/journal.pone.0078204.t002

where C_{sur} is the gas concentration in surface water, C_{eq} is the gas concentration when in equilibrium with the atmosphere at ambient temperature (global atmospheric concentrations were used), and k is the gas exchange velocity calculated as:

$$k = k_{600}\left(\frac{Sc}{600}\right)^{-0.5}$$

where Sc is the Schmidt number calculated from empirical third-order polynomial fit to water temperature and corrected at 20°C. The gas exchange coefficient k_{600} of Cole and Caraco [49] was used as a first approximation:

$$k_{600} = 2.07 + 0.215 \times U_{10}^{1.7}$$

where U_{10} is the wind speed at 10 m above ground. However, this gas transfer model is not adequate for small aquatic systems (small fetched) where turbulence is controlled by heat exchange rather than wind [50]. Therefore, a correction factor (×0.2458) was applied, obtained from a series of simultaneous CO_2 flux measurements from a floating chamber connected to an EGM-4 (PP-Systems) performed at the same time as surface gas concentrations were collected [4] (data from 2007 to 2010, $n = 57$, $r^2 = 0.689$, $p<0.001$; unpubl. data).

Ebullition

Ebullition flux and bubble characterization (composition, $\delta^{13}C$ and δD, and ^{14}C dating; see below) were obtained from submerged funnels. Bubble samples were collected in pre-combusted (500°C for 2 h), miliQ-rinsed, 125 mL glass bottles, helium flushed and vacuumed, with butyl rubber caps. Funnels were installed in polygonal ponds BYL1 and 80 from 18 June to 13 July 2011. Ice was present at the bottom of BYL80 from 18 to 22 June, while no ice was present in BYL1. Ebullition flux (F_e) was obtained from passive accumulation of gas in funnels, and calculated as:

$$F_e = (pGas \times V)/(A \times MV \times time)$$

where V is the gas volume collected, A is the funnel area (0.3526 m^2), and MV the gas molar volume at ambient air temperature. In addition, gas was collected from 22 to 26 June from stirred sediments for stable isotopes and ^{14}C dating in ponds BYL27 and 38, since ebullition rate did not provide sufficient gas and funnels were too large for proper installation in shallow and narrow runnel ponds.

Stable isotopes

Stable isotopes of C and H in CO_2 and CH_4 ($\delta^{13}CO_2$, $\delta^{13}CH_4$, and δD_{CH4}) were analyzed at the Biochemistry Laboratory of the School of Earth and Ocean Sciences (University of Victoria, Canada). Gas samples in Wheaton bottles were analyzed for $\delta^{13}CH_4$ by introducing the gas onto a GSQ PLOT column (0.32 mm ID, 30 m) using a Valco 6-port valve and sample loop. After chromatographic separation, the CH_4 passes through an oxidation oven (1030°C), a Nafion water trap, and open-split interface to a Continuous Flow-Isotope Ratio Mass Spectrometer (CF-IRMS). The $\delta^{13}CO_2$ was measured similarly, but without the combustion oven. Precision for the $\delta^{13}CH_4$ and $\delta^{13}CO_2$ analyses was ±0.2‰. Hydrogen isotope ratios of CH_4 (δD_{CH4}) were measured by a TC/EA pyrolysis unit (1450°C) interfaced to a CF-IRMS. Precision for the δD_{CH4} analyses was ±3‰, relative to VSMOW.

$\Delta^{14}C$ analysis

Methane and CO_2 were separated by a continuous flow line consisting of purification and combustion traps [51] as follows: first, CO_2 was frozen in liquid nitrogen (LN_2), second, carbon monoxide (CO) was oxidized to CO_2 in a 300°C CuO furnace and frozen in a second LN_2 trap, finally, non-condensable CH_4 was oxidized to CO_2 in a CuO furnace at 975°C (Lindberg/Blue M Tube Furnace, Thermo Scientific). The resulting CO_2 and H_2O from CH_4 combustion were further separated cryogenically on the vacuum line. Purified CO_2 was graphitized using the sealed tube zinc reduction method [52]. The ^{14}C analysis was conducted at the Keck Carbon Cycle AMS (KCCAMS) facility at the University of California, Irvine (UCI), on a compact accelerator mass spectrometer (AMS) system from National Electrostatics Corporation (NEC 0.5MV 1.5SDH-2 AMS), with a modified NEC MC-SNIC ion-source [53–54]. The in-situ simultaneous AMS $\delta^{13}C$ measurement allowed for fractionation corrections occurring inside the AMS system and during graphitization, significantly improving the precision and accuracy, with a day-to-day analysis

relative error of 2.5 to 3.1‰ based on secondary standards, and including extraction, graphitization and AMS measurement.

Archaeal diversity

Surface water was filtered sequentially through a 3 µm pore size polycarbonate filter and a 0.2 µm Sterivex unit (Millipore). Filters were immersed in buffer (40 mM EDTA; 50 mM Tris at pH 8.3; 0.75 M sucrose), stored in liquid nitrogen in the field (≤2 weeks), and then stored at −80°C until extraction. Cellular DNA was extracted from both filters, with a phenol:chloroform:Indole-3-Acetic Acid (25:24:1) and chloroform:Indole-3-Acetic Acid (24:1) separation and DNA quantified by spectrophotometry (Nanodrop ND-1000). Surface sediment samples were collected using a cut 60 mL sterile plastic syringe to depth of around 6.5 cm, placed in sterile plastic bags and homogenized. A sub-sample of 3 mL was squeezed from the bag into 5 mL cryotubes with buffer and stored as above. DNA was extracted using the MO BIO Kit (RNA Powersoil total RNA isolation kit #12866-25 and DNA elution accessory kit #12867-25) allowing both RNA and DNA to be extracted at the same time, but only DNA was sequenced for this study. Once extracted the DNA was quantified as above.

A PCR reaction mixture of 1× HF buffer (NEB), 200 µM dNTP (Feldan Bio), 0.4 mg mL^{-1} BSA (Fermentas), 0.2 µM of each 454 primer (969F: ACGCGHNRAACCTTACC and 1401R: CRGTGWGTRCAAGGRGCA) [55], 1 U of Phusion High-Fidelity DNA polymerase (NEB), and 0.1–1 µL of template DNA for sediment samples, or 2 µL for water samples. Three separate DNA concentrations were used for each sample, from 1× to 2.22×, to reduce PCR bias. Amplification cycles included denaturing at 98°C for 30 s, 30 cycles of denaturing at 98°C for 10 s, annealing at 55°C for 30 s, extension at 72°C for 30 s, and a final extension at 72°C for 5 min. For each sample, the triplicate reactions were pooled together for purification (QIAquick PCR purification kit; QIAGEN) and quantification (Nanodrop ND-1000). The resulting sample coded amplicons were mixed in equal proportions and sequenced on a Roche 454 GS-FLX Titanium platform at Université Laval Plateforme d'analyses Génomiques. Raw reads were submitted to NCBI Sequence Read Archive (SRA) under the accession number SRA039814, with a Sequence Read Experiment (SRX) number SRX319084. Resulting reads were subjected to pyrotag pre-processing, quality control, and taxonomic analyses [55]. Low-quality reads were identified and removed if they contained any non assigned nucleotides (N's), were <150 bp not including the adaptor and sample tag-code, if they exceed the expected amplicon size, and if the Forward primer sequence was incorrect. The remaining reads were then trimmed if there were nucleotide bases after the reverse primer. Next, reads were aligned using mother [56–57] against SILVA reference alignments, and then manually checked to remove misaligned reads. The number of reads after processing ranged from 1921 to 2105, and for downstream analysis was randomly resampled to 1921 reads. The SILVA database (version 108) was used for archaeal identifications, including additional previously generated clone library sequences [41,58–59] from the C. Lovejoy laboratory.

Supporting Information

File S1 Figure S1, Seasonal melting and freezing. Surface water temperature for one polygonal pond (BYL1) and one runnel pond (BYL24), from July 2008 to July 2009. **Figure S2, Diffusive greenhouse gas flux from polygonal and runnel ponds.** Data collected from summer 2009, 2010 and 2011, including 33 measurements from polygonal ponds and 58 from runnel ponds. The diffusive flux was calculated using the wind-based model of Cole and Caraco [41], but estimations were corrected with a regression equation comparing floating chamber CO_2 flux to wind-based flux (see Methods). **Table S1, Methane emission ranges (median value in parenthesis) through diffusion (N = 4) and ebullition (N = 8) from two polygonal ponds (BYL1 and BYL80), and diffusive flux from 12 other polygonal ponds and 14 other runnel ponds located on the same site measured from 18 June to 16 July 2011. Table S2, Range (median) of $\delta^{13}CO_2$, $\delta^{13}CH_4$, and δD_{CH4} values for diffusion and ebullition gas samples, also given separately for polygonal and runnel thaw ponds.**
(PDF)

Acknowledgments

We thank P.-G. Rossi, V. Gélinas, P. N. Bégin, C. Girard, L. Boutet, and G. Deslongchamps for their efficient help in the field and laboratory, A. Comeau for his precious help at the molecular laboratory and for pyrosequencing data processing, We also thank G. Gauthier for sharing his logistics allocation.

Author Contributions

Conceived and designed the experiments: KN IL CL. Performed the experiments: KN IL. Analyzed the data: KN IL XX MJW PEG. Contributed reagents/materials/analysis tools: IL CL XX MJW. Wrote the paper: KN IL CL PEG XX MJW.

References

1. Fortier D, Allard M (2004) Late Holocene syngenetic ice-wedge polygons development, Bylot Island, Canadian Arctic Archipelago. Can J of Earth Sci 41: 997–1012.
2. Rowland JC, Jones CE, Altmann G, Bryan R, Crosby BT, et al. (2010) Arctic Landscapes in Transition: Responses to Thawing Permafrost. Eos Trans AGU 91: 229–230. doi:10.1029/2010EO260001
3. Tank SE, Lesack LFW, Hesslein RH (2009) Northern Delta Lakes as Summertime CO_2 absorbers within the Arctic Landscape. Ecosystems 12: 144–157.
4. Laurion I, Vincent WF, MacIntyre S, Retamal L, Dupont C, et al. (2010) Variability in greenhouse gas emissions from permafrost thaw ponds. Limnol Oceanogr 55: 115–133.
5. Abnizova A, Siemens J, Langer M, Boike J (2012) Small ponds with major impact: The relevance of ponds and lakes in permafrost landscapes to carbon dioxide emissions. Glob Biogeochem Cy 26: GB2041–GB2050.
6. Tranvik LJ, Downing JA, Cotner JB, Loiselle SA, Striegl RG, et al. (2009) Lakes and reservoirs as regulators of carbon cycling and climate. Limnol Oceanogr 54: 2298–2314.
7. Muster S, Langer M, Heim P, Westermann S, Boike J (2012) Subpixel heterogeneity of ice-wedge polygonal tundra: a multi-scale analysis of land cover and evapotranspiration in the Lena River Delta, Siberia. Tellus B 64: 17301. doi: 10.3402/tellusb.v64i0.17301.
8. Zimov SA, Voropaev YV, Semiletov IP, Davidov SP, Prosiannikov SF, et al. (1997) North Siberian lakes: a methane source fueled by Pleistocene carbon. Science 277: 800–802.
9. Wagner D, Lipski A, Embacher A, Gattinger A (2005) Methane fluxes in permafrost habitats of the Lena Delta: effects of microbial community structure and organic matter quality. Environ Microbiol 7: 1582–1592.
10. Zona D, Oechel WC, Peterson KM (2008) Carbon fluxes across vegetated drained lakes of different ages on the arctic coastal plain, Alaska. AGU Fall Meeting Abstracts A421+
11. Grosse G, Harden J, Turetsky M, McGuire AD, Camill P, et al. (2011) Vulnerability of high-latitude soil organic carbon in North America to disturbance. J Geophys Res 116: 2005–2012.
12. Schuur EAG, Bockheim J, Canadell JG, Euskirchen E, Field CB, et al. (2008) Vulnerability of permafrost carbon to climate chagne: implications for the global carbon cycle. BioScience 58: 701–714.
13. Shirokova LS, Pokrovsky OS, Kirpotin SN, Desmukh C, Pokrovsky BG, et al. (2013) Biogeochemistry of organic carbon, CO_2, CH_4, and trace elements in

thermokarst water bodies in discontinuous permafrost zones of Western Siberia. Biogeochem 113: 573–593.
14. Breton J, Vallière C, Isabelle L (2009) Limnological properties of permafrost thaw ponds in northeastern Canada. Can J Fish Aquat Sci 66: 1635–1648.
15. Walter KM, Chanton JP, Chapin FS, Schuur EAG, Zimov SA, et al. (2008) Methane production and bubble emissions from arctic lakes: Isotopic implications for source pathways and ages. J Geophys Res 113: G00A08.
16. Berggren M, Ström L, Laudon H, Karlsson J, Jonsson A, et al. (2010) Lake secondary production fueled by rapid transfer of low molecular weight organic carbon from terrestrial sources to aquatic consumers. Ecol Lett 13: 870–880.
17. Guillemette F, Del Giorgio PA (2011) Reconstructing the various facets of dissolved organic carbon bioavailability in freshwater ecosystems. Limnol Oceanogr 56: 734–748.
18. Hornibrook ERC, Longstaffe FJ, Fyfe WS (1997) Spatial distribution of microbial methane production pathways in temperate zone wetland soils: stable carbon and hydrogen isotope evidence. Geochim Cosmochim Ac 61: 745–753.
19. Penning H, Conrad R (2007) Quantification of carbon flow from stable isotope fractionation in rice field soils with different organic matter. Org Geochem 38: 2058–2069.
20. Walter KM, Smith LC, Chapin II FS (2007) Methane bubbling from northern lakes: present and future contributions to the global methane budget. Phil Trans R Soc A 365: 1657–1676.
21. Michmerhuizen CM, Striegl RG, McDonald ME (1996) Potential methane emission from north-temperate lakes following ice melt. Limnol Oceanogr 41: 985–991.
22. Bastviken D, Cole J, Pace ML, Tranvik LJ (2004) Methane emissions from lakes: dependence of lake characteristics, two regional assessments, and a global estimate. Glob Biogeochem Cy 8: 4009–4021.
23. Smith LC, Sheng Y, MacDonald GM (2007) A first pan-Arctic assessment of the influence of glaciation, permafrost, topography and peatlands on northern hemisphere lake distribution. Permafrost Periglac 18: 201–208.
24. Borrel G, Joblin K, Guedon A, Colombet J, Tardy V, et al. (2011) *Methanobacterium lacus sp. nov.*, isolated from the profundal sediment of a freshwater meromictic lake. Int J Syst Evol Micr 62: 1625–1629.
25. Barber R, Zhang L, Harnack M, Olson M, Kaul R, et al. (2011) Complete genome sequence of *Methanosaeta concilii*, a specialist in aceticlastic methanogenesis. J Bacteriol 193: 3668–3669.
26. Deppenmeier U, Johann A, Hartsch T, Merkl R, Schmitz RA, et al. (2002) The genome of *Methanosarcina mazei*: evidence for lateral gene transfer between bacteria and archaea. J Mol Microb Biotech 4: 453–461.
27. Grosse G, Romanovsky V, Walter K, Morgenstern A, Lantuit H, et al. (2008) Distribution of thermokarst lakes and ponds at three yedoma sites in Siberia. (eds D L Kane and K M Hinkel), In Ninth International Conference on Permafrost Institute of Northern Engineering, University of Alaska Fairbanks. 551–556.
28. Sachs T, Wille C, Boike J, Kutzbach L (2008) Environmental controls on ecosystem-scale CH_4 emission from polygonal tundra in the Lena River Delta, Siberia. J Geophys Res 113: 2005–2012.
29. Zimov SA, Voropaev YV, Davydov SP, Zimova GM, Davydova AI, et al. (2001) Flux of methane from north Siberian aquatic systems: influence on atmospheric methane. Permafrost Response on Economic Development, Environmental Security and Natural Resources. NATO Science Series 76: 511–524. doi: 10.1007/978-94-010-0684-2_35.
30. Walter Anthony KM, Vas DA, Brosius L, Chapin FS III, Zimov SA, et al. (2010) Estimating methane emissions from northern lakes using ice-bubble surveys. Limnol Oceanogr-Meth 8: 592–609.
31. Hamilton JD, Kelly CA, Rudd JWM, Hesslein RH, Roulet NT (1994) Flux to the atmosphere of CH_4 and CO_2 from wetland ponds on the Hudson Bay Lowlands (HBLs). J Geophys I Res 99: 1495–1510.
32. Roehm CL, Giesler R, Karlsson J (2009) Bioavailability of terrestrial organic carbon to lake bacteria: The case of a degrading subarctic permafrost mire complex. J Geophys Res 114: G03006.
33. Wagner D, Gattinger A, Embacher A, Pfeiffer EM, Schloter M, et al. (2007) Methanogenic activity and biomass in Holocene permafrost deposits of the Lena Delta, Siberian Arctic and its implication for the global methane budget. Glob Change Bio 13: 1089–1099.
34. Zimov SA, Schuur EAG, Chapin FS III (2006) Climate Change: Permafrost and the global carbon budget. Science 312: 1612–1613.
35. Karadagli F, Rittmann BE (2007) A mathematical model for the kinetics of *Methanobacterium bryantii* M o H considering hydrogen thresholds. Biodegradation 18: 453–464.
36. Sakai S, Imachi H, Sekiguchi Y, Tseng IC, Ohashi A, et al. (2009) Cultivation of methanogens under low-hydrogen conditions by using the coculture method. Appl Environ Microbiol 75: 4892–4896.
37. Høj L, Olsen R, Torsvik V (2008) Effects of temperature on the diversity and community structure of known methanogenic groups and other Archaea in high Arctic peat. ISME J 2: 37–48.
38. Høj L, Olsen RA, Torsvik VL (2006) Archaeal communities in High Arctic wetlands at Spitsbergen, Norway (78°N) as characterized by 16S rRNA gene fingerprinting. FEMS Microbiol Ecol 53: 89–101.
39. Kobabe S, Wagner D, Pfeiffer EM (2004) Characterisation of microbial community composition of a Siberian tundra soil by fluorescence in situ hybridisation. FEMS Microbiology Ecology 50: 13–23.
40. Metje M, Frenzel P (2007) Methanogenesis and methanogenic pathways in a peat from subarctic permafrost. Environ Microbiol 9: 954–964.
41. Pouliot J, Galand PE, Lovejoy C, Vincent WF (2009) Vertical structure of archaeal communities and the distribution of ammonia monooxygenase A gene variants in two meromictic High Arctic lakes. Environmental Microbiology 11: 687–699.
42. Barbier BA, Dziduch I, Liebner S, Ganzert L, Lantuit H, et al. (2012) Methane-cycling communities in a permafrost-affected soil on Herschel Island, Western Canadian Arctic: active layer profiling of mcrA and pmoA genes. FEMS Microbiol Ecol: 1574–6941.
43. Borrel G, Jézéquel D, Biderre-Petit C, Morel-Desrosiers N, Morel JP, et al. (2011) Production and consumption of methane in freshwater lake ecosystems. Research in Microbiology 162: 832–847.
44. Juottonen H (2008) Archaea, bacteria, and methane production along environmental gradients in fens and bogs. *(Unpublished doctoral dissertation)*.
45. Brosius LS, Walter Anthony KM, Grosse G, Chanton JP, Farquharson LM, et al. (2012) Using the deuterium isotope composition of permafrost meltwater to constrain thermokarst lake contributions to atmospheric CH_4 during the last deglaciation. J Geophys Res 117: G01022.
46. Stainton M, Capel MJ, Armstrong A (1977) The chemical analysis of freshwater. Can Fish Mar Serv Misc Spec Publ 25.
47. Chappaz A, Gobeil C, Tessier A (2008) Geochemical and anthropogenic enrichments of Mo in sediments from perennially oxic and seasonally anoxic lakes in Eastern Canada. Geochim Cosmochim Ac 72: 170–184.
48. Hesslein RH, Rudd J, Kelly C, Ramlal P, Hallard K (1991) Carbon dioxide pressure in surface waters of Canadian lakes. In Air-water mass transfer. Amr Soc Eng p. 413–431.
49. Cole J, Caraco NF (1998) Atmospheric exchange of carbon dioxide in a low-wind oligotrophic lake measured by the addition of SF6. Limnol Oceanogr 43: 647–656.
50. MacIntyre S, Jonsson A, Jansson M, Aberg J, Turney DE, et al. (2010) Buoyancy flux, turbulence, and the gas transfer coefficient in a stratified lake. Geophys Res Lett 37: L24604.
51. Xu X, Pack MA, Stills A, Lupascu M, Czimczik CI (2012) A rapid method for preparing high concentration CH_4 gas samples for ^{14}C analysis by AMS. Abstract in The 21th Radiocarbon Conference, Paris.
52. Xu X, Trumbore SE, Zheng S, Southon JR, McDuffee KE, et al. (2007) Modifying a sealed tube zinc reduction method for preparation of AMS graphite targets: reducing background and attaining high precision. Nucl Instrum Meth 259: 320–329.
53. Southon J, Santos G (2004) Ion source development at KCCAMS, University of California, Irvine. Radiocarbon 46: 33–39.
54. Southon J, Santos GM (2007) Life with MC-SNICS. Part II: further ion source development at the keck carbon cycle AMS facility. Nucl Instrum Meth 259: 88–93.
55. Comeau AM, William KW, Tremblay JE, Carmack EC, Lovejoy C (2011) Arctic ocean microbial community structure before and after the 2007 record sea ice minimum. PLoS ONE 6: e27492.
56. Schloss PD, Westcott SL, Ryabin T, Hall JR, Hartmann M, et al. (2009) Introducing mothur: Open source, platform-independent, community-supported software for describing and comparing microbial communities. Appl Environ Microbiol 75: 7537–7541.
57. Schloss PD (2009) A high-throughput DNA sequence aligner for microbial ecology studies. PLoS ONE 4: e8230.
58. Galand PE, Lovejoy C, Vincent WF (2006) Remarkably diverse and contrasting archaeal communities in a large arctic river and the coastal Arctic Ocean. Aquat Microb Ecol 44: 115–126.
59. Comeau AM, Harding T, Galand PE, Vincent WF, Lovejoy C (2012) Vertical distribution of microbial communities in a perennially stratified Arctic lake with saline, anoxic bottom waters. Sci Rep 2: #604.

8 ANNEXE – Preuve de soumission du 2e article

De : "Polar Biology (POBI)" <dilip.rajasekar@springer.com>
Objet : POBI - Submission Confirmation
Date : 6 décembre 2013 15:18:24 HNE
À : Laurion Isabelle <Isabelle.Laurion@ete.inrs.ca>

Dear Dr. Isabelle Laurion,

Thank you for submitting your manuscript, Arctic thaw pond morphology influences bacterial communities and associated greenhouse gas emissions, to Polar Biology.

During the review process, you can keep track of the status of your manuscript by accessing the following web site:

http://pobi.edmgr.com/

Should you require any further assistance please feel free to e-mail the Editorial Office by clicking on "Contact Us" in the menu bar at the top of the screen.

With kind regards,
Springer Journals Editorial Office
Polar Biology

Now that your article will undergo the editorial and peer review process, it is the right time to think about publishing your article as open access. With open access your article will become freely available to anyone worldwide and you will easily comply with open access mandates. Springer's open access offering for this journal is called Open Choice (find more information on www.springer.com/openchoice). Once your article is accepted, you will be offered the option to publish through open access. So you might want to talk to your institution and funder now to see how payment could be organized; for an overview of available open access funding please go to www.springer.com/oafunding.
Although for now you don't have to do anything, we would like to let you know about your upcoming options.